

# Functional precision medicine for pediatric myeloid neoplasms

Doctoral thesis at the Medical University of Vienna  
for obtaining the academic degree  
**Doctor of Philosophy**

Submitted by

**Ben Haladik, BSc, MSc**

Supervisor

Univ.-Prof. Dr. med. Kaan Boztug, MBA

St. Anna Children's Cancer Research Institute

Zimmermannplatz 10, 1020 Vienna Austria

Medical University of Vienna, Department of Pediatrics and  
Adolescent Medicine, Vienna, Austria

CeMM Research Center for Molecular Medicine of the Austrian  
Academy of Sciences, Vienna, Austria

Vienna, 10/2025

# Declaration

This doctoral thesis was written by Ben Haladik (B.H.) and contains one published manuscript. B.H. is first author of the manuscript and has written all chapters of this thesis with feedback from Kaan Boztug. The experiments and analyses in this thesis have been performed in the St. Anna Children's Cancer Research Institute (CCRI) and the Research Center for Molecular Medicine of the Austrian Academy of Sciences (CeMM), which are both located in Vienna, Austria. The work presented here was supported by members of the Kaan Boztug laboratory at CeMM, the Giulio Superti-Furga laboratory at CeMM and the Michael N. Dworzak laboratory at CCRI. The published manuscript in the results section indicates individual author contributions. All other text was written by B.H. without the use of any AI algorithms for generation, translation or paraphrasing of any text included in this thesis.

The manuscript in chapter 3.2 was published in **Cell Reports Medicine** under the Creative Commons CC-BY 4.0 license has been reprinted with permission from the publisher Elsevier.

**Image-based drug screening combined with molecular profiling identifies signatures and drivers of therapy resistance in pediatric AML.**

Haladik B, Maurer-Granofszky M, Zoescher P, Jimenez-Heredia R, Frohne A, Segarra-Roca A, Casey C, Kartnig F, Giuliani S, Rashkova C, Repiscak P, Dworzak MN\*, Superti-Furga G\*, Boztug K\*. (2025) Cell Reports Medicine. Aug 19:102304. doi: 10.1016/j.xcrm.2025.102304. Epub ahead of print. \* equal contribution

Figures 1, 4, and 7 were reprinted with permission from Springer Nature under the Creative Commons Non-commercial License. Figure 2 was reprinted with kind permission from Cold Spring Harbor Laboratory Press. Figures 5 and 6 were reprinted with kind permission from the American Association for Cancer Research.

# Table of contents

## Table of Contents

Declaration .....	ii
Table of contents .....	iii
List of figures .....	v
Abstract .....	vi
Zusammenfassung .....	viii
Publications arising from this thesis .....	x
Abbreviations .....	xi
Acknowledgements .....	xii
1. Introduction .....	1
1.1. The unique biology of pediatric cancers .....	2
1.1.1. Germline predispositions .....	4
1.1.2. Oncogenic pathogens and compromised immune surveillance .....	5
1.1.3. Developmental tumorigenesis .....	5
1.2. Pediatric acute myeloid leukemia in the context of healthy hematopoiesis .....	7
1.2.1. The hematopoietic hierarchy and cell surface antigens .....	9
1.2.2. The hematopoietic hierarchy and transcription factors .....	12
1.2.3. Pediatric AML as a disease of aberrant transcription .....	17
1.2.4. The evolution of treatment of acute childhood leukemias .....	24
1.2.5. The current treatment landscape of pediatric AML .....	25
1.2.6. Emerging treatment options for pediatric AML .....	28
1.2.7. Mechanisms of treatment resistance in pediatric AML .....	31
1.3. Genomic and functional precision medicine .....	33
1.3.1. Genomic precision medicine .....	34
1.3.2. Functional Precision Medicine .....	35
1.3.3. Recent advances in functional precision medicine .....	36
1.4. Precision Medicine in pediatric malignancies .....	37
1.5. Aims of this thesis .....	39
2. Results .....	40
2.1. Prologue .....	40
2.2. Image-based drug screening combined with molecular profiling identifies signatures and drivers of therapy resistance in pediatric AML .....	41
3. Discussion .....	88
3.1. Functional Precision Medicine in pediatric cancers .....	88
3.1.1. Technical considerations for functional precision medicine studies .....	88

3.1.2.	Translational considerations for functional precision medicine studies .....	90
3.2.	Multi-omics insights into pediatric AML .....	93
3.2.1.	Clonality and genomic targetability of pediatric AML .....	93
3.2.2.	Cellular differentiation states and risk in pediatric AML.....	94
3.2.3.	The functional landscape of pediatric AML .....	95
3.2.4	Conclusions and future prospects.....	97
4.	Materials and Methods .....	99
References	.....	100
Appendix	.....	120
CV	.....	120

# List of figures

<b>Figure 1. Somatic coding mutation frequencies in pediatric and adult cancers.....</b>	<b>3</b>
<b>Figure 2. Age dependent incidence of early onset and late onset cancers.....</b>	<b>7</b>
<b>Figure 3. Simplified overview of hematopoiesis and marker expression profiles with focus on myeloid development.....</b>	<b>11</b>
<b>Figure 4. Development of hierarchical models of hematopoiesis over time. ....</b>	<b>15</b>
<b>Figure 5. Survival of pediatric AML patients with different oncogenic fusions .....</b>	<b>18</b>
<b>Figure 6. UMAP of pedAML transcriptomes. ....</b>	<b>22</b>
<b>Figure 7. Development of overall survival and event-free survival in the AML-BFM trials from 1987 to 2012.....</b>	<b>27</b>

# Abstract

Pediatric acute myeloid leukemia (AML) is a group of rare hematological malignancies that is mainly driven by oncogenic fusion proteins affecting epigenetic or transcriptional regulators. Studies over the past decades have dramatically improved overall survival of pediatric AML patients to 60-80% in the western world and overall survival rates of more than 90% have been achieved in selected subgroups. However, many subgroups still fare poorly and improvements in overall survival have stagnated over the past years, indicating that the previous approach of improving outcome via chemotherapy intensification, risk and response adjusted therapy and improvements in supportive care may have reached its limits. Therefore, novel treatment approaches to further improve outcome in pediatric AML are urgently needed.

Previous studies have elucidated the genomic landscape of the disease to an unprecedented extent and have uncovered a lower mutational burden when compared to adult AML and a substantially higher rate of structural mutations when compared to point mutations. There are only few targeted treatments available for the oncogenic drivers in pediatric AML and thus, genomic approaches alone may not be sufficient to identify novel treatment options in high-risk patients.

To address these challenges, we set out to comprehensively characterize pediatric AML using advanced drug response profiling (DRP) and multi-omics data integration. We established image-based high-content DRP in pediatric AML that allowed us to accurately distinguish malignant blasts and on-target cell killing and validated this methodology using orthogonal assays. Using this methodology, we profiled a retrospective cohort of 45 patients that were sampled at diagnosis with our DRP approach, whole exome sequencing, RNA sequencing and Assay for Transposase-Accessible Chromatin (ATAC) sequencing. We identified venetoclax combinations and chemotherapy drugs from standard treatment protocols as the main drivers of variation in our patient cohort. In an integrative analysis approach, we mapped pediatric AML ATAC-sequencing profiles to their most similar healthy counterpart and found samples that were more similar to either hematopoietic stem cells (HSCs) or to monocytes to be significantly more likely to be high-risk and unresponsive to induction chemotherapy. Additionally, we identified recurring drug sensitivity profiles for these groups where HSC-like samples were more sensitive to HDAC inhibitors and certain venetoclax combinations and monocyte-like samples were more sensitive to Fludarabine and other drugs. Finally, we demonstrated that the drug response profiles we identified are predictive of patient risk and non-response.

Overall, our study demonstrates feasibility of advanced image-based DRP for pediatric AML and provides proof-of-concept for functional precision medicine studies in pediatric leukemias

and other rare malignancies. Our integrative analysis approach highlights risk associations and vulnerabilities of cellular differentiation phenotypes and thus provides novel insights into these under-appreciated phenotypes. The predictivity of drug response profiles for patient risk indicates that DRP may be a useful stratification tool already at diagnosis and supports the application of functional precision medicine approaches beyond relapsed or refractory disease.

# Zusammenfassung

Die pädiatrische akute myeloische Leukämie (AML) umfasst eine Gruppe seltener Blutkrebskrankungen, die hauptsächlich von krebserzeugenden Fusionsproteinen verursacht wird. Diese bestehen in der Regel aus Proteinen, die die Transkription oder das Epigenom regulieren. Das Überleben von Patienten mit pädiatrischer AML hat sich in den letzten Jahrzehnten stark verbessert, so dass Überlebensraten in der westlichen Welt heutzutage zwischen 60 und 80% liegen. Bei gewissen Risikogruppen liegt die Überlebenschance sogar bei über 90%. Dennoch gibt es immer noch Subtypen mit deutlich schlechteren Überlebenschancen und das Überleben von Patient:innen mit pädiatrischer AML hat sich in den letzten Jahren weniger stark verbessert als zuvor. Die bisher verwendeten Strategien wie Intensivierung der Chemotherapie, Therapie-Adaptierung anhand von Risikofaktoren und Ansprechen der Patient:innen, und bessere Pflege scheinen nicht mehr auszureichen, um das Überleben der Patient:innen weiter zu verbessern. Deshalb werden neue Strategien, zur Verbesserung der Behandlung der pädiatrischen AML dringend benötigt.

Einige Studien der letzten Jahre haben die genomischen Eigenschaften dieser Krebsart umfassend charakterisiert und unter anderem eine deutlich niedrigere Mutationsrate als in Erwachsenen mit AML identifiziert, und eine höhere Rate von strukturellen Mutationen im Vergleich zu Punktmutationen beschrieben. Es gibt nur wenige Medikamente, die auf krebserzeugende Mutationen in pädiatrischer AML zugeschnitten sind und genetische Ansätze allein sind möglicherweise nicht ausreichend, um neue Therapieansätze für Patient:innen in Hochrisikogruppen zu finden.

Um diesen Herausforderungen zu begegnen haben wir eine umfassende Charakterisierung von Proben mit pädiatrischer AML vorgenommen, bei der wir fortgeschrittenes *Drug Response Profiling* (DRP) und multi-modale Datenintegration miteinander kombiniert haben. Wir haben ein bildbasiertes DRP-Verfahren für pädiatrische AML etabliert, das uns erlaubt die krebserzeugende Population der myeloischen Blasten und das Überleben von Zellen genau zu messen und diesen Ansatz mit orthogonalen Methoden validiert. Mit diesem Ansatz und Exome Sequenzierung, RNA-Sequenzierung und *Assay for Transposase-Accessible Chromatin* (ATAC) Sequenzierung haben wir 45 Proben aus der initialen Diagnose in einer retrospektiven Kohorte umfassend charakterisiert. Unser Ansatz hat Venetoklax Kombinationen und Chemotherapeutika aus üblichen Behandlungsprotokollen als Treiber der Variation zwischen Patient:innen hervorgehoben. In einer integrativen Analyse haben wir AML Proben den ähnlichsten gesunden Blutzelltypen zugeordnet. Proben, die eine hohe Ähnlichkeit zu hämatopoetischen Stammzellen oder Monozyten hatten, waren signifikant mit hohem Patient:innenrisiko und Resistenz gegen die Induktionstherapie assoziiert. Zusätzlich haben



wir konsistente Wirksamkeiten verschiedener Medikamente für diese Gruppen gefunden. HDAC Inhibitoren und bestimmte Venetoclax-Kombinationen waren gegen Stammzell-ähnliche Leukämien besonders wirksam und Fludarabine und andere Medikamente waren besonders gegen Monozyten-ähnliche Leukämien wirksam. Weiterhin konnten wir zeigen, dass unsere DRP-Messungen möglicherweise Patientenrisiko und Nicht-Ansprechen auf Therapie vorhersagen können.

Unsere Arbeit demonstriert die Machbarkeit von technisch fortgeschrittenen DRP-Ansätzen in pädiatrischer AML und ist ein Modellansatz für Studien im Bereich der funktionellen Präzisionsmedizin in pädiatrischen Leukämien und anderen seltenen Krebserkrankungen. Unsere integrative Analyse hebt Assoziationen zwischen Patientenrisiko und zellulärer Differenzierung hervor und ermöglicht so neue Einsichten in diese unter-erforschten Phänotypen. Die Vorhersagekraft unserer DRP-Methode für das Patientenrisiko hebt hervor, dass DRP ein nützliches Werkzeug zur Stratifizierung von Patient:innen ab Diagnose sein kann und zeigt, dass DRP auch über rezidierte Fälle und Fälle in späten Stadien hinaus anwendbar und nützlich sein kann.

# Publications arising from this thesis

**Image-based drug screening combined with molecular profiling identifies signatures and drivers of therapy resistance in pediatric AML.**

Haladik B, Maurer-Granofszky M, Zoescher P, Jimenez-Heredia R, Frohne A, Segarra-Roca A, Casey C, Kartnig F, Giuliani S, Rashkova C, Repiscak P, Dworzak MN\*, Superti-Furga G\*, Boztug K\*. (2025) Cell Reports Medicine. Aug 19:102304. doi: 10.1016/j.xcrm.2025.102304. Epub ahead of print. \* equal contribution

# Abbreviations

AML acute myeloid leukemia  
AMKL acute megakaryoblastic leukemia  
ALL acute lymphoblastic leukemia  
B-ALL B-cell acute lymphoblastic leukemia  
BFM Berlin Frankfurt Münster study group  
CLP common lymphoid progenitor  
CMP common myeloid progenitor  
DRP drug response profiling  
EBV Epstein-Barr Virus  
FAB French American British  
GMP Granulocyte macrophage progenitor  
FPM functional precision medicine  
GPM genomic precision medicine  
HSC hematopoietic stem cell  
LMPP lymphoid primed multipotent progenitor  
LSC leukemic stem cell  
MDP Monocyte dendritic cell progenitor  
MPP multipotent progenitor  
MRD measurable residual disease  
NGS next-generation sequencing  
pedAML pediatric acute myeloid leukemia  
pedALL pediatric acute lymphoblastic leukemia  
T-ALL T-cell acute lymphoblastic leukemia

# Acknowledgements

First and foremost, I thank my supervisor Kaan Boztug. This thesis would not have been possible without his support and guidance. We had started this work with the ambition to advance pediatric precision oncology in Vienna and his ambition, drive and perseverance always motivated me and enabled us to push this project through reach our common goal. I also thank Giulio Superti-Furga, who co-supervised me and kindly hosted me with his laboratory during my PhD. His continuous guidance and strategic thinking kept this project and me on track. Last but not least, I thank Michael N. Dworzak for his clinical input and continued support. He always inspired me to ultimately focus my work on the benefits for patients.

I want to thank all patients and their families who participated in the study in this manuscript and the other work we did. Translational research projects like the ones presented here are not possible without their active participation and consent and I am grateful for their contributions.

Additionally, I thank CCRI and CeMM for providing the environment that enabled this work. I want to thank Anita Ender and the staff at CeMM in particular for creating an amazing environment to do science. CeMM has been a wonderful place and the members of its administration and IT staff are the unsung heroes of every scientific project that makes it from the building into the world.

I thank the Boztug lab who I still rightfully advertise as the nicest people I ever had the pleasure of working with, and the GSF lab which hosted some of the most interesting characters I ever encountered. There are too many people here to name every individual, but both laboratories have been wonderful to work at and I cherish the memories of them for the rest of my life.

A PhD is a long and arduous journey and like all long and arduous journeys it is not possible – or at least much less enjoyable - without friends and family. I could write a page about each of them, but I will keep it shorter. The 2018 CeMM PhD cohort was my first friend group in Vienna and even though we are in many different countries now, we are still connected and I will be forever grateful for the time we spent together. In particular, I want to thank Daria Romanovskaia for the coffee breaks, the scientific discussions, and all the rants. Next, there are my german-speaking friends from the Jumpstreet, Frankfurt, and Offenbach. I never expected to find as much joy in my life as I found with all of who. I thank Theresia, who is the most amazing partner anyone could ever hope for and who shows me every day and one can always have more love in their life. Finally, I thank my family - from whom I inherited my stubbornness - Guido, Hanni, Werner and my Mom. You have always been there for me, and I am forever grateful.

# 1. Introduction

Pediatric acute leukemias are the most common cancers in childhood (Bhakta *et al*, 2019). Among these, pediatric acute myeloid leukemia (pedAML) represents approximately 20% of cases, but represents a disproportionately higher number of deaths compared to the more prevalent pediatric acute lymphoblastic leukemia (pedALL) that makes up approximately 80% of cases (Bonaventure *et al*, 2017). Advances in genomic characterization have substantially improved patient diagnosis and stratification in the past decades (Cooper *et al*, 2023; Rasche *et al*, 2018) and recent studies have elucidated the genomic landscape of pedAML to an unprecedented extent (Bolouri *et al*, 2018; Umeda *et al*, 2024). However, these advances in the understanding of the genomics of pedAML only partially translated into novel treatments for this disease. Some promising targeted agents are being evaluated, but only targeted inhibition of *FLT3* mutated AML has made it into standard clinical practice so far (Egan & Tasian, 2025). This is at least partially due to the fact that the majority of driving lesions in pediatric AML are structural aberrations and are not directly targetable with conventional approaches (Bolouri *et al*, 2018).

Thus, novel approaches for identifying promising treatment options in pedAML are urgently needed. One particular promising strategy to accomplish this are functional precision medicine (FPM) approaches, where drug response profiling (DRP) on primary patient cells can directly identify personalized treatment options *ex-vivo* (Letai, 2022). These approaches are feasible and can improve outcome in high-risk hematological malignancies (Snijder *et al*, 2017; Kornauth *et al*, 2022). Additionally, application of FPM in an integrated fashion with comprehensive genomic characterization is an attractive route to further our understanding of hematological malignancies by direct functional and molecular characterization of primary patient material (Malani *et al*, 2022; Irmisch *et al*, 2021).

These approaches have not yet been applied systematically in pedAML. Here, the integrated application of functional precision medicine and comprehensive molecular profiling is a particularly promising tool for patient stratification and the identification of promising treatments, as DRP results can be directly related to molecular phenotypes and can thus identify treatment options where genomic profiling alone may not be able to identify targetable lesions. This introductory chapter will first provide a broader context for such an approach by covering the following aspects:

1. A general overview of pediatric cancers and their differences to adult cancers. This section discusses the unique aspects of the biology of pediatric cancers with a

particular focus on the developmental origins of pediatric cancers as a key property that differentiates them from adult cancers.

2. Pediatric leukemias and their relationship to healthy hematopoiesis. This section first provides an overview of hematopoiesis in terms of cell surface markers and the transcriptional control of hematopoietic development and uses this overview as a frame of reference to describe the biology of pedAML
3. Genomic precision medicine and functional precision medicine. This section provides a brief overview of the history of both precision medicine approaches and discusses how the corresponding approaches have emerged as promising routes for treatment prioritization in recent years by discussing the early history of functional assays, the era of genomic precision medicine and the more recent advances in functional precision medicine
4. Precision medicine in pediatric oncology. This section describes precision medicine efforts in pediatric oncology, the key studies that demonstrated feasibility and potential benefits of these approaches and the unique challenges in pursuing precision medicine in pediatric oncology.

## 1.1. The unique biology of pediatric cancers

Cancer is an umbrella term describing a plethora of diseases that are characterized by the uncontrolled proliferation of cells from individual somatic clones, leading to malignant growth, infiltration of other tissues by metastases, organ failure and ultimately death. This behavior is encapsulated in the proposed eight hallmarks of cancer, which have been defined as sustaining proliferative signaling, evading growth suppressors, avoiding immune destruction, enabling replicative immortality, tumor promoting inflammation, activating invasion and metastases, inducing or accessing vasculature, genome instability and mutation, resisting cell death and deregulating cellular metabolism (Hanahan, 2022; Hanahan & Weinberg, 2000, 2011). More recently, four additional hallmarks - phenotypic plasticity, nonmutational epigenetic reprogramming, polymorphic microbiomes and senescent cells in the tumor microenvironment - have been proposed as additional enabling characteristics (Hanahan, 2022). These hallmarks that are most commonly acquired through a Darwinian evolutionary process where an initial fitness advantage in a somatic clone enables further acquisition of mutations until the oncogenic transformation is completed and an individual presents with overt cancer (Merlo *et al*, 2006; Nowell, 1976). The continuous acquisition of these mutations is due to different factors that span from environmental exposures to individual behaviors and germline predispositions (Greaves & Maley, 2012). In line with this reasoning, cancer

incidence increases with age and several hallmarks of aging are causally linked to oncogenesis (López-Otín *et al*, 2023; Siegel *et al*, 2025).

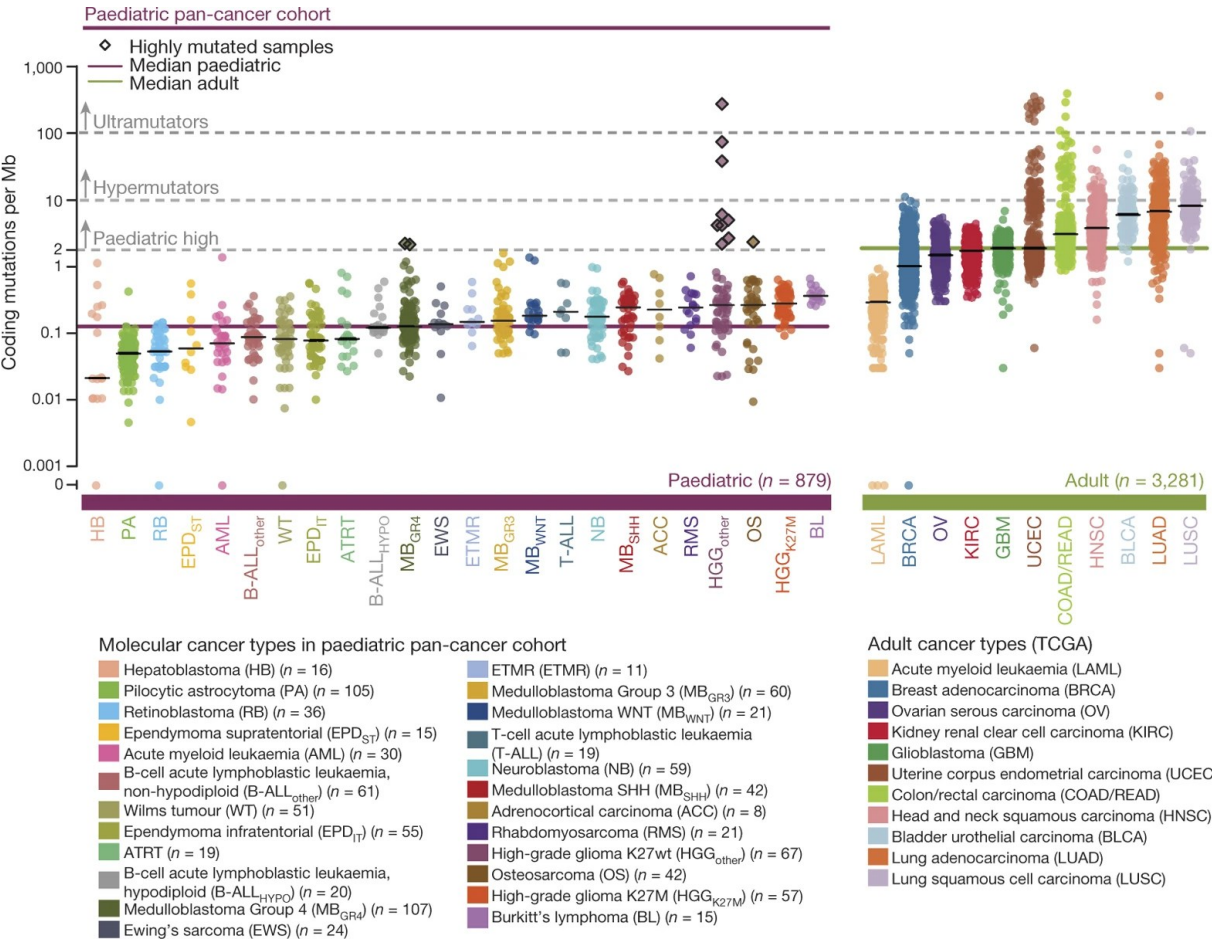


**Figure 1. Somatic coding mutation frequencies in pediatric and adult cancers**

Swarm plot of coding mutation frequencies per megabase (Mb) in 879 tumor samples 24 pediatric cancer types and 3281 tumor samples from 11 adult cancer types from the cancer genome atlas. Reprinted from (Gröbner *et al*, 2018) under the creative commons license.

However, this line of reasoning provides an incomplete if not false rationale for the oncogenesis of pediatric cancers. Pediatric malignancies have a distinct biology from their adult cancers, which is reflected in their unique genetic landscapes with overall lower mutational burden and a higher rate of structural variation than in adult cancers (Ma *et al*, 2018; Gröbner *et al*, 2018) (Fig. 1). The genetic drivers in pediatric cancer are also different. One large-scale study identified 142 candidate driver genes in pediatric cancer genomes of which only 45% matched the drivers found in large scale adult studies (Ma *et al*, 2018) and unique drivers have been identified in a substantial fraction of pediatric malignancies (Grünwald *et al*, 2018; Beird *et al*, 2022; Filbin & Monje, 2019). Furthermore, pediatric cancers commonly arise from developing

tissues, which is only rarely the case for adult cancers (Downing *et al*, 2012; Filbin & Monje, 2019; Marshall *et al*, 2014). Some childhood malignancies have specific alterations in common oncogenes that also play a role in adult malignancies such as *MYCN* amplifications that are indicative of high risk in neuroblastoma (Matthay *et al*, 2016) or the germline *RAS* mutations that predispose patients suffering from so-called *RAS*-opathies to leukemias (Niemeyer, 2014). However, many other pediatric cancers have distinct mutations that are largely restricted to that particular cancer type such as the *EWS::FLI1* fusion that is the single most important driver of Ewing sarcoma (Grünwald *et al*, 2018). Similarly, mutations that are largely restricted to younger patients have been identified in pediatric leukemias, where particular oncogenic fusion events such as *KMT2A* fusions, *NUP98* fusions and *GLIS2* fusions are far more prevalent in pediatric and adolescent leukemia patients than in adult patients (Bolouri *et al*, 2018). Conversely, some of the more commonly mutated genes in adult cancers are only affected rarely in pediatric cancers, such as *TP53* (Gröbner *et al*, 2018; Ma *et al*, 2018). These properties reflect distinct mechanisms of oncogenesis in pediatric cancers. They can arise from germline predispositions, oncogenic viruses and impaired immune surveillance or developmental mutations.

### 1.1.1. Germline predispositions

Germline predisposition may be the most intuitive mechanism for the oncogenesis of pediatric cancers, as oncogenesis in these cases can often be linked to well-studied oncogenes and tumor-suppressor genes. Early seminal studies have identified hereditary predisposing mutations for pediatric cancers such as Wilm's Tumor (Rahman *et al*, 1996) or retinoblastoma (Cavenee *et al*, 1986; Friend *et al*, 1986). Large-scale sequencing studies of pediatric cancer patients identified such predisposing genetic lesions in 6-8.5% of cases, but the true fraction of germline predisposition pediatric cancers is most likely higher at around 10% (Gröbner *et al*, 2018; Zhang *et al*, 2015; Maris, 2015; Kratz *et al*, 2021). Childhood cancer predisposition is often associated with specific syndromic features which are manifested in several well-known cancer predisposition syndromes, such as Fanconi-Anemia, Noonan Syndrome and other *RAS*-opathies (Rudelius *et al*, 2023). Similarly, bone marrow failure syndromes such as severe congenital neutropenias can be considered as pre-leukemic diseases and substantially increase the risk of myelodysplasias or AML (Skokowa *et al*, 2017; Dong *et al*, 1995; Xia *et al*, 2018). Notably, the proportion of patients with an underlying cancer predisposition strongly varies by tumor type and the driving mutations commonly occur in either genes involved in DNA damage repair, mitotic cell division and developmental signaling with an enrichment for transcriptional regulators (Gröbner *et al*, 2018; Kratz *et al*, 2021; Kentsis, 2020). Pediatric cancers with germline predispositions have a distinct biology from those without predisposition



and this becomes particularly evident when comparing treatment regimens for cancers of the same type in either group. For example, pediatric AML patients with predispositions caused by Down syndrome, *GATA2* deficiency, or DNA repair defects require different treatment approaches than patients *de-novo* AML (Sahoo *et al*, 2020; Hirabayashi *et al*, 2017; Wachter & Pikman, 2024).

### 1.1.2. Oncogenic pathogens and compromised immune surveillance

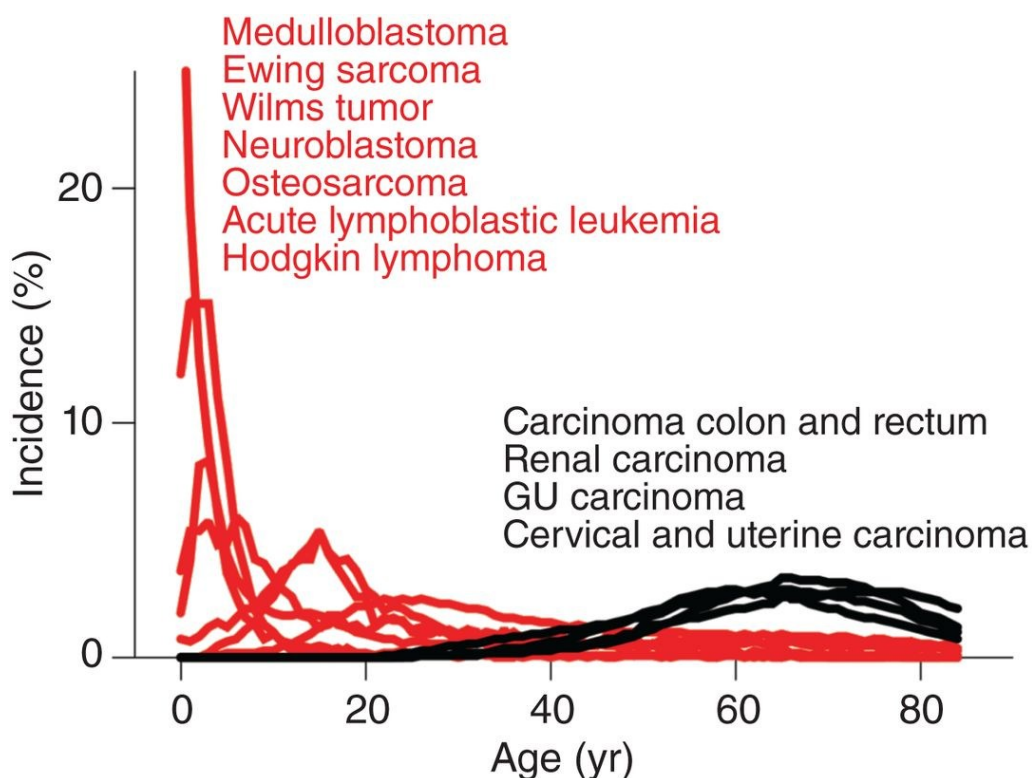
While environmental factors usually play a minor role in the development of pediatric cancers, there are exposures that can induce oncogenesis when combined in specific genetic backgrounds. A particularly intriguing example are oncogenic viruses such as Epstein-Barr virus (EBV), human papilloma virus (HPV), Merkel cell polyomavirus, and human T-cell lymphotropic virus (HTLV). EBV infections have been shown to cause lymphoproliferative neoplasms in immunodeficiency patients (Latour & Winter, 2018), but can also promote lymphoma in otherwise healthy individuals (Küppers, 2003). Additionally, EBV infections have been linked to several solid tumors, such as smooth muscle cell carcinoma, a subset of gastric carcinomas and nasopharyngeal carcinomas (Taylor *et al*, 2015). HPV infections are associated with a substantial fractions of cancers worldwide (de Martel *et al*, 2017). While cervical cancer is the most common cancer that is caused by HPV, it can also lead to oropharyngeal cancers in pediatric patients and has been linked to oral cancers in younger adults (Muzio *et al*, 2021). Merkel cell polyomavirus infection can cause Merkel cell carcinoma in children, where it leads to a more aggressive disease than in adults (Paulson & Nghiem, 2019). Furthermore, HTLV infections at birth have been shown to cause T-cell leukemia or lymphoma in some cases (Pombo-de-Oliveira *et al*, 2002).

The compromised immune system of patients suffering from inborn errors of immunity (IEI) makes them particularly vulnerable to cancer in general and especially to cancers caused by oncogenic viruses. Overall, it is estimated that IEI patients have a substantially higher risk of cancer than the general population due to impaired immune surveillance with an estimated 4-25% of them developing cancer (Jonkman-Berk *et al*, 2015; Shapiro, 2011). Notably, the mechanisms of oncogenesis in IEI patients are diverse and the tumor predisposition in these patients is often derived from the same molecular defect as the immune deficiency (Hauck *et al*, 2018).

### 1.1.3. Developmental tumorigenesis

Most pediatric cancers are thought to arise from developing tissues, leading to the hypothesis that they are caused by distinct mutational mechanisms that are restricted to development and

may be the result of impaired DNA damage repair in a stem or progenitor cell population and/or the introduction of mutations via the activation of endogenous DNA nucleases (Kentsis, 2020). In line with this reasoning, some cancers that occur early in life can be explained by somatic mosaicism, where mutations in cancer susceptibility genes occur *in utero* already and cause oncogenesis of sporadic cancers (Gerstung *et al*, 2020; Pareja *et al*, 2022). An additional intriguing mechanism attributes the oncogenesis of pediatric cancers to the activity of endogenous DNA nucleases during development. These nucleases may act as developmental mutators and introduce cancer-predisposing mutations early in development. Work in B-cell acute lymphoblastic leukemia (B-ALL) supports an oncogenic mechanism via the activation of endogenous DNA nucleases, where aberrant activity of *RAG1/2* and *AID*, together with a subsequent inflammatory stimulus can drive malignant transformation of a pre-leukemic clone that was already present *in utero* (Greaves, 2018). Similar studies have identified developmental mutators in solid tumors. The identification of the transposase *PGBD5* as a developmental mutator that can promote the development of medulloblastoma in mice is just one example (Yamada *et al*, 2024). Collectively, these data and others implicate the non-exclusive activity of somatic mutations in cancer susceptibility genes and developmental mutators as genetic drivers of childhood cancer development (Kentsis, 2024). In this context, one would expect cancers that predominantly occur in childhood to arise from mechanisms that are restricted to developing tissues and this should be reflected in the underlying genetic events and mutational profiles.



Incidence of pediatric cancers (red) and age associated cancers (black) (y-axis) over time (x-axis) based on data of 8,662,369 malignant cases collected in the SEER database. Reprinted with kind permission from cold spring harbor laboratory press. © Cold Spring Harbor Laboratory Press

Indeed, several developing tissues are far more frequently affected by cancer in children than in adults, such as the developing sympathetic nervous system for neuroblastoma, and soft tissue and bone tissue for Ewing sarcoma and osteosarcoma respectively (Fig. 2) (Beird *et al*, 2022; Grünewald *et al*, 2018; Kentsis, 2024; Matthay *et al*, 2016), indicating that these arise from distinct mechanisms that are silenced or inaccessible after some disease specific age and development threshold has passed. Further support for this model comes from several lines of evidence suggesting pre-natal origins for neuroblastoma, transient myeloproliferative disease, myeloid leukemia that progressed from down syndrome, B-ALL and medulloblastoma (Marshall *et al*, 2014).

**Figure 2. Age dependent incidence of early onset and late onset cancers.**

Collectively, these studies on the genetic landscapes and oncogenic mechanisms in pediatric cancers emphasize the dogma of pediatric oncology that *Children are not small adults*. Instead, pediatric cancers commonly arise from distinct genetic events that often target epigenetic or otherwise gene-regulatory processes and only specific developmental stages and tissues seem to be susceptible to oncogenic transformation by the underlying lesions (Filbin & Monje, 2019). Next, we will focus on pedAML as a model disease to discuss its oncogenesis in the context of healthy hematopoiesis, the underlying oncogenic fusion events as drivers of pedAML specifically, and their importance in the context of patient treatment and precision medicine for pedAML.

## 1.2. Pediatric acute myeloid leukemia in the context of healthy hematopoiesis

The hematopoietic system is a constantly developing tissue where the pool of hematopoietic cells in the blood and other tissues is continuously replenished by hematopoietic stem cells (HSCs) that reside in the bone marrow. This property enabled a vast body of research, as the life-long regenerative capacity and the relatively easy access to hematopoietic cells have made it an ideal model system to study tissue development and cellular differentiation. Based on the considerations in the previous section, one may even expect that due to this constant self-

renewal and the maintenance of HSCs throughout life, childhood leukemias should be very similar to their adult counterparts in terms of their genetic landscape.

However, this is not the case. Instead, pediatric leukemias follow a similar pattern as other childhood cancers and present with unique genetic landscapes that are presumably due to distinct oncogenic mechanisms. The mutational burden in pedAML is one of the lowest among childhood cancers and substantially lower than in adult AML. Another differentiating feature is the substantially higher fraction of structural aberrations and a distinct set of recurrently mutated genes (Bolouri *et al*, 2018). Intriguingly, the most common childhood cancers are of hematopoietic origin, and particularly early in life pediatric leukemias are far more prevalent than any other pediatric cancer (Steliarova-Foucher *et al*, 2017).

The life-long regenerative capacity of the hematopoietic system has made it an ideal tissue to study development and differentiation and probably one of the best understood human tissues (Orkin & Zon, 2008; Doulatov *et al*, 2012). Human hematopoietic cells arise from the bone marrow in adults, but the process undergoes multiple waves at different sites during development. The initial wave arises from the yolk sack, then in the aorta-gonad mesonephros region and subsequently in the fetal liver, thymus and spleen until the bone marrow is being colonized as the final site of hematopoiesis (Orkin & Zon, 2008).

Hematopoietic stem cells (HSCs) enable the production of all blood cell types through their almost infinite capacity for self-renewal and maintaining their pluripotent state. The traditional view of the production of all blood cell types from HSCs is as follows: HSCs use asymmetric cell-division to give rise to their more differentiated progenies that become gradually more differentiated. They first differentiate into a multipotent progenitor (MPP), which then gives rise to the common myeloid progenitor (CMP), or the lymphoid primed multipotent progenitor (LMPP). The LMPP gives rise to the common lymphoid progenitor (CLP) from which T- B- and NK-cells arise in further steps, but our focus will be the myeloid path. Here, the CMP can further differentiate into megakaryocyte erythrocyte precursors (MEPs) and granulocyte monocyte precursor cells (GMPs). The former develop into megakaryocytes and erythrocytes, whereas the latter develop into monocytes or granulocytes, such as basophils, eosinophils and neutrophils (Fig. 3).

This model has received several revisions over the past decades - particularly for the very early stages of HSC differentiation (Perié & Duffy, 2016; Velten *et al*, 2017; Orkin & Zon, 2008). However, it is still very useful to understand how different cell types arise from each other and particularly how they were initially identified. Therefore, we will use it as a reference for the first parts of this section. Overall, our aim here is to explore the current understanding of hematopoiesis with a focus on myeloid development and then use this as a context to

discuss the biology of pedAML. First, we will give an overview of the different hematopoietic sub-populations, their identification and their distinguishing features, cell surface markers and the key transcription factors that control the underlying processes. Thus, we will be viewing hematopoiesis first from the cell surface as the outside of the cell and then in terms of transcriptional control from the inside of the cell. After having discussed the gene-regulatory underpinnings of healthy hematopoiesis, we will finally discuss the aberrant behavior of pedAML and how it hijacks hematopoietic development pathways. Based on this, we will later discuss the relationship between leukemia differentiation state, the underlying oncogenic fusion events and patient risk.

### 1.2.1. The hematopoietic hierarchy and cell surface antigens

The differential expression of cluster of differentiation (CD) cell surface markers has enabled researchers to study individual sub-populations in isolation by separating them with fluorescence activated cell sorting (FACS) and thus made the functional interrogation of the developing hematopoietic system accessible. A common strategy of early seminal works (Akashi *et al*, 2000; Kondo *et al*, 1997) was to isolate different hematopoietic subsets via FACS and subsequently use colony formation assays to infer the clonogenic potential of these subsets and the different sub-populations that they can form. Based on these approaches several key features of human hematopoietic subpopulations could be identified based on their antigen expression and functional characterization.

HSCs are most commonly isolated by sorting for CD34<sup>+</sup> cells. This marker is usually expressed by 1-1.5% of bone marrow mononuclear cells and the most prominent surface marker for HSCs as it is used for a variety of clonogenic assays (Anjos-Afonso & Bonnet, 2023). Different studies have tried to further refine this definition of HSCs and the more differentiated MPPs that are not capable of long-term self-renewal. The discovery that CD34<sup>+</sup>CD38<sup>-</sup>CD45RA<sup>-</sup>CD90<sup>+</sup> cells initiate long-term cultures and could engraft in SCID mice whereas CD34<sup>+</sup>CD38<sup>-</sup>CD45RA<sup>-</sup>CD90<sup>-</sup> cells do not give rise to a CD34<sup>+</sup>CD90<sup>+</sup> population placed them at the top of the hematopoietic hierarchy (Majeti *et al*, 2007). However, a later study used an engraftment model to attribute and identified lower efficiency of engraftment of CD90<sup>-</sup> cells rather than a lack of long-term self-renewal and differentiation capabilities and instead proposed CD49f as the differentiating marker for HSCs and MPPs (Notta *et al*, 2011). Still, recent studies use Lin<sup>-</sup>CD34<sup>+</sup>CD38<sup>-</sup>CD90<sup>+</sup>CD10<sup>-</sup> to identify HSCs and Lin<sup>-</sup>CD34<sup>+</sup>CD38<sup>-</sup>CD90<sup>-</sup>CD10<sup>-</sup> to identify MPPs (Corces *et al*, 2016). Further delineating multipotent progenitors, Adolfsson and colleagues identified a Lin<sup>-</sup>Sca-1<sup>+</sup>c-kit<sup>+</sup>Flt3<sup>+</sup> lymphoid primed multipotent progenitor (LMPP) population within the Lin<sup>-</sup>Sca-1<sup>+</sup>c-kit<sup>+</sup> HSC compartment, that gives rise to lymphoid and myeloid cells, but not to megakaryocytes or erythroid cells and attribute lymphoid priming to

this population due to IL7R up-regulation (Adolfsson *et al*, 2005). Notably, some studies did report the existence of a rare CD34<sup>-</sup> HSC population that could populate the bone marrow of mice with severe combined immunodeficiency (SCID) and expresses CD93 (Bhatia *et al*, 1998). Anjos-Afonso and colleagues postulated that this population is on top of the hematopoietic developmental hierarchy (Anjos-Afonso *et al*, 2013). Collectively, these findings indicate that the HSC population is a heterogeneous pool where individual subpopulations may already be biased towards certain lineages (Laurenti & Göttgens, 2018).

CMPs were identified after the identification of common lymphoid progenitor cells (CLPs) as IL7Ra expressing progenitors of all lymphoid cell types (Kondo *et al*, 1997). Akashi and colleagues first identified this subset by investigating the colony forming unit activity of IL7Ra<sup>-</sup> Lin<sup>-</sup>c-Kit<sup>-</sup> murine bone marrow cells (Akashi *et al*, 2000). Nowadays, commitment to the myeloid branch of hematopoietic development is often associated with expression of the marker CD123, which acts as the receptor for the developmental cytokine interleukin 3 and is thus also called IL-3Ra. Work by Manz and colleagues defined these cells as IL-3Ra<sup>lo</sup>CD45RA<sup>-</sup> and demonstrated limited self-renewing capacity for these cells, but a capacity to generate GMPs and MEPs, thus distinguishing them from HSCs and lymphoid committed cells (Manz *et al*, 2002). Current approaches use the marker profile Lin<sup>-</sup>CD34<sup>+</sup>CD38<sup>+</sup>CD123<sup>+</sup>CD45RA<sup>-</sup> to isolate these cells (Corces *et al*, 2016).

GMPs are usually distinguished from the more primitive hematopoietic cell types via expression of CD45RA, which is seen as the defining lineage commitment marker for this subpopulation (Manz *et al*, 2002; Rieger & Schroeder, 2012). Earlier work differentiated GMPs from other myeloid progenitors via the expression of the FC gamma receptor (Akashi *et al*, 2000). The functional diversity of the GMP descendants monocytes, macrophages, basophils, eosinophils and neutrophils makes this subset particularly interesting due to its plasticity. GMPs are a heterogeneous group where more primitive precursors express FLT3 (Böiers *et al*, 2010). Intriguingly, Yanez and colleagues postulate that GMPs and monocyte dendritic cell precursors (MDPs) are on the same level in the hematopoietic hierarchy, rather than MDPs being derived from GMPs (Yáñez *et al*, 2017).

MEPs have been identified as a CD34<sup>+</sup>CD38<sup>mid</sup> population among hematopoietic progenitors and give rise to committed precursors of megakaryocytes and erythrocytes in a *MYB* mediated fashion (Sanada *et al*, 2016). Notably, there were some doubts on whether this marker profile is indicative of the true bipotent MEP population due to the massive imbalance between megakaryocyte progenitors and erythroid progenitors that can be derived from it. Additionally, cells that are restricted to either the erythroid lineage or the megakaryocytic lineage have been observed outside of the proposed MEP CD34<sup>+</sup>CD38<sup>mid</sup> population (Xavier-Ferruccio & Krause, 2018).

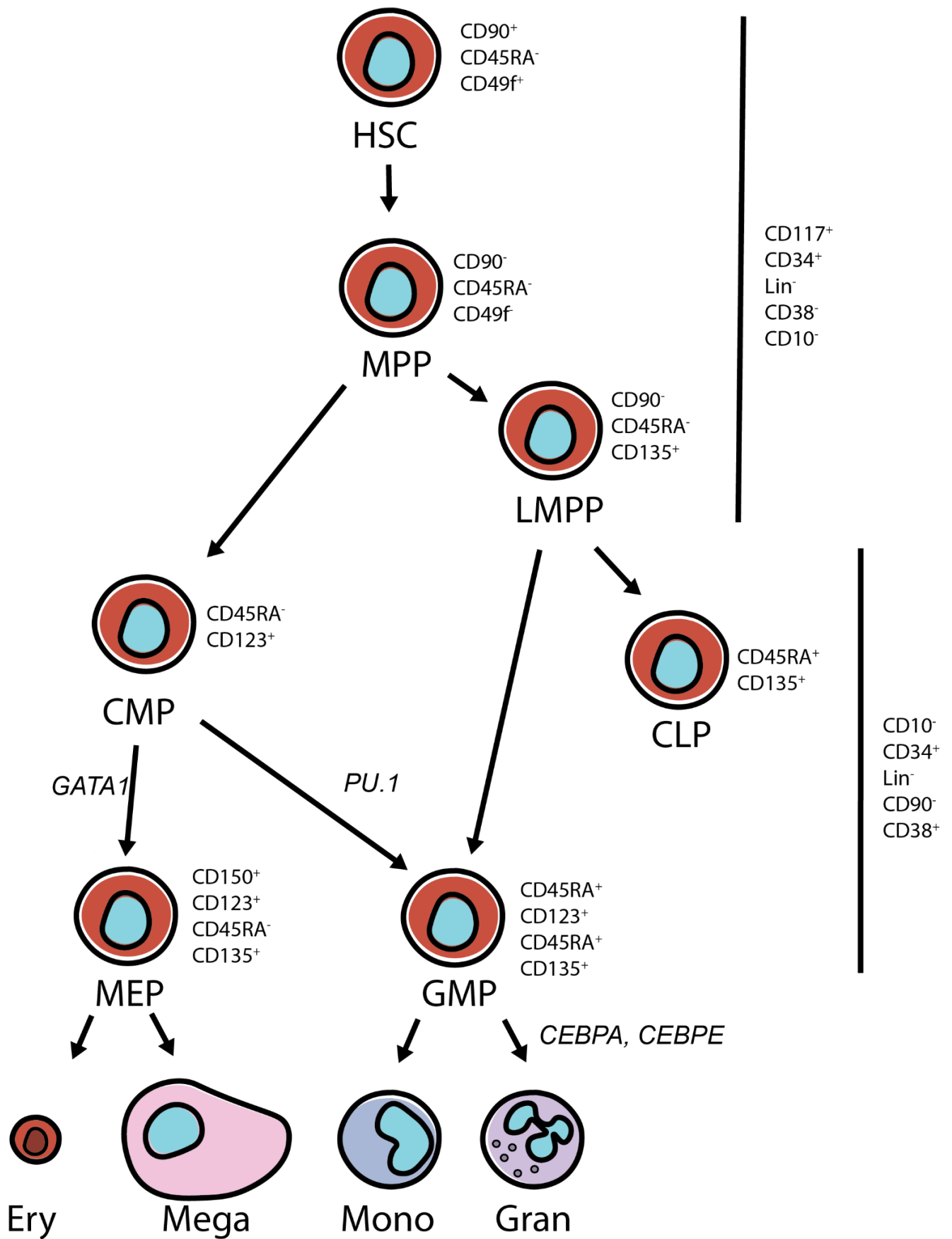


**Figure 3. Simplified overview of hematopoiesis and marker expression profiles with focus on myeloid development**

Individual cells indicate hematopoietic cell types. Arrows indicate the direction of development. Abbreviations are

as in main text. Smaller text on the right of individual cell types and next to straight lines indicates cell type specific surface antigen expression as described in (Corces *et al*, 2016) and (Rieger & Schroeder, 2012). Text next to arrows indicates key transcription factors.

Overall, advances in the characterization of surface marker expression and transcriptional profiling over the past three decades have enabled a detailed understanding of the hematopoietic system and shaped the current understanding of hematopoietic fate decision as a tightly regulated process that requires precise control of transcription and chromatin accessibility (Shivdasani & Orkin, 1996; Orkin & Zon, 2008). Recent single-cell studies have further advanced our understanding of the hematopoietic system and increased appreciation for the heterogeneity and functional diversity of hematopoietic precursor populations (Notta *et al*, 2016; Velten *et al*, 2017). Thus, the understanding of this cellular hierarchy has progressed from a view of discrete states to one as a more continuous process (Zhang *et al*, 2018). In the following section, we will discuss how transcriptional control shapes hematopoietic identity and provide an overview of the key findings in the field.

### 1.2.2. The hematopoietic hierarchy and transcription factors

While cell surface markers are commonly used to distinguish the different hematopoietic subsets, the maintenance and development of these identities is governed by a tightly coordinated network of transcription factors – many of which have also been implicated in the oncogenesis of pedAML and pediatric ALL (pedALL).

Seminal studies in murine models, together with investigations of cis-regulatory elements and genes that are altered in human leukemias have shaped our initial understanding of transcription factors as key drivers of cellular identity and lineage commitment (Orkin & Zon, 2008; Orkin, 1995). Broadly speaking, these studies investigated how knockout of individual TFs affects primitive hematopoiesis and definitive hematopoiesis. These processes are largely conserved across vertebrates and mammals specifically. Primitive hematopoiesis denotes the first wave of hematopoietic cell generation in the yolk sac that produces macrophages and erythrocytes – mainly to facilitate oxygen transport by erythrocytes. After an intermediate wave of transient definitive hematopoiesis in the blood islands, definitive hematopoiesis generates HSCs first in the fetal liver and subsequently in the bone marrow (Jagannathan-Bogdan & Zon, 2013). Here, we will initially focus on a core transcriptional network of HSCs – often termed the HSC heptad TFs – consisting of TAL1, LYL1, LMO2, GATA2, RUNX1, ERG and FLI1 (Diffner *et al*, 2013).

Differential chromatin accessibility at key regulatory elements of these TFs has been shown to be predictive of cellular identity (Thoms *et al*, 2021) and knockout of the majority of them is



embryonically lethal due to a lack of blood formation at different stages as shown by seminal studies in murine models. Loss of *TAL1*, *LMO2* and *GATA2* leads to a lack of hematopoiesis in the yolk sack and defects in later stages of hematopoiesis have also been demonstrated for these TFs (Robb *et al*, 1995, 1996; Tsai *et al*, 1994; Porcher *et al*, 1996; Yamada *et al*, 1998; Warren *et al*, 1994). Loss of *RUNX1* and *ERG* leads to a failure of definitive hematopoiesis in the fetal liver (Okuda *et al*, 1996; Loughran *et al*, 2008). Later studies demonstrated that this was due to *RUNX1* being required for the generation of HSCs from endothelial cells (Chen *et al*, 2009). Knockout of *FLI1* in mice has been shown to impair vascular development and megakaryopoiesis (Hart *et al*, 2000). Data in *Xenopus* and zebrafish indicate that *FLI1* activity is required for the development of hemangioblasts – the common precursors of blood and endothelial cells – and thus suggests that *FLI1* acts at the very beginning of hematopoietic development (Liu *et al*, 2008). Deletion of *LYL1* is not embryonically lethal, but leads to severe functional and proliferative impairment in murine HSCs (Capron *et al*, 2006). Collectively, these observations contributed to their designation as master regulators of hematopoiesis. Further work in murine HSCs identified closely coordinated binding on DNA of these TFs and suggested that they act in a combinatorial fashion (Wilson *et al*, 2010). This work and later work in human HSCs (Beck *et al*, 2013) solidified our current understanding that combinatorial activity of these TFs governs HSC maintenance. More recent work by Subramanian and colleagues indicates that the combinatorial binding of these TFs changes over the differentiation trajectory and may thus prime genes that are required for cell type transition for expression. For example, the authors describe increased binding of *GATA2*, *TAL1*, *LYL1* and *LMO2* to the *GATA1* locus in MEPs when compared to GMPs, CMPs and HSCs (Subramanian *et al*, 2023). Several other key TFs for early hematopoietic development have been identified in similar experimental setups. *MEIS1* for example is also required for definitive hematopoiesis and may drive expression of *RUNX1* in murine HSCs (Azcoitia *et al*, 2005). Later work has identified critical roles for *MEIS1* in controlling the metabolic phenotype of HSCs (Kocabas *et al*, 2012) and in the generation of *RUNX1* expressing cells in the epithelial to hematopoietic transition that precedes hematopoiesis (Coulombe *et al*, 2023).

More broadly, these studies suggest that this core set of HSC TFs primes the genome for differentiation by making regions accessible to subsequently acting lineage-defining transcription factors. Further downstream the hematopoietic differentiation landscape, several lineage-defining TFs and underlying processes have been identified. The most prominent among them for myeloid differentiation are *PU.1* for early myeloid commitment, *GATA1* together with the *GATA*-family TFs for commitment towards the MEP-lineage and HSC maintenance, and *CEBPA* and the *CEBP*-family TFs with a multifaceted role in the commitment to granulocytes and HSC homeostasis.

*PU.1* is a member of the ETS family transcription factor family and the key TF for myeloid development. It was long thought that the balance of *GATA1* and *PU.1* decides commitment to either MEPs or GMPs. However, more recent data used a murine reporter system for both *PU.1* and *GATA1* and did not identify a myeloid population that expresses both *PU.1* and *GATA1*, but instead found commitment to either lineage to be preceding the expression of either TF (Hoppe *et al*, 2016).

Erythroid development has been shown to be dependent on *GATA1*. Early work in mice has shown that *GATA1* deficient mice are incapable of erythropoiesis (Shivdasani & Orkin, 1996). More recently *GATA2*, *TAL1* and *ERG* were also shown to be involved in differentiation of HSCs towards MEPs (Thoms *et al*, 2021).

Monocytes and Granulocytes are the most differentiated cells in the myeloid branch of hematopoietic differentiation. Monocytes are derived either from GMPs or MDPs, that may develop from GMPs (Guilliams *et al*, 2018) or be generated independently (Yáñez *et al*, 2017). In addition to the key TFs for hematopoiesis discussed above, *PU.1*, *IRF8*, and *KLF4* are known to be required for monocytic development, since perturbation of each of these factors has been shown to reduce peripheral blood monocytes (Alder *et al*, 2008; Hambleton *et al*, 2011; McKercher *et al*, 1996). At the final steps of monocyte generation, proliferative CXCR4<sup>+</sup> pre-monocytes differentiate into functionally Ly6C<sup>hi</sup>CXCR4<sup>-</sup> mature monocytes (Chong *et al*, 2016).

The *CEBP* transcription factors have been identified as key TFs for myelopoiesis (Yamanaka *et al*, 1998). CEBPA and CEBPE are particularly prominent, due to their role in the generation of neutrophils and other granulocytes – particularly CEBPA and CEBPE. *CEBPE* has been shown to be required for the terminal differentiation of granulocyte precursor cells, as mice with *CEBPE* null mutations lack functional neutrophils and eosinophils and die prematurely due to opportunistic infections (Yamanaka *et al*, 1997). Similarly, *CEBPA* has been identified as a key TF that is required for neutrophil generation (Zhang *et al*, 1997). The authors also identified an overabundance of myeloid blasts in *CEBPA* KO mice, indicating that this TF may also be involved in other aspects of hematopoietic differentiation and HSC homeostasis. Indeed, a later study identified CEBPA as a key TF for the switch from fetal HSCs to adult HSCs (Ye *et al*, 2013).

Given this understanding of the transcriptional and epigenetic requirements for HSC generation, maintenance, and differentiation from multipotent progenitors towards fully differentiated cell types, a large body of research aimed at further dissecting the transcriptional control along the hematopoietic differentiation trajectory to gain a more precise understanding of the dynamics and interactions for the different key TFs in hematopoiesis. Particularly single-cell technologies enabled a more detailed understanding of the dynamics of different precursor

populations and challenged two key concepts in hematopoiesis: the understanding of hematopoiesis as a discrete stepwise process that was informed by transplantation studies and clonogenic assays, and the classical fully hierarchical model of the hematopoietic tree (Fig. 4A) (Perié & Duffy, 2016; Laurenti & Göttgens, 2018).

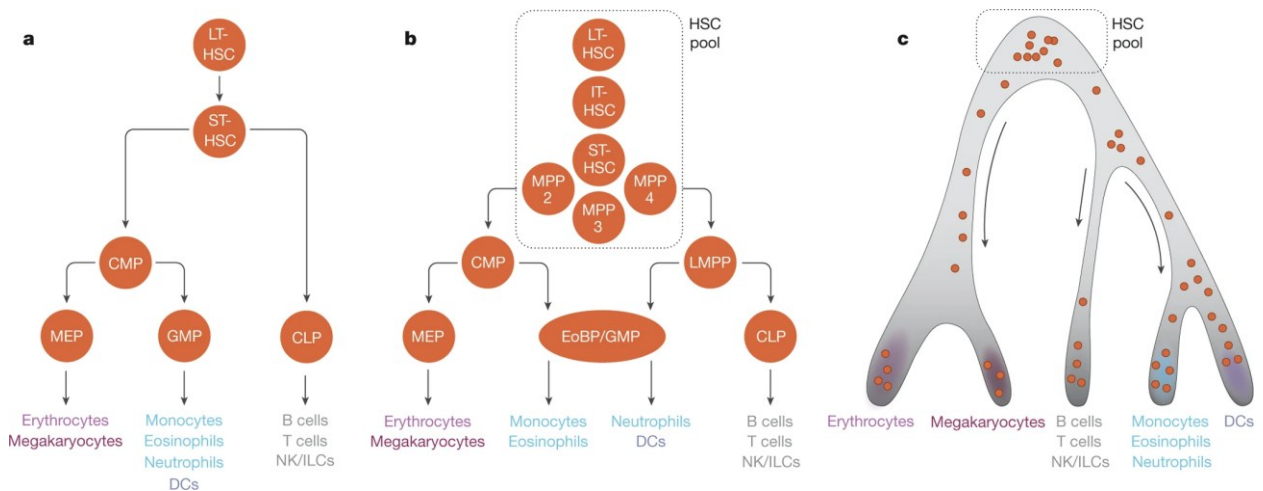


**Figure 4. Development of hierarchical models of hematopoiesis over time.**

**A** Hierarchical model representing the understanding around the year 2000. LT-HSC: Long-term HSC, ST-HSC: Short-term HSC. **B** Prevailing model of hematopoiesis from the 2000s to the early 2010s, including heterogeneity in the HSC-pool, the LMPP and heterogeneity in the GMP compartment with an eosinophil basophil progenitor (EoBP). **C** Model of hematopoiesis from 2016 onwards, understanding hematopoiesis as a continuous process where each dot indicates an individual cell. Reprinted from (Laurenti & Göttgens, 2018) with kind permission from Springer Nature.

In particular, these studies provided evidence for lineage bias of early precursors and therefore suggested that lineage commitment may occur even before the characteristic markers for a specific sub-population are expressed. In the context of LMPPs, a cellular barcoding study by Naik and colleagues found that they can give rise to myeloid, lymphoid and dendritic cells. By investigating the clonal output of single LMPPs they found that daughter cells often give rise to very similar cell types, suggesting that LMPPs are already primed to produce specific cell types in their presumably primitive state (Naik *et al*, 2013). Similar work in myeloid progenitors also identified lineage priming effects with single cell RNA-sequencing (Paul *et al*, 2015). This work challenged established marker panels for the identification of myeloid sub populations by demonstrating transcriptional profiles of progenitors of megakaryocytes, erythrocytes, dendritic cells and basophils within the  $CD34^{+}FcGr^{mid}$  population that would usually be defined as a CMP population. Additionally, the authors identified several small subpopulations that expressed key lineage defining genes TFs together with HSC-associated TFs such as *Meis1*

and *ApoE*, providing further evidence for lineage biased precursors that are not clearly identifiable via FACS. Further work deepened our understanding of biased precursor populations and proposed so-called metastable transcriptional states that precede binary cell fate choices, in particular by identifying counteracting gene-regulatory networks driven by *Irf8* and *Gfi1* that determine differentiation towards macrophages or neutrophils respectively (Olsson *et al*, 2016). Similarly, work by numerous groups identified striking similarities between HSCs and megakaryocytes and proposed HSC populations that were biased towards megakaryocytic differentiation (Woolthuis & Park, 2016). An even more comprehensive study aimed at reconstructing the hematopoietic tree using comprehensive FACS, single cell RNA sequencing and cultures derived from single cells (Velten *et al*, 2017). This study went even one step further and proposed that early hematopoiesis is a fully continuous process where lineage restriction only starts with the upregulation of CD38.

In addition to these findings, the role of gene-regulatory proteins beyond TFs, such as chromatin factors and epigenetic modifiers has also been increasingly appreciated in recent years. For example, chromatin factors and epigenetic modifiers have been identified as central determinants of hematopoiesis in mice. Lara-Astasio and colleagues screened 142 different chromatin factors *in-vivo* (Lara-Astasio *et al*, 2023). Notably they identify a substantial amount of mouse orthologs to human genes with known roles in AML that affect hematopoietic differentiation such as *Kmt2a*, *Dot1l*, *Men1*, and *Cebp* and also demonstrate that knockout of *Kmt2a* and *Men1* can increase cellular differentiation and reduce leukemic cell fitness in a *Flt3* and *Npm1c* driven model. Metabolic priming has also been identified as an important factor for lineage commitment in early progenitor populations. For example, work by Nakamura-Ishizu and colleagues demonstrated that HSCs can be metabolically primed towards the megakaryocytic lineage by thrombopoietin (Nakamura-Ishizu *et al*, 2018).

Collectively, these studies indicate that HSCs are a heterogeneous pool, where maintenance of the truly long-term HSCs is governed by a key set of TFs that act in a combinatorial fashion with each other and with lineage defining TFs to prime HSCs towards their cell fate (Fig. 4B,C). This priming may still be of stochastic nature until a certain threshold of decreasing multilineage potential is crossed and an individual cell is fully determined to its fate. Our understanding of the causal effects of these TFs is still limited due to technical limitations in non-invasively identifying HSC subpopulations due to small population sizes and ambiguity in marker expression. Most of the studies mentioned above still rely on FACS-based cell isolation and subsequent expansion with subsequent characterization. However, we still lack data that clarifies the developmental dynamics of TF requirements – ie which TFs are required during which precise stages of hematopoietic development. Yet, these data provide an essential

foundation to understand the disease-causing mechanisms of pedAML as most driving lesions in this disease affect epigenetic or transcriptional regulators.

### 1.2.3. Pediatric AML as a disease of aberrant transcription

Pediatric AML is thought to arise from mutations that occur during hematopoietic development and particularly infant AML is known to have a pre-natal origin (Camiolo *et al*, 2024). Early studies have provided evidence for malignant transformations *in utero* by demonstrating the presence of leukemic cells at birth (Ford *et al*, 1993; Gale *et al*, 1997; Maia *et al*, 2004) and infant AML is increasingly recognized as a biologically distinct subgroup with an enrichment for high-risk alterations such as *KMT2A*-rearrangements, *CBFA2T3::GLIS2* or *MNX1::ETV6* fusions (Masetti *et al*, 2015; Creutzig *et al*, 2012). These observations indicate that fetal hematopoiesis may be particularly vulnerable to a subset of driving AML fusions and thus demonstrate a need to understand how oncogenic fusions and structural aberrations affect early hematopoietic development and lead to leukemic transformation.

Pediatric acute leukemias are commonly caused by oncogenic fusion genes that occur in the developing hematopoietic system and pedAML is a prototypic example for this concept. The disease is already on the lower end of the spectrum of mutational burden when compared to all cancers (Kandoth *et al*, 2013), but also when compared to all pediatric cancers (Gröbner *et al*, 2018; Ma *et al*, 2018). As observed in other pediatric malignancies, the mutational landscape of pedAML is driven by structural variants which are largely distinct from its adult counterpart (Bolouri *et al*, 2018). Not only are structural lesions 2-3 times more likely in you patients with AML than in adult and elderly patients, but there are also marked differences in the affected genes. *DNMT3A* and *TP53* mutations for example are almost absent in pediatric AML patients but affect roughly a third of adult patients. Conversely mutations in *NRAS* affect approximately a third of pediatric patients, but less than 10% of adult patients.

In line with the hypothesis, that different lineage priming states are susceptible to leukemic transformation by distinct oncogenic fusions, these structural mutations are at least partially associated with specific differentiation phenotypes reflecting their most similar healthy phenotype, as outlined in the French American British (FAB) classification. This classification was used for staging of AML in the past and classifies AML cells into 8 classes M0-M7 based on the phenotypic similarity to healthy cells where for example M0 describes undifferentiated AML, M1 and M2 describe AML with minimal maturation and with maturation respectively, M3 describes acute promyelocytic leukemia (APL), M4 describes acute myelomonocytic leukemia, M5 describes monocytic AML, M6 describes erythroblastic AML, and M7 describes megakaryoblastic AML (Vardiman *et al*, 2002). While more recent schemes focus more on

defining genomic lesions to classify and stage pedAML (Loghavi *et al*, 2024; Umeda *et al*, 2024), associations between FAB type and oncogenic fusions may still be informative of the underlying disease biology and the developmental stage at which the oncogenic fusion occurred. *CBFB::MYH11* fusions are most commonly associated with the M4 phenotype (acute myelomonocytic AML), *RUNX1::RUNX1T1* with M2 (AML with maturation), *KMT2A*-rearrangements with M4 or M5 (acute monocytic leukemia), *DEK::NUP214* with M4 or M2 and *PML::RARA* exclusively with M3 (acute promyelocytic leukemia) (Martens & Stunnenberg, 2010). These associations of cellular differentiation states and oncogenic fusions also reflect commonalities between earlier risk stratification schemes based on FAB classes and more modern genetics based risk stratification as outlined in the most recent WHO guidelines (Khoury *et al*, 2022) and the current ELN classification for AML (Döhner *et al*, 2022). A more recently proposed stratification scheme further refines this approach and proposes mutually exclusive genomic categories that are notably almost exclusively structural (Umeda *et al*, 2024) (Fig. 5).

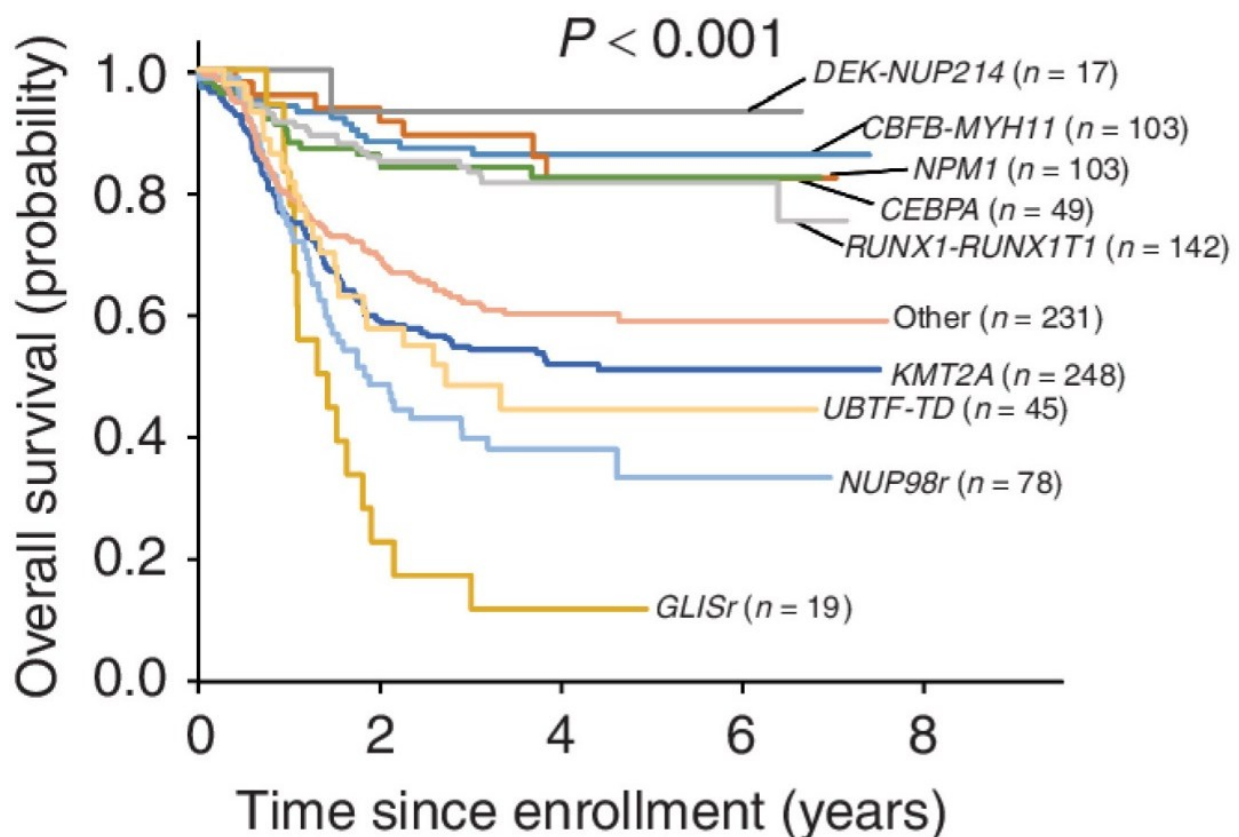


**Figure 5. Survival of pediatric AML patients with different oncogenic fusions**

Kaplan Meier curves of different genetic subgroups in the AAML1031 cohort as depicted in (Umeda *et al*, 2022). Reprinted with kind permission from the American Association for Cancer Research.

Due to their central role in both mechanistic disease understanding and risk stratification in pedAML, we will review the most common genomic lesions in pediatric AML in terms of risk associations, the physiological role of the wild type proteins and the current understanding of the mechanistic basis of their contribution to disease.

Leukemias with *PML::RARA* fusions are part of one of the success stories of modern medicine. These fusions result in acute promyelocytic leukemia (APL) of the FAB M3 class. The fusion protein is the product of a balanced translocation that fuses the *promyelocytic leukemia (PML)* gene to the *retinoic acid receptor alpha (RARA)*. If detected early enough, patients receive differentiating chemotherapy with arsenic trioxide and tretinoin which leads to rapid differentiation of the malignant blasts and – in most cases – an effective cure of the patient (Yilmaz *et al*, 2021).

*CBFB::MYH11* fusions and *RUNX1::RUNX1T1* fusions are considered as low risk by several study groups (de Rooij *et al*, 2015). Leukemias with these underlying lesions are commonly called core binding factor (CBF) leukemias as both *RUNX1* and *CBFB* are part of one of the core binding factor complexes (Speck & Gilliland, 2002). The chromosomal events leading to both fusions were among the earliest identified recurrent genomic lesions in AML. The corresponding genes were identified in the early 1990s (Miyoshi *et al*, 1991; Liu *et al*, 1993) and thus subject of a substantial amount of research since their initial discovery. Despite their commonalities in both complex membership and patient risk, the fusions lead to distinct phenotypes where *RUNX1::RUNX1T1* most commonly presents as M2 leukemia and *CBFB::MYH11* often presents as M4Eo leukemia, but may also present with an M2 or M5 phenotype (Sangle & Perkins, 2011). Notably, neither fusion is sufficient to induce leukemia in murine models, but instead requires additional mutations for malignant transformation (Castilla *et al*, 1999; Higuchi *et al*, 2002). Such cooperating mutations usually occur in the *RAS* pathway or upstream and the most common events occur in *NRAS*, *KIT*, *FLT3* and *KRAS*. Other common cooperating mutations that occur in genes such as *NF1* or *WT1* (Faber *et al*, 2016). Together with other CBF fusions, *RUNX1::RUNX1T1* and *CBFB::MYH11* dominantly inhibit CBF-mediated transcription, and it has been hypothesized that this inhibition hinders differentiation of hematopoietic progenitors and makes them susceptible to malignant transformation (Sangle & Perkins, 2011). Notably, both genes are required at the early steps of hematopoiesis. *RUNX1* is required for the generation of the earliest hematopoietic precursors from vascular endothelial cells as shown by experiments in the mouse (Chen *et al*, 2009). Similarly, *CBFB* is required at the same developmental stage and knockout of *CBFB* leads to a similar embryonically lethal phenotype, as *CBFB* knockout also abrogates *RUNX1* activity (Wang *et al*, 1996). While *RUNX1* seems to not be required after the developmental

stage (Chen *et al*, 2009), murine conditional knockout models showed a marked pancytopenia due to differentiation blocks and an expansion of HSCs (Wang *et al*, 2015). While these fusions are commonly grouped together due to their similar risk profile and common mechanisms, it has to be noted that the gene expression patterns of *RUNX1::RUNX1T1* and *CBFB::MYH11* are different (Fig. 6).

*KMT2A*-rearrangements can be found in ALL, AML and biphenotypic leukemias (Krivtsov & Armstrong, 2007). They were also among the earliest identified oncogenic fusion events which lead to the initial designation of the *KMT2A* gene as Mixed Lineage Leukemia (MLL) (Ziemin-van der Poel *et al*, 1991). Patients with *KMT2A*-rearrangements are mostly classified as high risk, but the precise risk stratification depends on the individual fusion partner gene (von Neuhoff *et al*, 2010). More than 80 fusion partners for *KMT2A* have been described (Meyer *et al*, 2009) and the three most common in pedAML are *MLLT3* – a member of the super elongation complex, *MLLT10* – a cofactor of *DOT1L*, and *AFDN* (*MLLT4*, *AF6*) – which is essential for the binding of adherence junctions (Krivtsov & Armstrong, 2007). Some *KMT2A*-rearrangements are sufficient to induce leukemia in mice, such as *KMT2A::MLLT3* (*KMT2A::AF9*) (Corral *et al*, 1996) and *KMT2A::MLLT1* (Lavau *et al*, 1997), further indicating the strong oncogenic potential of these fusions and implicating dysregulated activity of *KMT2A* as the driving force of the malignant transformation in this disease subgroup. Indeed, *KMT2A* fusions largely derive their oncogenic activity from a gain-of-function in *KMT2A* (Ayton & Cleary, 2001). The gene belongs to a family of methyltransferases that are implicated in a variety of cancers. Physiologically, it poises genomic sites for transcription via H3K4 methylation in a complex with several other proteins – most notably Menin. Within this complex, it activates a specific set of target genes of which particularly *HOXA* genes, *MEIS1* and *MYC* have well known roles in cancer and stem-cell maintenance (Rao & Dou, 2015). Early work in murine models indicated that *KMT2A* positively regulates *HOX* expression (Yu *et al*, 1995) and later work clarified that this positive regulation required additional binding partners such as Menin and is necessary for leukemogenesis of oncogenic *KMT2A* fusions (Yokoyama *et al*, 2005). The most common co-occurring mutations for *KMT2A*-rearrangements are in *NRAS* or *KRAS* (de Rooij *et al*, 2015), although they are usually thought of as secondary events.

*NUP98*-rearrangements lead to a particularly aggressive disease and mostly affect less differentiated cell types, leading to substantially lower overall survival than for most other oncogenic fusions (Fig. 5). Over 30 fusion partners have been identified and while *NUP98*-rearrangements have been identified in MDS, CML and T-ALL, they are most commonly found in pedAML where they occur in approximately 5% of patients (Michmerhuizen *et al*, 2020). Recent data indicate that the most common fusion partner for *NUP98* is *NSD1* (Struski *et al*, 2017). Overall, *NUP98*-rearrangements can be divided into two groups where the first is the



one with homeodomain moieties and is mostly comprised of *HOX* genes and the second is lacking homeodomain moieties and consists of diverse partners such as *NSD1*, *KDM5A*, *MLLT10* and others (Gough *et al*, 2011). Physiologically, *NUP98* is a member of the nuclear pore complex where it mediates selective transport in of RNA, It has also been demonstrated to mediate gene expression (Kalverda *et al*, 2010) and its phosphorylation has been shown to be a rate limiting step in mitotic nuclear pore complex disassembly (Laurell *et al*, 2011). *NUP98*-rearrangements lead to the upregulation of several genes with well-known roles in development in general and pedAML specifically such as *HOXA* genes and *MEIS1* (Gough *et al*, 2011): This led to initial hypotheses that *NUP98*-rearrangements may behave similarly as *KMT2A*-rearrangements, which is further supported by in-vivo experiments that showed that *KMT2A* knockout delays leukemogenesis in a *NUP98::HOXA9*-driven mouse model (Xu *et al*, 2016). However, some *NUP98* fusions also upregulate *HOXB* genes, leading to a gene expression signature that is distinct from *KMT2A*-rearrangements (Michmerhuizen *et al*, 2020) (Fig. 6).

*CBFA2T3::GLIS2* fusions are a peculiar subgroup with dismal prognosis that most often occurs in infants and are absent in adults. Notably, this fusion is also the most common oncogenic fusion in non-Down Syndrome AMKL and is absent from Down Syndrome AMKL, indicating more restricted requirements for oncogenic transformations when compared to other oncogenic fusions (Masetti *et al*, 2019). *CBFA2T3::GLIS2* fusions have been hard to detect due to the underlying cryptic inversion of chromosome 16 and thus have only been characterized more recently with the advent of NGS technologies (Gruber *et al*, 2012). Mechanistic work on this fusion revealed that the fusion protein leads to differentiation towards the megakaryocytic lineage and promotes self-renewal in a presumably *ERG*-dependent manner (Thirant *et al*, 2017). Further modeling of the disease in human inducible pluripotent stem cells indicate that oncogenesis requires the homeobox factor *DLX3* and that the fusion induces increased accessibility of *RUNX1* and *RUNX2* motifs and ETS motifs such as those for *FLI1* and *ERG* (Boudia *et al*, 2025).

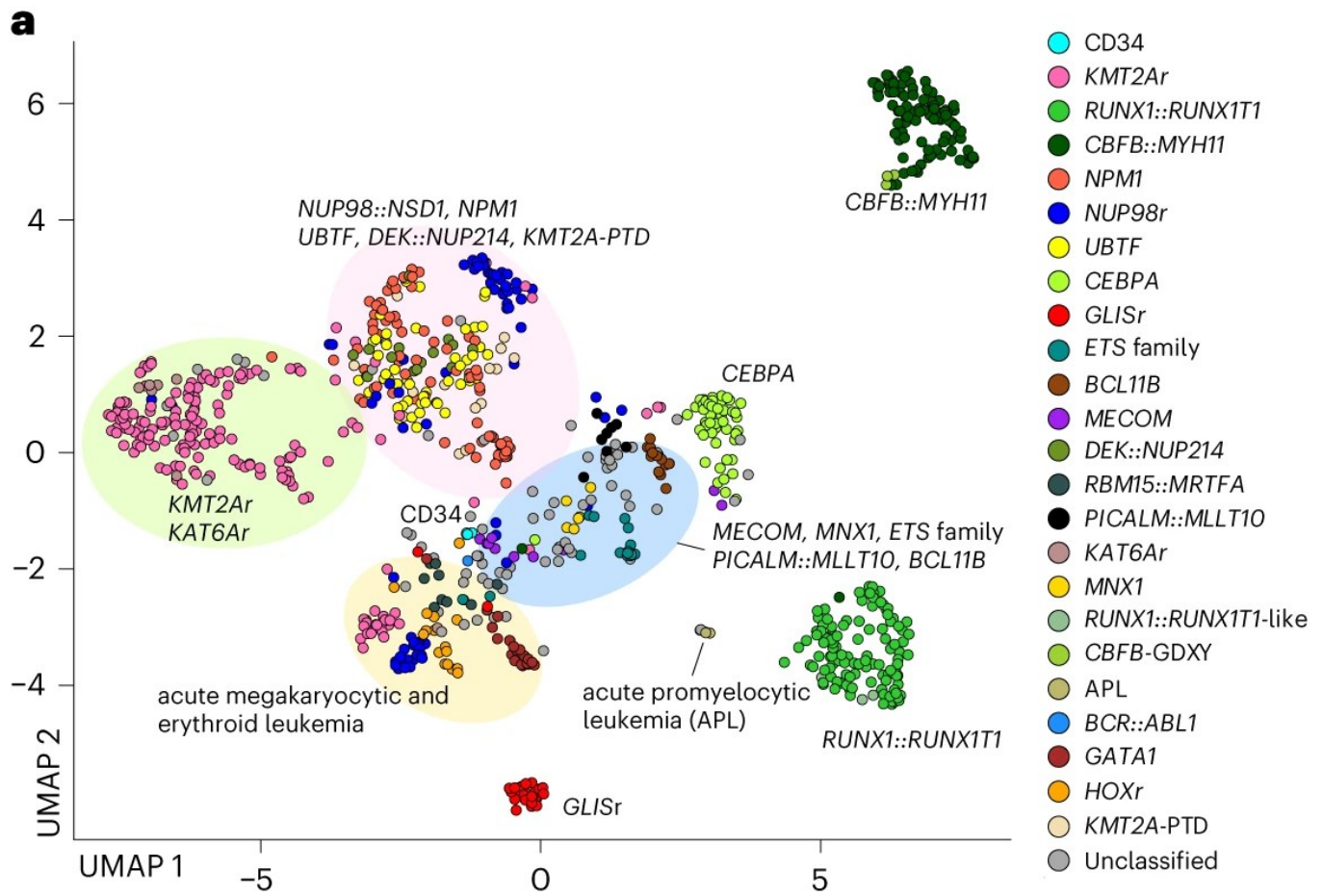


**Figure 6. UMAP of pedAML transcriptomes.**

UMAP representation of the transcriptomes of different pedAML genomic subsets (n=887) and CD34+ healthy controls based on the 315 most variable genes. Dots indicate individual samples and are colored according to the legend on the right. Semi-transparent ellipses indicate annotated transcriptional clusters. Reprinted from (Umeda *et al*, 2024) under the creative commons license.

In addition to the groups that are defined by oncogenic fusion proteins described above, *NPM1* and *CEBPA* mutations are also risk-defining lesions in several protocols, where *NPM1*-mutated AML and *CEBPA* double mutated AML are both defined as lower risk (Cooper *et al*, 2023). Additionally, the more recently recognized group of pedAML with *UBTF* tandem duplications (*UBTF*-TD) is emerging as a novel high risk entity (Umeda *et al*, 2022).

*NPM1* mutations in AML are usually associated with low risk. The most common mutation is usually denoted as *NPM1c* and causes a frameshift that leads to a truncation of the protein and a new nuclear export signal. This causes mis localization of *NPM1c* to the cytoplasm and activation of *HOX* genes (Falini *et al*, 2020). More recently, it was shown that *NPM1c* binds to chromatin targets and interacts with the *KMT2A* complex to regulate oncogenic gene expression (Uckelmann *et al*, 2023).

*CEBPA* has a well known role in granulopoiesis and *CEBPA* mutated AML cells have a committed myeloid progenitor phenotype (Pulikkan *et al*, 2017). Loss of function mutations in *CEBPA* have been demonstrated as causative for familial AML, which is due to a tumor suppressor function in hematopoietic cells (Smith *et al*, 2004). However, the causative effects of *CEBPA* mutations on transcriptional control in AML are not fully elucidated yet (Pulikkan *et al*, 2017).

*UBTF*-TD is a novel entity in pedAML that has only been identified in a recent study. Here, Umeda and colleagues identified tandem duplications in exon 13 of *UBTF* in 9% of 136 relapsed pedAML cases and further demonstrated increased proliferation and clonogenic activity of CD34<sup>+</sup> cells transduced with *UBTF*-TD when compared to transduction with *UBTF*-WT (Umeda *et al*, 2022). A subsequent large-scale genomic study confirmed that these events are mutually exclusive with other known driving lesions in pedAML and thus proposed *UBTF*-TD as an entity defining alteration in pedAML (Umeda *et al*, 2024). Similar work also proposed *UBTF*-TD AML as a distinct entity in adult AML (Duployez *et al*, 2023). *UBTF*-TD AMLs have a similar transcriptional profile to *NUP98*-rearranged and *NPM1c* AMLs (Fig. 6) and recent work has demonstrated co-occupation of DNA of *UBTF*-TD with *KMT2A* and Menin, suggesting a similar leukemogenic mechanism as in *NPM1c*, *NUP98*-, and *KMT2A*-rearranged leukemias (Barajas *et al*, 2024).

These different characteristics underline that a detailed understanding of the transcriptional outcomes of these different oncogenic fusions and other risk-conferring mutations is crucial to determine the molecular basis of treatment response and disease progression in pedAML. Accordingly, RNA sequencing has increased in relevance for pedAML and recent works have identified clear relationships between oncogenic fusions and transcriptional signatures (Fig. 6) (Umeda *et al*, 2024). As already alluded to above, we also observe interactions between several of these oncogenic fusions and the key TFs of early hematopoietic development and hematopoiesis, such as the increased accessibility of motifs for *RUNX1*, *RUNX2*, *FLI1* and *ERG* in *CBFA2T3::GLIS2* pedAML (Boudia *et al*, 2025), or the activation of *MEIS1* in *NUP98*- and *KMT2A*-rearranged pedAML (Michmerhuizen *et al*, 2020; Rao & Dou, 2015), implicating these subtype defining oncogenic lesions as drivers of HSC-like expression patterns in pedAML. In line with this reasoning, a study that used a comprehensive set of epigenetic approaches including analysis of cis-regulatory elements and transcription factor occupancy identified an AP-1 driven signature as common to the studied AML subtypes *CEBPAdm*, *RUNX1::RUNX1T1*, *NPM1c* and others whereas increased activity of *MEIS1* was exclusive to samples with *NPM1c*, further indicating that the activity of HSC-associated TFs is dependent on the underlying genomic lesion (Assi *et al*, 2019).

In line with these observations on the association between high-risk genomic lesions and expression of HSC-associated genes, work in adult AML has identified a leukemic stem cell signature consisting of 17 genes that is indicative of patient risk (Ng *et al*, 2016). Subsequent work has shown that this signature is also risk-predictive in pediatric populations (Duployez *et al*, 2019), indicating that stemness is a common risk factor in AML that is common to different underlying genomic alterations. However, further work in pediatric AML identified that the LSC17 score loses its predictiveness when applied within risk groups, indicating that the underlying genetic events affect expression of LSC17 genes and that LSC expression signatures may depend on the underlying genetic lesions (Huang *et al*, 2022). The authors of this study then established a new signature consisting of 47 genes that was risk predictive within their defined genetic subgroups. Further work from the laboratory of John E. Pimanda has identified a signature based on *ERG* and the previously described heptad of key HSC TFs that is indicative of patient risk and described the regulation of the *ERG* enhancer by these heptad TFs (Diffner *et al*, 2013). Collectively, these results indicate that gene expression signatures that are indicative of stemness may not only be predictive of patient risk, but also drive disease progression and relapse.

Notably, these associations may at least partially be mediated by the underlying genetic events. One hint towards this are the associations between FAB classes and oncogenic fusions described further above. In line with this reasoning, several genomic classes that are more restricted to individual FAB types form tighter transcriptional clusters that are more separate from other genomic classes as observed for the pedAML samples with *CBFB::MYH11*, *RUNX1::RUNX1T1* and *CBFA2T3::GLIS2* fusions (Fig. 6).

#### 1.2.4. The evolution of treatment of acute childhood leukemias

The scarcity of patients and severity of the diseases have fueled international collaborative trials in pediatric leukemias and led to substantial improvements in survival in both pediatric ALL and AML patients over the past decades. In the 1940s an acute leukemia diagnosis in childhood was a death sentence, until the seminal work of Sydney Farber produced the first temporary remissions after the administration of the antifolate aminopterin (Farber & Diamond, 1948). Subsequent work by George Hitchings and Gertrude Elion established antipurines as a promising additional component of chemotherapy and particularly established the use of 6-Mercaptopurine as a chemotherapeutic agent which remains a cornerstone of pedALL therapy until today (Hitchings & Elion, 1954; Elion *et al*, 1954). Subsequent work by Frei and colleagues studying the effects of combining 6-mercaptopurine and methotrexate demonstrated improvements in response rates by combining chemotherapeutic agents with different modes of action and thus laid the foundation for modern combination chemotherapy

treatment regimens (Frei *et al*, 1961). Based on these results, Pinkel and colleagues hypothesized that combining even more agents and thus inhibiting several growth pathways simultaneously may finally enable the cure of pedALL and termed this concept *total therapy*. This approach led to the establishment of combination therapy with vincristine, aminopterin, mercaptopurine and prednisolone (VAMP) and indeed, the resulting VAMP regimen enabled the first cures for pedALL (Pinkel, 1971; Aur *et al*, 1971), representing a major milestone for the treatment of pedALL in particular and for cancer therapy in general (Pui & Evans, 2013).

Treatment progress in pedAML closely followed this approach and led to the establishment of the 7+3 regimen consisting of cytarabine and daunorubicin in 1973 (Lichtman, 2013). While these seminal works identified the key compounds that enabled potentially curative treatment of pediatric leukemias, the risk factors underlying response rates remained poorly understood. After the first cytogenetic studies in pedALL in 1958, work by Secker-Walker and colleagues in 1978 finally established cytogenetic characteristics as prognostic markers for pedALL by demonstrating increased remission duration in patients with hyperdiploid pedALL (Secker-Walker *et al*, 1978), thus laying the foundation for modern genetics- and cytogenetics-based risk stratification. Again, similar progress has been achieved in pedAML and a plethora of works from the 1970s onwards identified associations between cytogenetic abnormalities and prognosis (Sakurai & Sandberg, 1973; Benedict *et al*, 1979; Shiraishi *et al*, 1982). Due to the rarity of the disease and disparities between treatment protocols, these earlier studies were still limited in their statistical power, but these limitations were overcome in studies on similarly treated patients (Berger *et al*, 1987) and large-scale collaborative studies identified robust associations between cytogenetics and prognosis in pediatric and adult AML (Grimwade *et al*, 1998). Continuous efforts over the following decades further refined the categorization of cytogenetic abnormalities and their prognostic significance for treatment response; the success of hematopoietic stem cell transplantation (HSCT), and the risk of relapse (Cooper *et al*, 2023). These seminal works laid the foundation for modern risk-adapted therapy approaches that combine genetic identification of risk-conferring lesions, continuous monitoring of measurable residual disease and major advances in supportive care (Cooper *et al*, 2023; Rasche *et al*, 2018).

### 1.2.5. The current treatment landscape of pediatric AML

The most recent trials report 5 year OS of 60%-80% in pedAML (Rasche *et al*, 2018; Tierens *et al*, 2024; Zwaan *et al*, 2015; Aplenc *et al*, 2020). These dramatic advances in outcome were achieved through substantial improvements in supportive care, increasingly sensitive methodologies for detecting MRD and the introduction of risk-adapted therapy coupled with highly optimized chemotherapy regimens and supportive measures for the detection of high-

risk events, such as CNS involvement. Successes in the treatment of patients with *DEK::NUP214* represent a valuable example for the advances from risk adapted therapy. The outcome of these patients in trials of the Children's Oncology Group improved dramatically with 5 year overall survival rates increasing from 58% in the 2006-2010 trial to 94% in the 2011-2019 trial, due to higher intensity chemotherapy and faster allocation to HSCT (Tarlock *et al*, 2021). Despite these successes, improvements in survival across risk genetic subgroups have largely stagnated over the past 10 years (Rasche *et al*, 2018), indicating that that the further optimization of clinical practice along this route may have reached its limits. In this section, we will review the current treatment landscape of pediatric AML, novel treatments for high-risk patients and the subgroups that may still profit from novel drugs.

Today, most patients with pediatric AML are treated with high-dose induction chemotherapy regimen consisting of cytarabine, daunorubicin, mitoxantrone and etoposide with response assessment via morphology, PCR or flow-cytometry after every chemotherapy cycle (Rasche *et al*, 2018; Aplenc *et al*, 2020; Tierens *et al*, 2024) (Fig. 7A). Particularly in the AML-BFM study group trials the dosages for anthracyclines have steadily increased over time (Fig. 7A) and overall survival steadily increased over time (Fig. 7B). Notably, these advances were largely achieved through improved OS in non-standard risk patients (Fig. 7C) and while 5-year EFS has not changed substantially between the 1987 trial and the 2012 trial (Fig. 7D), particularly HSCT-related deaths have been reduced dramatically (Fig. 7D). Initial risk stratification is largely based on the underlying fusion oncogene and response during the induction cycles. Notably, initial response is highly predictive of long-term response even well into relapse (Rasche *et al*, 2021; Brodersen *et al*, 2020; Tierens *et al*, 2016), indicating that early chemoresistance may persist over the full course of the disease and representing a need for additional biomarkers of resistant disease.

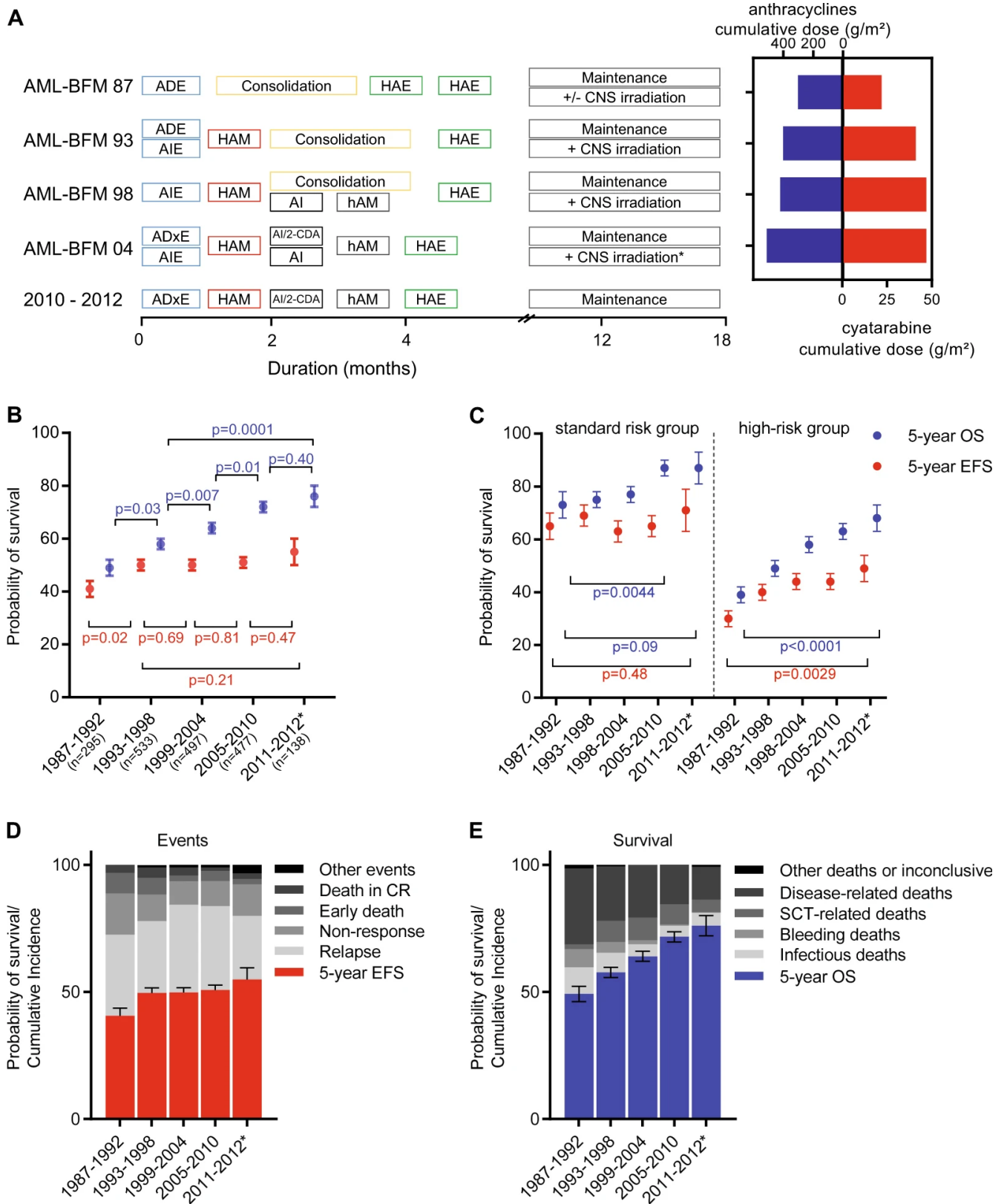


**Figure 7. Development of overall survival and event-free survival in the AML-BFM trials from 1987 to 2012.**

**A** Left: Treatment protocols for patients within the AML studies from 1987 to 2012 as flowcharts. Block widths are approximately proportional to treatment duration. ADE: Cytarabine, Daunorubicin, Etoposide; ADxE: Cytarabine, liposomal Daunorubicin, Etoposide; AHE: high-dose Cytarabine, Etoposide; AI: Cytarabine, Idarubicin; AIE: Cytarabine, Idarubicin, Etoposide; Consolidation: 6-thioguanine, Prednisone, Vincristine, Cytarabine, Doxorubicin

or Idarubicin; HAE: high-dose Cytarabine, Etoposide; HAM: high-dose Cytarabine, Mitoxantrone; hAM: intermediate-dose cytarabine, mitoxantrone; 2-CDA: 2-chloro-2-deoxyadenosine; CNS: central nervous system. Right: Bar chart of cumulative doses of anthracyclines and cytarabine e based on the maximum doses in each study. **B** Probability of overall survival and event-free survival per study. Points indicate the mean and error bars around points indicate the standard error. P-values are based on log-rank test. Color coding as in C. **C** Same as in B, but separated into standard risk group on the left and all other patients indicated as high risk group on the right. **D** Stacked bar chart of probability of events per study. **E** Stacked bar chart of probability of survival and causes of death per study. **D,E** Error bars indicate standard error. Reprinted under the Creative Commons non-commercial license from (Rasche *et al*, 2018).

Targeted therapies only slowly made their way into treatment of pediatric AML patients, which is largely due to the low frequencies of targetable lesions and the overall scarcity of patients. However, there are some remarkable successes in recent trials indicating that targeted treatments can improve both overall survival and event-free survival in ped AML. Probably the most prominent example is the application of Midostaurin or Sorafenib in patients with *FLT3* mutations. Trials for both drugs led to improvements in outcome (Pollard *et al*, 2022; Stone *et al*, 2017). Further advances have been made in immunotherapy by targeting the HSC associated cell surface protein CD33. The antibody drug conjugate Gemtuzumab Ozogamicin – consisting of an anti-CD33 antibody coupled to calicheamicin - has improved event free survival by reducing relapse risk in pedAML (Gamis *et al*, 2014). The additional benefit seems to mainly occur in the standard risk and intermediate risk groups and driven by CD33 expression (Fournier *et al*, 2020; Pollard *et al*, 2016). While these the latest successes from stage 3 clinical trials are encouraging, it has to be noted that FLT3 inhibitors are the only example where targeted treatments for high-risk genomic lesions enabled better outcomes (Egan & Tasian, 2025). However, recent advances in the understanding of unique vulnerabilities of several pedAML subgroups have enabled the development of a number of targeted agents with encouraging results. We will discuss these more novel treatment options for particular pedAML subtypes in the following section.

### 1.2.6. Emerging treatment options for pediatric AML

While the aforementioned large-scale efforts have led to substantial improvements for many pedAML subgroups, several genetically defined groups still fare poorly. Particularly patients with *KMT2A*-rearrangements, *NUP98*-rearrangements, the novel *UBTF*-TD subtype and *CBFA2T3::GLIS2* fusions still experience high rates of relapse and non-response. Thus, focused efforts over the past years have attempted to identify novel targets and drugs for these subgroups. Broadly speaking, current efforts focus on mutations in the *RAS* pathway, cell surface antigens, *BCL2* expression, and the Menin vulnerability that seems to be present in



several genomic subgroups (Pommert & Tarlock, 2022). This section provides an overview of ongoing efforts towards molecularly guided therapy.

As in other hematological malignancies, immunotherapy is a promising avenue for the treatment of high-risk pediatric AML. Substantial successes in B-ALL with anti-CD19 CAR T-cells spurred similar developments across several cancers and in pediatric AML. While the identification of cancer specific antigens has proven to be difficult – which is at least partially because pedAML blasts usually express markers that are common to other hematopoietic precursor populations - there are notable recent successes. Folate Receptor 1 (*FOL1R*) has been identified as a cancer specific antigen in *CBFA2T3::GLIS2* leukemias that can be targeted by CAR T-cells (Le *et al*, 2022).

Inhibition of anti-apoptotic signaling in the BCL2 pathway has emerged as another promising route towards outcome improvement after promising results of the BCL2 inhibitor venetoclax in older adults that were unfit for chemotherapy (Pollyea *et al*, 2019). Particularly the combination of venetoclax and the hypomethylating agent Azacytidine has improved overall survival and complete remission rates in elderly patients with previously untreated AML (DiNardo *et al*, 2020a). Successes of venetoclax have been based on a number of preclinical studies and a detailed understanding of the BCL2 pathway. The BCL2 pathway regulates apoptosis via permeabilization of the outer mitochondrial membrane and its major players can be grouped into four categories. The oligomerization of the pore formers BAX and BAK leads mitochondrial outer membrane polarization (MOMP) and subsequent cell death. These pore formers are regulated by three further member groups. The activators BID and BIM and the antiapoptotic members BCL-X<sub>L</sub>, BCL2 and MCL1 interact with BAX and BAK directly in an activating and inhibitory manner respectively. Furthermore, the sensitizers of the BH3 family BAD and NOXA can inhibit activity of the anti-apoptotic proteins by binding to BCL family proteins and thus freeing the activators (Kale *et al*, 2018). The poised state of these antiapoptotic family members for the release of BAX and BAK proteins and subsequent apoptosis has been termed apoptotic priming or mitochondrial priming and seminal work in AML has demonstrated that this status is predictive of chemotherapy response via an assay termed BH3 profiling (Vo *et al*, 2012; Ni Chonghaile *et al*, 2011). Subsequent work has further demonstrated that this concept can be therapeutically exploited as a cancer specific vulnerability in AML with the BCL2 inhibitor venetoclax (Pan *et al*, 2014). venetoclax acts in a similar manner to these BH3-family proteins by inhibiting BCL2 and thus enabling MOMP mediated apoptosis (Leverson *et al*, 2017). Recent studies mainly apply venetoclax in combination with other drugs, such chemotherapy with low dose Cytarabine alone (Wei *et al*, 2019), the FLAG regimen (fludarabine, cytarabine, granulocyte colony-stimulating factor) (DiNardo *et al*, 2021) or with hypomethylating agents such as azacitidine (DiNardo *et al*, 2020a,

2018a). After promising results in adults in both relapsed/refractory and untreated adult patients (Konopleva *et al*, 2016; Pollyea *et al*, 2019; DiNardo *et al*, 2020a), venetoclax has also been investigated in a pedAML and while patient numbers were often limited and the experience is less extensive than in adults the results have been encouraging. Two retrospective studies with 37 and 31 patients respectively evaluated responses to venetoclax and found complete responses in 42% of patients with AML in the former study and 58% of patients across myelodysplasias in the latter study (Masetti *et al*, 2023; Niswander *et al*, 2023). Both of these studies had heavily pre-treated patient populations with high-risk disease. Beyond the relapsed refractory setting, safety and efficacy of a venetoclax based regimen was also demonstrated in a prospective study in previously untreated pedAML patients (Wen *et al*, 2024).

Another particularly promising class of novel drugs are Menin inhibitors, such as revumenib and ziftomenib, which are under consideration for pedAML with *KMT2A*-rearrangements, *NUP98*-rearrangements and truncating *NPM1* mutations. Menin can positively and negatively regulate gene expression and has been shown to interact with diverse proteins which can be broadly categorized as transcriptional activators, transcriptional repressors, cell signaling proteins and other proteins (Matkar *et al*, 2013). The observation that the binding between Menin and *KMT2A* in *KMT2A*-rearranged leukemias is required for leukemogenesis – presumably via joint binding to the *HOXA9* promoter – spurred further enthusiasm for therapeutic targeting of the Menin-*KMT2A* interaction (Yokoyama *et al*, 2005) and focused research efforts over the subsequent 15 years have yielded the first Menin inhibitors (Issa *et al*, 2021), which can be considered as substantial successes in high risk leukemias. Revumenib has recently been granted FDA approval due to promising results in the AUGMENT-101 trial, where it was shown to increase overall survival and complete remission rates in relapsed/refractory *KMT2A*-rearranged leukemias (Aldoss *et al*, 2024; Martínez-Gamboa & Kaner, 2025). More recent work indicates that *NUP98*-rearranged leukemias and leukemias with *UBTF*-TD may also profit from treatment with Menin inhibitors, due to their dependency on the *KMT2A*-Menin interaction (Heikamp *et al*, 2022; Rasouli *et al*, 2023; Barajas *et al*, 2024).

These advances highlight the substantial improvements in outcome that can be achieved through basic research and the identification of novel vulnerabilities and particularly the emerging treatment options for pedAML with *KMT2A*-, or *NUP98*-rearrangements and *CBFA2T3::GLIS2* fusions (Egan & Tasian, 2025). However, several high risk groups still do not have established targeted treatment options, such as leukemias with *ETV6::MNX1*, or the approximately 10% of cases that cannot be assigned to genomic categories yet (Umeda *et al*, 2024).

Additionally, there are other factors than genetics that are independently predictive of outcome. Recent larger studies have indicated that initial response to induction is an independent prognostic factor for long-term OS – even after relapse (Rasche *et al*, 2021; Tierens *et al*, 2016; Brodersen *et al*, 2020). Intriguingly, joint stratification of patients by genetically determined risk group and MRD status revealed that early non-responders in low risk groups have equivalent survival to responders in intermediate groups (Umeda *et al*, 2024). This indicates that there must be additional, early present functional properties of pediatric leukemias that determine responses over a long time.

Collectively the advances and challenges in the treatment and stratification of pedAML outlined above indicate that there is a substantial need for an increased functional understanding of this disease, particularly in terms of emerging treatment resistance. While the collective understanding of the genetic basis of the disease has reached a point where driving lesions can be identified for a vast majority of patients, a mechanistic understanding of the basis for treatment resistance within genomic subgroups and the functional link between genetics and patient outcome are yet to be elucidated. The next section discusses some of the advances in understanding treatment resistance of pedAML to broaden our understanding of treatment resistance beyond the driving oncogenic fusions.

### 1.2.7. Mechanisms of treatment resistance in pediatric AML

The importance of oncogenic fusion events for pediatric AML biology and patient risk is further reflected in the risk stratification schemes used for the disease. Risk stratification is mainly based on the underlying gene fusions as identified by clinical genetics and response to therapy quantified as measurable residual disease (MRD). For example, fusion events resulting in *CBFBC::MYH11* or *RUNX1::RUNX1T1* transcripts, or biallelic *CEBPA* mutations are usually associated with good prognosis whereas fusions involving *NUP98*- and *KMT2A*-rearrangements or the *CBFA2T3::GLIS2* fusion are usually associated with poor prognosis (Elgarten & Aplenc, 2020). Notably, while our understanding of the leukemogenic potential of different lesions and their influence on the aggressiveness of the disease has been studied extensively (Krivtsov & Armstrong, 2007; Barajas *et al*, 2024; Rasouli *et al*, 2024; Gruber *et al*, 2012), far less is known about the biological basis of treatment resistance in the disease. Stark differences in patient risk and therapy response between cytogenetically defined subgroups are widely recognized and given the scarcity of individual high-risk mutations combined with the overall rarity of the disease, large collaborative efforts are the main drivers of progress in outcome (Zwaan *et al*, 2015). Several studies have investigated the molecular basis of treatment resistance via different approaches such as pharmacogenomics, longitudinal sampling with deep genomic characterization and functional assays.

For example, two studies used deep genomic sequencing to delineate the changes in clonal architecture over the course of treatment in selected cases (Masetti *et al*, 2016; McNeer *et al*, 2019). Both observed general changes in clonal frequencies, a reduction in *WT1*-mutated clones in individual samples and the emergence of mutations during treatment that were not present at diagnosis. Indicating that pedAML blasts undergo clonal selection during treatment. Intriguingly, their studies did not identify genetic lesions that would support straight-forward hypotheses on the mechanistic basis of the emergence of subclones under treatment, indicating that non-genetic mechanisms may play a greater role in therapy resistance in pediatric AML than previously appreciated.

This role of non-genetic mechanisms of resistance has been increasingly recognized in recent years. This type of resistance is usually attributed to the phenotypic plasticity of persister cells (Marine *et al*, 2020). In AML specifically, this is usually attributed to a population of HSC-like cells residing in the bone marrow (Misaghian *et al*, 2009). Indeed, a study that aimed to identify the cell origin in relapsed adult AML identified an HSC-like cells at relapse that were already present at diagnosis (Shlush *et al*, 2017). Intriguingly, the same study also found cells with a lineage committed phenotype that fueled relapse, and had an HSC-like expression profile, despite the committed immunophenotype. Further work on resistance to BET inhibitors in adult AML identified a similar transcriptional program driving resistance and linked the establishment of this program to the capacity to modulate enhancers termed *enhancer switching* (Bell *et al*, 2019), providing additional evidence for an epigenetic basis of drug resistance.

These data suggest that HSC-like AML cells are drivers of therapy resistance which may be due to their ability to stay quiescent. Given the different risk profiles of genetic lesions in pediatric AML, one may hypothesize that more high-risk lesions are also associated with more HSC-like regulatory phenotypes. The connection of HSC-like transcriptional signatures and poor response is well established in AML as demonstrated by previous studies that describe risk-predictive HSC-like transcriptional signatures (Diffner *et al*, 2013; Huang *et al*, 2022; Ng *et al*, 2016). Additionally, recent studies describe more stem cell-like transcriptional programs in high-risk pedAML and upon relapse (Umeda *et al*, 2024).

In line with this reasoning, Lambo and colleagues performed single cell sequencing of both RNA and accessible chromatin to illuminate the gene-regulatory basis of treatment and resistance (Lambo *et al*, 2023). This approach uncovered subgroup-dependent transcriptional programs and cell-type compositions that at least partially agree with the commonly observed patterns of association between FAB classes and oncogenic fusions: *KMT2A*-rearranged samples had higher fractions of monocyte-like cells, whereas *RUNX1*-rearranged samples had higher proportions of progenitor-like cells. Notably, the authors identified the emergence of hematopoietic stem-cell (HSC) and lymphoid epigenetic and transcriptional programs during

relapse, indicating that treatment resistant blasts transition away from myeloid transcriptional programs. These results may indicate that HSC-like cells may be less susceptible to chemotherapy than other more differentiated cell types.

These findings indicate that genetic, epigenetic and transcriptional states of cancer cells can all contribute to treatment resistance. While genetically mediated resistance can occur at diagnosis or emerge under selection from treatment pressure, epigenetic and transcriptionally mediated resistance are usually considered as emerging properties. These different treatment resistance factors clearly indicate a need for novel drugs and substantial progress has been made on this front over the past decades. The next section will provide an overview of these advances by first discussing genomic and functional precision medicine broadly and then reviewing the latest advances in precision medicine approaches for pediatric oncology.

### 1.3. Genomic and functional precision medicine

Precision Medicine is an umbrella term that is mostly used to describe the broad notion of giving the right drug to the right patient at the right time to cure disease. Currently, this term is used almost ubiquitously and can be attributed to diverse advances in the contexts of drug-development, drug target discovery, biomarker discovery, patient stratification or treatment optimization (Collins & Varmus, 2015). This section focuses on two groups of approaches that essentially pursue the same goal: Genomic Precision Medicine (GPM) and Functional Precision Medicine (FPM). Both approaches describe the means to identify the right drug for the right patient.

GPM approaches are mainly concerned with identifying targetable lesions, mutations that can be linked to a known drug vulnerability, requiring that the mutated protein is required for cancer growth and survival. GPM approaches have been instrumental for many of the novel cancer drugs that have been developed since the 1970s, but there have been challenges in scaling them to more mutated proteins and across larger patient populations.

FPM approaches on the other hand can be considered agnostic to the patient genotype. They aim to identify the best drug for a given patient by simply testing a large collection of drugs on patient material *ex-vivo*. While this idea sounds incredibly attractive, these approaches have long been considered as insufficient in recapitulating patient-specific vulnerabilities. However, major technological advancements and particularly single-cell readouts have propelled FPM approaches into relevance and recent studies finally describe improvements in patient outcome.

Both approaches have been enabled by technological advances that have been achieved over the past decades and have seen substantial successes. GPM approaches have propelled drug development on a plethora of mutated targets and enabled new standard of care treatments with matched targeted therapy. FPM approaches have so far not been applied on similar scales. However, recent studies have demonstrated outcome improvements in heavily pre-treated patient populations.

### 1.3.1. Genomic precision medicine

The discovery of the Philadelphia chromosome and subsequent success of *BCR::ABL1* inhibitors such as Imatinib then jumpstarted the era of genomic precision medicine (Druker *et al*, 1996), and sparked the development of a plethora of targeted inhibitors for cancer-specific lesions and recurrently mutated proteins (Zhang *et al*, 2009). Improvements in outcome through the introduction of targeted kinase inhibitors have substantially improved outcome in several cases, such as BRAF inhibitors for melanoma (Hauschild *et al*, 2012; Hertzman Johansson & Egyhazi Brage, 2014). For AML, several targeted agents have emerged with a similar rationale. Targeting mutated isocitrate dehydrogenase 1 and 2 with Ivosidenib has been shown to be an effective strategy for relapsed or refractory AML with the corresponding mutations (DiNardo *et al*, 2018b; Stein *et al*, 2017) after both genes were identified as recurrently mutated in adult AML. Perhaps the most prominent recent strategies involve inhibitors of *FLT3*. These inhibitors have emerged as viable treatment options for both adult AML (Stone *et al*, 2017) and pediatric AML (Sexauer & Tasian, 2017). Notably, the introduction of targeted inhibitors and improved genetic diagnoses have substantially improved outcome in pediatric AML, with *DEK::NUP214* fusions as a particularly prominent example. These fusions often co-occur with *FLT3* mutations and the combination of chemotherapy intensification, early allocation to HSCT and Gilteritinib administration for patients with *FLT3*-ITD has dramatically improved outcome for children with *DEK::NUP214* driven AML and effectively brought the overall survival of this subgroup to a level that is comparable with standard risk patients (Tarlock *et al*, 2021). These and other developments sparked further enthusiasm, leading to several basket trials where patients were not matched to treatments based on the originating tissue of the tumor, but rather based on the targetable lesions that were presumed to be tumor drivers such as the NCI-MATCH study (O'Dwyer *et al*, 2023). This study was started in 2015 and remains one of the largest precision oncology trials to date with approximately 6,000 recruited patients. The trial identified targetable lesions with a targeted NGS panel in 37.6% of recruited patients. However, only 12.4% of patients received targeted treatment in one of the 38 sub-studies that evaluated the matched targeted inhibitors. Broadly, these results may indicate that genomic profiling alone is not sufficient to increase the number of effective

therapies for patients who did not respond to standard therapy for their respective disease. However, advances in trial design and the incorporation of more molecular characterization assays could substantially improve the rate of patients with identifiable targets and outcome for patients who received treatment based on their genomic lesions. The MASTER trial comprehensively characterized the genome and additionally the transcriptome of 1,310 cancer patients (Horak *et al*, 2021). Using this approach, the authors were able to provide evidence-based disease management recommendations in 88% of cases and demonstrated improved overall response rates in the 31.8% of patients that received targeted therapy based on their molecular characterization. Similar successes have also been achieved in pediatric populations in later studies.

### 1.3.2. Functional Precision Medicine

Functional precision medicine (FPM) approaches have more recently emerged as a promising route for identifying promising treatments in high risk patients (Letai, 2022, 2017; Letai *et al*, 2022). Technical advances in the culturing of primary cells and improved drug response readouts have enabled the first studies that demonstrated efficacy for functional precision medicine guided treatment of late-stage aggressive hematological malignancies (Kornauth *et al*, 2022). Broadly speaking, these approaches rely on applying high throughput drug screening on primary patient samples to identify the most effective drug for an individual patient in a personalized fashion.

Attempts at identifying treatment options by culturing cells with drugs can be traced back to the very early days of cancer research, as the availability of affordable cytotoxicity and cell viability assays has enabled large scale evaluations of compounds and high-content screening approaches. Fluorometric and colorimetric assays enabled measuring cellular viability in response to hundreds of different treatments and thus quantitative high-throughput studies of toxicity. However, these approaches are limited as they only measure drug responses in bulk and thus can not consider cell-to-cell heterogeneity in terms of response to the given drugs (Ramirez *et al*, 2010). Still, these assays are widely used and have shown to be predictive of *in-vivo* response in recent work (Acanda De La Rocha *et al*, 2024; Liebers *et al*, 2023). Flow-cytometry based assays (Kuusanmäki *et al*, 2020; Spinner *et al*, 2020; Strachan *et al*, 2022) and image-based assays (Kornauth *et al*, 2022; Snijder *et al*, 2017) have filled this gap by enabling the interrogation of drug responses of single cells in a high-throughput fashion and enabled some of the first trials that demonstrated response predictivity and efficacy for FPM guided treatment.

### 1.3.3. Recent advances in functional precision medicine

FPM approaches have demonstrated several successes recently, which were largely due to novel trial designs and technological advances with better cell culturing systems and single cell readouts. These advances cover the areas of feasibility demonstration and biomarker discovery in observational non-interventional trials and prospective trials that demonstrated clinical benefit of FPM approaches.

Non-interventional FPM approaches have mainly focused on leukemias and lymphomas which is largely due to the easier access to malignant tissue and initially focused on demonstrating feasibility and predictiveness for patient response. Flow-cytometry (FCM) based assays are particularly attractive in this setting because they enable the quantification of on-target drug responses as they can precisely identify the malignant cell population within the blood or bone marrow samples that are usually taken (Kuusanmäki *et al*, 2020). Spinner and colleagues further advanced this methodology by establishing a fully automated FCM-based approach for MDS and AML where they tested 74 drugs and 36 drug combinations. This approach enabled them to accurately predict clinical response and deliver reports within 15 days (Spinner *et al*, 2020). Similarly, the SMART trial demonstrated predictiveness of ex-vivo profiling for hematological malignancies using the CellTiter Glo assay with an even faster turnover time of 7 days (Liebers *et al*, 2023). Further studies have applied FPM in integrated multi-omics approaches for biomarker discovery and to enable multi-omics informed molecular tumor boards, similar to the previously described GPM studies that integrated several NGS approaches. To date, there is a plethora of studies that apply functional and genomic assays in an integrated fashion to identify promising treatment options and demonstrate the feasibility of FPM for treatment recommendations (Pemovska *et al*, 2013; Kropivsek *et al*, 2023; Lee *et al*, 2024). Ongoing trials aim to advance these approaches even further to enable real-time multi-omics characterization that can inform molecular tumor boards (Irmisch *et al*, 2021; Malani *et al*, 2022).

The demonstration of clinical benefit of FPM in a prospective setting however requires both innovative trial designs and advanced assays. An interim report from the EXALT trial for example illustrates both angles well (Snijder *et al*, 2017). The trial used an innovative design where it evaluated the potential benefits of FPM by comparing responses of FPM treated patients to the response to the most recent regimen within the same patient. Furthermore, they used an innovative image-based high-content screening approach that enabled them to quantify the on-target response as the preferential killing of cancer cells with respect to healthy cells from the same patient within the same treated well. A follow-up publication was able to demonstrate clinical benefit for FPM guided treatment with this technology when compared to treatment by physicians choice (Kornauth *et al*, 2022). In addition to demonstrating clinical



benefit as measured by more than 1.3-fold progression-free survival compared to the previous therapy, the authors also identified exceptional responses that lasted three times longer than expected in 40% of responders.

## 1.4. Precision Medicine in pediatric malignancies

These observations from both GPM and FPM approaches in adult cancers have sparked enthusiasm for precision medicine trials in pediatric malignancies across entities. Additional work that highlighted differences in genetic dependencies between cell lines from pediatric cancers when compared to those from adult cancers further highlighted the need for additional genetic profiling studies in pediatric cancer populations (Dharia *et al*, 2021). Furthermore, large scale genetic studies across pediatric cancer entities indicated that more than 50% of pediatric cancer types may harbor targetable events and thus motivate more comprehensive molecular profiling studies (Gröbner *et al*, 2018).

Thus, a number of different trials aimed at identifying personalized targets in pediatric leukemias and some even provided patients with targeted treatment options. The LEAP consortium clinical exome panel sequencing and RT PCR and RNA sequencing in selected cases for pediatric high risk, relapsed and refractory leukemias, with the goal of providing personalized therapy recommendations (Pikman *et al*, 2021). 18% of patients received a high tier recommendation and while clinical responses to targeted treatments were variable, the comprehensive NGS characterization enabled the reclassification of several patients and additional drug sensitivity testing identified vulnerability of RAS mutated AML samples to MEK inhibitors, emphasizing the value of these approaches even when the number of patients eligible for matched targeted treatments is limited. The PRISM trial from the Zero Childhood Cancer Initiative performed comprehensive NGS characterization of high risk pediatric cancer patients with whole genome, transcriptome and methylome profiling and was able to identify therapeutic targets in a substantially higher proportion of patients of 71.4%. 31% of patients who received matched targeted therapy in this study showed objective evidence of clinical benefit (Wong *et al*, 2020). Notably, 61% of identified reportable variants in this study were based on either WGS or RNA-seq. This finding indicated that these approaches are complimentary for target detection and may explain the higher proportion of identified targetable events when compared to other studies that purely rely on target panels or DNA sequencing. A further follow-up of this study indicated that targeted treatment based on this molecular profiling strategy significantly improved outcome in the study cohort (Lau *et al*, 2024). Similar observations have been made in studies with the INFORM registry. Here, patient samples were subjected to whole genome sequencing, exome sequencing, DNA methylation

analysis and RNA sequencing. This multi-omics approach identified actionable targets in 85.9% of patients, emphasizing the increase in target discovery rate when several sequencing approaches are combined. While only 20 out of 519 patients received matched targeted therapy based on the findings from sequencing data, these patients had a substantially longer progression free survival of 204 days compared to 117 days for all other patients (van Tilburg *et al*, 2021).

Similarly to the efforts to advance GPM in pediatric oncology, several FPM studies in this setting have been published recently and illustrate an increasing diversity of approaches. As in adult cancers, earlier studies were enabled by technological innovation and focused on demonstrating feasibility and high-risk disease. One important use case for these studies is the identification of effective drugs for patients for whom no molecular target could be identified using NGS approaches. This was demonstrated for solid tumors in a recent report from the INFORM program (Peterziel *et al*, 2022). Here, the authors profiled solid tumors from pediatric patients with high-risk disease and were able to derive treatment recommendations in 80% of patients that lacked targetable events. Several earlier studies also evaluated the clinical benefit of FPM in pediatric oncology in selected cases. For example, image-based drug screening for pedALL in a co-culture system to mimic the bone marrow niche identified recurrent patterns of sensitivity and enabled FPM informed treatment of a patient with refractory T-ALL that achieved a durable remission (Frismantas *et al*, 2017). Further work in pedAML demonstrated predictivity of drug sensitivity profiling for MRD with an automated flow-cytometry based assay (Strachan *et al*, 2022) and another study in pedAML achieved remission in two of five patients that were treated based on FPM results (Wang *et al*, 2022). More recently, Acanda de la Rocha and colleagues demonstrated feasibility of FPM for pediatric patients in a prospective setting (Acanda De La Rocha *et al*, 2024). Among the 21 patients tested in this study, six received FPM-guided treatment and five of them showed greater than 1.3-fold improvement in progression free survival.

Collectively, these results make a strong case for integrated FPM in pediatric oncology and particularly in pedAML. Several studies have demonstrated feasibility of FPM in pediatric cancers and the utility of these approaches for biomarker discovery and response prediction (Acanda De La Rocha *et al*, 2024; Strachan *et al*, 2022; Wang *et al*, 2022). pedAML may be the ideal target for these approaches due to its particularly low mutational burden (Gröbner *et al*, 2018), the long-term predictivity of initial therapy response (Rasche *et al*, 2021; Brodersen *et al*, 2020; Tierens *et al*, 2016) and the relatively low number of targetable genomic lesions (Pommert & Tarlock, 2022; Egan & Tasian, 2025).

## 1.5. Aims of this thesis

The paucity of targetable mutations in pediatric AML and the observation that early resistance translates into increased patient risk at later stages of therapy and even after relapse makes this disease an almost ideal target for FPM approaches, as these may enable the identification of novel vulnerabilities that cannot be identified via molecular profiling alone.

Therefore, we set out to perform functional profiling and multi-omics characterization of pedAML to demonstrate feasibility of advanced functional profiling and identify functional genomic signatures of patient risk by performing advanced functional profiling of primary pedAML cells at diagnosis. More specifically, we pursued the following aims:

1. Establish advanced image-based drug screening for pedAML with orthogonally validated read outs and a disease specific compound library.
2. Perform functional profiling on a retrospectively sampled cohort of pedAML patients to map the chemosensitivity landscape of pedAML and identify recurrent patterns of drug sensitivity.
3. Characterize this retrospective cohort with comprehensive molecular profiling to identify the molecular underpinnings of *in-vivo* patient treatment response and *ex-vivo* drug sensitivities.
4. Evaluate the predictiveness of functional profiling for patient risk and response.

## 2. Results

### 2.1. Prologue

To achieve the aforementioned goals, we built upon the previously established *Pharmacoscopy* technology for image-based drug response profiling (Snijder *et al*, 2017; Kornauth *et al*, 2022). We established advanced image-based drug screening specific for pedAML with an accurate detection of blasts and accurate discrimination between viable and non-viable cells. We applied this technology to a retrospectively sampled cohort of pedAML 45 patients who were sampled at diagnosis and performed additional comprehensive molecular characterization that incorporated whole exome sequencing, RNA sequencing and ATAC-sequencing to generate a multi-omics landscape of pedAML that would allow us to identify functional-genomic signatures of patient risk.

This enabled us to map out the chemosensitivity landscape of pedAML and identify opposing axes of chemosensitivities that may discriminate patients based on their drug sensitivity profiles. Our in-depth analysis of ATAC-seq data allowed us to map pedAML blasts to their most similar healthy counterpart and identify an association between cellular differentiation state and patient risk. Integrating this analysis with our functional profiling data then allowed us to identify specific vulnerability profiles for these epigenetically defined and risk-associated cell states. Finally, an analysis with simple machine learning models demonstrated that our chemosensitivity profiles were predictive of initial response to induction chemotherapy and patient risk.

## 2.2. Image-based drug screening combined with molecular profiling identifies signatures and drivers of therapy resistance in pediatric AML

This section contains a full reprint of the manuscript below. The author of this thesis is the first author of this article, which has been reprinted from Elsevier under the Creative Commons License.

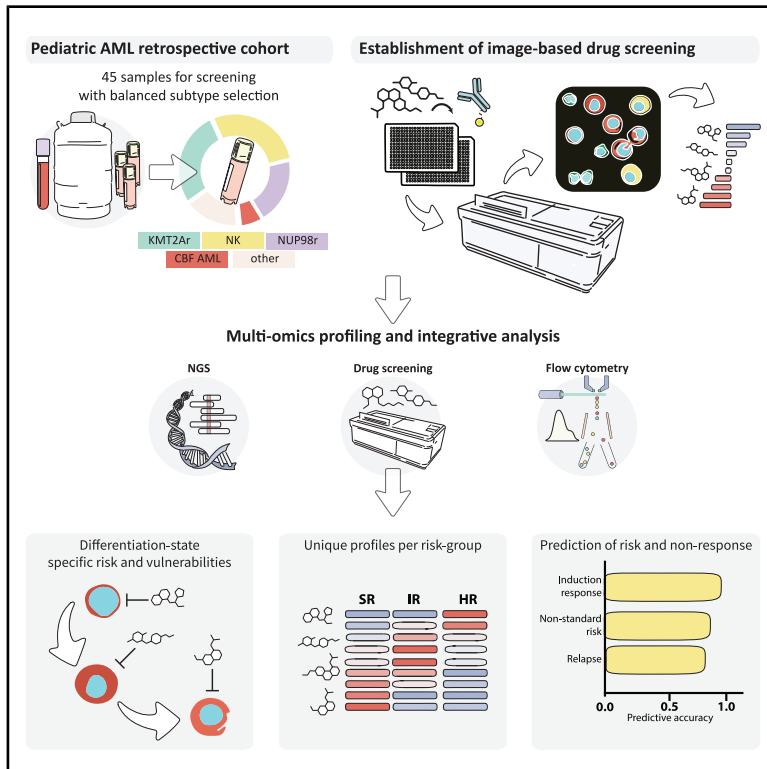
### **Image-based drug screening combined with molecular profiling identifies signatures and drivers of therapy resistance in pediatric AML.**

Haladik B, Maurer-Granofszky M, Zoescher P, Jimenez-Heredia R, Frohne A, Segarra-Roca A, Casey C, Kartnig F, Giuliani S, Rashkova C, Repiscak P, Dworzak MN\*, Superti-Furga G\*, Boztug K\*. (2025) Cell Reports Medicine. Aug 19:102304. doi: 10.1016/j.xcrm.2025.102304. Epub ahead of print. \* equal contribution

The Author Contributions section on page 15 of the article lists the contributions of all authors in detail.

# Image-based drug screening combined with molecular profiling identifies signatures and drivers of therapy resistance in pediatric AML

## Graphical abstract



## Authors

Ben Haladik, Margarita Maurer-Granofszky, Peter Zoescher, ..., Michael N. Dworzak, Giulio Superti-Furga, Kaan Boztug

## Correspondence

kaan.boztug@ccri.at

## In brief

Haladik et al. establish high-content imaging and deep-learning-based drug response profiling for pediatric acute myeloid leukemia. Combined with multi-omics profiling, they identify treatment options for epigenetically defined chemotherapy-resistant cell states and demonstrate the predictivity of drug response profiles for patient risk and response.

## Highlights

- Establishment of image-based drug response profiling for pediatric AML
- Identification of pediatric AML differentiation states with ATAC-seq
- Pediatric AML differentiation states exhibit distinct drug response and risk profiles
- Pediatric AML drug response profiling at diagnosis may predict therapy response

## Article

# Image-based drug screening combined with molecular profiling identifies signatures and drivers of therapy resistance in pediatric AML

Ben Haladik,<sup>1,2</sup> Margarita Maurer-Granofszky,<sup>1</sup> Peter Zoescher,<sup>1</sup> Raul Jimenez-Heredia,<sup>1,3</sup> Alexandra Frohne,<sup>1</sup> Anna Segarra-Roca,<sup>1</sup> Chloe Casey,<sup>1</sup> Felix Kartnig,<sup>2,4</sup> Sarah Giuliani,<sup>1</sup> Christina Rashkova,<sup>1,3</sup> Peter Repiscek,<sup>1</sup> Michael N. Dworzak,<sup>1,3,6,8</sup> Giulio Superti-Furga,<sup>2,5,8</sup> and Kaan Boztug<sup>1,2,3,6,7,8,9,\*</sup>

<sup>1</sup>St. Anna Children's Cancer Research Institute, Vienna, Austria

<sup>2</sup>CeMM Research Center for Molecular Medicine of the Austrian Academy of Sciences, Vienna, Austria

<sup>3</sup>Medical University of Vienna, Department of Pediatrics and Adolescent Medicine, Vienna, Austria

<sup>4</sup>Medical University of Vienna, Department of Internal Medicine III, Division of Rheumatology, Vienna, Austria

<sup>5</sup>Medical University of Vienna, Center for Physiology and Pharmacology, Vienna, Austria

<sup>6</sup>St. Anna Children's Hospital, Vienna, Austria

<sup>7</sup>Clinic for Pediatric Immunology and Rheumatology, Center for Pediatrics and Adolescent Medicine, University Hospital Bonn, Bonn, Germany

<sup>8</sup>These authors contributed equally

<sup>9</sup>Lead contact

\*Correspondence: [kaan.boztug@ccri.at](mailto:kaan.boztug@ccri.at)

<https://doi.org/10.1016/j.xcrm.2025.102304>

## SUMMARY

Despite recent advances in the understanding of the genomic landscape of pediatric acute myeloid leukemia (pedAML), targeted treatments are only available for selected genomic alterations, and the functional link between genotype and outcome remains partially elusive. Functional precision medicine approaches to investigate treatment resistance and patient risk have not been applied systematically for pedAML. Here, we describe an advanced functional screening platform combining high-content imaging and deep learning-based phenotyping. In 45 patients with pedAML, we identify BCL2 and FLT3 inhibitors and standard chemotherapy as major drivers of the chemosensitivity landscape, reveal substantial differential sensitivities between risk groups, and may effectively predict individual measurable residual disease and patient risk. Integration with genomic and epigenomic data uncovers a chemotherapy-resistant primitive state vulnerable to combined BCL2 and MDM2 inhibition and HDAC inhibition. Overall, we identify early signatures of therapy resistance across genetic subgroups and prioritize targeted treatments for these functionally and epigenetically defined patient subsets.

## INTRODUCTION

Pediatric acute myeloid leukemia (pedAML) is a rare hematological malignancy with poorer outcome than its lymphoblastic counterpart in children and adolescents and fundamentally different biology than in adult patients.<sup>1,2</sup> These differences are characterized by the disproportionately higher prevalence of structural aberrations in pedAML such as, for instance, *KMT2A* or *NUP98* rearrangements. Frequencies of non-structural mutations also differ markedly: *NRAS*, *KRAS*, *KIT*, and *WT1*, for example, are more commonly affected in younger patients, whereas variants in *DNMT3A*, *TP53*, and *NPM1* are more frequent in older patients.<sup>1</sup> Through rigorous optimization of treatment protocols over the past decades, 5-year overall survival (OS) rates have dramatically increased in most countries of the world,<sup>2</sup> and recent clinical trials now report 5-year OS between 60% and 80% in Western European countries<sup>3–5</sup> and the US.<sup>6</sup> Large-scale efforts in recent years have furthered our

understanding of the genetic determinants of patient risk and poor outcome in this disease,<sup>1,7</sup> revealed novel genomic subtypes,<sup>8</sup> and elucidated the trajectories of cellular composition hierarchies between diagnosis and relapse.<sup>9</sup> Furthermore, several studies in recent years have addressed poor outcome in selected genetically defined subgroups by identifying targetable disease mechanisms and novel therapeutic agents with menin inhibitors being particularly promising in *KMT2A*- and *NUP98*-rearranged leukemias.<sup>10,11</sup>

A systematic understanding of the functional basis of treatment resistance and poor response in pedAML has remained elusive, and individual contributions of subclonal evolution, pharmacogenomics, and germline variants have increasingly been recognized. Deep sequencing of genomic DNA in matched samples of diagnosis and non-response or relapse revealed patient-specific expansions of subclones with more prevalent genetic variants,<sup>12</sup> which may at least partially drive therapy resistance.<sup>7,13</sup> Pharmacogenomic efforts over the past decades

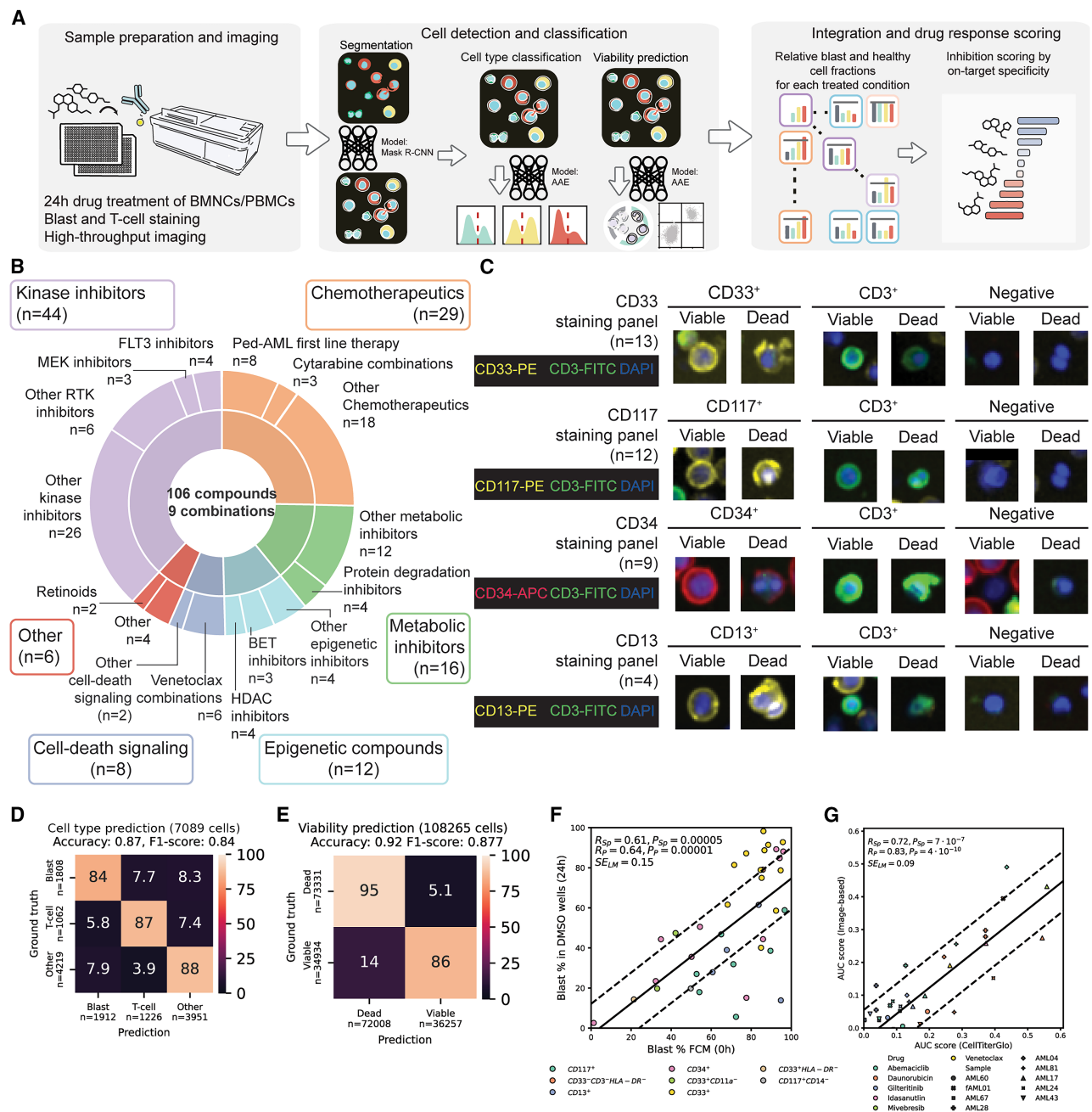


**Figure 1. Establishing an image-based drug sensitivity profiling platform for pedAML**

(A) Workflow. Mononuclear cells from either peripheral blood (PBMCs) or bone marrow (BMNCs) were incubated on plates with pre-printed compounds. After 24 h of incubation, these cells were stained with blast- and T-cell-specific markers and imaged. A custom pipeline then used deep learning models to classify cells by their marker expression profile and viability.

(B) Compound library overview. Pie-chart of relative abundancies per drug class in our custom compound library of 106 compounds and 9 combinations. RTK, receptor tyrosine kinase.

(C) Example images for the four most common staining panels in our pipeline covering  $n = 38$  samples. Each row indicates a staining panel. Images are contrast adjusted single-cell images for the three channels indicated for each row.

(D) Normalized confusion matrix for cell type prediction for  $n = 7,089$  cells in the testing dataset.

(E) Normalized confusion matrix for viability prediction for  $n = 108,265$  cells in the testing dataset.

(F) Scatterplot of relative blast abundancies among viable cells for flow cytometry (x axis) and image-based profiling (y axis) for  $n = 38$  samples where flow cytometry-based blast fractions were available. The black line indicates the linear model fit for flow cytometry and image-based values. Dashed lines indicate the

(legend continued on next page)



have identified several variants that affect drug metabolism, and seminal work in acute lymphoblastic leukemia has uncovered genetic determinants of anti-cancer activity or increased off-target toxicities for commonly used anti-leukemic agents.<sup>14,15</sup> Similarly, though not investigated at the same level of detail to date, more recent work in pedAML indicated that patients with SNPs that affect cellular accumulation of the active metabolite of cytarabine, cytarabine triphosphate, have inferior outcomes.<sup>16,17</sup> Furthermore, there are several germline variants that predispose to pedAML. For example, patients with Fanconi anemia, GATA2 deficiency, or Down syndrome all have a tendency to develop pedAML and require distinct treatment approaches.<sup>18–20</sup> In addition to these genetic drivers of predisposition and patient risk, several studies demonstrated that measurable residual disease (MRD) after induction—a surrogate for *in vivo* treatment response—provides prognostic value over the years and even well into relapse,<sup>8,21–24</sup> indicating that characteristics beyond the broadly recognized risk-stratifying mutations and genomic aberrations are further determinants of patient outcome. Thus, collectively, the identification of additive risk-conferring functional properties may allow to better predict outcome and optimally match patients to clinical trials.

One particularly promising strategy to address the aforementioned challenges in predicting individual patient response to therapy is to employ so-called functional precision medicine approaches, which aim to identify efficacious agents in a personalized fashion by directly measuring the effects of candidate drugs in primary patient material.<sup>25</sup> Recent work in this field has shown promise for improving outcome in late-stage hematological malignancies in adults,<sup>26,27</sup> in several high-risk pediatric populations,<sup>28–30</sup> and therefore highlighted the potential use of functional screenings as a stratification and discovery tool.<sup>31,32</sup> While these studies demonstrated promising results for biological discovery and potential improvements in outcome, challenges such as the interpretation of screening hits, the applicability of functional screening alongside established treatment concepts, and the identification of meaningful molecular correlates of *ex vivo* drug responses to derive robust insights from contextualizing compound screening data with molecular profiling data still remain largely unaddressed.

We here set out to systematically characterize patients with pedAML by advancing our previously established functional drug sensitivity profiling platform and integrating the resulting profiles with comprehensive genomic, transcriptomic, and epigenomic data. Through the comprehensive characterization of 45 patients, retrospectively sampled at diagnosis, we identified clearly distinguishable chemosensitivity profiles between risk groups as defined by the Associazione Italiana di Ematologia e Oncologia Pediatrica - Berlin Frankfurt Münster (AIEOP-BFM) AML consortium (EUCT: 2022-500783-35-00), revealed intriguing associations of drug response with cellular hierarchy compositions, and demonstrated the predictivity of *ex vivo* profiles for key clinical parameters.

## RESULTS

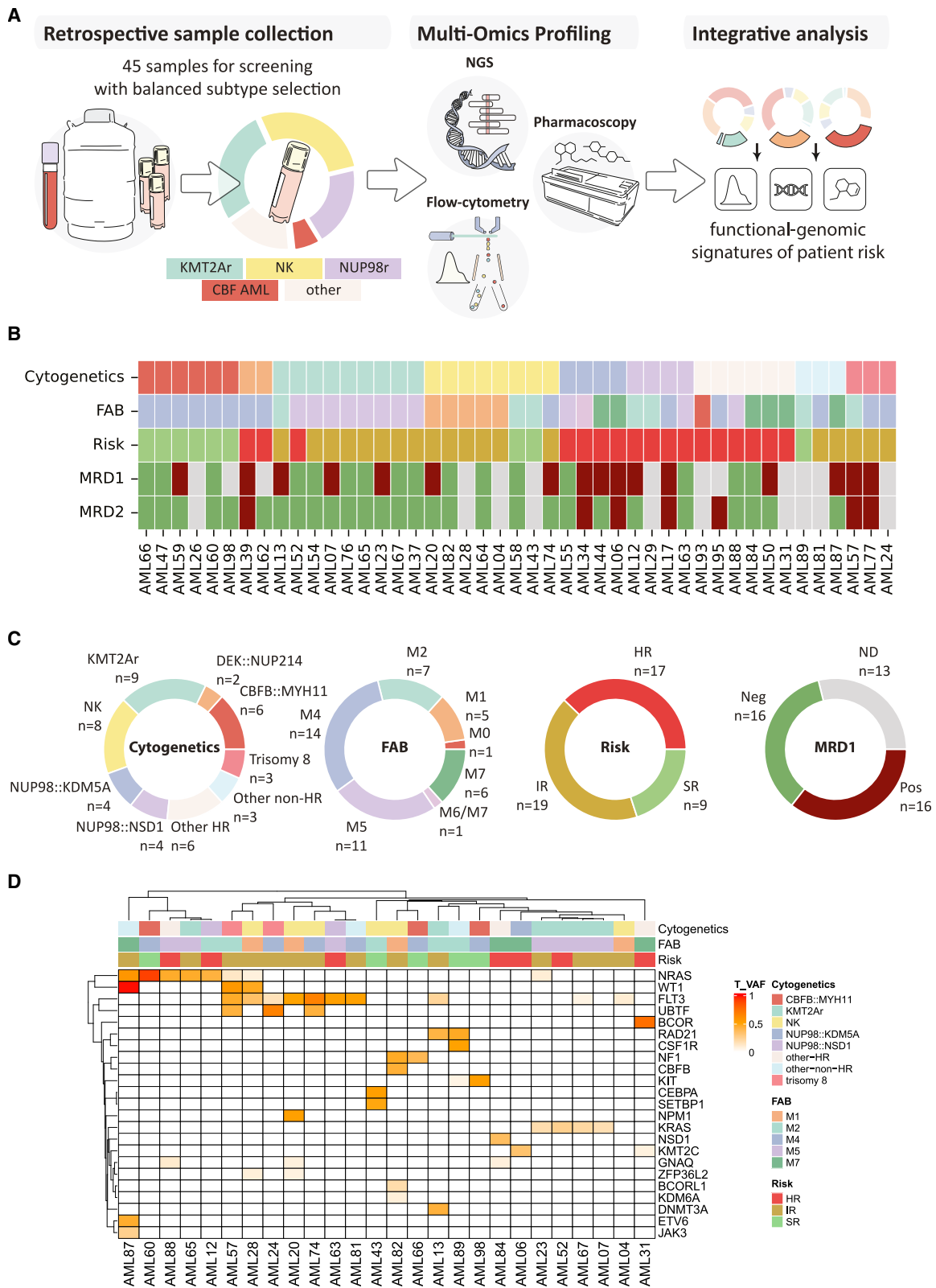
### Establishment of an image-based high-throughput compound screening platform for pedAML

To dissect the integrated chemosensitivity landscape of pedAML, we first set out to tailor our established image-based functional screening platform—previously termed Pharmacoscopy<sup>26,27</sup>—to some of the specific challenges in pedAML, such as heterogeneity in material amounts and blast fractions at diagnosis, the lack of universal blast-specific markers across cases and entities, and the challenges with *ex vivo* testing of myeloid blasts as described elsewhere.<sup>33</sup>

Hence, we established an image-based drug screening platform to quantify on-target drug activity against malignant blasts in primary mononuclear cells from blood or bone marrow. We treated cells with a custom, pedAML-specific compound library of 115 compounds and subsequently stained for markers as identified via our well-established flow cytometry based blast identification,<sup>34</sup> thereby explicitly accounting for the patient- and blast-specific immunophenotype (Figures 1A and 1B; Table S1). Our custom image analysis pipeline segmented cells with the Mask-R-CNN model<sup>35</sup> and classified them into viable and non-viable cells as well as marker-positive or marker-negative cells with adversarial autoencoders<sup>36</sup> (Figures 1A and 1C). Our cell type prediction accurately assessed cell marker positivity with an accuracy of 92% (Figure S1A) and roughly uniform predictive power across markers (Figure S1B), leading to an overall accuracy of 87% for the distinction between blasts, T cells, and other cells (Figure 1D). Our viability prediction model predicted cell viability as measured by staining for cells with fractured membranes with 92% accuracy (Figure 1E, STAR Methods). These approaches led to good agreement with orthogonal methods: leukemic blast fractions in untreated negative control wells correlated significantly with blast fractions as determined via flow cytometry (Pearson  $R = 0.64$ ,  $p = 0.00001$ , Spearman  $R = 0.61$ ,  $p = 0.00005$ , Figure 1F), which is similar to the performance described in a previous study.<sup>26,37–41</sup> We further assessed the robustness of our predictive viability model by performing image-based drug sensitivity profiling and measurements of metabolic activity via CellTiter-Glo in parallel and also found significant and high correlations of these orthogonal viability measurements across the 8 samples and 6 compounds we measured (Pearson  $R = 0.83$ ,  $p = 4 \cdot 10^{-10}$ , Spearman  $R = 0.72$ ,  $p = 7 \cdot 10^{-7}$ ; Figure 1G). Notably, these correlations largely remained robust to 2- and 4-fold decreases in cell numbers (Figure S1C). Additional measurements of replicate samples further confirmed the robustness of this approach with Pearson correlations between replicates consistently above 0.8 across readouts—similar to other studies<sup>38</sup> (Figure S1D). Thus, our high-throughput imaging approach and custom image analysis pipeline allowed us to faithfully distinguish between blasts and healthy cells and to calculate on-target drug responses enabling targeted drug sensitivity profiling in pedAML.

standard error. Abbreviations:  $R_{Sp}$ , Spearman rank correlation coefficient;  $P_{Sp}$ ,  $p$  value of Spearman rank correlation;  $R_p$ , Pearson correlation coefficient;  $P_p$ ,  $p$  value of Pearson correlation;  $SE_{Lm}$ , normalized standard error of the linear model.

(G) Scatterplot of inhibition scores for CTG ( $x$  axis) and image-based profiling ( $y$  axis) for  $n = 9$  samples and the 6 drugs tested. Lines and abbreviations are as in (F). Compounds were tested at four concentrations in technical quadruplicates per concentration (STAR Methods).



(legend on next page)

### Molecular and clinical cohort characteristics

We hypothesized that systematic application of this platform integrated with comprehensive molecular characterization may enable the identification of actionable early predictors of patient risk and non-response. Therefore, we combined our image-based chemosensitivity testing approach with detailed molecular profiling via whole-exome sequencing (WES), RNA sequencing, and assay for transposase accessible chromatin using sequencing (ATAC-seq) (Figure 2A). We applied this strategy to 45 fresh-frozen samples taken at diagnosis, thereby generating a comprehensive dataset comprising patients sampled at equivalent time points and treated according to highly similar treatment algorithms with a common cytarabine- and anthracycline-based chemotherapy backbone as established by the AIEOP-BFM study group.<sup>3</sup> We used five additional fresh pedAML samples for assay optimization and benchmarking. Initially, we selected available samples to cover all major cytogenetic subgroups and achieve enrichment for intermediate-risk (IR) and high-risk (HR) cases and subsequently categorized them based on diagnostic reports and our WES data. Samples with a normal karyotype, *CBFB::MYH11* fusions, and *KMT2A* rearrangements made up the most frequent subtypes in our cohort (Figures 2B and 2C). In addition to this grouping by recurring cytogenetic alterations, we assigned samples with cytogenetic alterations that occurred only once or had an unknown genetic subtype in our cohort into the groups other-non-HR (1 × *RUNX1::RUNX1T1*, 2 × unknown genetic alteration) and other-HR (*ETV6::MNX1*, *RPN1::MECOM*, *BCR::ABL1*, *CBFA2T3::GLIS2*, monosomy 7, complex karyotype). We further classified samples by risk according to the criteria established in the AIEOP-BFM-AML 2020 trial (EUCT: 2022-500783-35-00), based on genomic findings and response to induction therapy. Additionally, we annotated our cohort with data on MRD after induction at measurement time point 1 at day 21 or day 28 after first induction and time point 2 at day 56 after second induction and with a threshold of 0.1% blasts in bone marrow as detected by either flow cytometry or PCR. Thus, we generated a comprehensive overview of patient risk and early response for most patients (Tables 1 and S2).

Subsequently, we analyzed our WES data to identify additional, potentially risk-conferring mutations in our cohort and to delineate the clonality of these mutations by quantifying tumor variant allele frequencies (T-VAFs). Intriguingly, we found several rare entities within our cohort, such as three cases with *UBTF* tandem duplications in samples with trisomy 8 or a normal karyotype and a sample with the *CBFB* *GDX1* insertion and a normal karyotype. Further hierarchical clustering analysis of T-VAFs revealed three main clusters that largely recapitulated

the expected patterns of co-occurrence (Figure 2D). Both *KMT2A* and *NUP98* rearrangements were mostly associated with mutations in *RAS* family genes or *FLT3*. While *KRAS* mutations in our cohort were exclusively associated with *KMT2A* rearrangements, *FLT3* mutations co-occurred with mutations in *WT1* (2 samples) and *UBTF* (3 samples). Most mutations occurred within major subclones, whereas mutations in *KRAS*, *KMT2C*, *BCORL1*, and others were restricted to minor subclones. Given these findings, we classified our cohort with respect to newly described, molecularly unique risk groups.<sup>8</sup> Re-classification mainly affected samples with a normal karyotype, trisomy 8, and the two basket categories for HR and non-HR (Figure S2; Table S2).

Having established our methodology and a cohort that covers the majority of risk-conferring genetic lesions in pedAML, we used scoring based on the relative blast fraction (RBF) to quantify the on-target activity of each compound and concentration and subsequently calculated the approximate area under the dose-response curve for these values to derive RBF-area under the curve (AUC) scores similar to our previous work<sup>26,27</sup> (STAR Methods). Selected case vignettes illustrating the reporting format of our drug sensitivity profiling are displayed in Figure S3. For instance, we investigated a patient with *KMT2A::MLL1* and a monoblastic M5a phenotype according to the French American British (FAB) classification that responded well to chemotherapy *ex vivo* and achieved stable remission from the first induction cycle onward (Figures S3A–S3D). Another patient in our cohort with an FAB M2 phenotype, classified as high risk according to the AML-BFM 2020 study protocol due to trisomy of chromosome 8 and mutations in *NRAS*, *WT1*, and *FLT3*, showed resistance in our *ex vivo* profiling and did not respond to induction chemotherapy but could eventually undergo successful allogeneic hematopoietic stem cell transplantation after late response and has remained in remission since (Figures S3E–S3H).

### Inter-patient chemosensitivity heterogeneity is driven by response to chemotherapy and venetoclax combinations

Given these anecdotal observations linking *ex vivo* drug sensitivities and individual clinical courses, we sought to identify the drivers of the functional landscape in pedAML and their associations with clinical characteristics. Across compounds, unsupervised clustering of RBF-AUC scores revealed substantial heterogeneity between patients and initially showed no association with classical clinical parameters such as cellular identity as indicated by FAB class, cytogenetic subgroups, or initial response as quantified by silhouette coefficients (Figures 3 and S4A).

### Figure 2. Workflow and cohort overview

(A) Workflow: fresh-frozen samples from 45 patients, which were taken at diagnosis, were profiled for this study. After thawing, samples were profiled with flow cytometry and subjected to image-based drug screening and comprehensive next generation sequencing (NGS) characterization.

(B) Cohort characteristics: the cohort contains samples from all major cytogenetic subgroups with an enrichment for IR and HR cases. Top: patient characteristics. Each column represents a patient. Color codes in the respective columns indicate cytogenetic subgroup, FAB class, risk according to the AIEOP-BFM-AML 2020 study protocol, and measurable residual disease (MRD) after induction 1 and 2, respectively, and are the same as in (C).

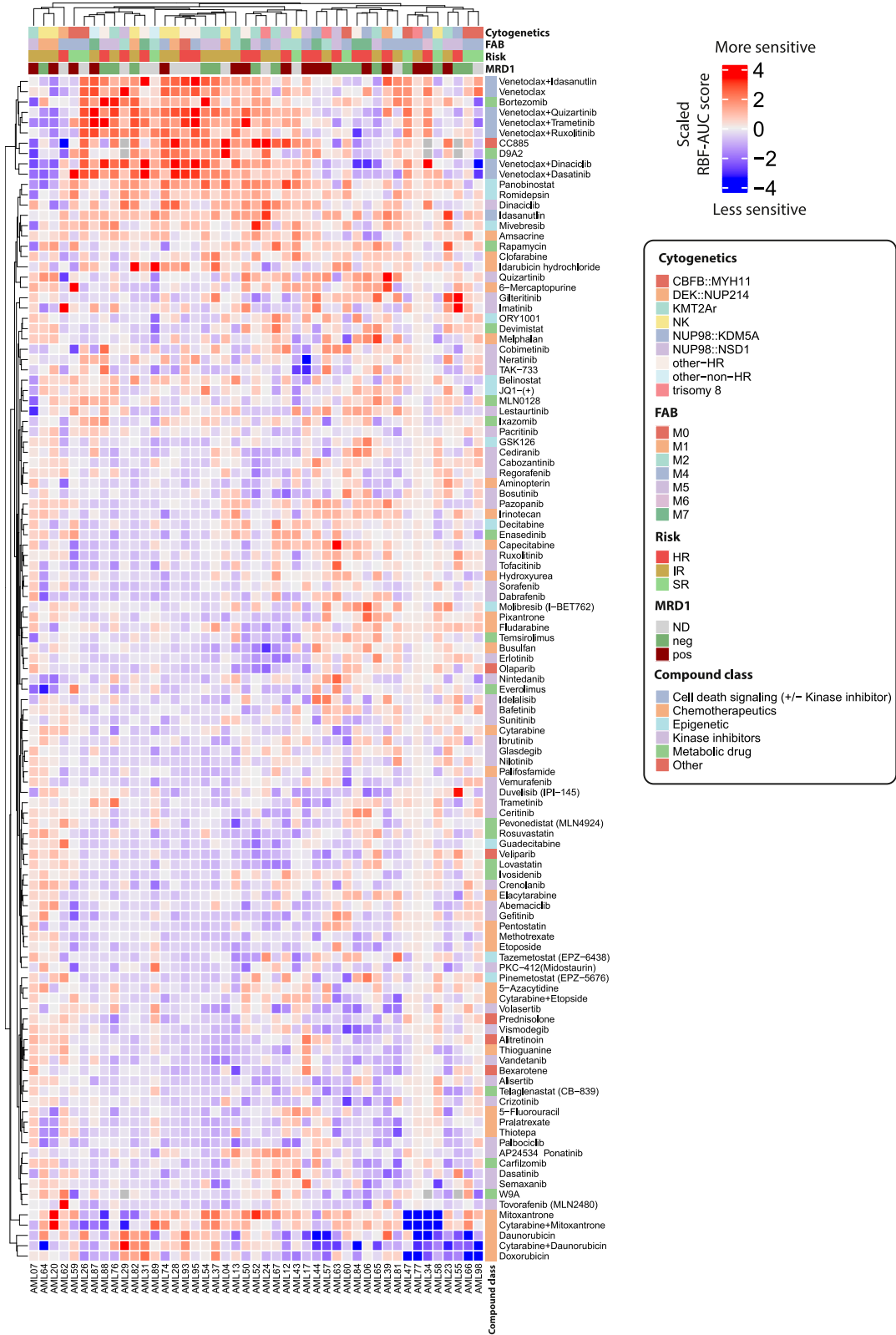
(C) Subtype frequencies. Pie charts indicate the relative abundance of the cytogenetic subgroups, FAB classes, risk groups, and MRD positivity after induction 1, respectively.

(D) Clustered heatmap of tumor variant allele frequencies for  $n = 26$  samples where whitelisted protein-altering mutations could be detected.

**Table 1. Patient clinical characteristics**

ID	FAB	Genetic subgroup	MRD Ind1	MRD Ind2	Risk at diagnosis	Time to death (days)	Time to relapse (days)	Time to SCT (days)	Time to FUP (days)
AML04	M1	NK	ND	ND	IR	534	277	357	534
AML06	M7	<i>NUP98::KDM5A</i>	pos	pos	HR	254	154	no SCT	254
AML07	M5b	<i>KMT2A::MLLT3</i>	pos	neg	IR	alive	no relapse	no SCT	979
AML12	M2	<i>NUP98::NSD1</i>	pos	neg	HR	alive	463	159	463
AML13	M2	<i>KMT2A::MLLT1</i>	pos	neg	IR	alive	326	625	938
AML17	M4	<i>NUP98::NSD1</i>	pos	pos	HR	alive	no relapse	137	137
AML20	M1	NK	pos	neg	IR	alive	no relapse	no SCT	603
AML23	M5a	<i>KMT2A::MLLT1</i>	pos	neg	IR	alive	293	no SCT	1,441
AML24	M4	trisomy 8	ND	ND	IR	alive	421	519	2,191
AML26	M4Eo	<i>CBFB::MYH11</i>	ND	ND	SR	alive	no relapse	no SCT	2,457
AML28	M1	NK	ND	ND	IR	472	314	394	472
AML29	M2	<i>NUP98::NSD1</i>	ND	ND	HR	alive	397	146	4,190
AML31	M7	<i>BCR::ABL1</i>	ND	ND	HR	alive	no relapse	139	2,230
AML34	M6/M7	<i>NUP98::KDM5A</i>	pos	pos	HR	alive	no relapse	no SCT	258
AML37	M5a	<i>KMT2A::MLLT1</i>	neg	neg	IR	alive	no relapse	no SCT	1,091
AML39	M4	<i>DEK::NUP214</i>	pos	pos	HR	alive	no relapse	134	322
AML43	M2	NK ( <i>CEBPA</i> adm)	ND	ND	SR	alive	no relapse	no SCT	1,735
AML44	M7	<i>NUP98::KDM5A</i>	pos	neg	HR	alive	no relapse	no SCT	911
AML47	M4Eo	<i>CBFB::MYH11</i>	neg	neg	SR	alive	no relapse	no SCT	237
AML50	M7	<i>CBFA2T3::GLIS2</i>	pos	neg	HR	alive	no relapse	no SCT	1,368
AML52	M5	<i>KMT2A::MLLT10</i>	neg	neg	HR	alive	no relapse	153	956
AML54	M5	<i>KMT2A::MLLT3</i>	neg	neg	IR	342	237	175	342
AML55	M5	<i>NUP98::KDM5A</i>	neg	neg	HR	alive	no relapse	181	543
AML57	M2/MDS	trisomy 8	pos	pos	IR	alive	no relapse	67	246
AML58	M2	NK ( <i>CEBPA</i> adm)	neg	neg	SR	alive	no relapse	no SCT	555
AML59	M4Eo	<i>CBFB::MYH11</i>	pos	neg	SR	alive	no relapse	no SCT	2,313
AML60	M4Eo	<i>CBFB::MYH11</i>	neg	neg	SR	alive	1,069	1,175	1,667
AML62	M4	<i>DEK::NUP214</i>	ND	neg	HR	alive	no relapse	134	1,362
AML63	M5a	<i>NUP98::NSD1</i>	neg	neg	HR	alive	973	973	1,635
AML64	M1	NK	neg	neg	IR	alive	no relapse	no SCT	1,868
AML65	M5	<i>KMT2A::MLLT3</i>	neg	neg	IR	alive	no relapse	no SCT	410
AML66	M4Eo	<i>CBFB::MYH11</i>	neg	neg	SR	alive	no relapse	no SCT	1,207
AML67	M5a	<i>KMT2A::MLLT3</i>	neg	neg	IR	alive	no relapse	no SCT	1,730
AML74	M4	NK	pos	neg	IR	745	303	no SCT	745
AML76	M5	<i>KMT2A::MLLT3</i>	neg	neg	IR	alive	no relapse	no SCT	1,583
AML77	M4	trisomy 8	pos	pos	IR	66	no relapse	63	66
AML81	M4	Other	ND	ND	IR	alive	no relapse	no SCT	2,961
AML82	M1	NK	neg	neg	IR	alive	798	no SCT	1,358
AML84	M7	Complex	neg	neg	HR	alive	no relapse	no SCT	607
AML87	M7	NK	pos	neg	IR	949	413	no SCT	949
AML88	M5	monosomy 7	neg	neg	HR	alive	no relapse	32	2,190
AML89	M2	<i>RUNX1::RUNX1T1</i>	ND	ND	SR	alive	no relapse	no SCT	3,499
AML93	M0	<i>ETV6::MNX1</i>	ND	ND	HR	668	480	100	668
AML95	M4	<i>inv(3)(q21q26) RPN1::MECOM</i>	ND	pos	HR	319	190	93	319
AML98	M4Eo	<i>CBFB::MYH11</i>	ND	neg	SR	alive	no relapse	no SCT	2,343

Overview of patient clinical characteristics for each retrospective sample. Abbreviations are as follows: FAB, French American British classification; NK, normal karyotype; MRD, measurable residual disease; SR, standard risk; IR, intermediate risk; HR, high risk; SCT, hematopoietic stem cell transplantation; FUP, follow-up; ND, not determined.



(legend on next page)

Clustering of compounds indicated two main clusters that seemed to drive variation. One cluster comprised venetoclax combinations, together with bortezomib, the SLC9 degrader D9A2, and the cereblon modulator CC885, whereas the other comprised first-line chemotherapy compounds such as daunorubicin alone, mitoxantrone alone, or either drug in combination with cytarabine. While daunorubicin and doxorubicin clustered closely together and were in the same cluster as mitoxantrone, idarubicin was placed in a different cluster apart from these drugs. This is also reflected in the correlation coefficients for these compounds, where scaled RBF-AUC scores of daunorubicin and doxorubicin responses correlate significantly with each other, but this is not the case for the other anthracyclines, which may reflect different off-target toxicities of these drugs (Figure S4B). These compounds were also among the compounds with the highest variation of RBF-AUC values across all tested compounds (Figure S4C), indicating that these were drivers of variation. Previous work has already established a link between apoptotic priming and response to chemotherapy and more specifically topoisomerase inhibitors.<sup>42</sup> Given the additional established link between apoptotic priming and venetoclax response,<sup>43</sup> we investigated potential correlations between chemotherapy response and response to venetoclax. We did not observe any strong correlations between venetoclax and chemotherapy for our scaled RBF-AUC score, which may reflect the differential off-target effects between these compounds. However, using the AUC score on the absolute blast fraction, without consideration of the personalized healthy (non-malignant) control cells, revealed significant correlations between venetoclax response and response to the topoisomerase inhibitors daunorubicin and idarubicin, and the combinations of cytarabine with daunorubicin or mitoxantrone, whereas responses to cytarabine did not correlate with venetoclax responses using either quantification approach (Figures S5A and S5B), indicating that apoptotic priming may also be a determinant of chemotherapy response in pedAML but not necessarily informative of off-target effects. Intriguingly, the two targeted FLT3 inhibitors quizartinib and gilteritinib were also among the compounds driving variation, but neither of these agents clustered with venetoclax combinations or standard chemotherapeutics of the induction regimen. Thus, we investigated the correlations of RBF-AUC scores for the compounds that drive variation. Compounds in the venetoclax combination cluster formed one cluster of strongly correlating compounds and correlated significantly with several chemotherapy drugs and combinations, further indicating that these compounds jointly drive variation. Intriguingly, the FLT3 inhibitors gilteritinib and quizartinib correlated negatively with a majority of compounds in that cluster, indicating that combined BCL2 inhibition and FLT3 inhibition posed opposing axes of vulnerability in our cohort (Figure 4A). These intriguing correlations prompted us to further investigate the correlations between different drug classes (STAR Methods). By filtering for the most consistent correlations

between drug-class pairs, we identified general trends of positive correlations between HDAC inhibitors and proteasome inhibitors with venetoclax combinations and negative correlations between FLT3 inhibitors and venetoclax combinations as well as several other consistent pairs (Figure 4B). These results indicated that venetoclax may not be effective in patients who benefit from FLT3 inhibitors, whereas proteasome inhibitors, HDAC inhibitors, and venetoclax combinations may be effective in similar patient populations.

### Chromatin accessibility analysis delineates cellular hierarchy states

Given these observations, we set out to identify the molecular drivers of the observed chemosensitivity patterns. Recent work has identified distinctive associations of known and newly defined genomic classes with leukemic stem cell states.<sup>8</sup> Another recent study identified a trajectory toward a more primitive cell state upon relapse.<sup>9</sup> Together, these results indicated that leukemic cells that are more similar to hematopoietic stem cells (HSCs) may drive resistance to chemotherapy. Therefore, we hypothesized that cellular differentiation states and their underlying gene-regulatory phenotypes may drive differential responses to induction chemotherapy and that chemosensitivities in pedAML undergo profound changes along the differentiation trajectory.

Accordingly, we leveraged our ATAC-seq data to gain insights into cellular differentiation states in our cohort. First, we mapped ATAC-seq data against a healthy reference.<sup>44</sup> Principal component analysis (PCA) after batch correction placed a majority of pedAML samples in proximity to several progenitor populations (Figure 5A), whereas samples with an FAB M7 phenotype with characteristic lesions such as *NUP98* rearrangements and the *CBFA2T3::GLIS2* fusion clustered mainly with each other in proximity to erythroblasts and megakaryocyte erythroid progenitor cells. Variation seemed to be mainly driven by differences between undifferentiated progenitor populations and differentiated lymphoid cells on the first principal component and differences between M7 pedAML samples and monocytes on the second principal component, suggesting that the pedAML cells largely assume precursor-like identities.

Given these observations and previous data that suggested a transition toward more stem cell-like phenotypes upon relapse,<sup>9</sup> we applied a support vector classifier to map pedAML samples in our cohort to their closest healthy counterpart. Our model was able to reliably distinguish all healthy cell types except multipotent progenitors and hematopoietic stem cells (Figure S6A). Overall, the model classified a majority of samples as granulocyte-macrophage progenitors (GMPs) ( $n = 19$ ) or monocytes ( $n = 8$ ), followed by megakaryocyte erythroid progenitors (MEPs) ( $n = 5$ ) and common myeloid progenitors (CMPs) ( $n = 5$ ). HSCs, erythroblasts, and lymphoid-primed multipotent progenitors (lpMPPs) were predicted only once (Figure S6B). We further confirmed the validity of these predictions using

### Figure 3. The chemosensitivity landscape of pedAML

Scaled RBF-AUC scores for  $n = 45$  samples of the retrospective cohort and each compound and combination.

Positive values (red) indicate sensitivity. Negative values (blue) indicate resistance. Row and column annotations are indicated in the legend on the right. Compounds were tested at three concentrations with two technical replicates per concentration (STAR Methods).

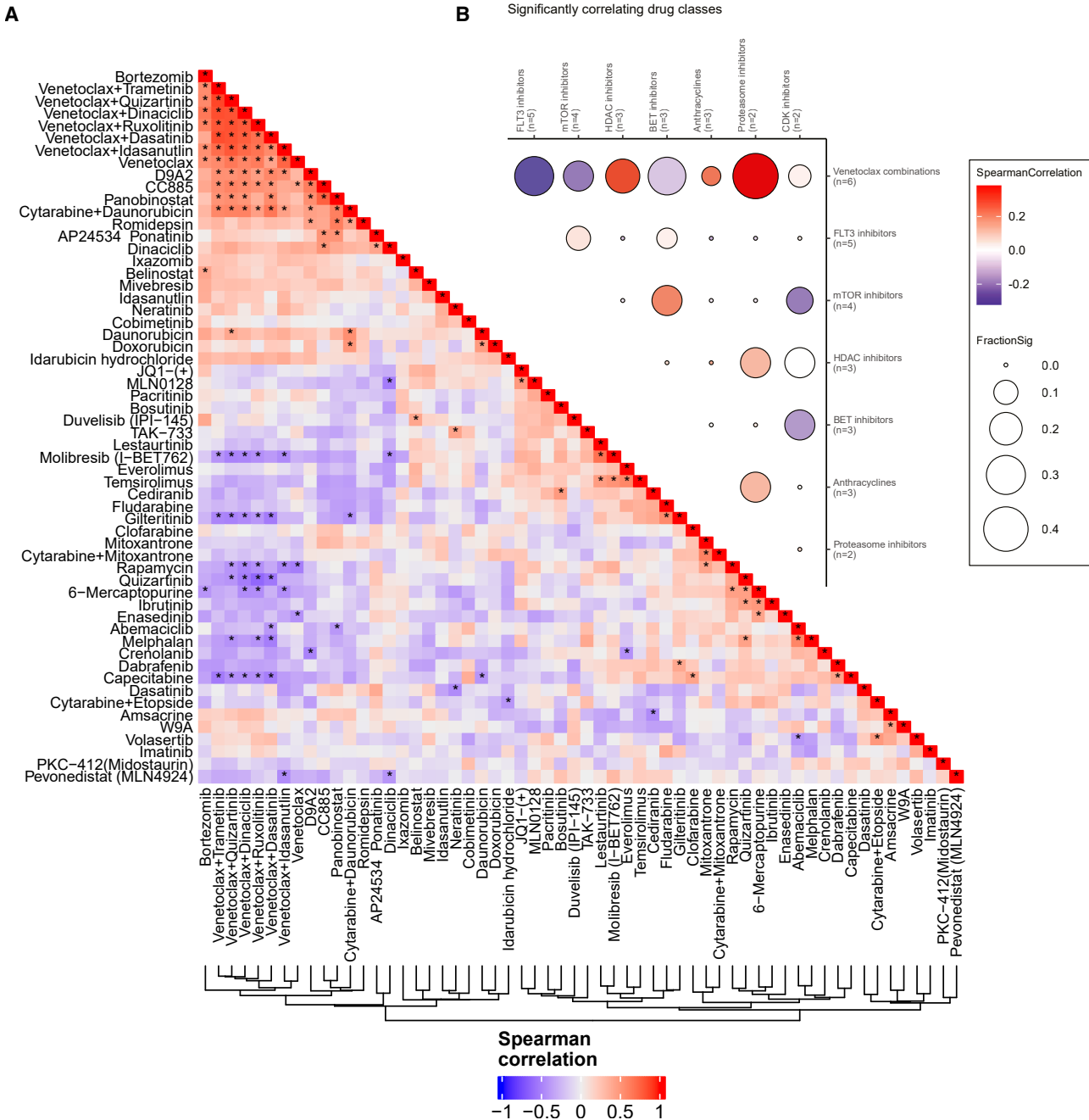


**Figure 4. Correlations analyses identify axes of vulnerability**

(A) Pairwise Spearman correlations of RBF-AUC scores for the 58 drugs with activity in at least 3 samples. Drugs are ordered by hierarchical clustering. Significant correlations after Benjamini-Hochberg multiple testing correction ( $p_{adj} < 0.05$ ) are highlighted with a star.

(B) Bubble plot of the seven drug classes with consistently correlating pairs where all pairs have either positive or negative correlations. Colors indicate the average Spearman correlations across all pairs between the two classes. Sizes indicate the fraction of significant pairs after Benjamini-Hochberg multiple testing correction ( $p_{adj} < 0.05$ ).

chromVAR analysis,<sup>45</sup> which demonstrated strong associations of *CEBP*-family transcription factor (TF) motifs with monocytic identities, *RUNX*-family motifs with precursor identities, and *GATA*-family motifs with erythroid and precursor identities (Figure S6C). ChromVAR scores for the respective TFs also

correlated strongly with expression of the respective genes, further supporting the validity of cell type and TF analyses (Figure S6D). Globally, we observed intriguing changes in TF activity along the differentiation trajectory, with partial overlaps along specific trajectories. HSC-like states were associated

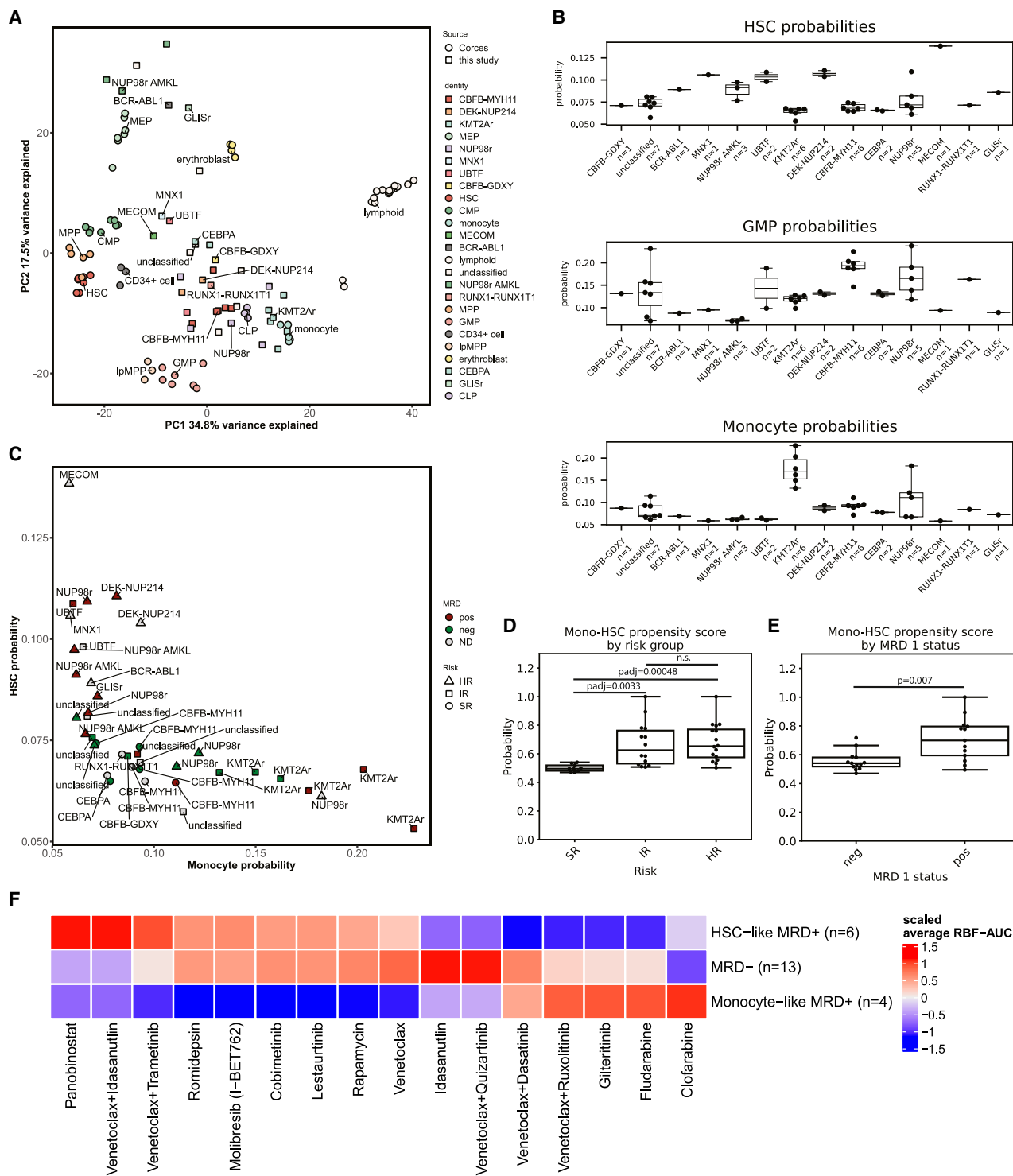


**Figure 5. Cellular differentiation states are associated with unique drug response signatures**

(A) PCA plot for this study ( $n = 39$ ) and the dataset from Corces et al. ( $n = 69$ ) using the 1,000 most variable consensus regions. Annotations indicate healthy precursors or groups defined by Umeda et al., respectively. Unclassified indicates all samples that could not be classified according to the scheme; lymphoid indicates B cells, T cells, and NK cells. MEP, megakaryocyte erythroid progenitor; HSC, hematopoietic stem cell; CMP, common myeloid progenitor; MPP, multipotent progenitor; GMP, granulocyte-macrophage progenitor; lpMPP, lymphoid-primed multipotent progenitor; CLP, common lymphoid progenitor.

(legend continued on next page)



with GATA-family TFs and TFs of the forkhead box (FOX) family (Figure S7A). The association with GATA-family TFs was largely retained for the CMP-, MEP-, and erythroblast-like states, whereas the association with FOX TFs partially changed and was finally lost in the erythroblast state (Figures S7B–S7D). Intriguingly, FOX TFs have mainly been implicated in lymphoid homeostasis,<sup>46</sup> indicating that lymphoid gene-regulatory programs may be co-opted for leukemic development in these states.<sup>9</sup> Monocytic and GMP-like states on the other hand were more associated with activity of interferon regulatory factors (IRFs) and STAT or CEBP-family TFs, respectively (Figures S7E and S7F), whereas IpMPP-like states had a distinct pattern of TF co-regulation (Figure S7G).

Intriguingly, the comparison of probabilities between genetic groups revealed group-specific patterns of similarity that recapitulated other recent work<sup>8</sup> (Figure 5B): *UBTF*-TD and *DEK::NUP214* leukemias were predicted to be more similar to HSCs than others, and *CBFB::MYH11* leukemias more similar to GMPs. Furthermore, *KMT2A*-rearranged samples in our cohort were predicted to be particularly similar to monocytes when compared to other samples.

### Cellular hierarchy states are associated with distinct clinical responses and ex vivo chemosensitivities

Given these associations with genetically defined risk groups, we hypothesized that the position along the differentiation trajectory from HSCs to monocytes may be associated with patient risk and outcome. Plotting the probabilities of HSCs and monocytes revealed an intriguing pattern, where the majority of samples had low probabilities for both HSC and monocyte identities. Samples with MRD or higher risk seemed to deviate from this state toward either a monocytic or an HSC-like state (Figure 5C). A more monocyte-like state was associated with intermediate- to high-risk *KMT2A*-rearranged AMLs, whereas a more HSC-like state was associated with *NUP98* fusions and *UBTF* tandem duplications. These data indicated that there was a higher propensity for high-risk genetics and non-response toward either end of the differentiation spectrum such that both the most differentiated and least differentiated cell states are associated with higher patient risk. Thus, we aimed to quantify this phenomenon by devising a Mono-HSC propensity score that quantifies this propensity away from the average phenotype in our cohort and toward a more HSC-like or more monocytic identity as  $\max\left(\frac{P_{mono}}{\max(P_{mono})}, \frac{P_{HSC}}{\max(P_{HSC})}\right)$  with the monocyte probability  $P_{mono}$  and the HSC probability  $P_{HSC}$ . In line with our expectations from the observed genetics at either ends of the differentiation spectrum, we found this score to be significantly associated with both patient risk and MRD after induction 1 (Figures 5D and 5E). Additional correlative analysis of our differentiation state probabilities and CIBERSORT scores from a

recent large-scale cohort study identified similar associations between genetic risk groups and differentiation states. We found significant correlations for primitive states and GMP-like states, whereas only the pro-monocytic state correlated significantly with our monocyte probability but not the monocyte score derived in the related work (Figures S8A–S8G). Devising a similar Mono-HSC propensity score as described earlier for the primitive score and the pro-monocytic score, we found significant differences between MRD-positive and -negative samples and between the different risk groups as defined by the AIEOP-BFM-AML study group (Figures S8H–S8I).

Associations between cellular differentiation state and patient risk and drug responses have been observed in a number of works in both pediatric and adult AML.

Given these associations of cellular hierarchies and clinical response, we hypothesized that these phenotypic differences would be mirrored in the blast chemosensitivities. Indeed, analysis of the top compounds for the more HSC-like MRD-positive samples (HSC-MRD+) and the more monocyte-like MRD-positive samples (Mono-MRD+) revealed distinct profiles, with panobinostat and the combination of venetoclax and idasanutlin as specific vulnerabilities of HSC-MRD+ samples, whereas chemotherapeutics such as irinotecan and thiotepe inhibited Mono-MRD+ samples more specifically. Previous research has identified monocytic cell states and RAS mutations as drivers of venetoclax resistance in adult AML,<sup>47,48</sup> prompting us to test whether there would be a differential influence of RAS mutations or monocytic cell states on venetoclax sensitivity. Indeed, our analysis indicated lower sensitivity to venetoclax in RAS-mutated monocytic samples than in GMP-like RAS wild-type samples or other samples (Figure S9A). Notably, combinations of venetoclax had an effect that was highly dependent on the combination partner, and combinations with kinase inhibitors showed less activity in HSC-MRD+ samples (Figure 5F). We further expanded this analysis to all predicted hematopoietic differentiation states and found venetoclax sensitivity to be most strongly associated with HSC and erythroblast states, whereas other states seemed to be more resistant to venetoclax as a single agent (Figure S9B). Intriguingly, the combinations of venetoclax with other agents had additional higher activity in CMPs, indicating that combination with other agents broadens the efficacy spectrum to more gene-regulatory backgrounds. Several compounds, such as quizartinib or pazopanib, showed inconsistent activity with respect to differentiation states, indicating that for some of these, other drivers may be more relevant for response.

### Chemosensitivity data are predictive of patient response

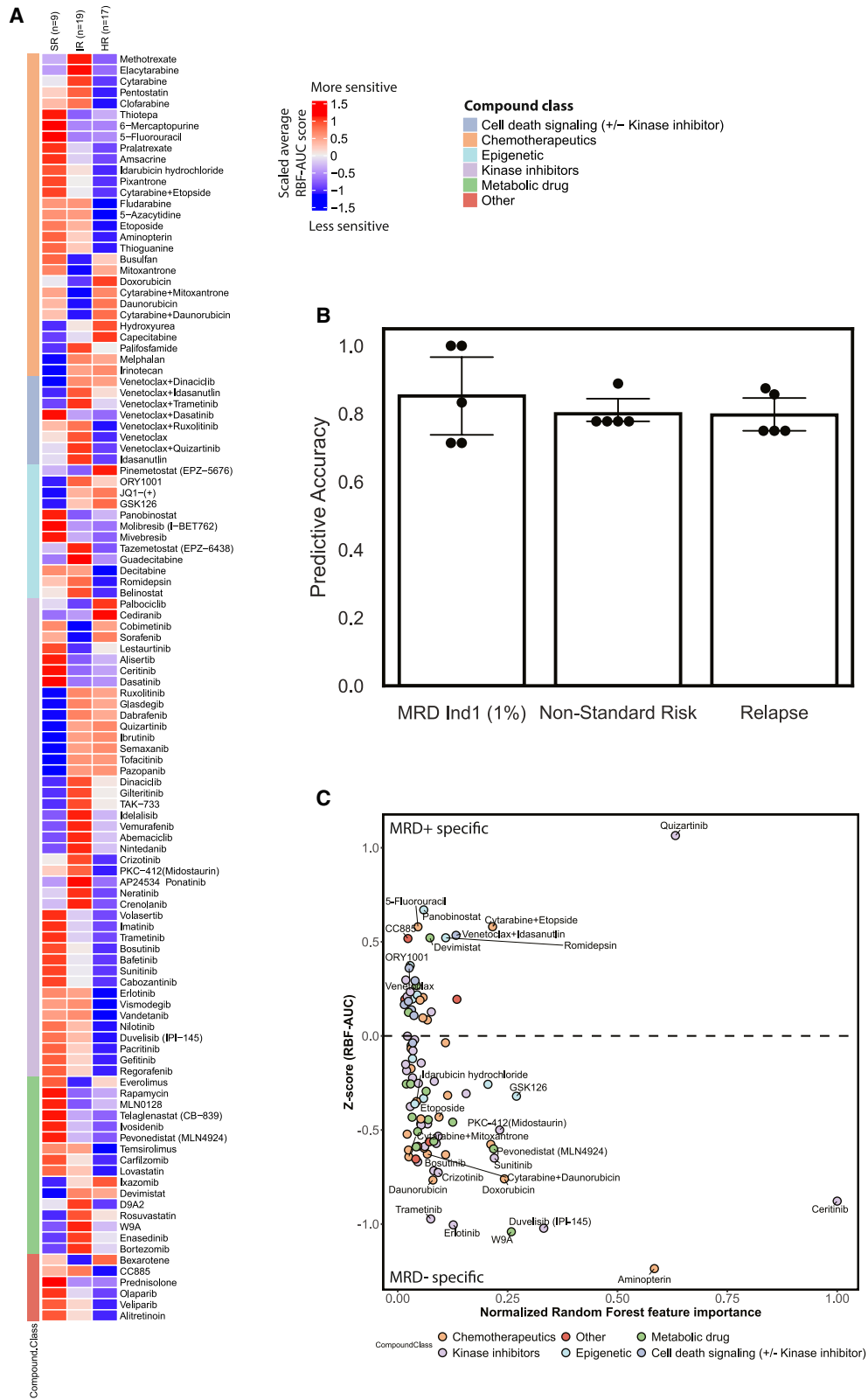
To better understand the potential clinical utility of our drug sensitivity profiling approach, we set out to further investigate the

(B) Boxplots of probabilities per genetic group as defined by Umeda et al. Boxes indicate the quartiles of the distribution and whiskers extend to points that are within 1.5 interquartile ranges. Dots indicate individual samples ( $n = 39$ ). Top: probabilities for hematopoietic stem cells (HSCs). Middle: probabilities for granulocyte-macrophage precursors (GMPs). Bottom: probabilities for monocytes.

(C) Scatterplot of HSC probability (x axis) against monocyte probability (y axis), colored by MRD1 ( $n = 39$ ).

(D and E) Scaled probability of monocytic/HSC identity by risk group ( $n = 39$ ) and MRD status ( $n = 26$ ). Significance was tested with the Mann-Whitney U test. Boxes and whiskers are indicated as in (B). Dots indicate values for individual samples.

(F) Heatmap of scaled average RBF-AUC scores for top 10 drugs of MRD-positive monocyte-like and MRD-positive HSC-like samples.



(legend on next page)

relationship between chemosensitivity, as quantified by RBF-AUC scores, and key clinical characteristics such as MRD, non-standard risk as defined in the AIEOP-BFM-AML 2020 trial, and early relapse. Specifically, we aimed to identify key differences in sensitivity patterns between risk groups by comparing RBF-AUC values and generating predictive models for MRD, risk, and early relapse.

We hypothesized that chemosensitivity differences between risk groups, as defined by the AIEOP-BFM-AML study group, may reveal actionable vulnerabilities. Analysis of responses by risk group revealed intriguing differences that were often concordant with compound mechanism of action between the standard-risk (SR), IR, and HR groups (Figure 6A). SR samples showed stronger responses to chemotherapy than HR samples in a majority of cases, particularly for nucleoside analogs such as 6-mercaptopurine or 5-fluorouracil, whereas cytarabine and anthracyclines such as idarubicin and daunorubicin seemed to be less specific to individual risk groups (Figure 6A). Furthermore, several targeted agents that are mainly considered in high-risk and relapse settings did not show the strongest activity in the HR group. Venetoclax alone and in combination most frequently showed activity in the IR group, and tyrosine kinase inhibitors showed stronger activity in the SR and IR groups than in the HR group. We found only a few vulnerabilities that were specific to the HR group, such as sensitivity to the CDK inhibitor palbociclib and the DOT1L inhibitor pinometostat (Figure 6A). Palbociclib is a CDK4/6 inhibitor, and CDK6 has been shown to be an essential target in both *NUP98*- and *KMT2A*-rearranged AML.<sup>49,50</sup> *NUP98* rearrangements are the most common genetic background among high-risk samples in our cohort.

More generally, our data indicate that chemotherapy sensitivity varies broadly by agent and that response profiles of genetically defined risk groups may only partially converge on individual targets, further emphasizing that drug sensitivity data do not simply recapitulate genetically defined risk. In line with these observations, our analysis of cluster concordance between drug sensitivity profiles and genetic status did not yield any associations between the two but rather indicated MRD and patient risk to be similarly concordant with drug sensitivity profiles (Figure S3A), indicating that drug sensitivity profiles reflect functional aspects of patient risk that are not recapitulated by genetics.

Given these differences between risk groups, we hypothesized that simple machine learning models may be able to predict key clinical parameters from RBF-AUC scores. Thus, we aimed to predict MRD status, non-standard risk, and early relapse from drug sensitivity profiles using RBF-AUC scores as input for random forest models in a cross-validation setting. Predictive accuracies ranged from 85.2% for the prediction of 1%

MRD after induction 1 to 79.9% for non-standard risk, further highlighting the predictive power of our approach (Figure 6B). Accuracy scores for the prediction of early relapse—defined as relapse within the first 12 months after diagnosis—were 79.2% and therefore slightly lower than those for MRD, indicating that chemosensitivity screening may be most predictive for events that are closer in time not at least because of inter-individual divergences in later treatment, such as stem cell transplantation. Overall, these results indicate that drug sensitivity profiling may have clinical utility for the early identification of non-responders and thus provide an additional tool for patient risk stratification—beyond the identification of promising treatments in high-risk settings.

Analyzing the relationship between feature importances and relative inhibition revealed drugs such as the antifolate aminopterin and the receptor tyrosine kinase inhibitors erlotinib and ceritinib to be more active in these MRD-negative samples (Figure 6C). The increased sensitivity to the antifolate aminopterin may indicate a stronger dependency on folate metabolism in low-risk patients, whereas the increased sensitivities to the unspecific tyrosine kinase inhibitors erlotinib and ceritinib may be more indicative of a broad dependency on tyrosine kinase signaling. The higher sensitivities in MRD-negative samples overall may indicate an increased susceptibility to apoptosis, which has been linked to better patient outcomes in earlier studies.<sup>51</sup> These results further support the observed predictivity of *ex vivo* testing for response from previous studies<sup>26,27,30,32</sup> and provide additional rationale for early integration of functional screening to predict response and identify early vulnerabilities in high-risk disease.

## DISCUSSION

Because of its rigorous logic, precision and personalized medicine have inspired the biomedical community over the last decade to achieve a patient-specific treatment rationale.<sup>52</sup> Indeed, our molecular mechanistic understanding of disease in a variety of cancers has tempted us to consider the granular stratification of patients based on genomic data and more recently additional -omics as an achievable goal.<sup>52</sup> However, recent experiences in adult cancers such as adult leukemia and lymphoma indicate that genetics-focused precision medicine approaches may not faithfully recapitulate the functional heterogeneity within samples from patients with cancer.<sup>25</sup> These observations imply that there are additional determinants of functional drug responsiveness that would be key to integrate into precision medicine-based approaches. Hence, the field of functional precision medicine has started to tackle these challenges by direct functional testing of cancer cells, either as an

### Figure 6. Chemosensitivity screening is predictive of key clinical parameters

- (A) Heatmap of scaled averaged responses per AIEOP-BFM-AML risk group as quantified by RBF-AUC scores for  $n = 45$  samples in our cohort.  
(B) Accuracy scores for each prediction target of 1% MRD ( $n = 32$  evaluable samples), non-standard risk ( $n = 45$  evaluable samples), and early relapse ( $n = 39$  evaluable samples) over the 5-fold cross-validation. Dots indicate accuracy scores per fold. The height of the bars indicates the mean accuracy over all folds, and error bars indicate the 95% confidence interval.  
(C) Scatterplot of Z score of inhibition for MRD1-positive (top) compared to MRD-negative (bottom) samples (y axis) against random forest feature importance (x axis), where compounds to the right contribute more to predictivity based on cross-validation over  $n = 32$  evaluable samples. Compounds are colored by compound class as in Figures 1 and 4.

alternative or conversely as a complementary approach to genomics-based precision medicine approaches.<sup>53,54</sup> However, the heterogeneity and relatively small sample sizes in pediatric tumors challenge the notion of clinical trial designs with genetics-based disease classification and treatment strategies.

In this study, we set out to study pedAML as a model disease to assess the feasibility of state-of-the-art image-based chemosensitivity profiling for integration into the clinical management of pedAML and to elucidate functional-genomic patterns of patient risk that may transcend genetically defined risk groups. Building upon our previously established approach with demonstrated clinical efficacy<sup>26,27</sup>—albeit with a relatively short incubation time—we here established an image-based screening platform that enables fast turnover times for a vast array of drugs with clinical relevance, such as chemotherapeutics in first-line therapy, compounds that target epigenetic regulators, BCL2 inhibitors, and a vast number of kinase inhibitors. Recent efforts have pursued similar goals with flow cytometry-based assays in diverse hematological malignancies<sup>32,39–41,55</sup> with a similar intention of employing single-cell readouts to define leukemic blast-specific drug response measurements. In our own experience, an image-based drug response platform as showcased here comes with the need of professional computational image analysis skills but arguably bears advantages when it comes to scalability with regard to costs per sample or the relative ease to expand or adapt platforms to individual patients or novel drugs to be included in a screen. The application of simple machine learning models enabled us to accurately predict key clinical parameters, such as non-standard risk, and MRD after the first induction cycle from drug sensitivity profiles, thus demonstrating the potential applicability of functional screening approaches for the early detection of patients at risk. While the detailed mechanistic and biological basis of the predictivity of drug sensitivity profiling is still a subject of active research and cannot be sufficiently addressed in this study due to sample size and the lack of a validation cohort, our work highlights the potential use of advanced drug sensitivity profiling for early identification of patients at risk and the identification of promising treatments. Future studies may overcome these hurdles and validate these findings by using this predictive approach in a prospective setting, where *ex vivo* screening will be performed at diagnosis and predictiveness can be evaluated at the respective time points for risk stratification, MRD assessment, and upon eventual relapse. Thus, while most functional profiling studies focus on patients with late-stage disease,<sup>26–28,30</sup> our study provides a rationale for testing patients at early time points, in line with the observation that early response in pedAML is a long-term predictor of outcome.<sup>21–24</sup>

The genetic heterogeneity of pedAML—with recent work distinguishing more than 20 genetically distinct entities<sup>8,56</sup>—makes it a particularly attractive target for functional precision medicine approaches. These approaches enable both targeted personalized treatments<sup>26</sup> and the elucidation of the corresponding disease-specific functional landscapes.<sup>54,57,58</sup> Several studies have highlighted functional heterogeneity in pedAML and other pediatric cancers<sup>31,59</sup> but did not identify any functional groupings that could be motivated from a molecular perspective. These heterogeneous results may be due to the relatively high percentages of healthy cells that are being screened together

with blasts in these assays. In contrast, our targeted and blast-specific approach indicates that response heterogeneity converges on sensitivity to conventional chemotherapy, HDAC inhibition, or sensitivity to BCL2 inhibition with or without kinase inhibition. Future studies will need to also comparatively test different emerging molecular and drug testing platforms with different treatment times and culturing conditions to understand platform- or technology-dependent advantages and disadvantages of various approaches.

Heterogeneity in treatment responses within genetically defined risk groups has been observed in several large pedAML cohorts.<sup>8,21</sup> However, the determining factors of this functional heterogeneity have remained elusive. On the epigenetic level, we observe that a propensity toward either more monocytic or more HSC-like states is indicative of risk and poor response. Associations of HSC-like gene expression signatures with patient risk in pediatric and adult AML are well known,<sup>60–62</sup> and recent data indicate a trajectory toward more primitive states upon relapse.<sup>9</sup> Several targeted treatment options for HSC-like states have been proposed,<sup>63</sup> but successes have been limited to few agents such as venetoclax. Indeed, we observed higher sensitivity to the combination of venetoclax and idasanutlin in HSC-like states and additionally higher sensitivity to the HDAC inhibitor panobinostat. HDAC inhibitors have been previously applied in clinical trials, but the results have been mixed,<sup>64,65</sup> which may be due to the lack of predictive biomarkers. Our results indicate that HDAC inhibition may be a promising route to target HSC-like states, thus providing a rationale for targeted evaluation of this agent. Furthermore, we observed higher sensitivity to the chemotherapeutic agents clofarabine and fludarabine in more monocyte-like states, indicating that especially this subset may profit from these chemotherapeutics. Hence, our results indicate that cellular differentiation is a targetable state in pedAML and suggest that selective chemotherapy may improve outcome in more differentiated leukemias and that targeted treatments with BCL2 or HDAC inhibition may improve outcome in more HSC-like leukemias. Collectively, our results implicate cellular differentiation states as a driver of treatment response heterogeneity and identify cell state-specific vulnerabilities that may enable personalized targeted treatments of poor responders.

Overall, our study underlines the feasibility and predictivity of *ex vivo* functional profiling for pedAML and other malignancies. The implementation of functional profiling in clinical practice has been in continuous discussion, and recent technological advances finally enable functional profiling in prospective settings.<sup>26,54,66,67</sup> Our data demonstrate that functional profiling enables risk prediction and the identification of targeted treatments for molecularly defined subgroups at even earlier time points, clearly showcasing the added value of functional profiling for patient stratification and response assessment. Looking forward, we envision that systematic application of functional profiling over the disease course will enable earlier identification of patients at risk and of promising drugs and has the potential to improve treatment outcome for broader patient populations.

#### Limitations of the study

While our study highlights the potential of advanced drug sensitivity profiling at diagnosis for patient stratification and risk

prediction and reveals intriguing associations of drug response and cellular differentiation state in pedAML, it does come with limitations. Given the rarity of pedAML, our patient cohort—while covering the broad spectrum of pedAML driving lesions—bears limitations for identifying associations between genetic background and drug response due to insufficient statistical power. Furthermore, our study is retrospective and does not provide an independent validation cohort to fully validate our findings. Prospective studies in larger cohorts are needed to demonstrate the utility of functional profiling in the clinics. Studies like ours bridge this gap by demonstrating the feasibility of functional profiling for patient stratification and treatment prioritization. Future efforts to implement functional profiling for personalized treatment prioritization will require international collaboration. Such efforts may further advance the substantial improvements in outcome for patients with pedAML that large-scale international trials achieved over the past decades.<sup>3,5,21</sup> Despite these limitations, our study provides substantial new data on the functional and epigenetic landscape of pedAML and provides a template for establishing advanced functional profiling for rare pediatric malignancies.

### RESOURCE AVAILABILITY

#### Lead contact

Further information and requests for resources and reagents should be directed to and will be fulfilled by the lead contact Dr. Kaan Boztug ([kaan.boztug@ccri.at](mailto:kaan.boztug@ccri.at)).

#### Materials availability

This study did not generate any new unique reagents.

#### Data and code availability

- ATAC-seq data of sorted blasts have been deposited in the Gene Expression Omnibus (GEO) under the accession number GEO: [GSE282258](https://www.ncbi.nlm.nih.gov/geo/query/acc.cgi?acc=GSE282258). RNA-seq data of sorted blasts have been deposited in GEO under the accession number GEO: [GSE282423](https://www.ncbi.nlm.nih.gov/geo/query/acc.cgi?acc=GSE282423). Raw exome-sequencing data have been deposited at the European Genome Phenome Archive (EGA) under the accession number EGA: EGAD50000001572. To request access, please submit an access request via the EGA website or contact Dr. Kaan Boztug ([kaan.boztug@ccri.at](mailto:kaan.boztug@ccri.at)). Raw imaging data will be made available upon request and uploaded to the appropriate platforms by the time of publication.
- Code and processed data to reproduce all figures in the manuscript are stored in a GitHub repository under [https://github.com/Boztug-lab/pedaml\\_screening](https://github.com/Boztug-lab/pedaml_screening).
- Any additional information required to reanalyze the data reported in this work is available from the [lead contact](#) upon request.

### ACKNOWLEDGMENTS

We thank all patients and families for their participation in the study. We further thank Michael Schuster and Christoph Bock from the Biomedical Sequencing Facility of the Research Center for Molecular Medicine of the Austrian Academy of Sciences (CeMM) for sequencing services and technical input. Additionally, we thank Anna Koren, Monika Malik, and Stefan Kubicek of the Molecular Discovery Platform of CeMM for their technical input and providing compounds and printed screening plates. We further thank Nora Mühlegger and Chiara Wertz for providing documentation of patient clinical characteristics. We also thank André Rendeiro for critical input on epigenetic analyses and Florian Grebien for invaluable critical review and discussion of the manuscript. This study was supported by funds from the Austrian Science Fund (FWF) (DOI: <https://doi.org/10.55776/KLI1056> to K.B.) and by additional

intramural funding by the St. Anna Children's Cancer Research Institute including donations. For open access purposes, the author has applied a CC BY public copyright license to any author accepted manuscript version arising from this submission.

### AUTHOR CONTRIBUTIONS

Conceptualization, B.H., M.M.-G., M.N.D., G.S.-F., and K.B.; methodology, B.H., P.Z., R.J.-H., A.F., A.S.-R., F.K., S.G., C.R., C.C., and P.R.; software, B.H., P.Z., C.C., and P.R.; formal analysis, B.H., M.M.-G., P.Z., and C.C.; investigation, B.H., M.M.-G., P.Z., R.J.-H., A.F., A.S.-R., F.K., S.G., C.R., and C.C.; resources, M.N.D., G.S.-F., and K.B.; data curation, B.H., M.M.-G., P.Z., and A.F.; writing – original draft, B.H. and K.B.; writing – review and editing, B.H., M.N.D., G.S.-F., and K.B.; visualization, B.H.; supervision, M.N.D., G.S.-F., and K.B.; funding acquisition, B.H., M.M.-G., M.N.D., G.S.-F., and K.B.

### DECLARATION OF INTERESTS

G.S.-F. has a patent EP3704484A1 pending and patent EP3198276A1. Both are licensed to Exscientia GmbH.

### STAR★METHODS

Detailed methods are provided in the online version of this paper and include the following:

- [KEY RESOURCES TABLE](#)
- [EXPERIMENTAL MODEL AND STUDY PARTICIPANT DETAILS](#)
- [METHOD DETAILS](#)
  - Drug treatment
  - Staining and image acquisition
  - Image analysis
  - Nucleus segmentation and segmentation model training
  - Cell type prediction
  - Viability prediction
  - Hyperparameter optimization for adversarial autoencoders
  - Benchmarking of image-based screening and CellTiterGlo data
  - Processing of dose response values and compound activity scoring
  - Drug-drug correlation analysis
  - Immunophenotyping for identification of markers for leukemic blasts
  - FACS staining for cell sorting
  - Cell number and cell viability assessment via flow cytometry
  - Transcriptome, exome and accessible chromatin sequencing
  - mRNA sequencing data analysis
  - ATAC-seq analysis
  - WES analysis
  - Predictions of healthy cell types and clinical variables
- [QUANTIFICATION AND STATISTICAL ANALYSIS](#)
- [ADDITIONAL RESOURCES](#)

### SUPPLEMENTAL INFORMATION

Supplemental information can be found online at <https://doi.org/10.1016/j.xcrm.2025.102304>.

Received: November 28, 2024

Revised: May 18, 2025

Accepted: July 24, 2025

### REFERENCES

1. Bolouri, H., Farrar, J.E., Triche, T., Jr., Ries, R.E., Lim, E.L., Alonzo, T.A., Ma, Y., Moore, R., Mungall, A.J., Marra, M.A., et al. (2018). The molecular landscape of pediatric acute myeloid leukemia reveals recurrent structural alterations and age-specific mutational interactions. *Nat. Med.* 24, 103–112.

- Bonaventure, A., Harewood, R., Stiller, C.A., Gatta, G., Clavel, J., Stefan, D.C., Carreira, H., Spika, D., Marcos-Gragera, R., Peris-Bonet, R., et al. (2017). Worldwide comparison of survival from childhood leukaemia for 1995–2009, by subtype, age, and sex (CONCORD-2): a population-based study of individual data for 89 828 children from 198 registries in 53 countries. *Lancet. Haematol.* *4*, e202–e217.
- Rasche, M., Zimmermann, M., Borschel, L., Bourquin, J.-P., Dworzak, M., Klingebiel, T., Lehrnbecher, T., Creutzig, U., Klusmann, J.-H., and Reinhardt, D. (2018). Successes and challenges in the treatment of pediatric acute myeloid leukemia: a retrospective analysis of the AML-BFM trials from 1987 to 2012. *Leukemia* *32*, 2167–2177. <https://doi.org/10.1038/s41375-018-0071-7>.
- Tierens, A., Arad-Cohen, N., Cheuk, D., De Moerloose, B., Fernandez Navarro, J.M., Hasle, H., Jahnukainen, K., Juul-Dam, K.L., Kaspers, G., and Kovalova, Z. (2024). Mitoxantrone Versus Liposomal Daunorubicin in Induction of Pediatric AML With Risk Stratification Based on Flow Cytometry Measurement of Residual Disease. *J Clin Oncol* *23*, 01841.
- Zwaan, C.M., Kolb, E.A., Reinhardt, D., Abrahamsson, J., Adachi, S., Aplenc, R., De Bont, E.S.J.M., De Moerloose, B., Dworzak, M., Gibson, B.E.S., et al. (2015). Collaborative efforts driving progress in pediatric acute myeloid leukemia. *J. Clin. Oncol.* *33*, 2949–2962. <https://doi.org/10.1200/JCO.2015.62.8289>.
- Aplenc, R., Meshinchi, S., Sung, L., Alonzo, T., Choi, J., Fisher, B., Gerbing, R., Hirsch, B., Horton, T., Kahwash, S., et al. (2020). Bortezomib with standard chemotherapy for children with acute myeloid leukemia does not improve treatment outcomes: a report from the Children’s Oncology Group. *Haematologica* *105*, 1879–1886.
- McNeer, N.A., Philip, J., Geiger, H., Ries, R.E., Lavallée, V.-P., Walsh, M., Shah, M., Arora, K., Emde, A.-K., Robine, N., et al. (2019). Genetic mechanisms of primary chemotherapy resistance in pediatric acute myeloid leukemia. *Leukemia* *33*, 1934–1943. <https://doi.org/10.1038/s41375-019-0402-3>.
- Umeda, M., Ma, J., Westover, T., Ni, Y., Song, G., Maciaszek, J.L., Rusch, M., Rahbarinia, D., Foy, S., Huang, B.J., et al. (2024). A new genomic framework to categorize pediatric acute myeloid leukemia. *Nat. Genet.* *56*, 281–293.
- Lambo, S., Trinh, D.L., Ries, R.E., Jin, D., Setiadi, A., Ng, M., Leblanc, V.G., Loken, M.R., Brodersen, L.E., Dai, F., et al. (2023). A longitudinal single-cell atlas of treatment response in pediatric AML. *Cancer Cell* *41*, 2117–2135.e12.
- Heikamp, E.B., Henrich, J.A., Perner, F., Wong, E.M., Hatton, C., Wen, Y., Barwe, S.P., Gopalakrishnapillai, A., Xu, H., Uckelmann, H.J., et al. (2022). The menin-MLL1 interaction is a molecular dependency in NUP98-rearranged AML. *Blood* *139*, 894–906.
- Aubrey, B.J., Cutler, J.A., Bourgeois, W., Donovan, K.A., Gu, S., Hatton, C., Perlee, S., Perner, F., Rahnamoun, H., Theall, A.C.P., et al. (2022). IKAROS and MENIN coordinate therapeutically actionable leukemogenic gene expression in MLL-r acute myeloid leukemia. *Nat. Cancer* *3*, 595–613.
- Farrar, J.E., Schuback, H.L., Ries, R.E., Wai, D., Hampton, O.A., Trevino, L.R., Alonzo, T.A., Guidry Auvil, J.M., Davidsen, T.M., Gesuwan, P., et al. (2016). Genomic profiling of pediatric acute myeloid leukemia reveals a changing mutational landscape from disease diagnosis to relapse. *Cancer Res.* *76*, 2197–2205.
- Masetti, R., Castelli, I., Astolfi, A., Bertuccio, S.N., Indio, V., Togni, M., Bellotti, T., Serravalle, S., Tarantino, G., Zecca, M., et al. (2016). Genomic complexity and dynamics of clonal evolution in childhood acute myeloid leukemia studied with whole-exome sequencing. *Oncotarget* *7*, 56746–56757.
- Rocha, J.C.C., Cheng, C., Liu, W., Kishi, S., Das, S., Cook, E.H., Sandlund, J.T., Rubnitz, J., Ribeiro, R., Campana, D., et al. (2005). Pharmacogenetics of outcome in children with acute lymphoblastic leukemia. *Blood* *105*, 4752–4758.
- Relling, M.V., and Evans, W.E. (2015). Pharmacogenomics in the clinic. *Nature* *526*, 343–350.
- Elsayed, A.H., Cao, X., Mitra, A.K., Wu, H., Raimondi, S., Cogle, C., Al-Mansour, Z., Ribeiro, R.C., Gamis, A., Kolb, E.A., et al. (2022). Polygenic Ara-C response score identifies pediatric patients with acute myeloid leukemia in need of chemotherapy augmentation. *J. Clin. Oncol.* *40*, 772–783.
- Amaki, J., Onizuka, M., Ohmachi, K., Aoyama, Y., Hara, R., Ichiki, A., Kawai, H., Sato, A., Miyamoto, M., Toyosaki, M., et al. (2015). Single nucleotide polymorphisms of cytarabine metabolic genes influence clinical outcome in acute myeloid leukemia patients receiving high-dose cytarabine therapy. *Int. J. Hematol.* *101*, 543–553.
- Wachter, F., and Pikman, Y. (2024). Pathophysiology of acute myeloid leukemia. *Acta Haematol.* *147*, 229–246.
- Sahoo, S.S., Kozyra, E.J., and Wlodarski, M.W. (2020). Germline predisposition in myeloid neoplasms: Unique genetic and clinical features of GATA2 deficiency and SAMD9/SAMD9L syndromes. *Best Pract. Res. Clin. Haematol.* *33*, 101197.
- Hirabayashi, S., Wlodarski, M.W., Kozyra, E., and Niemeyer, C.M. (2017). Heterogeneity of GATA2-related myeloid neoplasms. *Int. J. Hematol.* *106*, 175–182.
- Rasche, M., Zimmermann, M., Steidel, E., Alonzo, T., Aplenc, R., Bourquin, J.-P., Boztug, H., Cooper, T., Gamis, A.S., Gerbing, R.B., et al. (2021). Survival following relapse in children with acute myeloid leukemia: a report from AML-BFM and COG. *Cancers (Basel)* *13*, 2336.
- Tierens, A., Bjørklund, E., Siitonen, S., Marquart, H.V., Wulff-Juergensen, G., Pelliniemi, T.T., Forestier, E., Hasle, H., Jahnukainen, K., Lausen, B., et al. (2016). Residual disease detected by flow cytometry is an independent predictor of survival in childhood acute myeloid leukaemia; results of the NOPHO-AML 2004 study. *Br. J. Haematol.* *174*, 600–609.
- Brodersen, L.E., Gerbing, R.B., Pardo, M.L., Alonzo, T.A., Paine, D., Fritschle, W., Hsu, F.-C., Pollard, J.A., Aplenc, R., Kahwash, S.B., et al. (2020). Morphologic remission status is limited compared to  $\Delta N$  flow cytometry: a Children’s Oncology Group AAML0531 report. *Blood Adv.* *4*, 5050–5061.
- Buldini, B., Rizzati, F., Masetti, R., Fagioli, F., Menna, G., Micalizzi, C., Putti, M.C., Rizzari, C., Santoro, N., Zecca, M., et al. (2017). Prognostic significance of flow-cytometry evaluation of minimal residual disease in children with acute myeloid leukaemia treated according to the AIEOP-AML 2002/01 study protocol. *Br. J. Haematol.* *177*, 116–126.
- Letai, A. (2017). Functional precision cancer medicine-moving beyond pure genomics. *Nat. Med.* *23*, 1028–1035. <https://doi.org/10.1038/nm.4389>.
- Kornauth, C., Pemovska, T., Vladimer, G.I., Bayer, G., Bergmann, M., Eder, S., Eichner, R., Erl, M., Esterbauer, H., Exner, R., et al. (2022). Functional precision medicine provides clinical benefit in advanced aggressive hematologic cancers and identifies exceptional responders. *Cancer Discov.* *12*, 372–387. <https://doi.org/10.1158/2158-8290.CD-21-0538>.
- Snijder, B., Vladimer, G.I., Krall, N., Miura, K., Schmolke, A.-S., Kornauth, C., Lopez de la Fuente, O., Choi, H.-S., van der Kouwe, E., Gültekin, S., et al. (2017). Image-based ex-vivo drug screening for patients with aggressive hematological malignancies: interim results from a single-arm, open-label, pilot study. *Lancet. Haematol.* *4*, e595–e606. [https://doi.org/10.1016/S2352-3026\(17\)30208-9](https://doi.org/10.1016/S2352-3026(17)30208-9).
- Frismantas, V., Dobay, M.P., Rinaldi, A., Tchinda, J., Dunn, S.H., Kunz, J., Richter-Pechanska, P., Marovca, B., Pail, O., Jenni, S., et al. (2017). Ex vivo drug response profiling detects recurrent sensitivity patterns in drug-resistant acute lymphoblastic leukemia. *Blood* *129*, e26–e37. <https://doi.org/10.1182/blood-2016-09-738070>.
- Peterziel, H., Jamaladdin, N., ElHarouni, D., Gerloff, X.F., Herter, S., Fiesel, P., Berker, Y., Blattner-Johnson, M., Schramm, K., Jones, B.C., et al. (2022). Drug sensitivity profiling of 3D tumor tissue cultures in the pediatric precision oncology program INFORM. *NPJ Precis. Oncol.* *6*, 94. <https://doi.org/10.1038/s41698-022-00335-y>.
- Acanda De La Rocha, A.M., Berlow, N.E., Fader, M., Coats, E.R., Saghira, C., Espinal, P.S., Galano, J., Khatib, Z., Abdella, H., Maher, O.M., et al. (2024). Feasibility of functional precision medicine for guiding treatment of relapsed or refractory pediatric cancers. *Nat. Med.* *30*, 990–1000.

31. Wang, H., Chan, K.Y.Y., Cheng, C.K., Ng, M.H.L., Lee, P.Y., Cheng, F.W. T., Lam, G.K.S., Chow, T.W., Ha, S.Y., Chiang, A.K.S., et al. (2022). Pharmacogenomic profiling of pediatric acute myeloid leukemia to identify therapeutic vulnerabilities and inform functional precision medicine. *Blood Cancer Discov.* **3**, 516–535. <https://doi.org/10.1158/2643-3230.BCD-22-0011>.
32. Strachan, D.C., Gu, C.J., Kita, R., Anderson, E.K., Richardson, M.A., Yam, G., Pimm, G., Roselli, J., Schweickert, A., Terrell, M., et al. (2022). Ex Vivo Drug Sensitivity Correlates with Clinical Response and Supports Personalized Therapy in Pediatric AML. *Cancers (Basel)* **14**, 6240. <https://doi.org/10.3390/cancers14246240>.
33. Cucchi, D.G.J., Groen, R.W.J., Janssen, J.J.W.M., and Cloos, J. (2020). Ex vivo cultures and drug testing of primary acute myeloid leukemia samples: Current techniques and implications for experimental design and outcome. *Drug Resist. Updat.* **53**, 100730.
34. Maurer-Granofszky, M., Köhrer, S., Fischer, S., Schumich, A., Nebral, K., Larghero, P., Meyer, C., Mecklenbräuker, A., Mühlegger, N., Marschalek, R., et al. (2024). Genomic breakpoint-specific monitoring of measurable residual disease in pediatric non-standard-risk acute myeloid leukemia. *Haematologica* **109**, 740–750.
35. He, K., Gkioxari, G., Dollár, P., and Girshick, R. (2017). Mask R-CNN. Preprint at arXiv. <https://doi.org/10.48550/arxiv.1703.06870>.
36. Makhzani, A., Shlens, J., Jaitly, N., Goodfellow, I., and Frey, B. (2015). Adversarial Autoencoders. Preprint at arXiv. <https://doi.org/10.48550/arxiv.1511.05644>.
37. Kropivsek, K., Kachel, P., Goetze, S., Wegmann, R., Festl, Y., Severin, Y., Hale, B.D., Mena, J., van Droogen, A., Dietliker, N., et al. (2023). Ex vivo drug response heterogeneity reveals personalized therapeutic strategies for patients with multiple myeloma. *Nat. Cancer* **4**, 734–753.
38. Dietrich, S., Oleś, M., Lu, J., Sellner, L., Anders, S., Velten, B., Wu, B., Hüll-ein, J., da Silva Liberio, M., Walther, T., et al. (2018). Drug-perturbation-based stratification of blood cancer. *J. Clin. Investig.* **128**, 427–445. <https://doi.org/10.1172/JCI93801>.
39. Stieglitz, E., Gu, C.J., Richardson, M., Kita, R., Santaguida, M.T., Ali, K.A., Strachan, D.C., Dhar, A., Yam, G., Anderson, W., et al. (2023). Tretinoin Enhances the Effects of Chemotherapy in Juvenile Myelomonocytic Leukemia Using an Ex Vivo Drug Sensitivity Assay. *JCO Precis. Oncol.* **7**, e2300302.
40. Kuusanmäki, H., Leppä, A.-M., Pölonen, P., Kontro, M., Dufva, O., Deb, D., Yadav, B., Brück, O., Kumar, A., and Everaus, H. (2019). Phenotype-based drug screening reveals association between venetoclax response and differentiation stage in acute myeloid leukemia. *Haematologica* **105**, 708.
41. Spinner, M.A., Aleshin, A., Santaguida, M.T., Schaffert, S.A., Zehnder, J. L., Patterson, A.S., Gekas, C., Heiser, D., and Greenberg, P.L. (2020). Ex vivo drug screening defines novel drug sensitivity patterns for informing personalized therapy in myeloid neoplasms. *Blood Adv.* **4**, 2768–2778.
42. Vo, T.-T., Ryan, J., Carrasco, R., Neuberg, D., Rossi, D.J., Stone, R.M., DeAngelo, D.J., Frattini, M.G., and Letai, A. (2012). Relative mitochondrial priming of myeloblasts and normal HSCs determines chemotherapeutic success in AML. *Cell* **151**, 344–355.
43. Konopleva, M., Pollyea, D.A., Potluri, J., Chyla, B., Hogdal, L., Busman, T., McKeegan, E., Salem, A.H., Zhu, M., Ricker, J.L., et al. (2016). Efficacy and biological correlates of response in a phase II study of venetoclax monotherapy in patients with acute myelogenous leukemia. *Cancer Discov.* **6**, 1106–1117.
44. Corces, M.R., Buenrostro, J.D., Wu, B., Greenside, P.G., Chan, S.M., Koenig, J.L., Snyder, M.P., Pritchard, J.K., Kundaje, A., Greenleaf, W.J., et al. (2016). Lineage-specific and single-cell chromatin accessibility charts human hematopoiesis and leukemia evolution. *Nat. Genet.* **48**, 1193–1203.
45. Schep, A.N., Wu, B., Buenrostro, J.D., and Greenleaf, W.J. (2017). chromVAR: inferring transcription-factor-associated accessibility from single-cell epigenomic data. *Nat. Methods* **14**, 975–978.
46. Zaiss, D.M.W., and Coffey, P.J. (2018). Forkhead box transcription factors as context-dependent regulators of lymphocyte homeostasis. *Nat. Rev. Immunol.* **18**, 703–715.
47. Sango, J., Carcamo, S., Sirenko, M., Maiti, A., Mansour, H., Ulukaya, G., Tomalin, L.E., Cruz-Rodriguez, N., Wang, T., Olszewska, M., et al. (2024). RAS-mutant leukaemia stem cells drive clinical resistance to venetoclax. *Nature* **636**, 241–250.
48. Pei, S., Pollyea, D.A., Gustafson, A., Stevens, B.M., Minhajuddin, M., Fu, R., Riemondy, K.A., Gillen, A.E., Sheridan, R.M., Kim, J., et al. (2020). Monocytic subclones confer resistance to venetoclax-based therapy in patients with acute myeloid leukemia. *Cancer Discov.* **10**, 536–551.
49. Placke, T., Faber, K., Nonami, A., Putwain, S.L., Salih, H.R., Heidel, F.H., Krämer, A., Root, D.E., Barbie, D.A., Krivtsov, A.V., et al. (2014). Requirement for CDK6 in MLL-rearranged acute myeloid leukemia. *Blood* **124**, 13–23.
50. Schmoellerl, J., Barbosa, I.A.M., Eder, T., Brandstoetter, T., Schmidt, L., Maurer, B., Troester, S., Pham, H.T.T., Sagarajit, M., Ebner, J., et al. (2020). CDK6 is an essential direct target of NUP98 fusion proteins in acute myeloid leukemia. *Blood* **136**, 387–400.
51. Ni Chonghaile, T., Sarosiek, K.A., Vo, T.-T., Ryan, J.A., Tammareddi, A., Moore, V.D.G., Deng, J., Anderson, K.C., Richardson, P., Tai, Y.-T., et al. (2011). Pretreatment mitochondrial priming correlates with clinical response to cytotoxic chemotherapy. *Science* **334**, 1129–1133.
52. Torkamani, A., Andersen, K.G., Steinhilber, S.R., and Topol, E.J. (2017). High-Definition Medicine. *Cell* **170**, 828–843. <https://doi.org/10.1016/j.cell.2017.08.007>.
53. Letai, A. (2022). Precision medicine in AML: Function plus-omics is better than either alone. *Cancer Cell* **40**, 804–806.
54. Malani, D., Kumar, A., Brück, O., Kontro, M., Yadav, B., Hellesøy, M., Kuusanmäki, H., Dufva, O., Kankainen, M., Eldfors, S., et al. (2022). Implementing a functional precision medicine tumor board for acute myeloid leukemia. *Cancer Discov.* **12**, 388–401.
55. Schumich, A., Prchal-Murphy, M., Maurer-Granofszky, M., Hoelbl-Kovacic, A., Mühlegger, N., Pötschger, U., Fajmann, S., Haas, O.A., Nebral, K., von Neuhoff, N., et al. (2020). Phospho-Profilings Linking Biology and Clinics in Pediatric Acute Myeloid Leukemia. *Hemasphere* **4**, e312. <https://doi.org/10.1097/HS9.0000000000000312>.
56. Arber, D.A., Orazi, A., Hasserjian, R.P., Borowitz, M.J., Calvo, K.R., Kvasnicka, H.-M., Wang, S.A., Bagg, A., Barbuti, T., Branford, S., et al. (2022). International Consensus Classification of Myeloid Neoplasms and Acute Leukemias: integrating morphologic, clinical, and genomic data. *Blood* **140**, 1200–1228.
57. Tyner, J.W., Tognon, C.E., Bottomly, D., Wilmot, B., Kurtz, S.E., Savage, S. L., Long, N., Schultz, A.R., Traer, E., Abel, M., et al. (2018). Functional genomic landscape of acute myeloid leukaemia. *Nature* **562**, 526–531. <https://doi.org/10.1038/s41586-018-0623-z>.
58. Bottomly, D., Long, N., Schultz, A.R., Kurtz, S.E., Tognon, C.E., Johnson, K., Abel, M., Agarwal, A., Avaylon, S., Benton, E., et al. (2022). Integrative analysis of drug response and clinical outcome in acute myeloid leukemia. *Cancer Cell* **40**, 850–864.e9.
59. Lee, S.H.R., Yang, W., Gocho, Y., John, A., Rowland, L., Smart, B., Williams, H., Maxwell, D., Hunt, J., Yang, W., et al. (2023). Pharmacotypes across the genomic landscape of pediatric acute lymphoblastic leukemia and impact on treatment response. *Nat. Med.* **29**, 170–179. <https://doi.org/10.1038/s41591-022-02112-7>.
60. Huang, B.J., Smith, J.L., Farrar, J.E., Wang, Y.-C., Umeda, M., Ries, R.E., Leonti, A.R., Crowgey, E., Furlan, S.N., Tarlock, K., et al. (2022). Integrated stem cell signature and cytomolecular risk determination in pediatric acute myeloid leukemia. *Nat. Commun.* **13**, 5487.
61. Gentles, A.J., Plevritis, S.K., Majeti, R., and Alizadeh, A.A. (2010). Association of a leukemic stem cell gene expression signature with clinical outcomes in acute myeloid leukemia. *JAMA* **304**, 2706–2715.

62. Duployez, N., Marceau-Renaut, A., Villenet, C., Petit, A., Rousseau, A., Ng, S.W.K., Paquet, A., Gonzales, F., Barthélémy, A., Leprêtre, F., et al. (2019). The stem cell-associated gene expression signature allows risk stratification in pediatric acute myeloid leukemia. *Leukemia* *33*, 348–357.
63. Pollyea, D.A., and Jordan, C.T. (2017). Therapeutic targeting of acute myeloid leukemia stem cells. *Blood* *129*, 1627–1635.
64. Van Tilburg, C.M., Milde, T., Witt, R., Ecker, J., Hielscher, T., Seitz, A., Schenk, J.-P., Buhl, J.L., Riehl, D., Frühwald, M.C., et al. (2019). Phase I/II intra-patient dose escalation study of vorinostat in children with relapsed solid tumor, lymphoma, or leukemia. *Clin. Epigenetics* *11*, 188.
65. Goldberg, J., Sulis, M.L., Bender, J., Jeha, S., Gardner, R., Pollard, J., Aquino, V., Laetsch, T., Winick, N., Fu, C., et al. (2020). A phase I study of panobinostat in children with relapsed and refractory hematologic malignancies. *Pediatr. Hematol. Oncol.* *37*, 465–474.
66. Letai, A., Bholra, P., and Welm, A.L. (2022). Functional precision oncology: testing tumors with drugs to identify vulnerabilities and novel combinations. *Cancer Cell* *40*, 26–35.
67. Irmisch, A., Bonilla, X., Chevrier, S., Lehmann, K.-V., Singer, F., Toussaint, N.C., Esposito, C., Mena, J., Milani, E.S., Casanova, R., et al. (2021). The Tumor Profiler Study: integrated, multi-omic, functional tumor profiling for clinical decision support. *Cancer Cell* *39*, 288–293.
68. Casteels, T., Bajew, S., Reiniš, J., Enders, L., Schuster, M., Fontaine, F., Müller, A.C., Wagner, B.K., Bock, C., and Kubicek, S. (2022). SMNDC1 links chromatin remodeling and splicing to regulate pancreatic hormone expression. *Cell Rep.* *40*.
69. Abdulla, W. Mask R-CNN for object detection and instance segmentation on Keras and TensorFlow. [https://github.com/matterport/Mask\\_RCNN](https://github.com/matterport/Mask_RCNN).
70. Kromp, F., Bozsaky, E., Rifatbegovic, F., Fischer, L., Ambros, M., Berneder, M., Weiss, T., Lazic, D., Dörr, W., Hanbury, A., and Beiske, K. (2020). An annotated fluorescence image dataset for training nuclear segmentation methods. *Sci. Data* *7*, 262.
71. Gunesli, G.N., Sokmensuer, C., and Gunduz-Demir, C. (2020). Attention-Boost: Learning what to attend for gland segmentation in histopathological images by boosting fully convolutional networks. *IEEE Trans. Med. Imaging* *39*, 4262–4273.
72. Korfhage, N., Muehling, M., Ringshandl, S., Becker, A., Schmeck, B., and Freisleben, B. (2020). Detection and segmentation of morphologically complex eukaryotic cells in fluorescence microscopy images via feature pyramid fusion. *PLoS Comput. Biol.* *16*, e1008179.
73. Caicedo, J.C., Goodman, A., Karhohs, K.W., Cimini, B.A., Ackerman, J., Haghighi, M., Heng, C., Becker, T., Doan, M., McQuin, C., and Rohban, M. (2019). Nucleus segmentation across imaging experiments: the 2018 Data Science Bowl. *Nat. Methods* *16*, 1247–1253.
74. Reichl, S., Ergüner, B., Barreca, D., Folkman, L., Dobnikar, L., and Bock, C. (2024). Ultimate ATAC-Seq Data Processing & Quantification Pipeline (v1.1.0) (Zenodo). <https://doi.org/10.5281/zenodo.11087225>.
75. Auwera, G.A., and O'Connor, B.D. (2020). Genomics in the cloud: using Docker, GATK, and (WDL in Terra).
76. Kim, S., Scheffler, K., Halpern, A.L., Bekritsky, M.A., Noh, E., Källberg, M., Chen, X., Kim, Y., Beyter, D., Krusche, P., and Saunders, C.T. (2018). Strelka2: fast and accurate calling of germline and somatic variants. *Nat. Methods* *15*, 591–594.
77. Chen, X., Schulz-Trieglaff, O., Shaw, R., Barnes, B., Schlesinger, F., Källberg, M., Cox, A.J., Kruglyak, S., and Saunders, C.T. (2016). Manta: rapid detection of structural variants and indels for germline and cancer sequencing applications. *Bioinformatics* *32*, 1220–1222.



## STAR★METHODS

### KEY RESOURCES TABLE

REAGENT or RESOURCE	SOURCE	IDENTIFIER
<b>Antibodies</b>		
CD117-PE	BD Biosciences	Cat# 555714; RRID:AB_396058
CD34-APC	BD Biosciences	Cat# 555714; RRID:AB_396058
CD3-FITC	BD Biosciences	Cat# 345763; RRID:AB_2811220
CD3-APC	BD Biosciences	Cat# 345767; RRID:AB_2833003
CD11a-APC	BD Biosciences	Cat# 550852; RRID:AB_398466
CD33-PE	BioLegend	Cat# 366608; RRID:AB_2566107
HLA-DR-FITC	BioLegend	Cat# 307604; RRID:AB_314682
CD13-PE	EXBIO Praha	Cat# 1P-396-T100; RRID:AB_10736238
<b>Critical commercial assays</b>		
CellTiter-Glo	Promega	Cat# G7573
Qiagen AllPrep DNA/RNA mini kit	Qiagen	Cat# 80204
Twist Library Preparation EF Kit	Twist Biosciences	Cat# 104207
Tagment DNA TDE1 Enzyme and Buffer Kits	Illumina	Cat# 20034198
<b>Deposited data</b>		
Healthy reference ATAC-seq data from Corces et al.	Gene Expression Omnibus	GEO: GSE74912
ATAC-seq data from this study	Gene Expression Omnibus	GEO: <a href="https://www.ncbi.nlm.nih.gov/geo/query/acc.cgi?acc=GSE282258">GSE282258</a>
RNA-seq data from this study	Gene Expression Omnibus	GEO: <a href="https://www.ncbi.nlm.nih.gov/geo/query/acc.cgi?acc=GSE282423">GSE282423</a>
Exome sequencing data from this study	European Genome Phenome Archive	EGA: EGAD50000001572
<b>Software and algorithms</b>		
Code repository for main analyses in this study	GitHub	DOI: <a href="https://doi.org/10.5281/zenodo.16368448">https://doi.org/10.5281/zenodo.16368448</a>
Code repository for image-based screening pipeline	GitHub	DOI: <a href="https://doi.org/10.5281/zenodo.16330001">https://doi.org/10.5281/zenodo.16330001</a>
Code repository for models to predict cell types and cell viabilities	GitHub	DOI: <a href="https://doi.org/10.5281/zenodo.16330095">https://doi.org/10.5281/zenodo.16330095</a>
<b>Other</b>		
SpectraMax i3 plate reader	Molecular Devices	N/A
Opera Phenix High Content Screening System	Perkin Elmer	RRID:SCR_021100

### EXPERIMENTAL MODEL AND STUDY PARTICIPANT DETAILS

Fresh-frozen samples of primary bone-marrow mononuclear cells (MNCs) were acquired from the biobank of the St. Anna Children's Hospital Vienna, Austria covering a total of 45 patients. All patients or their respective legal guardians gave written informed consent prior to the study. Samples are standardized to contain 10 million MNCs per vial. Fresh samples for testing and optimization of 5 additional patients aged 0–18 years were taken from leftover material that was obtained during routine diagnostic procedures. Of these, one sample with the ID fAML01 was used for assessing correlations between Image-based viability assessment and CellTiterGlo, two samples with the IDs fAML02 and fAML03 were additionally used for viability model training and two samples with the IDs pAML01 and pAML02 were additionally used to train the cell type model. These samples were only used for the technical benchmarking in this study and thus not subjected to further characterization. All samples were acquired under the appropriate ethics approval by the independent ethics committee of the Medical University of Vienna (institutional review board vote No.1500/2014). Patients were aged 0–18 years at the time of sample acquisition, selected in a gender- and sex-balanced fashion ( $n = 20$  female,  $n = 25$  male) and are of European descent. More information on individual samples can be found in [Table S2](#).

### METHOD DETAILS

#### Drug treatment

Screening plates were acquired from the Molecular Discovery Platform of the Center for Molecular Medicine of the Austrian Academy of Sciences (CeMM) and stored at  $-80^{\circ}\text{C}$  until screening.

Every sample was screened on two screening plates spotted with a total of 115 compounds in 3 concentrations and duplicates. All compounds were dissolved in DMSO. Additionally, each plate contains 32 control wells spotted with DMSO. Compounds were spotted onto plates in a randomized layout. Plates were thawed in the dark for 3 h before screening.

Bone-marrow mononuclear cells (MNCs) were either thawed from frozen vials or isolated from fresh bone marrow via Ficoll gradient separation. Subsequently, cells were resuspended in IMDM with 10% FCS and 1% Penicillin and Streptomycin and seeded onto plates at a density of 9,000 cells per well and incubated at 37°C with 5% CO<sub>2</sub> for 24 h.

Additional drug treatment for benchmarking of Pharmacoscopy and CellTiterGlo (Figure 1G) was performed using the compounds described in the respective figure in quadruplicates at concentrations of 10 nM, 100 nM, 1 μM and 10 μM.

### Staining and image acquisition

Treatment incubation was stopped by adding 15 μL of fixation-permeabilization buffer (PBS with 0.5% Formaldehyde, 0.1% X-114), incubating for 15 min and subsequently washing three times with PBS. Then, 15 μL of PBS were added to all wells. Subsequently, cells were stained with sample specific staining solution containing 10 mM solutions of DAPI and Hoechst in a concentration of 1:1500 each, leading to a total concentration of 1:750, and the appropriate antibody cocktail to among the following antibodies: CD117-PE (BD Biosciences Cat# 555714, RRID:AB\_396058), CD34-APC (BD Biosciences Cat# 345804, RRID:AB\_2686894), CD3-FITC (BD Biosciences Cat# 345763, RRID:AB\_2811220), CD3-APC (BD Biosciences Cat# 345767, RRID:AB\_2833003), CD11a-APC (BD Biosciences Cat# 550852, RRID:AB\_398466), CD33-PE (BioLegend Cat# 366608, RRID:AB\_2566107), HLA-DR-FITC (BioLegend Cat# 307604, RRID:AB\_314682), CD13-PE (EXBIO Praha Cat# 1P-396-T100, RRID:AB\_10736238). The antibodies for CD3 and CD13 were added in a concentration of 1:150. CD11a was added in a concentration of 1:200. All other antibodies were added in a concentration of 1:250. 15 μL of staining solution were added to each well. The first plate was incubated for 6 h at room temperature and the second one overnight at 4°C until imaging with 4 h at RT before imaging for the second plate. Images were acquired with a PerkinElmer Opera Phenix microscope at 20× resolution, leading to 25 images at a resolution of 1080x1080 pixels, covering the full well for each well and each channel.

Viability staining was performed with Live-or-Dye fixable viability staining kit (Biotium, San Francisco, CA, USA) according to the manufacturer's recommendations. In brief, cells were washed 2× with PBS. Subsequently, 15 μL of viability dye solution at a concentration of 1:300 was added to each well. After 30 min of incubation away from light, cells were prepared for imaging as described in before in this paragraph.

### Image analysis

After image acquisition and export, images were analyzed with CellProfiler (v4.2.1, RRID:SCR\_007358).<sup>68</sup> We added custom modules for nuclear segmentation - described further below - and gamma correction with corresponding function from the scikit-image library (v0.18.1). CellProfiler outputs were written to sqlite databases for further analyses. Subsequently, we performed quality control by first excluding images that were likely to be improperly stained by excluding wells with average intensities at least 4 standard deviations away from the average well intensity for each imaged channel. Furthermore, we excluded artifacts and improperly segmented cells by thresholding on morphological descriptors for intensity, texture and cell-shape. After this QC step, we applied our AAE models for cell type and viability prediction as described in the following section. Our pipeline then enumerated all viable cells for each marker and wrote them into a single table for further analysis. More details can be found in the code repository referenced in the data and code availability section.

### Nucleus segmentation and segmentation model training

We adapted a Mask-R-CNN implementation<sup>35,69</sup> with pre-trained ImageNet weights for nucleus segmentation and compiled a custom training dataset from 4 different sources<sup>70–73</sup>, as well as a small selection of images that were annotated in-house. The training dataset comprises a total of 1523 images and 43519 nuclei. We randomly split the dataset into 80% training images and 20% testing images, subsequently trained the model for 100 epochs and picked the weights from the epoch with the lowest combined loss value on the testing dataset as our final model for further segmentation tasks.

### Cell type prediction

To train a predictive model to classify cells by their marker expression profile, we generated an in-house dataset comprising of 16553 cells imaged over 550 fields of view from 11 samples. Samples were selected to cover all cell surface markers that were stained across the full cohort. We then randomly sampled 50 image patches with sizes of 500x500 pixels per plate and manually annotated cells as positive or negative for the given markers using the VGG image annotator. Subsequently, we trained an adversarial autoencoder (AAE) with hyperparameter optimization to derive a model that predicts marker positivity from image data. Our model receives two-channel patches with a size of 32x32 pixels as input that contain the DAPI channel and the current channel of interest. Models were trained with tensorflow (v2.11.0) and keras (v2.11.0). Model hyperparameter optimization was performed with keras-tuner (v1.1.0).

### Viability prediction

We performed automated labeling of nuclei for semi-supervised viability learning based on morphology and viability dye intensity jointly. Assuming that distinct cell-subpopulations have different protein contents, and will therefore have different viability dye

intensities, we first performed UMAP dimensionality reduction of nuclei morphology features, followed by unsupervised clustering of nuclei in the reduced feature space using HDBSCAN (v0.8.38.post2). Subsequently, we fit Gaussian mixture models comprised of two independent Gaussian distributions on the viability dye intensities for each cluster. To finally derive high-confidence labels of cell viability, we performed two additional filtering steps. First, we only assigned labels to cells that were at least 3 standard deviations away from the respective positive or negative distribution respectively. Then, we fit a K nearest neighbors (KNN) model on the data using the distribution fits as labels, and only kept labels were distribution fits and KNN clusters agreed with each other. The model was then trained on 1000 randomly sampled fields of view from 5 samples, yielding roughly 1.8 million cells with a labeling rate of 29.5%.

### Hyperparameter optimization for adversarial autoencoders

We performed hyperparameter optimization using keras-tuner (v1.1.0) with Bayesian optimization on patches of a size 32x32 pixels for an adversarial autoencoder with a set of convolutional layers, followed by dense layers with 500 neurons and used the following hyperparameter ranges: Number of dense layers: 2,3; z-dimensionality:25,100,500; Number of filters per convolutional layer: [16, 128, 16, 128, 16], [128, 16, 128, 16, 128], [128, 128, 64, 64, 16], [128, 128, 64, 64, 16, 16], [128, 64, 128, 16, 64, 16], [16, 16, 64, 64, 128], [16, 16, 64, 64, 128, 128], [16, 16, 128, 128, 128]; class learning rate: 0.0001, 0.00001; Optimizer: Adam, Nadam; Augmentation: Flip only, flip and random brightness changes. We additionally set a dropout rate of 0.2. We subsequently selected the architecture with the lowest classification loss. The final architecture for cell type prediction had a z-dimensionality of 100, a learning rate of  $10^{-4}$  a filter size of 3, 3 dense layers, used the Nadam optimizer, had [16,128,16,128,16] filters and was trained with flipping only. The final architecture for viability prediction had a z dimensionality of 25, a learning rate of  $10^{-4}$  a filter size of 5, 2 dense layers, used the Adam optimizer, had [16, 16, 128, 128, 128] filters and was trained with flipping only.

### Benchmarking of image-based screening and CellTiterGlo data

Cells were incubated in compound concentrations ranging from 10 nM to 10  $\mu$ M in quadruplicates for 24 h in different densities ranging from 9000 cells per well to 2250 cells per well. Treatment was performed in two 384 well plates per experiment. After the incubation period, CellTiterGlo (Promega) was performed according to the manufacturer's protocol. Fluorescent viability readouts were measured on a plate-reader (SpectraMax i3, Molecular Probes). Image-based screening was performed in parallel as described above.

### Processing of dose response values and compound activity scoring

Dose response values were first filtered for outliers by filtering wells with total cell numbers that were more than 4 standard deviations higher than the average number in the DMSO control. Subsequently, we filtered out outlier replicate values, by filtering out values that were 50% above the average value for the previous concentration point. We additionally filtered out concentrations with more than a 50% difference between replicates.

We scored compound activity using an approximate area under the curve (AUC) metric. First, we used linear interpolation to map all dose response values to the same concentration range. Then, we calculated relative blast fractions (RBFs) for each treated condition as described previously,<sup>26,27</sup> by dividing the viable blast fraction in treated wells by the mean viable blast fraction in negative control wells. Subsequently we calculated the approximate AUC by integrating over the average RBFs per concentration point and calculated the final RBF-AUC inhibition score as  $1 - \text{AUC}$ , such that higher values indicate stronger inhibitions. We fit dose-response curves as shown in [Figure 3](#) using a 3-parameter dose response model and normalized absolute blast fractions to the average of the negative DMSO control. RBF-AUC values were scaled by subtracting the mean and dividing by the standard deviation for cohort-level depictions such as [Figures 4, 5, and 6](#). Absolute response values - denoted as Blast AUC as shown in [Figure S4B](#) - were calculated analogously, but instead of dividing the viable fraction of blasts in treated wells by the mean viable blast fraction in negative control wells, we divided the absolute number of viable blasts in treated wells, by the mean absolute number of viable blasts in negative control wells, thus ignoring non-malignant populations.

### Drug-drug correlation analysis

To derive the most robust drug-drug pairs for subsequent correlation analysis, we first filtered for drugs with at least approximately 50% inhibition in at least 3 samples, by only keeping drugs with a Blast AUC value of 0.25 or higher in at least 3 samples. This analysis led to 58 of 115 drugs or combinations being kept. We quantified strength of correlation with Spearman correlation coefficients for each drug pair. For the analysis of correlation by drug-class, we manually annotated drugs to their respective classes ([Table S2](#)) and subsequently kept all pairs of classes where all drug-pairs between the two classes have either positive or negative Spearman Correlation coefficients.

### Immunophenotyping for identification of markers for leukemic blasts

Immunophenotyping has been performed at diagnosis on erythrocyte-lysed whole bone marrow (BM) samples using multiparameter flow cytometry (MFC). As in our previous work, we used a 10-color format cocktail across two tubes<sup>34</sup>: Tube 1 included HLA-DR, CD45, CD15, CD34, CD117, CD33, CD14, and CD11b, while Tube 2 contained HLA-DR, CD45, CD38, CD371, CD34, CD117,

CD33, CD99, CD123, and CD45RA. Patient-specific LAIP antigens, such as lymphoid markers (e.g., CD2, CD4, CD7, CD19, CD56) or other aberrant markers (e.g., CD11a, CD13, CD71, CD99, NG2), were included as “drop-ins” only in tube 1.

### FACS staining for cell sorting

Cells were washed using PBS with 2% FBS. After spinning down at 400g for 8 min at either room temperature or 4°C, the supernatant was removed, and the cells were resuspended in 300  $\mu$ L of PBS/2% FBS. Of this suspension, 250  $\mu$ L was transferred to a filter-cap FACS tube (Ref. nr. 352235). Patient-specific markers for leukemic blasts together with CD3, CD19 and CD45 were used to sort normal CD3 T cells or CD19 B cells and leukemic blasts. Following a brief vortex and 15-min incubation at room temperature in the dark, the cells were washed once, and the supernatant was removed. The cells were resuspended in PBS/2% FBS/25 mM HEPES and sorted using a FACS Aria (BD Biosciences) cell sorter.

### Cell number and cell viability assessment via flow cytometry

For determining absolute cell numbers and viability we used Trucount tubes (BD Biosciences) in conjunction with 7-AAD and CD45 staining as well as with antibodies for identification of leukemic blasts (as identified with immunophenotyping, i.e., CD117, CD34 or CD33) as well as normal T cells (CD3). Measurements were conducted on a FACS Symphony (BD Biosciences) analyzer.

### Transcriptome, exome and accessible chromatin sequencing

RNA and DNA from FACS isolated blasts and DNA healthy lymphoid cells were isolated using the Qiagen AllPrep DNA/RNA mini kit (Cat. No 80204) according to the manufacturer’s protocol. Amplification of cDNA was performed using the SmartSeq2 protocol. Library construction was performed using the Twist Library Preparation EF Kit (Twist Biosciences). DNA for ATAC-seq was isolated from 50,000 sorted blasts using the Tagment DNA TDE1 Enzyme and Buffer Kits (Illumina, CA, USA) RNA from isolated blasts.

### mRNA sequencing data analysis

We merged the unaligned.bam files using Picard v3.0.0 (RRID:SCR\_006525) and extracted UMI sequences for each read from “BC” tags (which contained sample index reads and UMIs) into “RX” tags using a custom Python script. We converted the unaligned.bam files to.fastq format using Picard v3.0.0, filtered according to quality and length with fastp v0.23.3, and aligned to the GRCh38 genome reference (Ensembl v102) with STAR v2.7.10. We then sorted the aligned reads using Picard v3.0.0, and transferred the RX tags containing the UMI sequences from the unaligned to the aligned.bam files using GATK v4.4.0. We added read mate information, grouped reads by UMIs, and called molecular consensus sequences using fgbio v2.1.0, then converted the resulting.bam files to.fastq format using SAMtools v1.17 (RRID:SCR\_002105) and subsequently quantified read counts using Salmon v1.9.0 in mapping based mode against a salmon index built from the GRCh38 transcriptome.

### ATAC-seq analysis

ATAC-seq data was analyzed as described in Casteels et al.<sup>68,74</sup> In brief, sequence adapter trimming and initial filtering were performed with fastp v0.20.1 and alignments to the GRCh38 human reference genome were performed using bowtie2 v2.4.4 with the `-very-sensitive` parameter. PCR duplicates were marked using Samblaster v0.1.24. Sorting, filtering of ENCODE blacklisted regions and subsequent indexing was performed using samtools v1.12 and peaks were called using MACS2 v2.2.7.1. Only samples with at least 40% of mapped reads, a duplication rate below 50% as detected via Samblaster and fractions of reads in peaks as detected by MACS2 of more than 10% were considered for further downstream analysis. Identified peak summits were then merged to generate a consensus region set. This analysis was performed for the dataset from this study and the healthy reference dataset from Corces et al.<sup>44</sup> independently, and reads from this study were subsequently quantified for the consensus regions derived from the healthy reference. Subsequent unsupervised analyses were performed on CQN normalized read counts using the CQN package and trimmed mean of M normalized library sizes as provided by the edgeR package. Batch correction was performed using reCombat.

### WES analysis

Raw sequencing reads were processed using the nf-core sarek WES pipeline version 2.7.2. Variant calling was conducted in a tumor-normal matched mode, utilizing CD3 or CD19 FACS-sorted cells as the matched normal samples. Three variant callers - Mutect2<sup>75</sup>, Strelka<sup>76</sup>, and Manta<sup>77</sup> - were employed for comprehensive variant identification. The resulting VCF files from Mutect2 and Strelka (following the best practices workflow) were normalized using bcftools norm (bcftools v1.9) and subsequently annotated with the Ensembl Variant Effect Predictor (VEP) (VEP v99.2). A coordinate-based filtering was conducted using the start and end coordinates of genes listed in an in-house AML gene panel.

### Predictions of healthy cell types and clinical variables

Predictive models for mapping to healthy references and for clinical variables were implemented using the scikit-learn (v1.3.2). Random Forest models for clinical variable prediction were initialized with balanced class weights, without bootstrapping and with 101 estimators. Support vector machines for healthy cell type prediction were initialized with radial-basis function kernels and balanced class weights on the 1000 most variable consensus regions.

### **QUANTIFICATION AND STATISTICAL ANALYSIS**

All statistical tests were performed using scipy (v1.13.0) in Python (v3.11.6). Significance of differences between quantitative measurements was assessed using the Mann-Whitney-U test unless otherwise indicated. Multiple testing correction was performed using Bonferroni correction unless otherwise indicated.

### **ADDITIONAL RESOURCES**

Risk stratification for samples in this study was performed according to the criteria established by the AIEOP-BFM-AML consortium: EUCT: 2022-500783-35-00.

Cell Reports Medicine, Volume 6

## Supplemental information

### **Image-based drug screening combined with molecular profiling identifies signatures and drivers of therapy resistance in pediatric AML**

**Ben Haladik, Margarita Maurer-Granofszky, Peter Zoescher, Raul Jimenez-Heredia, Alexandra Frohne, Anna Segarra-Roca, Chloe Casey, Felix Kartnig, Sarah Giuliani, Christina Rashkova, Peter Repiscak, Michael N. Dworzak, Giulio Superti-Furga, and Kaan Boztug**

# Supplementary Figures

## Figure S1

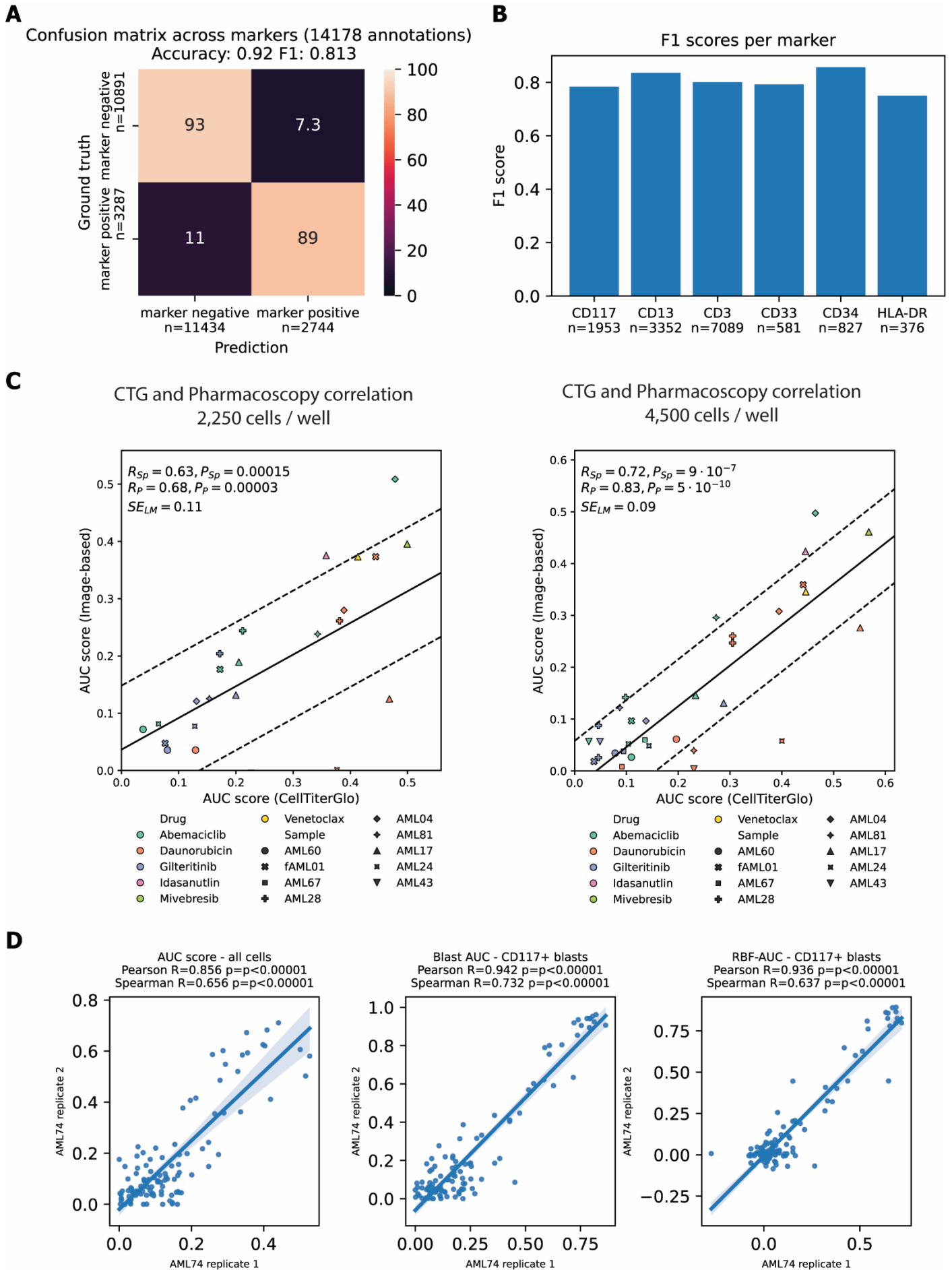


**Figure S1: Pharmacoscopy technical benchmarkings. Related to Figure 1**

**A** Confusion matrix for marker-positivity across all cells in the testing dataset for the celltype model. **B** Bargraph of F1 scores per surface antigen in the testing dataset. The bottom number indicates the number of cells **C** Left: Correlation between CTG inhibition scores and Pharmacoscopy inhibition scores for 6 drugs and 9 samples for a cell-density of 2.250 cells per well. Right: same as left, but with 4.500 cells per well. **D** Correlation between replicates across readouts for the AUC score on all cells (left), target cells only (middle) and the RBF-AUC score (right).



**Figure S2**

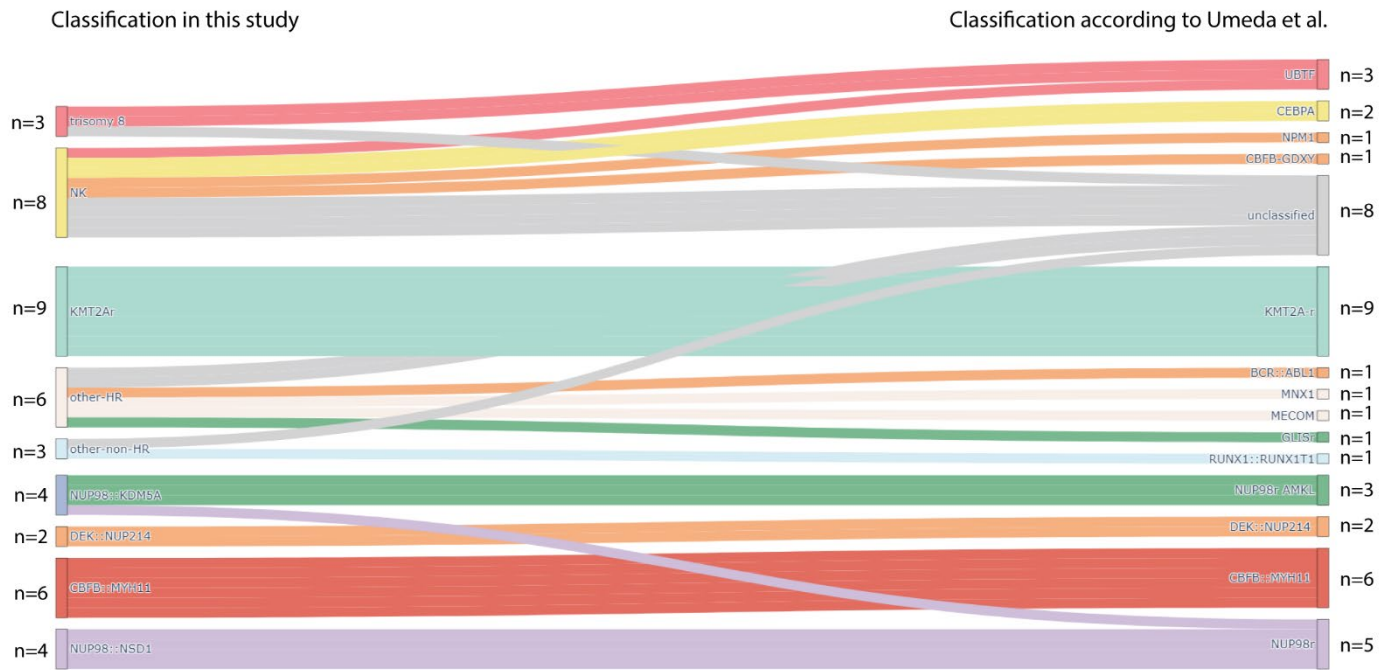


**Figure S2: Molecular re-classification of our cohort. Related to Figure 2**

Sankey chart indicating matchings between the classification in this study for the n=45 samples in our cohort and the classification in Umeda et al.

Figure S3

AML37 - *KMT2A::MLLT1*

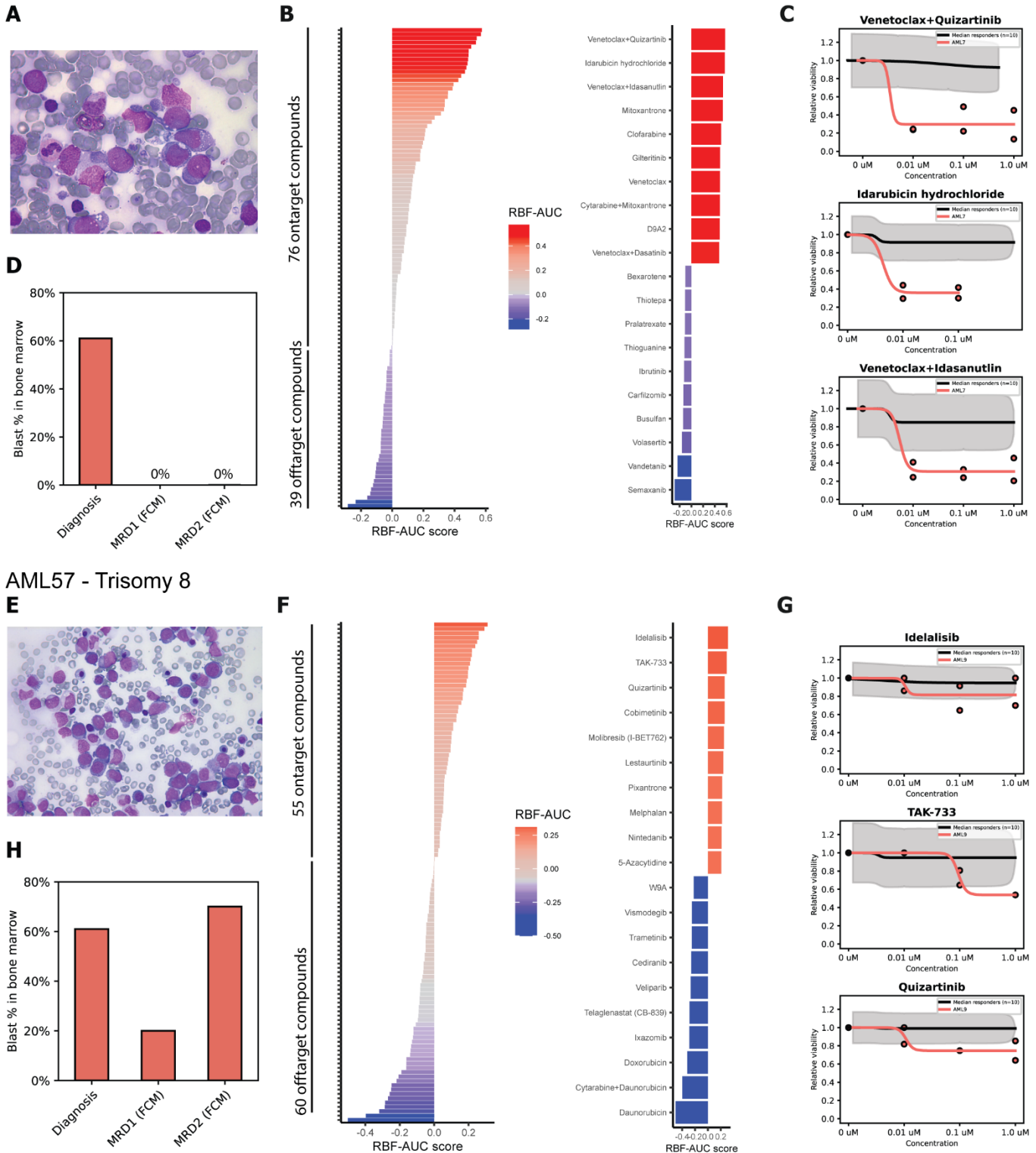


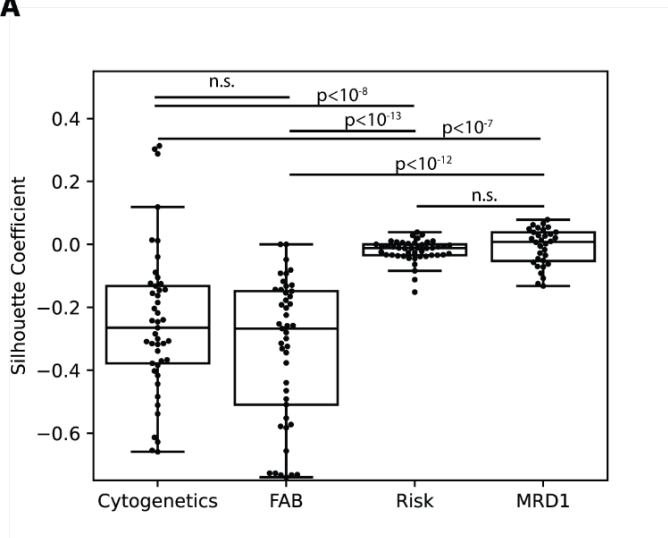
Figure S3: Case vignettes illustrating our drug sensitivity profiling reporting format. Related to Figure 3

**A** Bone marrow smear of sample AML37 (good responder). The patient had a monoblastic M5a phenotype and a *KMT2A::MLLT1* fusion. **B** Left: Bar chart of RBF-AUC scores for all tested compounds. Right: Bar chart of RBF-AUC scores for the 10 compounds with the highest and lowest RBF-AUC scores respectively and the induction regimen drugs Idarubicin and Mitoxantrone among the top 10 compounds. **C** Dose response curves for the patient (red) and 10 patients with RBF-AUC scores closest to the median score for the respective drug. Lines indicate the fit of the dose response curve. Dots indicate blast viability relative to the average of the DMSO control for each replicate after QC. The shaded grey area indicates the standard deviation around the curve fit for the 10 median responders. **D** Barplots of blast percentages at diagnosis and at MRD time points after induction 1 and 2 as determined by flow-cytometry (FCM) indicating complete response after the first induction cycle. **E** Bone marrow smear of sample AML57 (poor responder). The patient had an M2 phenotype, trisomy and mutations in *NRAS*, *WT1*, and *FLT3* **F** Barplots of RBF-AUC scores analogous with induction compounds Daunorubicin, Doxorubicin and the combination of

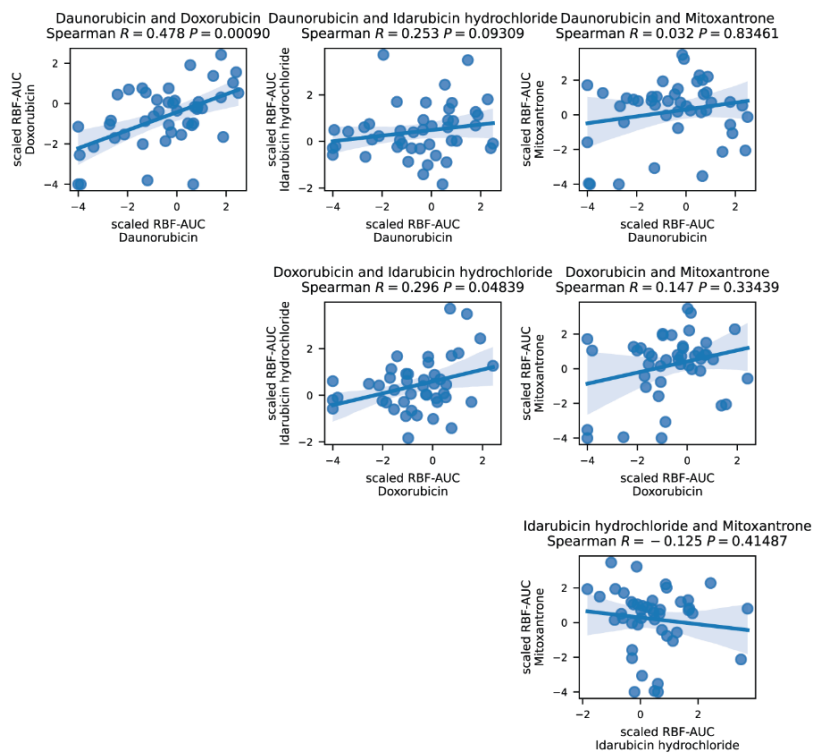
Cytarabine and Daunorubicin among the lowest scoring drugs analogous to **B**. **G** Dose response curves for top 3 drugs analogous to **C**. **H** Barplots of blast percentages at diagnosis and at MRD time points analogous to **D** indicating highly resistant disease.

**Figure S4: Clustering analysis of chemosensitivities**

**A**



**B**



**C**

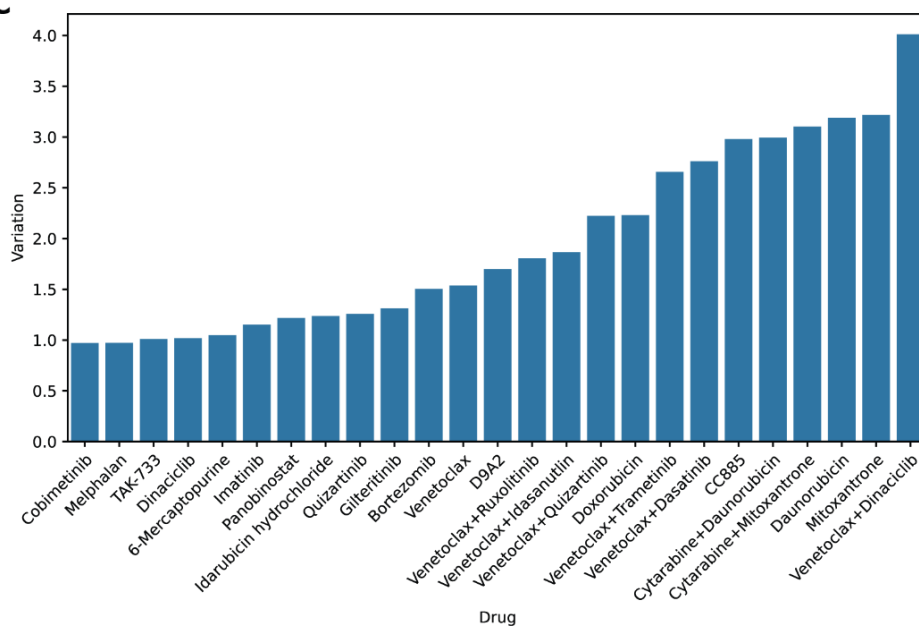


**Figure S4: Clustering analysis of chemosensitivities. Related to Figure 3**

**A** Silhouette coefficients of drug sensitivities per sample based on sample classification by cytogenetic group (n=45), FAB classification (n=45), risk group (n=45), and MRD status (n=32) respectively. P-values calculated with Mann-Whitney-U test. Dots indicate individual samples. Boxes represent quartiles. Whiskers extend to points that are within 1.5 interquartile ranges. **B** Correlations of RBF-AUC scores for selected chemotherapeutics for the n=45 samples profiled in this study. Individual dots indicate the scaled RBF-AUC score for individual samples and the respective compounds. Lines indicate a linear model fit. Shaded areas around lines indicate the 95% confidence interval. **C** Variation per compound for the 25 most variable compounds.

Figure S5

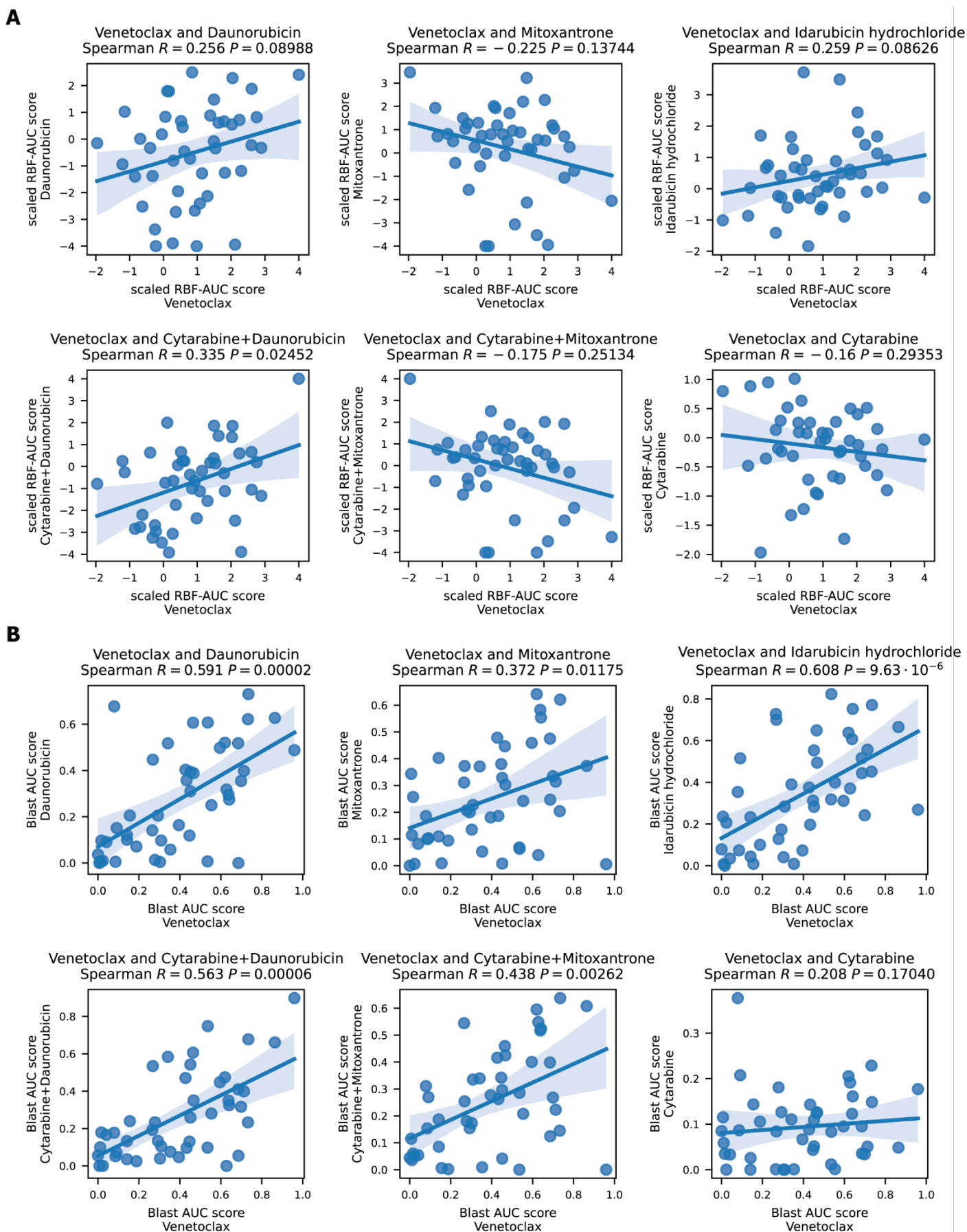


Figure S5: Correlation of Venetoclax and selected chemotherapeutic agents. Related to Figure 3

A Scatterplots and Spearman correlations between Venetoclax on the horizontal axes and selected chemotherapy compounds on the vertical axes for  $n=45$  samples in the cohort. Individual dots indicate the scaled RBF-AUC score for individual samples and

the respective compounds. Lines indicate a linear model fit. Shaded areas around lines indicate the 95% confidence interval. **B** Same as A, but dots indicate the absolute AUC score that only reflects responses of the blast population (Methods).

Figure S6

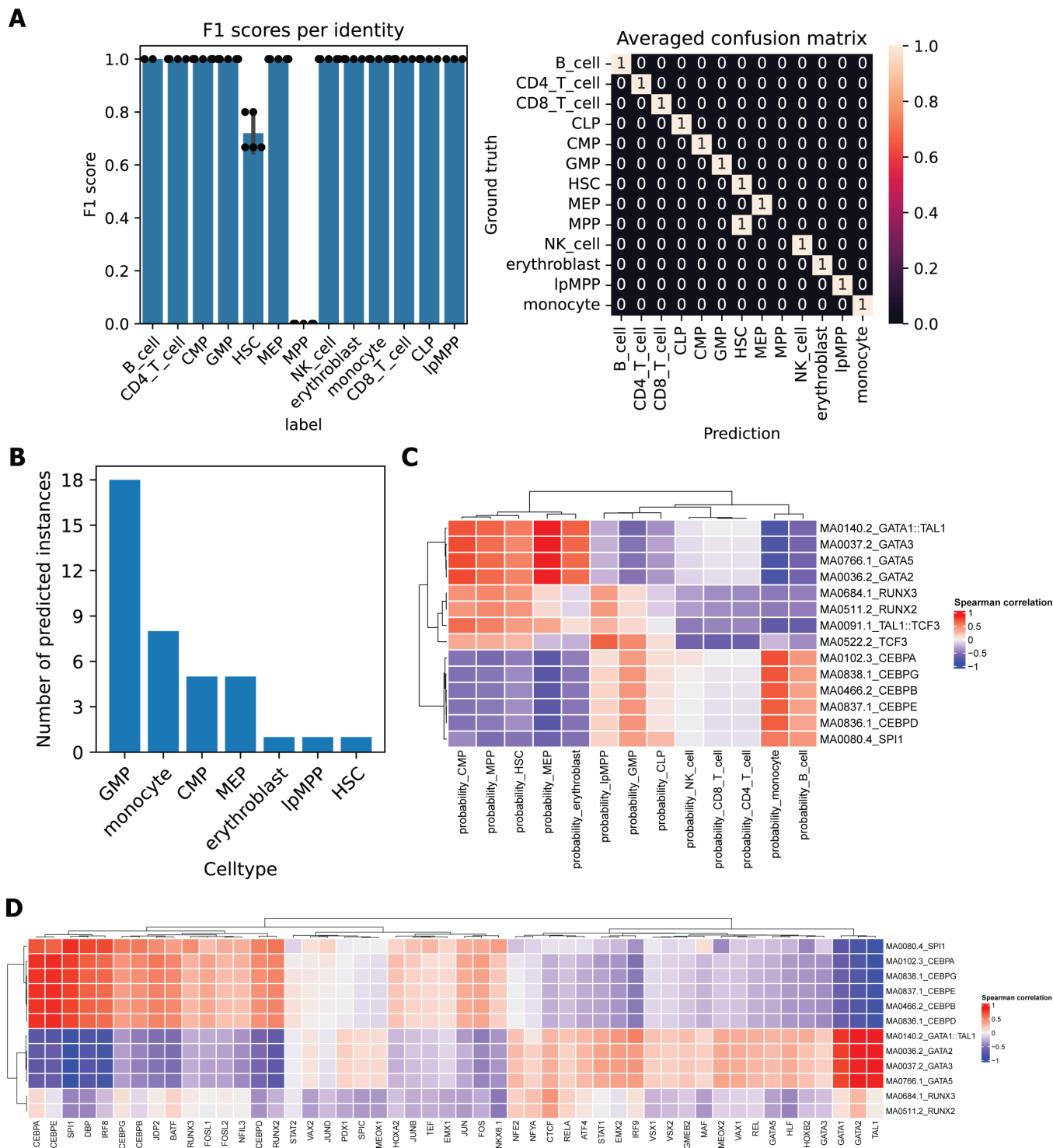
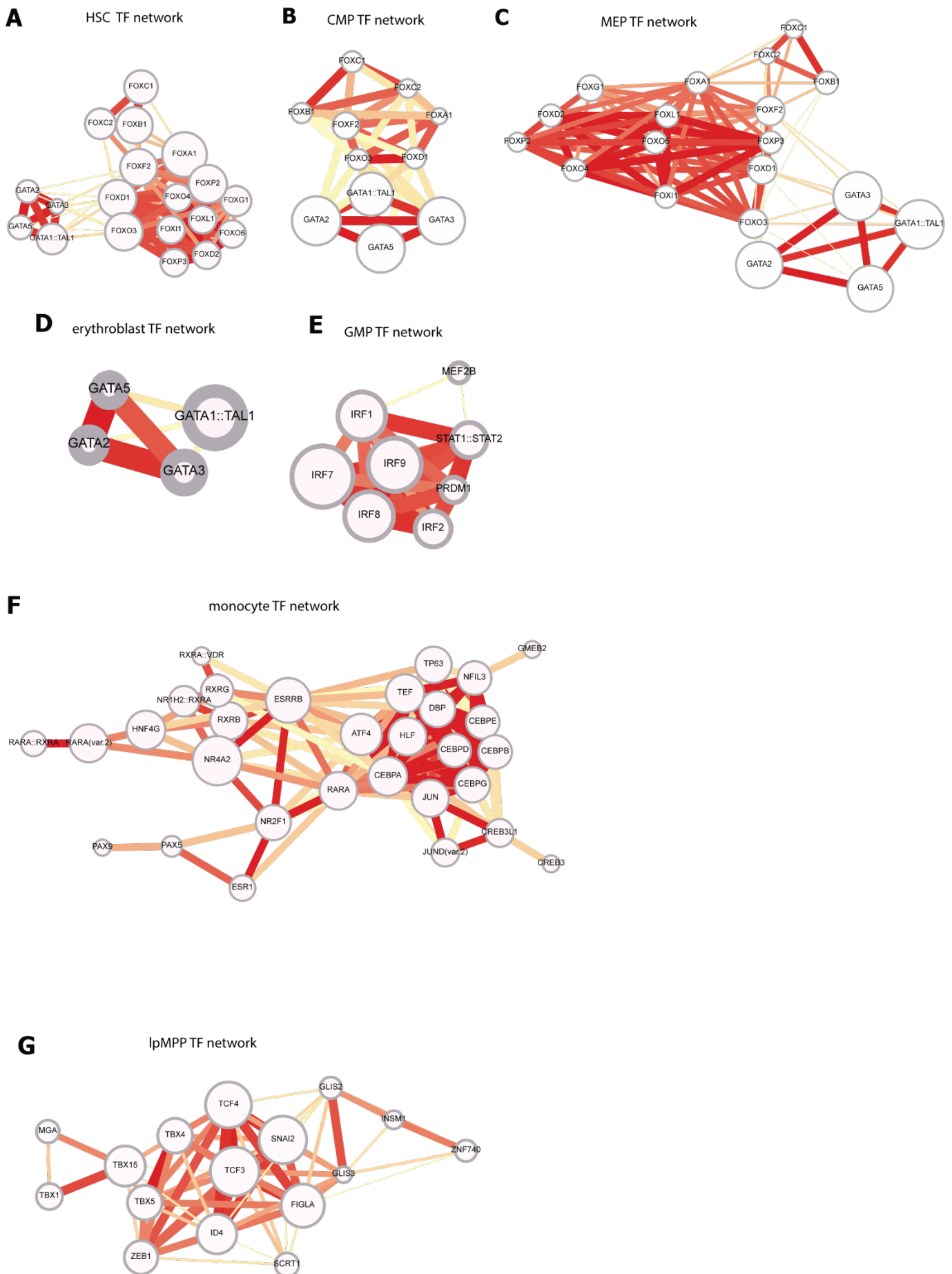


Figure S6: Mapping pedAML samples to their most similar healthy cell-types. Related to Figure 5

**A** Performance of the support vector classifier. Left: F1 scores per run and celltype in 5-fold cross-validation. Dots indicate F1 scores per run. Bar heights indicate mean F1 scores over all folds. Error bars indicate 95% confidence intervals. Right: Averaged confusion matrix over all runs. **B** Numbers of predicted healthy cell-types for samples in the ExTrAct-cohort. **C** Clustered heatmap of Spearman correlations for predicted probabilities of healthy cell-types and chromVAR deviation scores of key hematopoietic transcription factors **D** Spearman rank correlation for chromVAR scores for TF motifs from Supplementary Figure S4B and normalized expression levels of key hematopoietic transcription factors



**Figure S7**



**Figure S7: Transcription factor activity networks for predicted cell states. Related to Figure 5**

Networks represent the largest connected component correlating TF-activities that are significantly associated with the respective cell states for the n=38 samples with ATAC-seq data after QC. Node sizes are proportional to correlation between TF activity and

cell state probability. Edges represent Spearman correlations of at least 0.8 between individual TF activities (STAR methods). Edge widths and colors are proportional to correlation value. **A** HSC TF network. **B** CMP TF network. **C** MEP TF network. **D** erythroblast TF network. **E** GMP TF network. **F** monocyte TF network. **G** lpMPP TF network.

**Figure S8**

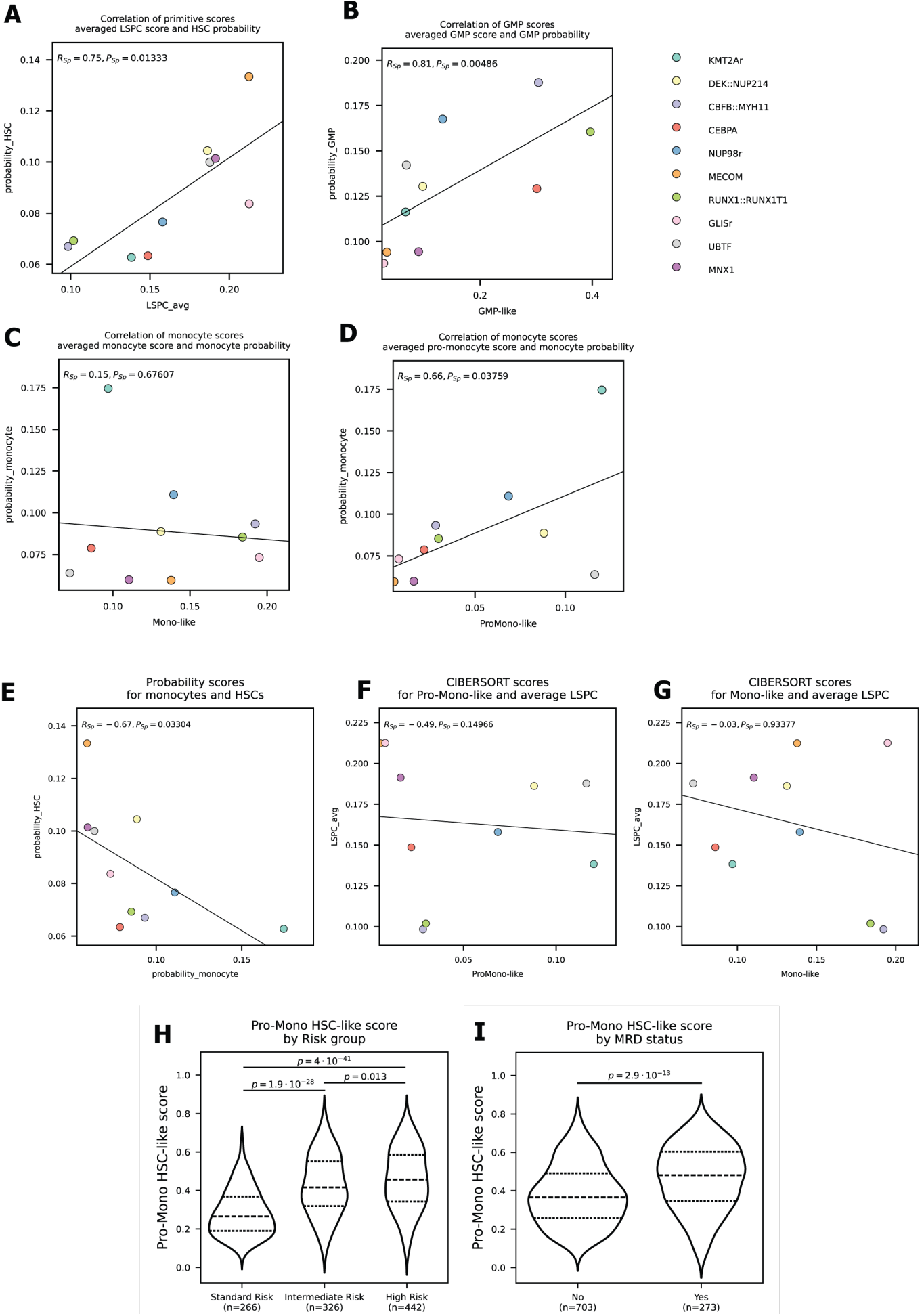


**Figure S8: Validation analysis of cell type differentiation states. Related to Figure 5**

**A-D** CIBERSORT scores from Umeda et al (x-axis) plotted against probabilities for cell differentiation states from this study (y-axis). Dots indicate median values per genetic subtype for *KMT2Ar* (n=6 this study; n=236 Umeda et al.), *DEK::NUP214* (n=2 this study, n=17 Umeda et al.), *CBFB::MYH11* (n=6 this study, n=102 Umeda et al.), *CEBPA* (n=2 this study, n=63 Umeda et al.), *NUP98r* (n=5 this study, n=77 Umeda et al.), *MECOM* (n=1 this study, n=11 Umeda et al.), *RUNX1::RUNX1T1* (n=1 this study, n=141 Umeda et al.), *GLISr* (n=1 this study, n=20 Umeda et al.), *UBTF* (n=2 this study, n=45 Umeda et al.), *MNX1* (n=1 this study, n=4 Umeda et al.) Black lines indicate linear model fit regression line. **A** Averaged LSPC CIBERSORT score and HSC probability **B** GMP-like CIBERSORT score and GMP probability **C** Mono-like CIBERSORT score and monocyte probability **D** Pro-Mono like CIBERSORT score and monocyte probability. **E-G** Dots and lines as in A-D. **E** HSC probability plotted against monocyte probability **F** averaged LSPC CIBERSORT score and Mono-like CIBERSORT score **G** averaged LSPC CIBERSORT score and Pro-Mono-like CIBERSORT score **H** Violin plot of Pro-Mono HSC score by AIEOP-BFM risk group **I** Violin plot of Pro-Mono HSC score by MRD status after induction 1. Widths are proportional to the number of samples within the corresponding value interval. Dashed lines in H and I separate the quartiles of the data.

**Figure S9**

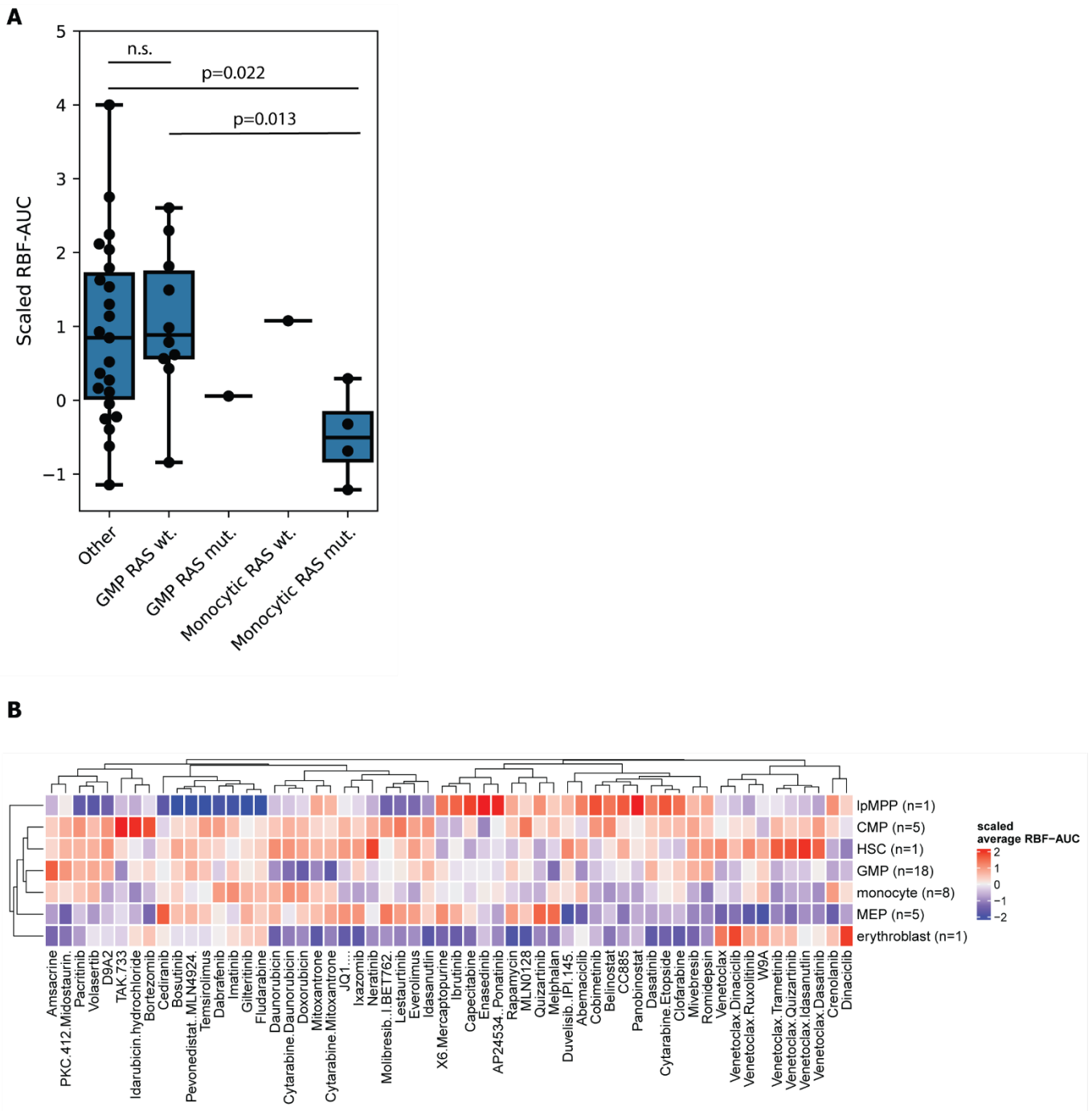


**Figure S9: Associations of drug response and cellular differentiation states. Related to Figure 5**

**A** Comparative analysis of Venetoclax response by RAS-mutation status and differentiation status for monocytic samples with mutated RAS (n=4), one monocytic sample with wild type RAS (n=1), one GMP-like sample with mutated RAS (n=1), GMP-like samples with wild type RAS (n=8) and samples that are neither GMP-like nor monocytic and have been termed Other (n=23). P-values were calculated using the Mann-Whitney-U Test. Dots indicate RBF-AUC values for individual samples. Boxes represent quartiles. Whiskers extend to points that are within 1.5 interquartile ranges. **B** Heatmap of scaled averaged RBF-AUC values for predicted differentiation states.

## Supplementary Tables

### Supplementary Table 1: Compound library overview. Related to Figure 1.

Compound	Compound MoA	Compound class	ConcPoint1 (micromolar)	ConcPoint2 (micromolar)	ConcPoint3 (micromolar)
Pentostatin	Adenosine deaminase inhibitor	Chemotherapeutic	1	0.1	0.01
Thiotepa	Alkylating agent	Chemotherapeutic	1	0.1	0.01
Palifosfamide	Alkylating agent	Chemotherapeutic	1	0.1	0.01
Busulfan	Alkylating agent	Chemotherapeutic	1	0.1	0.01
Melphalan	Alkylating agent	Chemotherapeutic	1	0.1	0.01
Aminopterin	Antimetabolite, Antifolate	Chemotherapeutic	1	0.1	0.01
Pralatrexate	Antimetabolite, Antifolate	Chemotherapeutic	0.7	0.07	0.007
Methotrexate	Antimetabolite, Antifolate	Chemotherapeutic	1	0.1	0.01
Doxorubicin	Antimetabolite, DNA intercalater	Chemotherapeutic	1	0.1	0.01
Idarubicin hydrochloride	Antimetabolite, DNA intercalater	Chemotherapeutic	1	0.1	0.01
Daunorubicin	Antimetabolite, DNA intercalater	Chemotherapeutic	1	0.1	0.01
Mitoxantrone	Antimetabolite, DNA intercalater, Topoisomerase 2 inhibitor	Chemotherapeutic	1	0.1	0.01
Pixantrone	Antimetabolite, DNA intercalater, Topoisomerase 2 inhibitor	Chemotherapeutic	1	0.1	0.01
Etoposide	Antimetabolite, DNA synthesis inhibitor	Chemotherapeutic	2	0.2	0.02
Hydroxyurea	Antimetabolite, DNA sythesis inhibitor, other effects	Chemotherapeutic	1	0.1	0.01
Amsacrine	Antimetabolite, DNA-intercalater	Chemotherapeutic	1	0.1	0.01
Thioguanine	Antimetabolite, Purines	Chemotherapeutic	1	0.1	0.01
6-Mercaptopurine	Antimetabolite, Purines	Chemotherapeutic	0.1	0.01	0.001
Clofarabine	Antimetabolite, Purines	Chemotherapeutic	1	0.1	0.01
Fludarabine	Antimetabolite, Purines	Chemotherapeutic	1	0.1	0.01
5-Fluorouracil	Antimetabolite, Pyrimidines	Chemotherapeutic	1	0.1	0.01
Cytarabine	Antimetabolite, Pyrimidines	Chemotherapeutic	1	0.1	0.01
Elacytarabine	Antimetabolite, Pyrimidines	Chemotherapeutic	1	0.1	0.01
Capecitabine	Antimetabolite, Pyrimidines	Chemotherapeutic	1	0.1	0.01
5-Azacytidine	Antimetabolite, Pyrimidines, Hypomethylating agent	Chemotherapeutic	3	0.3	0.03
Irinotecan	Antimetabolite, Topoisomerase 1 inhibitor	Chemotherapeutic	1	0.1	0.01
Venetoclax	BCL2-inhibitor	Cell death signaling (+/- Kinase inhibitor)	1	0.1	0.01
Molibresib (I-BET762)	BET inhibitor	Epigenetic	1	0.1	0.01
JQ1(+)	BET inhibitor	Epigenetic	0.96	0.096	0.0096
Mivebresib	BET inhibitor	Epigenetic	1	0.1	0.01
Venetoclax+Dasatinib	Combination	Cell death signaling (+/- Kinase inhibitor)	0.5+0.5	0.05+0.05	0.005+0.005
Venetoclax+Ruxolitinib	Combination	Cell death signaling (+/- Kinase inhibitor)	0.5+0.5	0.05+0.05	0.005+0.005
Venetoclax+Idasanutlin	Combination	Cell death signaling (+/- Kinase inhibitor)	0.5+0.5	0.05+0.05	0.005+0.005
Venetoclax+Dinaciclib	Combination	Cell death signaling (+/- Kinase inhibitor)	0.5+0.5	0.05+0.05	0.005+0.005
Venetoclax+Trametinib	Combination	Cell death signaling (+/- Kinase inhibitor)	0.5+0.5	0.05+0.05	0.005+0.005

Venetoclax+Quizartinib	Combination	Cell death signaling (+/- Kinase inhibitor)	0.5+0.5	0.05+0.05	0.005+0.005
Cytarabine+Daunorubicin	Combination, Antimetabolite	Chemotherapeutic	0.5+0.5	0.05+0.05	0.005+0.005
Cytarabine+Etoposide	Combination, Antimetabolite	Chemotherapeutic	0.5+0.5	0.05+0.05	0.005+0.005
Cytarabine+Mitoxantrone	Combination, Antimetabolite	Chemotherapeutic	0.5+0.5	0.05+0.05	0.005+0.005
Pinemetostat (EPZ-5676)	Epigenetic drug	Epigenetic	1	0.1	0.01
Romidepsin	Epigenetic drug, HDAC inhibitor	Epigenetic	2	0.2	0.02
Belinostat	Epigenetic drug, HDAC inhibitor	Epigenetic	1	0.1	0.01
Panobinostat	Epigenetic drug, HDAC inhibitor	Epigenetic	5	0.5	0.05
ORY1001	Epigenetic drug, Histone demethylase inhibitor	Epigenetic	1	0.1	0.01
Tazemetostat (EPZ-6438)	Epigenetic drug, Histone methyltransferase inhibitor	Epigenetic	1	0.1	0.01
Guadecitabine	Epigenetic drug, hypomethylating agent	Epigenetic	1	0.1	0.01
Decitabine	Epigenetic drug, hypomethylating agent	Epigenetic	1	0.1	0.01
GSK126	Epigenetic drug, Methyltransferase inhibitor	Epigenetic	1	0.1	0.01
Prednisolone	glucocorticoid	Other	1	0.1	0.01
Vismodegib	Hedgehog pathway inhibitor	Kinase inhibitor	2	0.2	0.02
Glasdegib	Hedgehog pathway inhibitor	Kinase inhibitor	1	0.1	0.01
Ivosidenib	IDH inhibitor	Metabolic drug	1	0.1	0.01
Enasidenib	IDH inhibitor	Metabolic drug	1	0.1	0.01
Ceritinib	Kinase inhibitor, ALK	Kinase inhibitor	1	0.1	0.01
Crizotinib	Kinase inhibitor, ALK	Kinase inhibitor	2	0.2	0.02
Alisertib	Kinase inhibitor, Aurora	Kinase inhibitor	1	0.1	0.01
Bafetinib	Kinase inhibitor, BCR-ABL	Kinase inhibitor	1	0.1	0.01
Imatinib	Kinase inhibitor, BCR-ABL	Kinase inhibitor	1	0.1	0.01
AP24534 Ponatinib	Kinase inhibitor, BCR-ABL	Kinase inhibitor	1	0.1	0.01
Dasatinib	Kinase inhibitor, BCR-ABL	Kinase inhibitor	1	0.1	0.01
Nilotinib	Kinase inhibitor, BCR-ABL	Kinase inhibitor	2	0.2	0.02
Bosutinib	Kinase inhibitor, BCR-ABL	Kinase inhibitor	1	0.1	0.01
Vemurafenib	Kinase inhibitor, BRAF	Kinase inhibitor	2	0.2	0.02
Dabrafenib	Kinase inhibitor, BRAF	Kinase inhibitor	1	0.1	0.01
Ibrutinib	Kinase inhibitor, BTK	Kinase inhibitor	1	0.1	0.01
Dinaciclib	Kinase inhibitor, CDK	Kinase inhibitor	1	0.1	0.01
Palbociclib	Kinase inhibitor, CDK	Kinase inhibitor	1	0.1	0.01
Abemaciclib	Kinase inhibitor, CDK	Kinase inhibitor	1	0.1	0.01
Neratinib	Kinase inhibitor, EGFR	RTK inhibitor	1	0.1	0.01
Erlotinib	Kinase inhibitor, EGFR	RTK inhibitor	2	0.2	0.02
Gefitinib	Kinase inhibitor, EGFR	RTK inhibitor	1	0.1	0.01
Gilteritinib	Kinase inhibitor, FLT3	RTK inhibitor	0.1	0.01	0.001
Quizartinib	Kinase inhibitor, FLT3	RTK inhibitor	1	0.1	0.01
Crenolanib	Kinase inhibitor, FLT3	RTK inhibitor	1	0.1	0.01
Lestaurtinib	Kinase inhibitor, FLT3	RTK inhibitor	1	0.1	0.01
Ruxolitinib	Kinase inhibitor, JAK	Kinase inhibitor	1	0.1	0.01
Tofacitinib	Kinase inhibitor, JAK	Kinase inhibitor	1	0.1	0.01
Pacritinib	Kinase inhibitor, JAK	Kinase inhibitor	1	0.1	0.01
Trametinib	Kinase inhibitor, MEK	Kinase inhibitor	1	0.1	0.01
Cobimetinib	Kinase inhibitor, MEK	Kinase inhibitor	1	0.1	0.01

TAK-733	Kinase inhibitor, MEK	Kinase inhibitor	1	0.1	0.01
Idelalisib	Kinase inhibitor, PI3K	Kinase inhibitor	1	0.1	0.01
Duvelisib (IPI-145)	Kinase inhibitor, PI3K	Kinase inhibitor	1	0.1	0.01
Volasertib	Kinase inhibitor, Plk	Kinase inhibitor	1	0.1	0.01
Sunitinib	Kinase inhibitor, RTK	RTK inhibitor	1	0.1	0.01
Nintedanib	Kinase inhibitor, RTK	RTK inhibitor	1	0.1	0.01
Cabozantinib	Kinase inhibitor, unspecific	RTK inhibitor	2	0.2	0.02
Regorafenib	Kinase inhibitor, unspecific	Kinase inhibitor	2	0.2	0.02
PKC-412(Midostaurin)	Kinase inhibitor, unspecific	RTK inhibitor	1	0.1	0.01
Sorafenib	Kinase inhibitor, unspecific	Kinase inhibitor	1	0.1	0.01
Vandetanib	Kinase inhibitor, VEGFR	RTK inhibitor	2	0.2	0.02
Semaxanib	Kinase inhibitor, VEGFR	RTK inhibitor	1	0.1	0.01
Pazopanib	Kinase inhibitor, VEGFR	RTK inhibitor	0.443	0.0443	0.00443
Cediranib	Kinase inhibitor, VEGFR	RTK inhibitor	1	0.1	0.01
Idasanutlin	MDM2 inhibitor	Cell death signaling (+/- Kinase inhibitor)	1	0.1	0.01
Temsirolimus	mTOR inhibitor	Metabolic drug	1	0.1	0.01
Everolimus	mTOR inhibitor	Metabolic drug	1	0.1	0.01
Rapamycin	mTOR inhibitor	Metabolic drug	1	0.1	0.01
MLN0128	mTOR inhibitor	Metabolic drug	1	0.1	0.01
MLN2480	mTOR inhibitor	Metabolic drug	1	0.1	0.01
Pevonedistat (MLN4924)	NEDD inhibitor	Metabolic drug	1	0.1	0.01
Veliparib	PARP inhibitor	Epigenetic	1	0.1	0.01
Olaparib	PARP inhibitor	Epigenetic	1	0.1	0.01
Carfilzomib	Proteasome inhibitor	Metabolic drug	0.000117	0.0000117	0.00000117
Ixazomib	Proteasome inhibitor	Metabolic drug	1	0.1	0.01
Bortezomib	Proteasome inhibitor	Metabolic drug	1	0.1	0.01
Bexarotene	Retinoid	Other	2	0.2	0.02
Alitretinoin	Retinoid receptor activator	Other	2	0.2	0.02
CC885	SLC9A1 degradation toxicity control	Other	1	0.1	0.01
D9A2	SLC9A1 degrader	Metabolic drug	1	0.1	0.01
W9A	SLC9A1 inhibitor	Metabolic drug	1	0.1	0.01
Rosuvastatin	Statin	Metabolic drug	1	0.1	0.01
Lovastatin	Statin	Metabolic drug	1	0.1	0.01
Telaglenastat (CB-839)	TCA cycle inhibitor, targets Glutaminase	Metabolic drug	1	0.1	0.01
Devimistat	TCA cycle inhibitor, targets Pyruvate Dehydrogenase	Metabolic drug	1	0.1	0.01



## Supplementary Table 2: Extended patient information. Related to Figure 2.

Extended information on patient samples in the cohort. (WES) next do detected mutations in the Additional alterations column indicates that the alterations have been identified via whole-exome sequencing. Abbreviations are the following: NK: Normal Karyotype; WES: Whole exome sequencing; ND: not detected/not assessed; Dx: Diagnosis; SCT: stem cell transplantation; FUP: follow up; MRD: Measurable residual disease; SR: Standard risk; IR: Intermediate risk; HR: High risk; pos: positive; neg: negative

Sample ID	Sex	Age at Dx (years)	FAB	Cytogenetics	Additional alterations	FCM - MRD (d21 or d28)	PCR MRD d28	MRD vote Ind1	FCM-MRD d56	PCR MRD d56	MRD vote Ind2	Risk BFM 2019	RISK BFM 2019 post Ind1	Time to death (days)	Time to relapse (days)	Time to SCT (days)	Time to FUP (days)	Treatment protocol	Umeda 2024 category
AML74	male	17,8	M4	NK	FLT3-ITD	7.50 %	ND	pos	ambiguous	nd	neg	IR	HR	745	303	no SCT	745	AML-BFM 04 mod	UBTF
AML20	female	3,8	M1	NK	FLT3-ITD NPM1	0.53 %	ND	pos	ambiguous	nd	neg	IR	HR	alive	no relapse	no SCT	603	AML-BFM 2012	NPM1
AML82	female	16,5	M1	NK		neg	ND	neg	neg	neg	neg	IR	IR	alive	798	no SCT	1358	AML-BFM 2013	CBFB-GDXY
AML64	male	5,7	M1	NK		neg	ND	neg	neg	nd	neg	IR	IR	alive	no relapse	no SCT	1868	AML-BFM 2004	unclassified
AML31	male	11,8	M7	BCR::ABL1		ND	ND	ND	nd	nd	ND	HR	HR	alive	no relapse	139	2230	AML04 Interim	BCR-ABL1
AML93	female	7,4	M0	ETV6::MNX1		ND	ND	ND	nd	nd	ND	HR	HR	668	480	100	668	AML04 Interim	MNX1
AML37	male	1,4	M5a	KMT2A::MLLT1		neg	<0,01 %	neg	neg	neg	neg	IR	IR	alive	no relapse	no SCT	1091	AML-BFM 2012	KMT2Ar
AML06	male	1,4	M7	NUP98::KDM5A		10.6 0%	2%	pos	0.104%	0.09%	pos	HR	HR	254	154	no SCT	254	AML-BFM 2012	NUP98r AMKL
AML57	male	18,3	M2/MDS !	trisomy 8	NRAS, WT1	20%	ND	pos	70%	nd	pos	IR	HR	alive	no relapse	67	246	AML-BFM 2004	UBTF
AML84	female	1,4	M7	complex		neg	ND	neg	neg	nd	neg	HR	HR	alive	no relapse	no SCT	607	AML-BFM 2012	unclassified
AML13	male	17,7	M2	KMT2A::MLLT1	FLT3-ITD, DNMT3A, RAD21	0.09 %	0.70%	pos	neg	<0,01 %	neg	IR	HR	alive	326	625	938	AML-BFM 2012	KMT2Ar
AML39	female	0,1	M4	DEK::NUP214	FLT3-ITD	3.10 %	ND	pos	2.20%	nd	pos	HR	HR	alive	no relapse	134	322	AML-BFM 2012	DEK-NUP214
AML44	female	12,8	M7	NUP98::KDM5A	KIT	0.38 %	ND	pos	neg	nd	neg	HR	HR	alive	no relapse	no SCT	911	AML-BFM 2012	NUP98r AMKL

AML66	female	8,9	M4Eo	CBFB::MYH11		neg	ND	neg	neg	nd	neg	SR	SR	alive	no relapse	no SCT	1207	AML-BFM 2012	CBFB-MYH11
AML47	male	17,4	M4Eo	CBFB::MYH11	NRAS, KIT	neg ambiguous	ND	neg	ambiguous	nd	neg	SR	SR	alive	no relapse	no SCT	237	AML-BFM 2012	CBFB-MYH11
AML58	male	4,4	M2	NK	CEBPAdm	neg	nd	neg	neg	nd	neg	SR	SR	alive	no relapse	no SCT	555	AML-BFM 2012	CEBPA
AML63	male	4,6	M5a	NUP98::NSD1	FLT3-ITD, GATA2	neg ambiguous	ND	neg	ambiguous	nd	neg	HR	HR	alive	973	973	1635	AML-BFM 04	NUP98r
AML62	female	14,2	M4	DEK::NUP214	FLT3-ITD	nd	ND	ND	neg	nd	neg	HR	HR	alive	no relapse	134	1362	AML-BFM 2004	DEK-NUP214
AML59	male	7,6	M4Eo	CBFB::MYH11		0.10 %	ND	pos	neg	nd	neg	SR	IR	alive	no relapse	no SCT	2313	AML04 Interim	CBFB-MYH11
AML77	male	8,5	M4	trisomy 8	GATA2	1.50 %	ND	pos	0.36%	nd	pos	IR	HR	66	no relapse	63	66	AML-BFM 04	unclassified
AML26	female	6,1	M4Eo	CBFB::MYH11		ND	ND	ND	nd	nd	ND	SR	SR	alive	no relapse	no SCT	2457	AML04 Interim	CBFB-MYH11
AML88	male	5,1	M5	monosomy 7	NRAS	neg	ND	neg	neg	nd	neg	HR	HR	alive	no relapse	32	2190	AML-BFM 2004	unclassified
AML95	male	15,4	M4	inv(3)(q21q26) RPN1/MECOM		ND	ND	ND	38%	nd	pos	HR	HR	319	190	93	319	AML-BFM 04	MECOM
AML54	male	0,1	M5	KMT2A::MLLT3		ambiguous 0,17 %	<0,01 %	neg	0.01%	0.03%	neg	IR	IR	342	237	175	342	AML-BFM 2012	KMT2Ar
AML07	female	15,3	M5b	KMT2A::MLLT3		neg	0.20%	pos	neg	<0,01 %	neg	IR	HR	alive	no relapse	no SCT	979	AML-BFM 2012	KMT2Ar
AML60	male	9,8	M4Eo	CBFB::MYH11		neg	nd	neg	neg	nd	neg	SR	SR	alive	1069	1175	1667	AML04 Interim	CBFB-MYH11
AML98	female	1,4	M4Eo	CBFB::MYH11		ND	ND	ND	neg	nd	neg	SR	SR	alive	no relapse	no SCT	2343	AML04 Interim	CBFB-MYH11
AML89	female	4,5	M2	RUNX1::RUNX1 T1		ND	ND	ND	nd	nd	ND	SR	SR	alive	no relapse	no SCT	3499	AML04 Interim	RUNX1-RUNX1T1
AML76	male	16,8	M5	KMT2A::MLLT3		neg	neg	neg	neg	neg	neg	IR	IR	alive	no relapse	no SCT	1583	AML-BFM 2004	KMT2Ar
AML87	male	8,9	M7	NK	ETV6, JAK3, WT1	0.54 %	0.30%	pos	neg	neg	neg	IR	HR	949	413	no SCT	949	AML-BFM 2012	unclassified
AML50	male	3,3	M7	CBFA2T3::GLIS2	GATA2	3.07 %	4%	pos	neg	neg	neg	HR	HR	alive	no relapse	no SCT	1368	AML-BFM 2012	GLISr
AML52	female	11	M5	KMT2A::MLLT10		neg	<0,01 %	neg	neg	neg	neg	HR	HR	alive	no relapse	153	956	AML-BFM 2012	KMT2Ar

AML65	female	11,3	M5	KMT2A::MLLT3	NRAS	neg	neg	neg	neg	neg	neg	IR	IR	alive	no relapse	no SCT	410	AML-BFM 2012	KMT2Ar	
AML23	female	7,2	M5a	KMT2A::MLLT1	GATA2, KRAS, NRAS	0.36 %	0.20%	pos	neg	neg	neg	IR	HR	alive	293	no SCT	1441	AML-BFM 2012	KMT2Ar	
AML67	female	1,1	M5a	KMT2A::MLLT3		neg	<10-4	neg	neg	neg	neg	IR	IR	alive	no relapse	no SCT	1730	AML-BFM 2004	KMT2Ar	
AML28	female	16,4	M1	NK	FLT3, NRAS, WT1 (WES)	ND	ND	ND	ND	ND	ND	IR	IR	472	314	394	472	AML-BFM 2004	unclassified	
AML24	male	10,3	M4	trisomy 8	FLT3-ITD, UBTF, (WES)	ND	ND	ND	ND	ND	ND	IR	IR	alive	421	519	2191	(AML-BFM 04) different therapy	UBTF	
AML43	male	17,8	M2	NK	CEBPAdm (WES)	ND	ND	ND	ND	ND	ND	SR	SR	alive	no relapse	no SCT	1735	AML-BFM 2004	CEBPA	
AML04	male	6,7	M1	NK	FLT3-ITD	ND	ND	ND	ND	ND	ND	IR	IR	534	277	357	534	AML-BFM 2004	unclassified	
AML81	female	12,6	M4	other	FLT3 (WES)	ND	ND	ND	ND	ND	ND	IR	IR	alive	no relapse	no SCT	2961	AML-BFM 2004	unclassified	
AML17	female	16,9	M4	NUP98::NSD1	FLT3	ambiguous	1%	pos	ambiguous	0.10%	pos	HR	HR	alive	no relapse	137	137	AML-BFM 2012	NUP98r	
AML12	male	10,8	M2	NUP98::NSD1	NRAS	32.7 1%	50%	pos	neg	0.04%	neg	HR	HR	alive	463	159	463	AML-BFM 2012	NUP98r	
AML29	female	3,9	M2	NUP98::NSD1		ND	ND	ND	ND	ND	ND	HR	HR	alive	397	146	4190	(AML-BFM 04) different therapy	NUP98r	
AML55	male	7,6	M5	NUP98::KDM5A		neg	<0,01 %	neg	neg		neg	HR	HR	alive	no relapse	181	543	AML-BFM recommendations 2019	NUP98r	
AML34	male	1,7	M6/M7	NUP98::KDM5A		0.21 %	0.40%	pos	0.34%		0.30%	pos	HR	HR	alive	no relapse	no SCT	258	AML-BFM recommendations 2019	NUP98r AMKL

## 3. Discussion

Advances in FPM approaches have propelled a previously nascent field substantially forward and particularly studies in high-risk adult cancers have demonstrated that FPM approaches can improve outcome for patients whose disease has progressed beyond standard treatment protocols (Kornauth *et al*, 2022; Snijder *et al*, 2017). Pediatric oncology patients have not profited from these developments to the same extent, which is at least partially due to their rarity, but also due to the inherent challenges in treating pediatric patients, such as limitations in available material and the overall lower number of technologically advanced centers that specialize in pediatric oncology.

Here, we generated a proof-of-concept for FPM in pedAML – a disease that may particularly profit from FPM approaches due to its low mutational burden and the lower number of targetable genetic alterations. Our study demonstrates that FPM in pedAML is feasible and that the application of FPM at diagnosis may be a valuable tool for patient stratification and to improve our understanding of the disease biology directly from primary samples.

### 3.1. Functional Precision Medicine in pediatric cancers

Several open questions around the application of FPM for pediatric cancers remain and while our study is limited in terms of sample size, lack of a validation cohort and due to its retrospective nature, it does provide useful guidance for designing future FPM studies. In particular, our work elucidates several technical and translational aspects of FPM studies that will need to be carefully considered in future studies.

#### 3.1.1. Technical considerations for functional precision medicine studies

The major technical deliberations for FPM projects concern the assay setup for drug response profiling (DRP) in terms of readout, culturing conditions and choice of drug library, and each of these aspects may have major implications for the subsequent findings.

We chose an image-based single-cell readout due to several advantages on a technical level. First, this setup enabled us to profile drug responses on a single-cell level and thus to accurately measure the responses of the malignant blast populations across patients, rather than a mixture which may include a substantial fraction of healthy cells. Until recently, studies using this type of assay were the only ones that could demonstrate improvements in patient

outcome (Kornauth *et al*, 2022; Snijder *et al*, 2017). A more recent study indicates that FPM studies may also be successful using simpler fluorometric assays across a variety of high-risk pediatric tumors (Acanda De La Rocha *et al*, 2024). However, inter-patient variability in malignant cell fraction may be a confounding factor when evaluating drug responses from such bulk assays. Our approach enabled the simultaneous measurement of up to three cell surface markers. The number of markers can be scaled up more easily with FCM-based approaches, which may be better suited to identify drug responses beyond cell death such as cellular differentiation, which is an important aspect in pedAML therapy. However, recent studies indicate that a combination of carefully selected markers and deep-learning based computational approaches can be used to substantially scale up the number of detectable markers in image-based screening approaches (Severin *et al*, 2022). These approaches and ours require substantial computational infrastructure and the development of dedicated software and thus may not be easy to establish in different centers. Nonetheless, our setup allowed us to test a relatively high number of 116 drugs or drug combinations, which is more than other related studies were able to test (Wang *et al*, 2022; Strachan *et al*, 2022; Kuusanmäki *et al*, 2020). Additionally, it allowed us to derive blast-specific drug responses from relatively low cell numbers of 9,000 cells per well with variable blast numbers, indicating that performing this assay is feasible even for low sample amounts. Collectively, these observations indicate that high-content drug screening is a well-suited technology for FPM approaches due to its scalability and the ability to measure single-cell responses.

We chose to perform drug treatment in regular medium without any added cytokines or stromal cells for 24 hours. While this enabled us to identify meaningful drug response profiles in terms of predictivity of key clinical parameters, it may have lead to some false negatives for slower acting drugs, where active drugs could not be identified because the incubation was stopped before they showed their effect. Similarly, the lack of additional cytokines may lower proliferation rates and thus artificially decrease responses to drugs that mainly act at specific cell-cycle stages. Particularly the novel Menin inhibitors are known to act more slowly and induce differentiation in AML blasts and our assay may not be well suited to evaluate responses to these drugs. Despite these limitations, our study measured meaningful responses to venetoclax combinations, chemotherapeutics, FLT3 inhibitors, HDAC inhibitors, and other drugs, indicating that 24 hours of treatment is sufficiently long to measure treatment responses to these drugs. Future FPM studies may have dedicated setups with varied incubation times depending on the target disease and the compounds of interest to overcome these limitations.

Drug libraries for FPM studies need to be carefully designed to consider both the clinical reality and the major pathways involved in the disease. While the inclusion of standard of care drugs

is a common choice in the design of such studies, whether and how to drug combinations should be included is not obvious and there is little evidence that would clearly indicate whether drug combinations need to be included in FPM studies. In our study, 58 of 116 different treatments – including 9 combinations - showed activity in at least three patient samples and all tested drug combination were among the treatments that showed activity. This may indicate that combinations are more likely to deliver a signal in DRP studies. Oncology patients only rarely receive a single drug for their treatment and it is currently unclear whether DRP assays need to model this explicitly by also applying drug combinations *ex-vivo*. FPM-guided treatment in the EXALT trial often contained combinations even though no combinations were tested *ex-vivo* (Kornauth *et al*, 2022). Yet, the study was able to demonstrate clinical benefit despite the lack of combinations in the *ex-vivo* assay. This may indicate that testing combinations is not required to inform patient treatments, but this has yet to be evaluated quantitatively and comprehensively. The combinatorial complexity of testing drug combinations at different ratios and the clinical reality that drugs in combination therapy are often administered at different doses and different schedules and dynamically adjusted based on patient response further complicates any assessment of whether *ex-vivo* DRP is a good proxy for *in-vivo* treatment response.

### 3.1.2. Translational considerations for functional precision medicine studies

In addition to the more technical factors considered above, several insights into key translational aspects for FPM studies can be derived by contextualizing our work with other recent studies. Our work highlights that meaningful insights into the biology of patient risk can be gained from non-prospective FPM studies. Based on these data, one may raise questions on the optimal time point for FPM study enrollment with respect to disease stage and the position of FPM studies in clinical decision making.

Most FPM studies focused on the application for high-risk tumors in a relapsed refractory setting. This is a reasonable approach as it is directly in line with the rationale to also apply novel drugs in such a high-risk setting first when patients have exhausted all other treatment options. Indeed, several FPM-based studies were able to demonstrate clinical benefit in these settings (Snijder *et al*, 2017; Kornauth *et al*, 2022; Acanda De La Rocha *et al*, 2024). However, it is currently unclear whether this is an optimal time point for performing DRP. Observational non-interventional studies such as ours and related work (Strachan *et al*, 2022; Liebers *et al*, 2023) demonstrate that DRP profiles are predictive of patient response. Considering data in pedAML that indicates that early response is a long-term predictor of

patient outcome (Tierens *et al*, 2016; Rasche *et al*, 2021; Brodersen *et al*, 2020), one may argue that DRP at early time points may be an effective tool to assign patients to more promising treatments before resistant disease emerges. Future trials may need to perform DRP at earlier time points to evaluate the time frame in which DRP results are predictive and to evaluate the potential benefits of FPM in patient populations which are less heavily pre-treated and may thus have less broadly resistant malignancies. However, the molecular changes in tumors under treatment will have to be carefully considered in such settings. Several studies have identified substantial molecular changes between samples at diagnosis and matched samples taken at relapse or during disease progression in pedAML (Lambo *et al*, 2023; McNeer *et al*, 2019; Masetti *et al*, 2016). Similar studies in solid tumors identified substantial genetic changes in matched samples that can also lead to a change in tumor classification upon relapse (Worst *et al*, 2016). These findings illustrate that the long-term predictiveness of functional assays will have to be carefully investigated and may depend on the tumor entity. Furthermore, treatment choices based on DRP results may not be straightforward. Our study used random forest models to predict patient risk and early response from drug response profiles rather than simply correlating *in-vivo* response and *ex-vivo* response. Furthermore, unsupervised clustering of drug response profiles did not yield strong associations between drug response profiles and clinical variables, indicating that the relationships between risk and response of an individual patient and their *ex-vivo* drug response profile is complex, just as contributions of individual drugs to the outcome of an individual patient are often unclear in modern treatment regimens. This may be at least partially due to the multi-modal nature of modern cancer therapy, where different biomarkers are usually considered in combination and patients receive drugs in combination, which are dynamically adjusted based on response and adverse effects. Thus, the interpretation of drug response profiles for therapy selection may also have to be multi-modal and consider the full complexity of an individual case.

The retrospective nature of our work and the lack of a validation cohort is a major limitation of our study. It is clear that prospective studies are needed to evaluate the true clinical benefit of FPM approaches. However, retrospective studies like ours fill a gap between technology establishment, biological understanding and translational application, as they enable an evaluation of feasibility for FPM before a prospective study takes place and may deepen the understanding of the respective malignancies. A particularly intriguing aspect in FPM studies is the correlation between targetable mutations and *ex-vivo* sensitivity. Our study was able to demonstrate a link between epigenetic cellular differentiation states, patient risk and *ex-vivo* drug response for the high-risk groups we identified. Similar findings have been made in adult AML in a recent study (Bottomly *et al*, 2022). Collectively, these results and ours indicate that cellular differentiation states may be an under-appreciated molecular predictor of sensitivity to

targeted treatments. We did not identify any strong associations between targetable genetic lesions and ex-vivo sensitivity to targeted agents alone, except for the association between monocytic *RAS*-mutated AML and resistance to venetoclax. This may be due to a lack of statistical power. However, there is good reason to believe that targeted treatment based on targetable genomic lesions alone may not be the optimal route to improve outcome in high-risk cancer patients. Only a relatively low number of GPM basket trials have demonstrated clinical benefit in recent years (Pishvaian *et al*, 2020; Burd *et al*, 2020; Sicklick *et al*, 2019; Lau *et al*, 2024). Notably, all of these studies applied combination therapies and matched targeted treatment did not necessarily directly target the actual mutated protein in these studies. Additionally, there is a relatively high number of reported FPM studies over the past decade that only report few if any associations between targetable alterations and ex-vivo responses to the corresponding drugs (Dietrich *et al*, 2018; Tyner *et al*, 2018). This may indicate that even fewer tumors may be susceptible to targeted treatment based on their lesion than currently thought and warrants an in-depth investigation of additional drivers of therapy resistance for targeted treatments.

Future studies that apply FPM approaches together with molecular profiling may further elucidate on the mechanisms of treatment resistance despite presence of a targetable lesion or vice versa. Comparative studies such as the EXALT-2 trial are a particularly interesting route to deepen our insight into the relationship between targetable lesions, FPM results and patient outcome. This study prospectively compares treatment GPM-based treatment, FPM-based treatment and physician's choice treatment and may reveal the superiority of either approach alone (Kazianka *et al*, 2025). Additionally, studies that combine functional and molecular characterization and jointly relate these to treatment response are under way and may shed further light on the predictivity of GPM and FPM approaches alone and in combination (Irmisch *et al*, 2021; Malani *et al*, 2022). The first results from a study of the Tumor Profiler project have been published recently and indicate that multi-omics trials that combine several functional and molecular biomarkers are feasible (Miglino *et al*, 2025), paving the way for future studies that compare more complex multi-omics biomarkers to better understand patient risk and response. Molecular profiling studies that incorporated different sequencing modalities such as the MASTER trial or the PRISM trial were able to identify targeted treatments and improve diagnoses in a substantial fraction of patients, indicating that multi-modal data collection is feasible and informative in clinical practice (Wong *et al*, 2020; Horak *et al*, 2021; Lau *et al*, 2024). Studies that combine different sequencing modalities with additional functional characterization may improve these rates even further and improve outcome through the implementation of multi-disciplinary molecular tumor boards (Irmisch *et al*, 2021; Malani *et al*, 2022).



## 3.2. Multi-omics insights into pediatric AML

As outlined previously, a number of novel agents are emerging as viable treatment options in ped AML, particularly venetoclax, Menin inhibitors and immunotherapy. Our study particularly highlights venetoclax and venetoclax combinations as treatment options for pedAML, but the implications of our integrated FPM approach go further. In the context of related work, our study further elucidates the role of clonality, cellular differentiation and functional cell states in pediatric AML.

### 3.2.1. Clonality and genomic targetability of pediatric AML

Our study indicated substantial clonality of pedAML blasts at diagnosis as indicated by differential variant allele frequencies of mutations identified via whole exome sequencing. The clonality of pedAML has usually been investigated by deep genomic sequencing of matched samples from diagnosis and relapse (Masetti *et al*, 2016; McNeer *et al*, 2019). Both of these studies and ours suggest the presence of 2-4 subclones at diagnosis – in line with the assumption that mutations in genes such as RAS or FLT3 are usually secondary events in pedAML and thus not present in all malignant cells. Our study substantially increases the available data on pedAML clonality at diagnosis to date and further supports the notion of pedAML as an inherently clonal disease.

This observation has important implications for targeted treatment in pediatric AML, particularly for targeted inhibitors for key mutations such as MEK inhibitors for mutations in the RAS pathway, or FLT3 inhibitors for activating FLT3 mutations. pedAML study protocols usually only recommend FLT3 inhibitors if the mutation is detected with a variant allele frequency above a certain threshold – usually 0.4 (Cooper *et al*, 2023). Given that particularly the KRAS mutations in our study only occurred in minor subclones, similar thresholds may have to be applied in trials for other targeted inhibitors, such as MEK inhibitors and future studies may explore the targeting of several different subclones simultaneously in line with the classical paradigm of *total therapy*.

Notably, our study did not identify any strong associations between targetable mutations and presence of the corresponding lesions. This is at least partially due to lack of statistical power. However, the clonality of targetable mutations may indicate that the next generation of clinical trials may consider to target individual subclones simultaneously rather than targeting individual lesions which only present in a fraction of leukemic cells in an individual patient.

### 3.2.2. Cellular differentiation states and risk in pediatric AML

Leukemia stem cells (LSCs) are the fraction of leukemic blasts that are considered to be fueling the blast population observed in a patients' blood and drivers of relapse and non-response (Misaghian *et al*, 2009). LSCs are postulated to be essentially the malignant counterpart of healthy HSCs and are considered to be largely quiescent and equipped with higher proliferative potential than the bulk of leukemic cells that can be detected in a regular biopsy. Thus, they are also postulated to have a more HSC-like transcriptional signature than the remaining majority of leukemic cells within the same patient. Earlier work identified these cells via serial transplantation studies and described them as heterogeneous in their capacity for self-renewal and leukemia generation in transplant recipients (Lapidot *et al*, 1994; Hope *et al*, 2004). Based on these findings, different transcriptional signatures of LSCs that can be detected in bulk AML samples have been identified and shown to be predictive of patient risk (Ng *et al*, 2016; Diffner *et al*, 2013; Huang *et al*, 2022).

However, the specificity to different genetic subgroups for these signatures and potential differential abundancies of LSCs depending on the leukemia subtype are yet to be fully elucidated. Recent studies in pedAML indicated differential LSC-like transcription between different genetic subgroups with subtypes that are classified as high-risk usually having a more HSC-like expression (Umeda *et al*, 2024). In line with this association of LSC-like expression and patient risk, another study identified the emergence of a more LSC-like transcriptional phenotype upon relapse (Lambo *et al*, 2023). Based on these findings, one may hypothesize that these phenotypes are either due to an increased LSC fraction, or they are due to a more LSC-like state in the majority of leukemic cells that were sequenced, indicating that this expression signature is an inherent feature of higher-risk leukemia regardless of the size of the LSC fraction.

Similarly to the studies mentioned above, our ATAC-seq data indicate HSC/LSC-like epigenetic states are associated with more high-risk genetic subtypes. Our ATAC-seq data were generated from isolated chromatin of 50,000 cells of an individual sample and ATAC-seq measures open chromatin rather than gene expression as RNA-seq does. Therefore, ATAC-seq data represents an average over all sequenced cells that weighs individual cells more or less equally, whereas bulk RNA-seq data can be confounded by over-expression of individual genes in a subset of cells. Given this context, it is unlikely that the signatures that we reported were due to an increased fraction of LSCs, but our results rather suggest that a more LSC-like epigenetic state in the bulk of the leukemia population is more indicative of patient risk.

In our study, we also reported an association between a more monocytic cell state and patient risk and MRD positivity. Such an association has not yet been reported to our knowledge and

should thus be considered carefully. Notably, the genetic subgroup with the highest similarity to monocytes were the KMT2A-rearranged samples. Thus, it should be considered that this phenomenon could be due to an over-representation of KMT2A-rearranged pedAMLs in our cohort or the risk-association could be restricted to KMT2A-rearranged pedAML.

Our study further describes the differential vulnerabilities of these risk-associated cellular differentiation states. Similar associations – although without the patient risk component – have also been described in adult AML (Bottomly *et al*, 2022). Successful treatment based on differentiation states has so far only been described for acute promyelocytic leukemia (Yilmaz *et al*, 2021), which is mainly driven by the *PML::RARA* fusion and thus also provides a genomic target. It is currently unclear to what extent cellular differentiation states are purely dependent on the genetic drivers or whether they reflect other independent factors such as the cell of origin of the leukemia in an individual patient. However, the associations between cellular differentiation state and patient risk that we and others have described (Lambo *et al*, 2023; Umeda *et al*, 2024) certainly indicate that this approach provides a useful rationale for considering patient risk and subgroups that may profit from similar treatments, as it provides a convenient way to abstract from the genomic complexity of pedAML and consider more the functional commonalities of the different genomic subgroups.

### 3.2.3. The functional landscape of pediatric AML

Our study provided a substantial amount of functional data on pedAML and highlights vulnerabilities to venetoclax combinations and chemotherapeutics in standard treatment protocols among others as drivers of variation in drug response profiles. Two other studies that describe DRP in pedAML have been published recently (Wang *et al*, 2022; Strachan *et al*, 2022). However, ours is the first that aims to identify functional groupings beyond responders and non-responders and associations with recurrent mutations.

In terms of the functional landscape of pedAML, we describe opposing axes of drug sensitivity variation, where FLT3 inhibitors, mTOR inhibitors and BET inhibitors consistently correlate negatively with venetoclax combinations. On the other hand anthracyclines, proteasome inhibitors and HDAC inhibitors consistently correlate positively with venetoclax combinations. These results indicate that patient groups who may profit from drugs in either group may not profit from the other and vice versa. Going further, data in the literature indicates that these correlations may reflect converging mechanisms of molecular dependencies that are indicated by these drug sensitivities.

The positive correlations of venetoclax combinations, HDAC inhibitors and proteasome inhibitors may be due to convergence on the BCL2 pathway. The BCL2 pathway has been

shown to be the primary cell-death pathway for HDAC inhibitor induced cell death (Matthews *et al*, 2012; Inoue *et al*, 2007). There is no direct data that links sensitivity to proteasome inhibitors to venetoclax or the BCL2 pathway to our knowledge and resistance to proteasome inhibitors remains only partially understood. However, the positive correlation between sensitivity to proteasome inhibition and combined BCL2 inhibition may be due to ATF4-mediated up-regulation of the BCL2-pathway members BIM and PUMA via the integrated stress response (Tian *et al*, 2024).

Consistent positive correlations between sensitivities to FLT3 inhibitors, mTOR inhibitors and BET inhibitors were overall weaker in our study than the correlations between venetoclax combinations, proteasome inhibitors, and HDAC inhibitors. However, there are data indicating that PI3K-AKT-mTOR signaling is a major driver of response for all three groups of compounds. Sensitivity to mTOR inhibitors has been found to be determined by AKT activity where increases in phosphorylated AKT have been associated with increased sensitivity to mTOR inhibition (Gera *et al*, 2004; Kurmasheva *et al*, 2006). The pathway has also been shown to be activated by FLT3 and particularly by constitutively active mutated FLT3 (Masson & Rönstrand, 2009). The relationship between BET dependency and the PI3K-AKT-mTOR pathway is less clear. However, there are data that indicate a co-dependency between BRD4 activity and activity of the PI3K-AKT-mTOR pathway, where BET inhibitors lowered PI3K signaling and reduced expression of receptor tyrosine kinases (Stratikopoulos *et al*, 2015).

Thus, the opposing axes of sensitivity in our cohort seem to be driven by BCL2 dependency on the one side and FLT3 mediated dependency on the PI3K-AKT-mTOR pathway on the other side. Additionally, several studies link FLT3 activity and resistance to venetoclax directly and may explain the negative correlation between sensitivity to FLT3 inhibitors and sensitivity to venetoclax combinations. Genomic analysis of patients in a phase II study for venetoclax in relapsed AML patients indicated that activating mutations in *FLT3* or mutations in *PTPN11* may confer resistance to venetoclax as patients with the corresponding mutations did not respond to venetoclax monotherapy (Chyla *et al*, 2018), thus providing a direct rationale for the negative correlation between response to venetoclax combinations and response to FLT3 inhibitors. Similarly, another study identified mutations in *FLT3* and *RAS* in samples with primary resistance to venetoclax and in emergent clones at relapse after venetoclax therapy (DiNardo *et al*, 2020b) Signaling downstream of FLT3 may also be involved in venetoclax resistance via the up-regulation of MCL-1 and BCL-xL. STAT5 has been shown to up-regulate BCL-xL after activation by constitutive FLT3-ITD activity (Yoshimoto *et al*, 2009) and in an IL3-dependent manner (Dumon *et al*, 1999). Intriguingly, this inverse relationship of FLT3 inhibitor sensitivity and venetoclax sensitivity has also been described in terms of FLT3 inhibitor resistance, where over-expression of BCL2 conferred resistance to a FLT3 inhibitor in a cell

line model (Kohl *et al*, 2007). These findings and ours further solidify the opposing roles of FLT3 signaling and the BCL2 pathway in AML that lead to inverse sensitivity patterns that we observed.

Collectively, these data suggest that venetoclax sensitivity and sensitivity to kinase inhibition, particularly FLT3 and downstream signaling via the PI3K-AKT-mTOR pathway may be mutually exclusive dependencies in pediatric AML, where samples are either sensitive to BCL2 inhibition or to inhibition of FLT3 and its downstream signaling targets.

Notably, the relationship between these observations and patient risk in pedAML is not fully clear and further work is needed to better elucidate these differential dependencies. However, some further hints on the nature of this relationship can be deduced from our data. We do observe a higher sensitivity to venetoclax combinations and the HDAC inhibitors panobinostat and romidepsin in MRD positive HSC-like samples in our cohort, whereas the FLT3 inhibitor gilteritinib shows higher activity in monocyte-like MRD positive samples. This grouping of samples does not fully recapitulate the proposed mutual exclusivity of dependencies though, indicating that this relationship is not fully aligned with clinically defined patient risk. In line with this observation, we observed sensitivity patterns between risk groups that were often concordant with mechanism of action, but did not yield any obvious patterns that discriminated between different risk groups based on pathway-level dependencies, indicating that genetically defined risk groups may only partially capture pathway-level dependencies.

### 3.2.4 Conclusions and future prospects

Based on our observations and the studies outlined above, our study makes a clear case for the benefit of FPM approaches in pedAML. Both clinical and translational studies in ped AML have been hindered by the rarity of the disease and the heterogeneity of driving lesions. To date, these limitations have mainly been addressed through large-scale international collaboration that enabled the dramatic improvements in outcome that we have observed over the past decades. Further work uncovered converging vulnerabilities for the plethora of different driving lesions such as the vulnerability to BCL2 inhibition in high-risk and relapsed/refractory pedAML or the sensitivity to Menin inhibition in AMLs that depend on the Menin-KMT2A interaction, such as those with *NPM1c*, *KMT2A*-rearrangements, *NUP98*-rearrangements or *UBTF-TD*. These advances have demonstrated the power of international collaboration and how both rigorous translational research and deep mechanistic insights into disease biology can inform the next generation of treatments.

Our study is among the first to provide an additional functional layer of understanding to this dismal disease and particularly highlights the value of functional profiling at diagnosis rather

than restricting the application of FPM approaches to the relapsed refractory setting. Thus, it provides a rationale for applying high-throughput FPM approaches for both patient stratification and biological discovery.

FPM approaches like ours may be used to improve the stratification for high-risk patients in clinical trials. Particularly outcome for patients receiving venetoclax may be further improved by this approach. Enrollment of pedAML patients in venetoclax trials has so far mainly been based on resistance to therapies within the standard of care, rather than truly response predictive biomarkers. Advanced DRP may provide such biomarkers by testing for resistance with ex-vivo assays before patients start the treatment, with the added benefit that DRP can also inform alternative options in case the assay indicates resistance to the intended treatment. Similarly, they may also be useful for evaluating promising drugs before patients are actually being enrolled in a trial and thus provide a useful additional data modality that can further enhance the pre-clinical data that usually informs such trials.

Similarly, FPM approaches like ours may be useful to identify converging patterns of drug sensitivity that are indicative of joint vulnerabilities across genomic subgroups. As mentioned above, the sensitivities to venetoclax or Menin inhibitors across genetically defined subgroups are clear indicators of common disease mechanisms that can be therapeutically exploited. Further vulnerabilities like these may exist in pedAML and other rare malignancies and FPM approaches are an attractive avenue to identify such vulnerabilities directly in patient material rather than relying on more artificial cell line models or model organisms that may behave differently. Thus, FPM-based approaches may identify treatment options for pedAML subgroups that still fare poorly, such as those with oncogenic fusions involving MECOM or relapsed pedAML for groups without defined genetic targets.

Beyond the treatment of relapsed/refractory patients, we envision FPM-approaches as an additional tool for patient stratification and biomarker identification. In line with the ambition to provide comprehensive genetic testing for most cancer patients, additional functional profiling may provide invaluable information for the identification of promising treatment options for non-responders and their early detection.

## 4. Materials and Methods

Materials and methods for the published manuscript have been extensively described in the manuscript.

# References

- Acanda De La Rocha AM, Berlow NE, Fader M, Coats ER, Saghira C, Espinal PS, Galano J, Khatib Z, Abdella H, Maher OM, *et al* (2024) Feasibility of functional precision medicine for guiding treatment of relapsed or refractory pediatric cancers. *Nat Med* 30: 990–1000
- Adolfsson J, Månsson R, Buza-Vidas N, Hultquist A, Liuba K, Jensen CT, Bryder D, Yang L, Borge O-J, Thoren LAM, *et al* (2005) Identification of Flt3<sup>+</sup> lympho-myeloid stem cells lacking erythro-megakaryocytic potential a revised road map for adult blood lineage commitment. *Cell* 121: 295–306
- Akashi K, Traver D, Miyamoto T & Weissman IL (2000) A clonogenic common myeloid progenitor that gives rise to all myeloid lineages. *Nature* 404: 193–197
- Alder JK, Georgantas RW, Hildreth RL, Kaplan IM, Morisot S, Yu X, McDevitt M & Civin CI (2008) Kruppel-like factor 4 is essential for inflammatory monocyte differentiation in vivo. *J Immunol* 180: 5645–5652
- Aldoss I, Issa GC, Blachly JS, Thirman MJ, Mannis GN, Arellano ML, DiPersio JF, Traer E, Zwaan CM, Shukla N, *et al* (2024) Updated Results and Longer Follow-up from the AUGMENT-101 Phase 2 Study of Revumenib in All Patients with Relapsed or Refractory (R/R) *KMT2Ar* Acute Leukemia. *Blood* 144: 211–211
- Anjos-Afonso F & Bonnet D (2023) Human CD34<sup>+</sup> hematopoietic stem cell hierarchy: how far are we with its delineation at the most primitive level? *Blood* 142: 509–518
- Anjos-Afonso F, Currie E, Palmer HG, Foster KE, Taussig DC & Bonnet D (2013) CD34(-) cells at the apex of the human hematopoietic stem cell hierarchy have distinctive cellular and molecular signatures. *Cell Stem Cell* 13: 161–174
- Aplenc R, Meshinchi S, Sung L, Alonzo T, Choi J, Fisher B, Gerbing R, Hirsch B, Horton T, Kahwash S, *et al* (2020) Bortezomib with standard chemotherapy for children with acute myeloid leukemia does not improve treatment outcomes: a report from the Children's Oncology Group. *Haematologica* 105: 1879–1886
- Assi SA, Imperato MR, Coleman DJL, Pickin A, Potluri S, Ptasinska A, Chin PS, Blair H, Cauchy P, James SR, *et al* (2019) Subtype-specific regulatory network rewiring in acute myeloid leukemia. *Nat Genet* 51: 151–162
- Aur RJ, Simone J, Hustu HO, Walters T, Borella L, Pratt C & Pinkel D (1971) Central nervous system therapy and combination chemotherapy of childhood lymphocytic leukemia. *Blood* 37: 272–281
- Ayton PM & Cleary ML (2001) Molecular mechanisms of leukemogenesis mediated by MLL fusion proteins. *Oncogene* 20: 5695–5707
- Azcoitia V, Aracil M, Martínez-A C & Torres M (2005) The homeodomain protein Meis1 is essential for definitive hematopoiesis and vascular patterning in the mouse embryo. *Dev Biol* 280: 307–320
- Barajas JM, Rasouli M, Umeda M, Hiltenbrand R, Abdelhamed S, Mohnani R, Arthur B, Westover T, Thomas ME, Ashtiani M, *et al* (2024) Acute myeloid leukemias with UBTF tandem duplications are sensitive to menin inhibitors. *Blood* 143: 619–630



- Beck D, Thoms JAI, Perera D, Schütte J, Unnikrishnan A, Knezevic K, Kinston SJ, Wilson NK, O'Brien TA, Göttgens B, *et al* (2013) Genome-wide analysis of transcriptional regulators in human HSPCs reveals a densely interconnected network of coding and noncoding genes. *Blood* 122: e12-22
- Beird HC, Bielack SS, Flanagan AM, Gill J, Heymann D, Janeway KA, Livingston JA, Roberts RD, Strauss SJ & Gorlick R (2022) Osteosarcoma. *Nat Rev Dis Primers* 8: 77
- Bell CC, Fennell KA, Chan Y-C, Rambow F, Yeung MM, Vassiliadis D, Lara L, Yeh P, Martelotto LG, Rogiers A, *et al* (2019) Targeting enhancer switching overcomes non-genetic drug resistance in acute myeloid leukaemia. *Nat Commun* 10: 2723
- Benedict WF, Lange M, Greene J, Derencsenyi A & Alfi OS (1979) Correlation between prognosis and bone marrow chromosomal patterns in children with acute nonlymphocytic leukemia: similarities and differences compared to adults. *Blood* 54: 818–823
- Berger R, Bernheim A, Ochoa-Noguera ME, Daniel MT, Valensi F, Sigaux F, Flandrin G & Boiron M (1987) Prognostic significance of chromosomal abnormalities in acute nonlymphocytic leukemia: a study of 343 patients. *Cancer Genet Cytogenet* 28: 293–299
- Bhakta N, Force LM, Allemani C, Atun R, Bray F, Coleman MP, Steliarova-Foucher E, Frazier AL, Robison LL, Rodriguez-Galindo C, *et al* (2019) Childhood cancer burden: a review of global estimates. *Lancet Oncol* 20: e42–e53
- Bhatia M, Bonnet D, Murdoch B, Gan OI & Dick JE (1998) A newly discovered class of human hematopoietic cells with SCID-repopulating activity. *Nat Med* 4: 1038–1045
- Böiers C, Buza-Vidas N, Jensen CT, Pronk CJH, Kharazi S, Wittmann L, Sitnicka E, Hultquist A & Jacobsen SEW (2010) Expression and role of FLT3 in regulation of the earliest stage of normal granulocyte-monocyte progenitor development. *Blood* 115: 5061–5068
- Bolouri H, Farrar JE, Triche T, Ries RE, Lim EL, Alonzo TA, Ma Y, Moore R, Mungall AJ, Marra MA, *et al* (2018) The molecular landscape of pediatric acute myeloid leukemia reveals recurrent structural alterations and age-specific mutational interactions. *Nat Med* 24: 103–112
- Bonaventure A, Harewood R, Stiller CA, Gatta G, Clavel J, Stefan DC, Carreira H, Spika D, Marcos-Gragera R, Peris-Bonet R, *et al* (2017) Worldwide comparison of survival from childhood leukaemia for 1995-2009, by subtype, age, and sex (CONCORD-2): a population-based study of individual data for 89 828 children from 198 registries in 53 countries. *Lancet Haematol* 4: e202–e217
- Bottomly D, Long N, Schultz AR, Kurtz SE, Tognon CE, Johnson K, Abel M, Agarwal A, Avaylon S, Benton E, *et al* (2022) Integrative analysis of drug response and clinical outcome in acute myeloid leukemia. *Cancer Cell* 40: 850-864.e9
- Boudia F, Baille M, Babin L, Aid Z, Robert E, Rivière J, Galant K, Alonso-Pérez V, Anselmi L, Arkoun B, *et al* (2025) Progressive chromatin rewiring by ETO2::GLIS2 revealed in a genome-edited human iPSC model of pediatric leukemia initiation. *Blood* 145: 1510–1525
- Brodersen LE, Gerbing RB, Pardo ML, Alonzo TA, Paine D, Fritschle W, Hsu F-C, Pollard JA, Aplenc R, Kahwash SB, *et al* (2020) Morphologic remission status is limited compared to ΔN flow cytometry: a Children's Oncology Group AAML0531 report. *Blood Adv* 4: 5050–5061
- Burd A, Levine RL, Ruppert AS, Mims AS, Borate U, Stein EM, Patel P, Baer MR, Stock W, Deininger M, *et al* (2020) Precision medicine treatment in acute myeloid leukemia using

- prospective genomic profiling: feasibility and preliminary efficacy of the Beat AML Master Trial. *Nat Med* 26: 1852–1858
- Camiolo G, Mullen CG & Ottersbach K (2024) Mechanistic insights into the developmental origin of pediatric hematologic disorders. *Exp Hematol* 136: 104583
- Capron C, Lécluse Y, Kaushik AL, Foudi A, Lacout C, Sekkai D, Godin I, Albagli O, Poullion I, Svinartchouk F, *et al* (2006) The SCL relative LYL-1 is required for fetal and adult hematopoietic stem cell function and B-cell differentiation. *Blood* 107: 4678–4686
- Castilla LH, Garrett L, Adya N, Orlic D, Dutra A, Anderson S, Owens J, Eckhaus M, Bodine D & Liu PP (1999) The fusion gene Cbfb-MYH11 blocks myeloid differentiation and predisposes mice to acute myelomonocytic leukaemia. *Nat Genet* 23: 144–146
- Cavenee WK, Murphree AL, Shull MM, Benedict WF, Sparkes RS, Kock E & Nordenskjold M (1986) Prediction of familial predisposition to retinoblastoma. *N Engl J Med* 314: 1201–1207
- Chen MJ, Yokomizo T, Zeigler BM, Dzierzak E & Speck NA (2009) Runx1 is required for the endothelial to haematopoietic cell transition but not thereafter. *Nature* 457: 887–891
- Chong SZ, Evrard M, Devi S, Chen J, Lim JY, See P, Zhang Y, Adrover JM, Lee B, Tan L, *et al* (2016) CXCR4 identifies transitional bone marrow premonocytes that replenish the mature monocyte pool for peripheral responses. *J Exp Med* 213: 2293–2314
- Chyla B, Daver N, Doyle K, McKeegan E, Huang X, Ruvolo V, Wang Z, Chen K, Souers A, Levenson J, *et al* (2018) Genetic biomarkers of sensitivity and resistance to venetoclax monotherapy in patients with relapsed acute myeloid leukemia. *Am J Hematol* 93: E202-5
- Collins FS & Varmus H (2015) A new initiative on precision medicine. *N Engl J Med* 372: 793–795
- Cooper TM, Alonzo TA, Tasian SK, Kutny MA, Hitzler J, Pollard JA, Aplenc R, Meshinchi S & Kolb EA (2023) Children’s Oncology Group’s 2023 blueprint for research: Myeloid neoplasms. *Pediatr Blood Cancer* 70 Suppl 6: e30584
- Corces MR, Buenrostro JD, Wu B, Greenside PG, Chan SM, Koenig JL, Snyder MP, Pritchard JK, Kundaje A, Greenleaf WJ, *et al* (2016) Lineage-specific and single-cell chromatin accessibility charts human hematopoiesis and leukemia evolution. *Nat Genet* 48: 1193–1203
- Corral J, Lavenir I, Impey H, Warren AJ, Forster A, Larson TA, Bell S, McKenzie AN, King G & Rabbitts TH (1996) An Mll-AF9 fusion gene made by homologous recombination causes acute leukemia in chimeric mice: a method to create fusion oncogenes. *Cell* 85: 853–861
- Coulombe P, Cole G, Fentiman A, Parker JDK, Yung E, Bilenky M, Degefie L, Lac P, Ling MYM, Tam D, *et al* (2023) Meis1 establishes the pre-hemogenic endothelial state prior to Runx1 expression. *Nat Commun* 14: 4537
- Creutzig U, van den Heuvel-Eibrink MM, Gibson B, Dworzak MN, Adachi S, de Bont E, Harbott J, Hasle H, Johnston D, Kinoshita A, *et al* (2012) Diagnosis and management of acute myeloid leukemia in children and adolescents: recommendations from an international expert panel. *Blood* 120: 3187–3205
- Dharia NV, Kugener G, Guenther LM, Malone CF, Durbin AD, Hong AL, Howard TP, Bandopadhyay P, Wechsler CS, Fung I, *et al* (2021) A first-generation pediatric cancer dependency map. *Nat Genet* 53: 529–538

- Dietrich S, Oleś M, Lu J, Sellner L, Anders S, Velten B, Wu B, Hüllein J, da Silva Liberio M, Walther T, *et al* (2018) Drug-perturbation-based stratification of blood cancer. *J Clin Invest* 128: 427–445
- Diffner E, Beck D, Gudgin E, Thoms JAI, Knezevic K, Pridans C, Foster S, Goode D, Lim WK, Boelen L, *et al* (2013) Activity of a heptad of transcription factors is associated with stem cell programs and clinical outcome in acute myeloid leukemia. *Blood* 121: 2289–2300
- DiNardo CD, Jonas BA, Pullarkat V, Thirman MJ, Garcia JS, Wei AH, Konopleva M, Döhner H, Letai A, Fenaux P, *et al* (2020a) Azacitidine and venetoclax in previously untreated acute myeloid leukemia. *N Engl J Med* 383: 617–629
- DiNardo CD, Lachowicz CA, Takahashi K, Loghavi S, Xiao L, Kadia T, Daver N, Adeoti M, Short NJ, Sasaki K, *et al* (2021) Venetoclax Combined With FLAG-IDA Induction and Consolidation in Newly Diagnosed and Relapsed or Refractory Acute Myeloid Leukemia. *J Clin Oncol* 39: 2768–2778
- DiNardo CD, Pratz KW, Letai A, Jonas BA, Wei AH, Thirman M, Arellano M, Frattini MG, Kantarjian H, Popovic R, *et al* (2018a) Safety and preliminary efficacy of venetoclax with decitabine or azacitidine in elderly patients with previously untreated acute myeloid leukaemia: a non-randomised, open-label, phase 1b study. *Lancet Oncol* 19: 216–228
- DiNardo CD, Stein EM, de Botton S, Roboz GJ, Altman JK, Mims AS, Swords R, Collins RH, Mannis GN, Pollyea DA, *et al* (2018b) Durable Remissions with Ivosidenib in IDH1-Mutated Relapsed or Refractory AML. *N Engl J Med* 378: 2386–2398
- DiNardo CD, Tiong IS, Quaglieri A, MacRaild S, Loghavi S, Brown FC, Thijssen R, Pomilio G, Ivey A, Salmon JM, *et al* (2020b) Molecular patterns of response and treatment failure after frontline venetoclax combinations in older patients with AML. *Blood* 135: 791–803
- Döhner H, Wei AH, Appelbaum FR, Craddock C, DiNardo CD, Dombret H, Ebert BL, Fenaux P, Godley LA, Hasserjian RP, *et al* (2022) Diagnosis and management of AML in adults: 2022 recommendations from an international expert panel on behalf of the ELN. *Blood* 140: 1345–1377
- Dong F, Brynes RK, Tidow N, Welte K, Löwenberg B & Touw IP (1995) Mutations in the gene for the granulocyte colony-stimulating-factor receptor in patients with acute myeloid leukemia preceded by severe congenital neutropenia. *N Engl J Med* 333: 487–493
- Doulatov S, Notta F, Laurenti E & Dick JE (2012) Hematopoiesis: a human perspective. *Cell Stem Cell* 10: 120–136
- Downing JR, Wilson RK, Zhang J, Mardis ER, Pui C-H, Ding L, Ley TJ & Evans WE (2012) The pediatric cancer genome project. *Nat Genet* 44: 619–622
- Druker BJ, Tamura S, Buchdunger E, Ohno S, Segal GM, Fanning S, Zimmermann J & Lydon NB (1996) Effects of a selective inhibitor of the Abl tyrosine kinase on the growth of Bcr-Abl positive cells. *Nat Med* 2: 561–566
- Dumon S, Santos SC, Debierre-Grockiego F, Gouilleux-Gruart V, Cocault L, Boucheron C, Mollat P, Gisselbrecht S & Gouilleux F (1999) IL-3 dependent regulation of Bcl-xL gene expression by STAT5 in a bone marrow derived cell line. *Oncogene* 18: 4191–4199
- Duployez N, Marceau-Renaut A, Villenet C, Petit A, Rousseau A, Ng SWK, Paquet A, Gonzales F, Barthélémy A, Leprêtre F, *et al* (2019) The stem cell-associated gene expression signature allows risk stratification in pediatric acute myeloid leukemia. *Leukemia* 33: 348–357

- Duployez N, Vasseur L, Kim R, Largeaud L, Passet M, L'Haridon A, Lemaire P, Fenwarth L, Geffroy S, Helevaut N, *et al* (2023) UBTF tandem duplications define a distinct subtype of adult de novo acute myeloid leukemia. *Leukemia* 37: 1245–1253
- Egan G & Tasian SK (2025) Precision medicine for high-risk gene fusions in pediatric AML: a focus on KMT2A, NUP98, and GLIS2 rearrangements. *Blood* 145: 2574–2586
- Elgarten CW & Aplenc R (2020) Pediatric acute myeloid leukemia: updates on biology, risk stratification, and therapy. *Curr Opin Pediatr* 32: 57–66
- Elion GB, Singer S & Hitchings GH (1954) Antagonists of nucleic acid derivatives. VIII. Synergism in combinations of biochemically related antimetabolites. *J Biol Chem* 208: 477–488
- Faber ZJ, Chen X, Gedman AL, Boggs K, Cheng J, Ma J, Radtke I, Chao J-R, Walsh MP, Song G, *et al* (2016) The genomic landscape of core-binding factor acute myeloid leukemias. *Nat Genet* 48: 1551–1556
- Falini B, Brunetti L, Sportoletti P & Martelli MP (2020) NPM1-mutated acute myeloid leukemia: from bench to bedside. *Blood* 136: 1707–1721
- Farber S & Diamond LK (1948) Temporary remissions in acute leukemia in children produced by folic acid antagonist, 4-aminopteroyl-glutamic acid. *N Engl J Med* 238: 787–793
- Filbin M & Monje M (2019) Developmental origins and emerging therapeutic opportunities for childhood cancer. *Nat Med* 25: 367–376
- Ford AM, Ridge SA, Cabrera ME, Mahmoud H, Steel CM, Chan LC & Greaves M (1993) In utero rearrangements in the trithorax-related oncogene in infant leukaemias. *Nature* 363: 358–360
- Fournier E, Duployez N, Ducourneau B, Raffoux E, Turlure P, Caillot D, Thomas X, Marceau-Renaut A, Chantepie S, Malfuson J-V, *et al* (2020) Mutational profile and benefit of gemtuzumab ozogamicin in acute myeloid leukemia. *Blood* 135: 542–546
- Frei E, Freireich EJ, Gehan E, Pinkel D, Holland JF, Selawry O, Haurani F, Spurr CL, Hayes DM, James GW, *et al* (1961) Studies of Sequential and Combination Antimetabolite Therapy in Acute Leukemia: 6-Mercaptopurine and Methotrexate. *Blood* 18: 431–454
- Friend SH, Bernards R, Rogelj S, Weinberg RA, Rapaport JM, Albert DM & Dryja TP (1986) A human DNA segment with properties of the gene that predisposes to retinoblastoma and osteosarcoma. *Nature* 323: 643–646
- Frismantas V, Dobay MP, Rinaldi A, Tchinda J, Dunn SH, Kunz J, Richter-Pechanska P, Marovca B, Pail O, Jenni S, *et al* (2017) Ex vivo drug response profiling detects recurrent sensitivity patterns in drug-resistant acute lymphoblastic leukemia. *Blood* 129: e26–e37
- Gale KB, Ford AM, Repp R, Borkhardt A, Keller C, Eden OB & Greaves MF (1997) Backtracking leukemia to birth: identification of clonotypic gene fusion sequences in neonatal blood spots. *Proc Natl Acad Sci USA* 94: 13950–13954
- Gamis AS, Alonzo TA, Meshinchi S, Sung L, Gerbing RB, Raimondi SC, Hirsch BA, Kahwash SB, Heerema-McKenney A, Winter L, *et al* (2014) Gemtuzumab ozogamicin in children and adolescents with de novo acute myeloid leukemia improves event-free survival by reducing relapse risk: results from the randomized phase III Children's Oncology Group trial AAML0531. *J Clin Oncol* 32: 3021–3032

- Gera JF, Mellinghoff IK, Shi Y, Rettig MB, Tran C, Hsu J, Sawyers CL & Lichtenstein AK (2004) AKT activity determines sensitivity to mammalian target of rapamycin (mTOR) inhibitors by regulating cyclin D1 and c-myc expression. *J Biol Chem* 279: 2737–2746
- Gerstung M, Jolly C, Leshchiner I, Dentro SC, Gonzalez S, Rosebrock D, Mitchell TJ, Rubanova Y, Anur P, Yu K, *et al* (2020) The evolutionary history of 2,658 cancers. *Nature* 578: 122–128
- Gough SM, Slape CI & Aplan PD (2011) NUP98 gene fusions and hematopoietic malignancies: common themes and new biologic insights. *Blood* 118: 6247–6257
- Greaves M & Maley CC (2012) Clonal evolution in cancer. *Nature* 481: 306–313
- Greaves M (2018) A causal mechanism for childhood acute lymphoblastic leukaemia. *Nat Rev Cancer* 18: 471–484
- Grimwade D, Walker H, Oliver F, Wheatley K, Harrison C, Harrison G, Rees J, Hann I, Stevens R, Burnett A, *et al* (1998) The importance of diagnostic cytogenetics on outcome in AML: analysis of 1,612 patients entered into the MRC AML 10 trial. *Blood* 92: 2322–2333
- Gröbner SN, Worst BC, Weischenfeldt J, Buchhalter I, Kleinheinz K, Rudneva VA, Johann PD, Balasubramanian GP, Segura-Wang M, Brabetz S, *et al* (2018) The landscape of genomic alterations across childhood cancers. *Nature* 555: 321–327
- Gruber TA, Larson Gedman A, Zhang J, Koss CS, Marada S, Ta HQ, Chen S-C, Su X, Ogden SK, Dang J, *et al* (2012) An Inv(16)(p13.3q24.3)-encoded CBFA2T3-GLIS2 fusion protein defines an aggressive subtype of pediatric acute megakaryoblastic leukemia. *Cancer Cell* 22: 683–697
- Grünewald TGP, Cidre-Aranaz F, Surdez D, Tomazou EM, de Álava E, Kovar H, Sorensen PH, Delattre O & Dirksen U (2018) Ewing sarcoma. *Nat Rev Dis Primers* 4: 5
- Guilliams M, Mildner A & Yona S (2018) Developmental and functional heterogeneity of monocytes. *Immunity* 49: 595–613
- Hambleton S, Salem S, Bustamante J, Bigley V, Boisson-Dupuis S, Azevedo J, Fortin A, Haniffa M, Ceron-Gutierrez L, Bacon CM, *et al* (2011) IRF8 mutations and human dendritic-cell immunodeficiency. *N Engl J Med* 365: 127–138
- Hanahan D & Weinberg RA (2000) The hallmarks of cancer. *Cell* 100: 57–70
- Hanahan D & Weinberg RA (2011) Hallmarks of cancer: the next generation. *Cell* 144: 646–674
- Hanahan D (2022) Hallmarks of cancer: New Dimensions. *Cancer Discov* 12: 31–46
- Hart A, Melet F, Grossfeld P, Chien K, Jones C, Tunnacliffe A, Favier R & Bernstein A (2000) Fli-1 is required for murine vascular and megakaryocytic development and is hemizygotously deleted in patients with thrombocytopenia. *Immunity* 13: 167–177
- Hauck F, Voss R, Urban C & Seidel MG (2018) Intrinsic and extrinsic causes of malignancies in patients with primary immunodeficiency disorders. *J Allergy Clin Immunol* 141: 59-68.e4
- Hauschild A, Grob J-J, Demidov LV, Jouary T, Gutzmer R, Millward M, Rutkowski P, Blank CU, Miller WH, Kaempgen E, *et al* (2012) Dabrafenib in BRAF-mutated metastatic

- melanoma: a multicentre, open-label, phase 3 randomised controlled trial. *Lancet* 380: 358–365
- Heikamp EB, Henrich JA, Perner F, Wong EM, Hatton C, Wen Y, Barwe SP, Gopalakrishnapillai A, Xu H, Uckelmann HJ, *et al* (2022) The menin-MLL1 interaction is a molecular dependency in NUP98-rearranged AML. *Blood* 139: 894–906
- Hertzman Johansson C & Egyhazi Brage S (2014) BRAF inhibitors in cancer therapy. *Pharmacol Ther* 142: 176–182
- Higuchi M, O'Brien D, Kumaravelu P, Lenny N, Yeoh E-J & Downing JR (2002) Expression of a conditional AML1-ETO oncogene bypasses embryonic lethality and establishes a murine model of human t(8;21) acute myeloid leukemia. *Cancer Cell* 1: 63–74
- Hirabayashi S, Wlodarski MW, Kozyra E & Niemeyer CM (2017) Heterogeneity of GATA2-related myeloid neoplasms. *Int J Hematol* 106: 175–182
- Hitchings GH & Elion GB (1954) The chemistry and biochemistry of purine analogs. *Ann N Y Acad Sci* 60: 195–199
- Hope KJ, Jin L & Dick JE (2004) Acute myeloid leukemia originates from a hierarchy of leukemic stem cell classes that differ in self-renewal capacity. *Nat Immunol* 5: 738–743
- Hoppe PS, Schwarzfischer M, Loeffler D, Kokkaliaris KD, Hilsenbeck O, Moritz N, Ende M, Filipczyk A, Gambardella A, Ahmed N, *et al* (2016) Early myeloid lineage choice is not initiated by random PU.1 to GATA1 protein ratios. *Nature* 535: 299–302
- Horak P, Heining C, Kreutzfeldt S, Hutter B, Mock A, Hülle J, Fröhlich M, Uhrig S, Jahn A, Rump A, *et al* (2021) Comprehensive Genomic and Transcriptomic Analysis for Guiding Therapeutic Decisions in Patients with Rare Cancers. *Cancer Discov* 11: 2780–2795
- Huang BJ, Smith JL, Farrar JE, Wang Y-C, Umeda M, Ries RE, Leonti AR, Crowgey E, Furlan SN, Tarlock K, *et al* (2022) Integrated stem cell signature and cytotoxic risk determination in pediatric acute myeloid leukemia. *Nat Commun* 13: 5487
- Inoue S, Riley J, Gant TW, Dyer MJS & Cohen GM (2007) Apoptosis induced by histone deacetylase inhibitors in leukemic cells is mediated by Bim and Noxa. *Leukemia* 21: 1773–1782
- Irmisch A, Bonilla X, Chevrier S, Lehmann K-V, Singer F, Toussaint NC, Esposito C, Mena J, Milani ES, Casanova R, *et al* (2021) The Tumor Profiler Study: integrated, multi-omic, functional tumor profiling for clinical decision support. *Cancer Cell* 39: 288–293
- Issa GC, Ravandi F, DiNardo CD, Jabbour E, Kantarjian HM & Andreeff M (2021) Therapeutic implications of menin inhibition in acute leukemias. *Leukemia* 35: 2482–2495
- Jagannathan-Bogdan M & Zon LI (2013) Hematopoiesis. *Development* 140: 2463–2467
- Jonkman-Berk BM, van den Berg JM, Ten Berge IJM, Bredius RGM, Driessen GJ, Dalm VASH, van Dissel JT, van Deuren M, Ellerbroek PM, van der Flier M, *et al* (2015) Primary immunodeficiencies in the Netherlands: national patient data demonstrate the increased risk of malignancy. *Clin Immunol* 156: 154–162
- Kale J, Osterlund EJ & Andrews DW (2018) BCL-2 family proteins: changing partners in the dance towards death. *Cell Death Differ* 25: 65–80

- Kalverda B, Pickersgill H, Shloma VV & Fornerod M (2010) Nucleoporins directly stimulate expression of developmental and cell-cycle genes inside the nucleoplasm. *Cell* 140: 360–371
- Kandoth C, McLellan MD, Vandin F, Ye K, Niu B, Lu C, Xie M, Zhang Q, McMichael JF, Wyczalkowski MA, *et al* (2013) Mutational landscape and significance across 12 major cancer types. *Nature* 502: 333–339
- Kazianka L, Pichler A, Agreiter C, Rohrbeck J, Kornauth C, Porpaczy E, Sillaber C, Sperr WR, Gleixner KV, Hauswirth A, *et al* (2025) Comparing functional and genomic-based precision medicine in blood cancer patients. *HemaSphere* 9: e70129
- Kentsis A (2020) Why do young people get cancer? *Pediatr Blood Cancer* 67: e28335
- Kentsis A (2024) Toward a unified theory of why young people develop cancer. *Cold Spring Harb Perspect Med* 14
- Khoury JD, Solary E, Abla O, Akkari Y, Alaggio R, Apperley JF, Bejar R, Berti E, Busque L, Chan JKC, *et al* (2022) The 5th edition of the World Health Organization Classification of Haematolymphoid Tumours: Myeloid and Histiocytic/Dendritic Neoplasms. *Leukemia* 36: 1703–1719
- Kocabas F, Zheng J, Thet S, Copeland NG, Jenkins NA, DeBerardinis RJ, Zhang C & Sadek HA (2012) Meis1 regulates the metabolic phenotype and oxidant defense of hematopoietic stem cells. *Blood* 120: 4963–4972
- Kohl TM, Hellinger C, Ahmed F, Buske C, Hiddemann W, Bohlander SK & Spiekermann K (2007) BH3 mimetic ABT-737 neutralizes resistance to FLT3 inhibitor treatment mediated by FLT3-independent expression of BCL2 in primary AML blasts. *Leukemia* 21: 1763–1772
- Kondo M, Weissman IL & Akashi K (1997) Identification of clonogenic common lymphoid progenitors in mouse bone marrow. *Cell* 91: 661–672
- Konopleva M, Pollyea DA, Potluri J, Chyla B, Hogdal L, Busman T, McKeegan E, Salem AH, Zhu M, Ricker JL, *et al* (2016) Efficacy and Biological Correlates of Response in a Phase II Study of Venetoclax Monotherapy in Patients with Acute Myelogenous Leukemia. *Cancer Discov* 6: 1106–1117
- Kornauth C, Pemovska T, Vladimer GI, Bayer G, Bergmann M, Eder S, Eichner R, Erl M, Esterbauer H, Exner R, *et al* (2022) Functional precision medicine provides clinical benefit in advanced aggressive hematologic cancers and identifies exceptional responders. *Cancer Discov* 12: 372–387
- Kratz CP, Jongmans MC, Cavé H, Wimmer K, Behjati S, Guerrini-Rousseau L, Milde T, Pajtler KW, Golmard L, Gauthier-Villars M, *et al* (2021) Predisposition to cancer in children and adolescents. *Lancet Child Adolesc Health* 5: 142–154
- Krivtsov AV & Armstrong SA (2007) MLL translocations, histone modifications and leukaemia stem-cell development. *Nat Rev Cancer* 7: 823–833
- Kropivsek K, Kachel P, Goetze S, Wegmann R, Festl Y, Severin Y, Hale BD, Mena J, van Drogen A, Dietliker N, *et al* (2023) Ex vivo drug response heterogeneity reveals personalized therapeutic strategies for patients with multiple myeloma. *Nat Cancer* 4: 734–753
- Küppers R (2003) B cells under influence: transformation of B cells by Epstein-Barr virus. *Nat Rev Immunol* 3: 801–812

- Kurmasheva RT, Huang S & Houghton PJ (2006) Predicted mechanisms of resistance to mTOR inhibitors. *Br J Cancer* 95: 955–960
- Kuusanmäki H, Leppä A-M, Pölönen P, Kontro M, Dufva O, Deb D, Yadav B, Brück O, Kumar A, Everaus H, *et al* (2020) Phenotype-based drug screening reveals association between venetoclax response and differentiation stage in acute myeloid leukemia. *Haematologica* 105: 708–720
- Lambo S, Trinh DL, Ries RE, Jin D, Setiadi A, Ng M, Leblanc VG, Loken MR, Brodersen LE, Dai F, *et al* (2023) A longitudinal single-cell atlas of treatment response in pediatric AML. *Cancer Cell* 41: 2117-2135.e12
- Lapidot T, Sirard C, Vormoor J, Murdoch B, Hoang T, Caceres-Cortes J, Minden M, Paterson B, Caligiuri MA & Dick JE (1994) A cell initiating human acute myeloid leukaemia after transplantation into SCID mice. *Nature* 367: 645–648
- Lara-Astiaso D, Goñi-Salaverri A, Mendieta-Esteban J, Narayan N, Del Valle C, Gross T, Giotopoulos G, Beinortas T, Navarro-Alonso M, Aguado-Alvaro LP, *et al* (2023) In vivo screening characterizes chromatin factor functions during normal and malignant hematopoiesis. *Nat Genet* 55: 1542–1554
- Latour S & Winter S (2018) Inherited Immunodeficiencies With High Predisposition to Epstein-Barr Virus-Driven Lymphoproliferative Diseases. *Front Immunol* 9: 1103
- Laurell E, Beck K, Krupina K, Theerthagiri G, Bodenmiller B, Horvath P, Aebersold R, Antonin W & Kutay U (2011) Phosphorylation of Nup98 by multiple kinases is crucial for NPC disassembly during mitotic entry. *Cell* 144: 539–550
- Lau LMS, Khuong-Quang D-A, Mayoh C, Wong M, Barahona P, Ajuyah P, Senapati A, Nagabushan S, Sherstyuk A, Altekoeester A-K, *et al* (2024) Precision-guided treatment in high-risk pediatric cancers. *Nat Med* 30: 1913–1922
- Laurenti E & Göttgens B (2018) From haematopoietic stem cells to complex differentiation landscapes. *Nature* 553: 418–426
- Lavau C, Szilvassy SJ, Slany R & Cleary ML (1997) immortalization and leukemic transformation of a myelomonocytic precursor by retrovirally transduced HRX-ENL. *EMBO J* 16: 4226–4237
- Lee S, Weiss T, Bühler M, Mena J, Lottenbach Z, Wegmann R, Sun M, Bihl M, Augustynek B, Baumann SP, *et al* (2024) High-throughput identification of repurposable neuroactive drugs with potent anti-glioblastoma activity. *Nat Med* 30: 3196–3208
- Letai A, Bhola P & Welm AL (2022) Functional precision oncology: Testing tumors with drugs to identify vulnerabilities and novel combinations. *Cancer Cell* 40: 26–35
- Letai A (2017) Functional precision cancer medicine-moving beyond pure genomics. *Nat Med* 23: 1028–1035
- Letai A (2022) Functional precision medicine: putting drugs on patient cancer cells and seeing what happens. *Cancer Discov* 12: 290–292
- Levenson JD, Sampath D, Souers AJ, Rosenberg SH, Fairbrother WJ, Amiot M, Konopleva M & Letai A (2017) Found in Translation: How Preclinical Research Is Guiding the Clinical Development of the BCL2-Selective Inhibitor Venetoclax. *Cancer Discov* 7: 1376–1393



- Le Q, Hadland B, Smith JL, Leonti A, Huang BJ, Ries R, Hylkema TA, Castro S, Tang TT, McKay CN, *et al* (2022) CBFA2T3-GLIS2 model of pediatric acute megakaryoblastic leukemia identifies FOLR1 as a CAR T cell target. *J Clin Invest* 132
- Lichtman MA (2013) A historical perspective on the development of the cytarabine (7days) and daunorubicin (3days) treatment regimen for acute myelogenous leukemia: 2013 the 40th anniversary of 7+3. *Blood Cells Mol Dis* 50: 119–130
- Liebers N, Bruch P-M, Terzer T, Hernandez-Hernandez M, Paramasivam N, Fitzgerald D, Altmann H, Roeder T, Kolb C, Knoll M, *et al* (2023) Ex vivo drug response profiling for response and outcome prediction in hematologic malignancies: the prospective non-interventional SMARTrial. *Nat Cancer* 4: 1648–1659
- Liu F, Walmsley M, Rodaway A & Patient R (2008) Fli1 acts at the top of the transcriptional network driving blood and endothelial development. *Curr Biol* 18: 1234–1240
- Liu P, Tarlé SA, Hajra A, Claxton DF, Marlton P, Freedman M, Siciliano MJ & Collins FS (1993) Fusion between transcription factor CBF beta/PEBP2 beta and a myosin heavy chain in acute myeloid leukemia. *Science* 261: 1041–1044
- Loghavi S, Kanagal-Shamanna R, Khoury JD, Medeiros LJ, Naresh KN, Nejati R, Patnaik MM & WHO 5th Edition Classification Project (2024) Fifth edition of the world health classification of tumors of the hematopoietic and lymphoid tissue: myeloid neoplasms. *Mod Pathol* 37: 100397
- López-Otín C, Blasco MA, Partridge L, Serrano M & Kroemer G (2023) Hallmarks of aging: An expanding universe. *Cell* 186: 243–278
- Loughran SJ, Kruse EA, Hacking DF, de Graaf CA, Hyland CD, Willson TA, Henley KJ, Ellis S, Voss AK, Metcalf D, *et al* (2008) The transcription factor Erg is essential for definitive hematopoiesis and the function of adult hematopoietic stem cells. *Nat Immunol* 9: 810–819
- Maia AT, Koechling J, Corbett R, Metzler M, Wiemels JL & Greaves M (2004) Protracted postnatal natural histories in childhood leukemia. *Genes Chromosomes Cancer* 39: 335–340
- Majeti R, Park CY & Weissman IL (2007) Identification of a hierarchy of multipotent hematopoietic progenitors in human cord blood. *Cell Stem Cell* 1: 635–645
- Manz MG, Miyamoto T, Akashi K & Weissman IL (2002) Prospective isolation of human clonogenic common myeloid progenitors. *Proc Natl Acad Sci USA* 99: 11872–11877
- Marine J-C, Dawson S-J & Dawson MA (2020) Non-genetic mechanisms of therapeutic resistance in cancer. *Nat Rev Cancer* 20: 743–756
- Maris JM (2015) Defining why cancer develops in children. *N Engl J Med* 373: 2373–2375
- Masetti R, Vendemini F, Zama D, Biagi C, Pession A & Locatelli F (2015) Acute myeloid leukemia in infants: biology and treatment. *Front Pediatr* 3: 37
- Ma X, Liu Y, Liu Y, Alexandrov LB, Edmonson MN, Gawad C, Zhou X, Li Y, Rusch MC, Easton J, *et al* (2018) Pan-cancer genome and transcriptome analyses of 1,699 paediatric leukaemias and solid tumours. *Nature* 555: 371–376
- Malani D, Kumar A, Brück O, Kontro M, Yadav B, Hellesøy M, Kuusanmäki H, Dufva O, Kankainen M, Eldfors S, *et al* (2022) Implementing a functional precision medicine tumor board for acute myeloid leukemia. *Cancer Discov* 12: 388–401

- Marshall GM, Carter DR, Cheung BB, Liu T, Mateos MK, Meyerowitz JG & Weiss WA (2014) The prenatal origins of cancer. *Nat Rev Cancer* 14: 277–289
- de Martel C, Plummer M, Vignat J & Franceschi S (2017) Worldwide burden of cancer attributable to HPV by site, country and HPV type. *Int J Cancer* 141: 664–670
- Martens JHA & Stunnenberg HG (2010) The molecular signature of oncofusion proteins in acute myeloid leukemia. *FEBS Lett* 584: 2662–2669
- Martínez-Gamboa DA & Kaner J (2025) Revumenib: a new era in acute leukemia treatment. *Trends Cancer* 11: 81–83
- Masetti R, Baccelli F, Leardini D, Gottardi F, Vendemini F, Di Gangi A, Becilli M, Lodi M, Tumino M, Vinci L, *et al* (2023) Venetoclax-based therapies in pediatric advanced MDS and relapsed/refractory AML: a multicenter retrospective analysis. *Blood Adv* 7: 4366–4370
- Masetti R, Bertuccio SN, Pession A & Locatelli F (2019) CBFA2T3-GLIS2-positive acute myeloid leukaemia. A peculiar paediatric entity. *Br J Haematol* 184: 337–347
- Masetti R, Castelli I, Astolfi A, Bertuccio SN, Indio V, Togni M, Belotti T, Serravalle S, Tarantino G, Zecca M, *et al* (2016) Genomic complexity and dynamics of clonal evolution in childhood acute myeloid leukemia studied with whole-exome sequencing. *Oncotarget* 7: 56746–56757
- Masson K & Rönstrand L (2009) Oncogenic signaling from the hematopoietic growth factor receptors c-Kit and Flt3. *Cell Signal* 21: 1717–1726
- Matkar S, Thiel A & Hua X (2013) Menin: a scaffold protein that controls gene expression and cell signaling. *Trends Biochem Sci* 38: 394–402
- Matthay KK, Maris JM, Schleiermacher G, Nakagawara A, Mackall CL, Diller L & Weiss WA (2016) Neuroblastoma. *Nat Rev Dis Primers* 2: 16078
- Matthews GM, Newbold A & Johnstone RW (2012) Intrinsic and extrinsic apoptotic pathway signaling as determinants of histone deacetylase inhibitor antitumor activity. *Adv Cancer Res* 116: 165–197
- McKercher SR, Torbett BE, Anderson KL, Henkel GW, Vestal DJ, Baribault H, Klemsz M, Feeney AJ, Wu GE, Paige CJ, *et al* (1996) Targeted disruption of the PU.1 gene results in multiple hematopoietic abnormalities. *EMBO J* 15: 5647–5658
- McNeer NA, Philip J, Geiger H, Ries RE, Lavallée V-P, Walsh M, Shah M, Arora K, Emde A-K, Robine N, *et al* (2019) Genetic mechanisms of primary chemotherapy resistance in pediatric acute myeloid leukemia. *Leukemia* 33: 1934–1943
- Merlo LMF, Pepper JW, Reid BJ & Maley CC (2006) Cancer as an evolutionary and ecological process. *Nat Rev Cancer* 6: 924–935
- Meyer C, Kowarz E, Hofmann J, Renneville A, Zuna J, Trka J, Ben Abdelali R, Macintyre E, De Braekeleer E, De Braekeleer M, *et al* (2009) New insights to the MLL recombinome of acute leukemias. *Leukemia* 23: 1490–1499
- Michmerhuizen NL, Klco JM & Mullighan CG (2020) Mechanistic insights and potential therapeutic approaches for NUP98-rearranged hematologic malignancies. *Blood* 136: 2275–2289

- Miglino N, Toussaint NC, Ring A, Bonilla X, Tusup M, Gosztonyi B, Mehra T, Gut G, Jacob F, Chevrier S, *et al* (2025) Feasibility of multiomics tumor profiling for guiding treatment of melanoma. *Nat Med* 31: 2430–2441
- Misaghian N, Ligresti G, Steelman LS, Bertrand FE, Bäsecke J, Libra M, Nicoletti F, Stivala F, Milella M, Tafuri A, *et al* (2009) Targeting the leukemic stem cell: the Holy Grail of leukemia therapy. *Leukemia* 23: 25–42
- Miyoshi H, Shimizu K, Kozu T, Maseki N, Kaneko Y & Ohki M (1991) t(8;21) breakpoints on chromosome 21 in acute myeloid leukemia are clustered within a limited region of a single gene, AML1. *Proc Natl Acad Sci USA* 88: 10431–10434
- Muzio LL, Ballini A, Cantore S, Bottalico L, Charitos IA, Ambrosino M, Nocini R, Malcangi A, Dioguardi M, Cazzolla AP, *et al* (2021) Overview of *Candida albicans* and Human Papillomavirus (HPV) Infection Agents and their Biomolecular Mechanisms in Promoting Oral Cancer in Pediatric Patients. *Biomed Res Int* 2021: 7312611
- Naik SH, Perié L, Swart E, Gerlach C, van Rooij N, de Boer RJ & Schumacher TN (2013) Diverse and heritable lineage imprinting of early haematopoietic progenitors. *Nature* 496: 229–232
- Nakamura-Ishizu A, Matsumura T, Stumpf PS, Umemoto T, Takizawa H, Takihara Y, O’Neil A, Majeed ABBA, MacArthur BD & Suda T (2018) Thrombopoietin Metabolically Primes Hematopoietic Stem Cells to Megakaryocyte-Lineage Differentiation. *Cell Rep* 25: 1772-1785.e6
- von Neuhoff C, Reinhardt D, Sander A, Zimmermann M, Bradtke J, Betts DR, Zemanova Z, Stary J, Bourquin J-P, Haas OA, *et al* (2010) Prognostic impact of specific chromosomal aberrations in a large group of pediatric patients with acute myeloid leukemia treated uniformly according to trial AML-BFM 98. *J Clin Oncol* 28: 2682–2689
- Ng SWK, Mitchell A, Kennedy JA, Chen WC, McLeod J, Ibrahimova N, Arruda A, Popescu A, Gupta V, Schimmer AD, *et al* (2016) A 17-gene stemness score for rapid determination of risk in acute leukaemia. *Nature* 540: 433–437
- Niemeyer CM (2014) RAS diseases in children. *Haematologica* 99: 1653–1662
- Niswander LM, Chung P, Diorio C & Tasian SK (2023) Clinical responses in pediatric patients with relapsed/refractory leukemia treated with azacitidine and venetoclax. *Haematologica* 108: 3142–3147
- Ni Chonghaile T, Sarosiek KA, Vo T-T, Ryan JA, Tammareddi A, Moore VDG, Deng J, Anderson KC, Richardson P, Tai Y-T, *et al* (2011) Pretreatment mitochondrial priming correlates with clinical response to cytotoxic chemotherapy. *Science* 334: 1129–1133
- Notta F, Doulatov S, Laurenti E, Poeppl A, Jurisica I & Dick JE (2011) Isolation of single human hematopoietic stem cells capable of long-term multilineage engraftment. *Science* 333: 218–221
- Notta F, Zandi S, Takayama N, Dobson S, Gan OI, Wilson G, Kaufmann KB, McLeod J, Laurenti E, Dunant CF, *et al* (2016) Distinct routes of lineage development reshape the human blood hierarchy across ontogeny. *Science* 351: aab2116
- Nowell PC (1976) The clonal evolution of tumor cell populations. *Science* 194: 23–28
- O’Dwyer PJ, Gray RJ, Flaherty KT, Chen AP, Li S, Wang V, McShane LM, Patton DR, Tricoli JV, Williams PM, *et al* (2023) The NCI-MATCH trial: lessons for precision oncology. *Nat Med* 29: 1349–1357

- Okuda T, van Deursen J, Hiebert SW, Grosveld G & Downing JR (1996) AML1, the target of multiple chromosomal translocations in human leukemia, is essential for normal fetal liver hematopoiesis. *Cell* 84: 321–330
- Olsson A, Venkatasubramanian M, Chaudhri VK, Aronow BJ, Salomonis N, Singh H & Grimes HL (2016) Single-cell analysis of mixed-lineage states leading to a binary cell fate choice. *Nature* 537: 698–702
- Orkin SH & Zon LI (2008) Hematopoiesis: an evolving paradigm for stem cell biology. *Cell* 132: 631–644
- Orkin SH (1995) Transcription factors and hematopoietic development. *J Biol Chem* 270: 4955–4958
- Pan R, Hogdal LJ, Benito JM, Bucci D, Han L, Borthakur G, Cortes J, DeAngelo DJ, Debose L, Mu H, *et al* (2014) Selective BCL-2 inhibition by ABT-199 causes on-target cell death in acute myeloid leukemia. *Cancer Discov* 4: 362–375
- Pareja F, Ptashkin RN, Brown DN, Derakhshan F, Selenica P, da Silva EM, Gazzo AM, Da Cruz Paula A, Breen K, Shen R, *et al* (2022) Cancer-Causative Mutations Occurring in Early Embryogenesis. *Cancer Discov* 12: 949–957
- Paulson KG & Nghiem P (2019) One in a hundred million: Merkel cell carcinoma in pediatric and young adult patients is rare but more likely to present at advanced stages based on US registry data. *J Am Acad Dermatol* 80: 1758–1760
- Paul F, Arkin Y, Giladi A, Jaitin DA, Kenigsberg E, Keren-Shaul H, Winter D, Lara-Astiaso D, Gury M, Weiner A, *et al* (2015) Transcriptional heterogeneity and lineage commitment in myeloid progenitors. *Cell* 163: 1663–1677
- Pemovska T, Kontro M, Yadav B, Edgren H, Eldfors S, Szwajda A, Almusa H, Beshpalov MM, Ellonen P, Elonen E, *et al* (2013) Individualized systems medicine strategy to tailor treatments for patients with chemorefractory acute myeloid leukemia. *Cancer Discov* 3: 1416–1429
- Perié L & Duffy KR (2016) Retracing the in vivo haematopoietic tree using single-cell methods. *FEBS Lett* 590: 4068–4083
- Peterziel H, Jamaladdin N, ElHarouni D, Gerloff XF, Herter S, Fiesel P, Berker Y, Blattner-Johnson M, Schramm K, Jones BC, *et al* (2022) Drug sensitivity profiling of 3D tumor tissue cultures in the pediatric precision oncology program INFORM. *NPJ Precis Oncol* 6: 94
- Pikman Y, Tasian SK, Sulis ML, Stevenson K, Blonquist TM, Apsel Winger B, Cooper TM, Pauly M, Maloney KW, Burke MJ, *et al* (2021) Matched Targeted Therapy for Pediatric Patients with Relapsed, Refractory, or High-Risk Leukemias: A Report from the LEAP Consortium. *Cancer Discov* 11: 1424–1439
- Pinkel D (1971) Five-year follow-up of “total therapy” of childhood lymphocytic leukemia. *JAMA* 216: 648–652
- Pishvaian MJ, Blais EM, Brody JR, Lyons E, DeArbeloa P, Hendifar A, Mikhail S, Chung V, Sahai V, Sohal DPS, *et al* (2020) Overall survival in patients with pancreatic cancer receiving matched therapies following molecular profiling: a retrospective analysis of the Know Your Tumor registry trial. *Lancet Oncol* 21: 508–518
- Pollard JA, Alonzo TA, Gerbing R, Brown P, Fox E, Choi J, Fisher B, Hirsch B, Kahwash S, Getz K, *et al* (2022) Sorafenib in combination with standard chemotherapy for children with

- high allelic ratio FLT3/ITD+ acute myeloid leukemia: A report from the children's oncology group protocol AAML1031. *J Clin Oncol* 40: 2023–2035
- Pollard JA, Loken M, Gerbing RB, Raimondi SC, Hirsch BA, Aplenc R, Bernstein ID, Gamis AS, Alonzo TA & Meshinchi S (2016) CD33 expression and its association with gemtuzumab ozogamicin response: results from the randomized phase III children's oncology group trial AAML0531. *J Clin Oncol* 34: 747–755
- Pollyea DA, Amaya M, Strati P & Konopleva MY (2019) Venetoclax for AML: changing the treatment paradigm. *Blood Adv* 3: 4326–4335
- Pombo-de-Oliveira MS, Dobbin JA, Loureiro P, Borducchi D, Maia RC, Fernandes MA, Cavalcanti GB, Takemoto S & Franchini G (2002) Genetic mutation and early onset of T-cell leukemia in pediatric patients infected at birth with HTLV-I. *Leuk Res* 26: 155–161
- Pommert L & Tarlock K (2022) The evolution of targeted therapy in pediatric AML: gemtuzumab ozogamicin, FLT3/IDH/BCL2 inhibitors, and other therapies. *Hematology Am Soc Hematol Educ Program* 2022: 603–610
- Porcher C, Swat W, Rockwell K, Fujiwara Y, Alt FW & Orkin SH (1996) The T cell leukemia oncoprotein SCL/tal-1 is essential for development of all hematopoietic lineages. *Cell* 86: 47–57
- Pui C-H & Evans WE (2013) A 50-year journey to cure childhood acute lymphoblastic leukemia. *Semin Hematol* 50: 185–196
- Pulikkan JA, Tenen DG & Behre G (2017) C/EBP $\alpha$  deregulation as a paradigm for leukemogenesis. *Leukemia* 31: 2279–2285
- Rahman N, Arbour L, Tonin P, Renshaw J, Pelletier J, Baruchel S, Pritchard-Jones K, Stratton MR & Narod SA (1996) Evidence for a familial Wilms' tumour gene (FWT1) on chromosome 17q12-q21. *Nat Genet* 13: 461–463
- Ramirez CN, Antczak C & Djaballah H (2010) Cell viability assessment: toward content-rich platforms. *Expert Opin Drug Discov* 5: 223–233
- Rao RC & Dou Y (2015) Hijacked in cancer: the KMT2 (MLL) family of methyltransferases. *Nat Rev Cancer* 15: 334–346
- Rasche M, Zimmermann M, Borschel L, Bourquin J-P, Dworzak M, Klingebiel T, Lehrnbecher T, Creutzig U, Klusmann J-H & Reinhardt D (2018) Successes and challenges in the treatment of pediatric acute myeloid leukemia: a retrospective analysis of the AML-BFM trials from 1987 to 2012. *Leukemia* 32: 2167–2177
- Rasche M, Zimmermann M, Steidel E, Alonzo T, Aplenc R, Bourquin J-P, Boztug H, Cooper T, Gamis AS, Gerbing RB, *et al* (2021) Survival Following Relapse in Children with Acute Myeloid Leukemia: A Report from AML-BFM and COG. *Cancers (Basel)* 13
- Rasouli M, Blair H, Troester S, Szoltysek K, Cameron R, Ashtiani M, Krippner-Heidenreich A, Grebien F, McGeehan G, Zwaan CM, *et al* (2023) The MLL-Menin Interaction is a Therapeutic Vulnerability in NUP98-rearranged AML. *HemaSphere* 7: e935
- Rasouli M, Troester S, Grebien F, Goemans BF, Zwaan CM & Heidenreich O (2024) NUP98 oncofusions in myeloid malignancies: An update on molecular mechanisms and therapeutic opportunities. *HemaSphere* 8: e70013
- Rieger MA & Schroeder T (2012) Hematopoiesis. *Cold Spring Harb Perspect Biol* 4

- Robb L, Elwood NJ, Elefanty AG, Köntgen F, Li R, Barnett LD & Begley CG (1996) The scl gene product is required for the generation of all hematopoietic lineages in the adult mouse. *EMBO J* 15: 4123–4129
- Robb L, Lyons I, Li R, Hartley L, Köntgen F, Harvey RP, Metcalf D & Begley CG (1995) Absence of yolk sac hematopoiesis from mice with a targeted disruption of the scl gene. *Proc Natl Acad Sci USA* 92: 7075–7079
- de Rooij JDE, Zwaan CM & van den Heuvel-Eibrink M (2015) Pediatric AML: from biology to clinical management. *J Clin Med* 4: 127–149
- Rudelius M, Weinberg OK, Niemeyer CM, Shimamura A & Calvo KR (2023) The International Consensus Classification (ICC) of hematologic neoplasms with germline predisposition, pediatric myelodysplastic syndrome, and juvenile myelomonocytic leukemia. *Virchows Arch* 482: 113–130
- Sahoo SS, Kozyra EJ & Wlodarski MW (2020) Germline predisposition in myeloid neoplasms: Unique genetic and clinical features of GATA2 deficiency and SAMD9/SAMD9L syndromes. *Best Pract Res Clin Haematol* 33: 101197
- Sakurai M & Sandberg AA (1973) Prognosis of acute myeloblastic leukemia: chromosomal correlation. *Blood* 41: 93–104
- Sanada C, Xavier-Ferrucio J, Lu Y-C, Min E, Zhang P-X, Zou S, Kang E, Zhang M, Zerafati G, Gallagher PG, *et al* (2016) Adult human megakaryocyte-erythroid progenitors are in the CD34+CD38mid fraction. *Blood* 128: 923–933
- Sangle NA & Perkins SL (2011) Core-binding factor acute myeloid leukemia. *Arch Pathol Lab Med* 135: 1504–1509
- Secker-Walker LM, Lawler SD & Hardisty RM (1978) Prognostic implications of chromosomal findings in acute lymphoblastic leukaemia at diagnosis. *Br Med J* 2: 1529–1530
- Severin Y, Hale BD, Mena J, Goslings D, Frey BM & Snijder B (2022) Multiplexed high-throughput immune cell imaging reveals molecular health-associated phenotypes. *Sci Adv* 8: eabn5631
- Sexauer AN & Tasian SK (2017) Targeting FLT3 signaling in childhood acute myeloid leukemia. *Front Pediatr* 5: 248
- Shapiro RS (2011) Malignancies in the setting of primary immunodeficiency: Implications for hematologists/oncologists. *Am J Hematol* 86: 48–55
- Shiraishi Y, Taguchi H, Niiya K, Shiomi F, Kikukawa K, Kubonishi S, Ohmura T, Hamawaki M & Ueda N (1982) Diagnostic and prognostic significance of chromosome abnormalities in marrow and mitogen response of lymphocytes of acute nonlymphocytic leukemia. *Cancer Genet Cytogenet* 5: 1–24
- Shivdasani RA & Orkin SH (1996) The transcriptional control of hematopoiesis [see comments]. *Blood* 87: 4025–4039
- Shlush LI, Mitchell A, Heisler L, Abelson S, Ng SWK, Trotman-Grant A, Medeiros JF, Rao-Bhatia A, Jaciw-Zurakowsky I, Marke R, *et al* (2017) Tracing the origins of relapse in acute myeloid leukaemia to stem cells. *Nature* 547: 104–108
- Sicklick JK, Kato S, Okamura R, Schwaederle M, Hahn ME, Williams CB, De P, Krie A, Piccioni DE, Miller VA, *et al* (2019) Molecular profiling of cancer patients enables personalized combination therapy: the I-PREDICT study. *Nat Med* 25: 744–750

- Siegel RL, Kratzer TB, Giaquinto AN, Sung H & Jemal A (2025) Cancer statistics, 2025. *CA Cancer J Clin* 75: 10–45
- Skokowa J, Dale DC, Touw IP, Zeidler C & Welte K (2017) Severe congenital neutropenias. *Nat Rev Dis Primers* 3: 17032
- Smith ML, Cavenagh JD, Lister TA & Fitzgibbon J (2004) Mutation of CEBPA in familial acute myeloid leukemia. *N Engl J Med* 351: 2403–2407
- Snijder B, Vladimer GI, Krall N, Miura K, Schmolke A-S, Kornauth C, Lopez de la Fuente O, Choi H-S, van der Kouwe E, Gültekin S, *et al* (2017) Image-based ex-vivo drug screening for patients with aggressive haematological malignancies: interim results from a single-arm, open-label, pilot study. *Lancet Haematol* 4: e595–e606
- Speck NA & Gilliland DG (2002) Core-binding factors in haematopoiesis and leukaemia. *Nat Rev Cancer* 2: 502–513
- Spinner MA, Aleshin A, Santaguida MT, Schaffert SA, Zehnder JL, Patterson AS, Gekas C, Heiser D & Greenberg PL (2020) Ex vivo drug screening defines novel drug sensitivity patterns for informing personalized therapy in myeloid neoplasms. *Blood Adv* 4: 2768–2778
- Stein EM, DiNardo CD, Pollyea DA, Fathi AT, Roboz GJ, Altman JK, Stone RM, DeAngelo DJ, Levine RL, Flinn IW, *et al* (2017) Enasidenib in mutant IDH2 relapsed or refractory acute myeloid leukemia. *Blood* 130: 722–731
- Steliarova-Foucher E, Colombet M, Ries LAG, Moreno F, Dolya A, Bray F, Hesselting P, Shin HY, Stiller CA & IICC-3 contributors (2017) International incidence of childhood cancer, 2001–10: a population-based registry study. *Lancet Oncol* 18: 719–731
- Stone RM, Mandrekar SJ, Sanford BL, Laumann K, Geyer S, Bloomfield CD, Thiede C, Prior TW, Döhner K, Marcucci G, *et al* (2017) Midostaurin plus Chemotherapy for Acute Myeloid Leukemia with a FLT3 Mutation. *N Engl J Med* 377: 454–464
- Strachan DC, Gu CJ, Kita R, Anderson EK, Richardson MA, Yam G, Pimm G, Roselli J, Schweickert A, Terrell M, *et al* (2022) Ex Vivo Drug Sensitivity Correlates with Clinical Response and Supports Personalized Therapy in Pediatric AML. *Cancers (Basel)* 14
- Stratikopoulos EE, Dendy M, Szabolcs M, Khaykin AJ, Lefebvre C, Zhou M-M & Parsons R (2015) Kinase and BET inhibitors together clamp inhibition of PI3K signaling and overcome resistance to therapy. *Cancer Cell* 27: 837–851
- Struski S, Lagarde S, Bories P, Puisieux C, Prade N, Cuccuini W, Pages MP, Bidet A, Gervais C, Lafage-Pochitaloff M, *et al* (2017) NUP98 is rearranged in 3.8% of pediatric AML forming a clinical and molecular homogenous group with a poor prognosis. *Leukemia* 31: 565–572
- Subramanian S, Thoms JAI, Huang Y, Cornejo-Páramo P, Koch FC, Jacquelin S, Shen S, Song E, Joshi S, Brownlee C, *et al* (2023) Genome-wide transcription factor-binding maps reveal cell-specific changes in the regulatory architecture of human HSPCs. *Blood* 142: 1448–1462
- Tarlock K, Alonzo TA, Gerbing RB, Wang Y-C, Ries RE, Hirsch BA, Lange B, Woods WG, Cooper TM, Gamis AS, *et al* (2021) Significant Improvements in Survival for Patients with t(6;9)(p23;q34)/ *DEK-NUP214* in Contemporary Trials with Intensification of Therapy: A Report from the Children’s Oncology Group. *Blood* 138: 519–519

- Taylor GS, Long HM, Brooks JM, Rickinson AB & Hislop AD (2015) The immunology of Epstein-Barr virus-induced disease. *Annu Rev Immunol* 33: 787–821
- Thirant C, Ignacimouttou C, Lopez CK, Diop M, Le Mouël L, Thiollier C, Siret A, Dessen P, Aid Z, Rivière J, *et al* (2017) ETO2-GLIS2 Hijacks Transcriptional Complexes to Drive Cellular Identity and Self-Renewal in Pediatric Acute Megakaryoblastic Leukemia. *Cancer Cell* 31: 452–465
- Thoms JAI, Truong P, Subramanian S, Knezevic K, Harvey G, Huang Y, Seneviratne JA, Carter DR, Joshi S, Skhinas J, *et al* (2021) Disruption of a GATA2-TAL1-ERG regulatory circuit promotes erythroid transition in healthy and leukemic stem cells. *Blood* 138: 1441–1455
- Tian X, Srinivasan PR, Tajiknia V, Sanchez Sevilla Uruchurtu AF, Seyhan AA, Carneiro BA, De La Cruz A, Pinho-Schwermann M, George A, Zhao S, *et al* (2024) Targeting apoptotic pathways for cancer therapy. *J Clin Invest* 134
- Tierens A, Arad-Cohen N, Cheuk D, De Moerloose B, Fernandez Navarro JM, Hasle H, Jahnukainen K, Juul-Dam KL, Kaspers G, Kovalova Z, *et al* (2024) Mitoxantrone versus liposomal daunorubicin in induction of pediatric AML with risk stratification based on flow cytometry measurement of residual disease. *J Clin Oncol* 42: 2174–2185
- Tierens A, Bjørklund E, Siitonen S, Marquart HV, Wulff-Juergensen G, Pelliniemi T-T, Forestier E, Hasle H, Jahnukainen K, Lausen B, *et al* (2016) Residual disease detected by flow cytometry is an independent predictor of survival in childhood acute myeloid leukaemia; results of the NOPHO-AML 2004 study. *Br J Haematol* 174: 600–609
- van Tilburg CM, Pfaff E, Pajtler KW, Langenberg KPS, Fiesel P, Jones BC, Balasubramanian GP, Stark S, Johann PD, Blattner-Johnson M, *et al* (2021) The Pediatric Precision Oncology INFORM Registry: Clinical Outcome and Benefit for Patients with Very High-Evidence Targets. *Cancer Discov* 11: 2764–2779
- Tsai FY, Keller G, Kuo FC, Weiss M, Chen J, Rosenblatt M, Alt FW & Orkin SH (1994) An early haematopoietic defect in mice lacking the transcription factor GATA-2. *Nature* 371: 221–226
- Tyner JW, Tognon CE, Bottomly D, Wilmot B, Kurtz SE, Savage SL, Long N, Schultz AR, Traer E, Abel M, *et al* (2018) Functional genomic landscape of acute myeloid leukaemia. *Nature* 562: 526–531
- Uckelmann HJ, Haarer EL, Takeda R, Wong EM, Hatton C, Marinaccio C, Perner F, Rajput M, Antonissen NJC, Wen Y, *et al* (2023) Mutant NPM1 directly regulates oncogenic transcription in acute myeloid leukemia. *Cancer Discov* 13: 746–765
- Umeda M, Ma J, Huang BJ, Hagiwara K, Westover T, Abdelhamed S, Barajas JM, Thomas ME, Walsh MP, Song G, *et al* (2022) Integrated genomic analysis identifies UBTF tandem duplications as a recurrent lesion in pediatric acute myeloid leukemia. *Blood Cancer Discov* 3: 194–207
- Umeda M, Ma J, Westover T, Ni Y, Song G, Maciaszek JL, Rusch M, Rahbarinia D, Foy S, Huang BJ, *et al* (2024) A new genomic framework to categorize pediatric acute myeloid leukemia. *Nat Genet* 56: 281–293
- Vardiman JW, Harris NL & Brunning RD (2002) The World Health Organization (WHO) classification of the myeloid neoplasms. *Blood* 100: 2292–2302



- Velten L, Haas SF, Raffel S, Blaszkiewicz S, Islam S, Hennig BP, Hirche C, Lutz C, Buss EC, Nowak D, *et al* (2017) Human haematopoietic stem cell lineage commitment is a continuous process. *Nat Cell Biol* 19: 271–281
- Vo T-T, Ryan J, Carrasco R, Neuberg D, Rossi DJ, Stone RM, Deangelo DJ, Frattini MG & Letai A (2012) Relative mitochondrial priming of myeloblasts and normal HSCs determines chemotherapeutic success in AML. *Cell* 151: 344–355
- Wachter F & Pikman Y (2024) Pathophysiology of acute myeloid leukemia. *Acta Haematol* 147: 229–246
- Wang CQ, Chin DWL, Chooi JY, Chng WJ, Taniuchi I, Tergaonkar V & Osato M (2015) Cbfb deficiency results in differentiation blocks and stem/progenitor cell expansion in hematopoiesis. *Leukemia* 29: 753–757
- Wang H, Chan KYY, Cheng CK, Ng MHL, Lee PY, Cheng FWT, Lam GKS, Chow TW, Ha SY, Chiang AKS, *et al* (2022) Pharmacogenomic profiling of pediatric acute myeloid leukemia to identify therapeutic vulnerabilities and inform functional precision medicine. *Blood Cancer Discov* 3: 516–535
- Wang Q, Stacy T, Miller JD, Lewis AF, Gu TL, Huang X, Bushweller JH, Bories JC, Alt FW, Ryan G, *et al* (1996) The CBFbeta subunit is essential for CBFalpha2 (AML1) function in vivo. *Cell* 87: 697–708
- Warren AJ, Colledge WH, Carlton MB, Evans MJ, Smith AJ & Rabbitts TH (1994) The oncogenic cysteine-rich LIM domain protein rbtn2 is essential for erythroid development. *Cell* 78: 45–57
- Wei AH, Strickland SA, Hou J-Z, Fiedler W, Lin TL, Walter RB, Enjeti A, Tiong IS, Savona M, Lee S, *et al* (2019) Venetoclax Combined With Low-Dose Cytarabine for Previously Untreated Patients With Acute Myeloid Leukemia: Results From a Phase Ib/II Study. *J Clin Oncol* 37: 1277–1284
- Wen X, Lu Y, Li Y, Qi P, Wu Y, Yu J, Zhang R, Huang Q, Huang P, Hou B, *et al* (2024) Remission rate, toxicity and pharmacokinetics of venetoclax-based induction regimens in untreated pediatric acute myeloid leukemia. *NPJ Precis Oncol* 8: 248
- Wilson NK, Foster SD, Wang X, Knezevic K, Schütte J, Kaimakis P, Chilarska PM, Kinston S, Ouwehand WH, Dzierzak E, *et al* (2010) Combinatorial transcriptional control in blood stem/progenitor cells: genome-wide analysis of ten major transcriptional regulators. *Cell Stem Cell* 7: 532–544
- Wong M, Mayoh C, Lau LMS, Khuong-Quang D-A, Pinese M, Kumar A, Barahona P, Wilkie EE, Sullivan P, Bowen-James R, *et al* (2020) Whole genome, transcriptome and methylome profiling enhances actionable target discovery in high-risk pediatric cancer. *Nat Med* 26: 1742–1753
- Woolthuis CM & Park CY (2016) Hematopoietic stem/progenitor cell commitment to the megakaryocyte lineage. *Blood* 127: 1242–1248
- Worst BC, van Tilburg CM, Balasubramanian GP, Fiesel P, Witt R, Freitag A, Boudalil M, Previti C, Wolf S, Schmidt S, *et al* (2016) Next-generation personalised medicine for high-risk paediatric cancer patients - The INFORM pilot study. *Eur J Cancer* 65: 91–101
- Xavier-Ferruccio J & Krause DS (2018) Concise Review: Bipotent Megakaryocytic-Erythroid Progenitors: Concepts and Controversies. *Stem Cells* 36: 1138–1145

- Xia J, Miller CA, Baty J, Ramesh A, Jotte MRM, Fulton RS, Vogel TP, Cooper MA, Walkovich KJ, Makaryan V, *et al* (2018) Somatic mutations and clonal hematopoiesis in congenital neutropenia. *Blood* 131: 408–416
- Xu H, Valerio DG, Eisold ME, Sinha A, Koche RP, Hu W, Chen C-W, Chu SH, Brien GL, Park CY, *et al* (2016) NUP98 Fusion Proteins Interact with the NSL and MLL1 Complexes to Drive Leukemogenesis. *Cancer Cell* 30: 863–878
- Yamada M, Keller RR, Gutierrez RL, Cameron D, Suzuki H, Sanghrajka R, Vaynshteyn J, Gerwin J, Maura F, Hooper W, *et al* (2024) Childhood cancer mutagenesis caused by transposase-derived PGBD5. *Sci Adv* 10: eadn4649
- Yamada Y, Warren AJ, Dobson C, Forster A, Pannell R & Rabbitts TH (1998) The T cell leukemia LIM protein Lmo2 is necessary for adult mouse hematopoiesis. *Proc Natl Acad Sci USA* 95: 3890–3895
- Yamanaka R, Barlow C, Lekstrom-Himes J, Castilla LH, Liu PP, Eckhaus M, Decker T, Wynshaw-Boris A & Xanthopoulos KG (1997) Impaired granulopoiesis, myelodysplasia, and early lethality in CCAAT/enhancer binding protein epsilon-deficient mice. *Proc Natl Acad Sci USA* 94: 13187–13192
- Yamanaka R, Lekstrom-Himes J, Barlow C, Wynshaw-Boris A & Xanthopoulos KG (1998) CCAAT/enhancer binding proteins are critical components of the transcriptional regulation of hematopoiesis (Review). *Int J Mol Med* 1: 213–221
- Yáñez A, Coetzee SG, Olsson A, Muench DE, Berman BP, Hazelett DJ, Salomonis N, Grimes HL & Goodridge HS (2017) Granulocyte-Monocyte Progenitors and Monocyte-Dendritic Cell Progenitors Independently Produce Functionally Distinct Monocytes. *Immunity* 47: 890-902.e4
- Ye M, Zhang H, Amabile G, Yang H, Staber PB, Zhang P, Levantini E, Alberich-Jordà M, Zhang J, Kawasaki A, *et al* (2013) C/EBPα controls acquisition and maintenance of adult haematopoietic stem cell quiescence. *Nat Cell Biol* 15: 385–394
- Yilmaz M, Kantarjian H & Ravandi F (2021) Acute promyelocytic leukemia current treatment algorithms. *Blood Cancer J* 11: 123
- Yokoyama A, Somerville TCP, Smith KS, Rozenblatt-Rosen O, Meyerson M & Cleary ML (2005) The menin tumor suppressor protein is an essential oncogenic cofactor for MLL-associated leukemogenesis. *Cell* 123: 207–218
- Yoshimoto G, Miyamoto T, Jabbarzadeh-Tabrizi S, Iino T, Rocnik JL, Kikushige Y, Mori Y, Shima T, Iwasaki H, Takenaka K, *et al* (2009) FLT3-ITD up-regulates MCL-1 to promote survival of stem cells in acute myeloid leukemia via FLT3-ITD-specific STAT5 activation. *Blood* 114: 5034–5043
- Yu BD, Hess JL, Horning SE, Brown GA & Korsmeyer SJ (1995) Altered Hox expression and segmental identity in Mll-mutant mice. *Nature* 378: 505–508
- Zhang DE, Zhang P, Wang ND, Hetherington CJ, Darlington GJ & Tenen DG (1997) Absence of granulocyte colony-stimulating factor signaling and neutrophil development in CCAAT enhancer binding protein alpha-deficient mice. *Proc Natl Acad Sci USA* 94: 569–574
- Zhang J, Walsh MF, Wu G, Edmonson MN, Gruber TA, Easton J, Hedges D, Ma X, Zhou X, Yergeau DA, *et al* (2015) Germline mutations in predisposition genes in pediatric cancer. *N Engl J Med* 373: 2336–2346

- Zhang J, Yang PL & Gray NS (2009) Targeting cancer with small molecule kinase inhibitors. *Nat Rev Cancer* 9: 28–39
- Zhang Y, Gao S, Xia J & Liu F (2018) Hematopoietic Hierarchy - An Updated Roadmap. *Trends Cell Biol* 28: 976–986
- Ziemin-van der Poel S, McCabe NR, Gill HJ, Espinosa R, Patel Y, Harden A, Rubinelli P, Smith SD, LeBeau MM & Rowley JD (1991) Identification of a gene, MLL, that spans the breakpoint in 11q23 translocations associated with human leukemias. *Proc Natl Acad Sci USA* 88: 10735–10739
- Zwaan CM, Kolb EA, Reinhardt D, Abrahamsson J, Adachi S, Aplenc R, De Bont ESJM, De Moerloose B, Dworzak M, Gibson BES, *et al* (2015) Collaborative efforts driving progress in pediatric acute myeloid leukemia. *J Clin Oncol* 33: 2949–2962

# Appendix

## CV

# Curriculum Vitae – Ben Haladik

ORCID: 0000-0001-6903-7379

Date/place of birth: 18.02.1993 Linz, Austria

### **Education**

- 09/2018 – present PhD Student, Medical University of Vienna  
Malignant Diseases Program  
PhD program of the Research Center for Molecular Medicine of the Austrian Academy of Sciences (CeMM). Jointly supervised by Prof. Giulio Superti-Furga and Univ. Prof. Kaan Boztug.
- 10/2016 – 11/2018 M.Sc. Bioinformatics, Institute for Mathematics and Computer Science  
Goethe University Frankfurt  
Thesis Title: “Exhaustive Bioinformatics Image Analysis of New and Recurrent Instances of Hodgkin Lymphoma using Machine Learning Methods”  
Molecular Bioinformatics group (Prof. Ina Koch)  
in collaboration with the Institute of Pathology (Prof. Martin-Leo Hansmann)
- 10/2012 – 06/2016 B.Sc. Bioinformatics, Institute for Mathematics and Computer Science  
Goethe University Frankfurt  
Thesis title: “Bioinformatical Application of Graphlets to Protein Structure Topologies”,  
Molecular Bioinformatics group (Prof. Ina Koch)

### **Research experience**

- 09/2018 – 06/2025 PhD Student, St. Anna Children’s Cancer Research Institute  
09/2018 – 03/2020 at Ludwig Boltzmann Institute for Rare and Undiagnosed Diseases  
Image-based drug screenings and data integration in pediatric leukemia  
Established computer vision pipelines with AI-based cell classification and orthogonal validation for image-based drug screening in pediatric leukemia primary samples and neuroblastoma cell lines  
Established workflows and reporting standards for image-based drug screenings on primary samples  
Standardized protocols for image-based drug screenings and trained technicians to achieve redundancy and fast turnover for drug screening and reporting on primary samples

Performed integrative analyses of drug screening data with ATAC-, RNA- and exome-sequencing data on pediatric AML patient cohort to investigate multi-modal drivers and signatures of patient risk

02/2016 – 08/2018 Part-time Research Assistant, Institute of Pathology  
University Hospital Frankfurt

Whole-slide-image analysis pipeline development using Machine Learning algorithms

Increased number of evaluable datasets 2-fold by establishing advanced segmentation algorithms

Established spatial statistics-based analysis framework for whole slide images

## **Further activities**

01/2020 – 06/2025 Deputy Data Manager, Research Center for Molecular Medicine  
of the Austrian Academy of Sciences

Helped establish standards for data documentation and user education according to FAIR principles

Re-organized and annotated data of 6 legacy projects according to FAIR principles for transfer to new HPC infrastructure

Data management introductions and data checkouts for ~2 users per year

01/2020 – 01/2021 PhD student representative, Research Center for Molecular  
Medicine of the Austrian Academy of Sciences (CeMM)

08/2015 – 08/2018 Member of Bioinformatics Student Council  
Goethe University Frankfurt

04/2015 – 01/2016 Tutor for Math and Bioinformatics (Part-time),  
Institute for Mathematics and Computer Science, Goethe  
University Frankfurt

## **Publications**

**Haladik B.**, Maurer-Granofszky M., Zoescher P., Jimenez-Heredia R., Frohne A., Segarra-Roca A., Casey C., Kartnig F., Giuliani S., Rashkova C., Repiscak P., Dworzak M.N., Superti-Furga G. & Boztug K. (2025). Image-based drug screening combined with molecular profiling identifies signatures and drivers of therapy resistance in pediatric AML. *Cell Reports Medicine*

Goldmann U., Wiedmer T., Garofoli A., Sedlyarov V., Bichler M., **Haladik B.**, Wolf G., Christodoulaki E., Ingles-Prieto A., Ferrada E., Frommelt F., Teoh ST., Leippe P., Onea G., Pfeifer M., Kohlbrenner M., Chang L., Selzer P., Reinhardt J., Digles D., Ecker G.F., Osthushenrich T., MacNamara A., Malarstig A., Hepworth D. & Superti-Furga G. (2025). Data- and knowledge-derived functional landscape of human solute carriers. *Molecular Systems Biology*

Troester S., Eder, T., Wukowits N., Piontek M., Fernández-Pernas P., Schmoellerl J., **Haladik B.**, Manhart G., Allram M., Maurer-Granofszky M., Scheidegger N., Nebral K., Superti-Furga G., Meisel R., Bornhauser B., Valent P., Dworzak M.N., Zuber J., Boztug K. & Grebien F. (2025). Transcriptional and epigenetic rewiring by the NUP98::KDM5A fusion oncoprotein directly activates CDK12. *Nature Communications*

Kalinichenko A., Perinetti Casoni G., Dupré L., Trotta L., Huemer J., Galgano D., German Y., **Haladik B.**, Pazmandi J., Thian M., Petronczki Ö.Y., Chiang S.C., Taskinen M., Hekkala A., Kauppila S., Lindgren O., Tapiainen T., Kraakman M.J., Vettenranta K., Lomakin A.J., Saarela J., Seppänen M.R.J., Bryceson Y.T. & Boztug K. (2021). RhoG deficiency abrogates cytotoxicity of human lymphocytes and causes hemophagocytic lymphocytosis. *Blood*.